Tampereen teknillinen korkeakoulu
Julkaisuja 344

Tampere University of Technology
Publications 344

Sami Repo

On-line Voltage Stability Assessment of Power System – An Approach of Black-box Modelling

Tampere 2001

Tampereen teknillinen korkeakoulu
Julkaisuja 344

Tampere University of Technology
Publications 344

Sami Repo

On-line Voltage Stability Assessment of Power System – An Approach of Black-box Modelling

Thesis for the degree of Doctor of Technology to be presented with due permission for public examination and criticism in Auditorium RG202, at Tampere University of Technology, on the 19th of October 2001, at 12 o'clock noon.

Tampere 2001

ISBN 952-15-0696-2 (printed)
ISBN 952-15-1473-6 (PDF)
ISSN 0356-4940

TTKK- PAINO, Tampere 2001

ABSTRACT

The management of power systems has become more difficult than earlier because power systems are operated closer to security limits, environmental constraints restrict the expansion of transmission network, the need for long distance power transfers has increased and fewer operators are engaged in the supervision and operation of power systems. Voltage instability has become a major concern in many power systems and many blackouts have been reported, where the reason has been voltage instability.

On-line voltage stability assessment is commonly based on a black-box modelling. Traditionally the model has been a two-dimensional security boundary, which is based on tabulation of data. The idea of the model-based approach presented in this study is to generalise the security boundary method and to take into account the uncertainty related to power system operation. The term “model-based approach” means in this thesis an approach which is based on black-box models. The model-based approach does not replace traditional analysis methods, rather these methods are urgently needed at the off-line computation step of the approach. The computation of the voltage stability margin is time-consuming and that is why these methods cannot be used in on-line applications.

The objective of the study was to develop a method to be applicable in practice for on-line voltage stability assessment of long-term large-disturbance voltage stability based on black-box model. The basis of the approach is appropriate modelling of power system voltage stability and computation of the most critical voltage stability margins. A large number of power system operation points and the most critical voltage stability margins are computed to create the model. An essential part of model creation is the selection and extraction of model inputs, on which the accuracy of the model is mainly based.

This thesis evinces new ideas for on-line voltage stability assessment of black-box model. The requirements and the proposed solution of all steps are presented to provide a step by step procedure for the use. The thesis describes first time an application of linear regression models to voltage stability margin approximation. The contributions of the thesis also include the improvement of maximum loading point algorithm, development of new voltage stability contingency ranking methods, and application of data analysis methods to voltage stability studies. The main results obtained in this thesis are an algorithm to compute the most critical voltage stability margin, a method to create a black-box modelling approach for on-line voltage stability assessment, and a method to approximate the most critical voltage stability margin accurately.

PREFACE

The research work was carried out at Tampere University of Technology since 1995. The supervisor of the thesis was Professor Pertti Järventausta. I would like to express my gratitude to him for his support in the course of this thesis. Professors Leena Korpinen and Erkki Lakervi have also advised me during the research work.

I would like to express my thanks to my colleague Juhani Bastman Lic.Tech. for the co-operation, support and many discussions. I wish to thank the personnel of the Institute of Power Engineering at Tampere University of Technology for creating an encouraging and pleasant research environment. I wish to express my special thanks to Ari Nikander Lic.Tech. and Vesa Latva-Pukkila M.Sc. for the rational and irrational discussions during the lunch and coffee breaks.

I wish to thank Ritva Hirvonen Dr. Tech. and the personnel of Fingrid Plc, especially Jarmo Elovaara M.Sc. and Mikko Koskinen M.Sc., for many discussions and advice during the research work. The co-operation and discussions with the personnel of Power System Laboratory of Helsinki University of Technology in Finland and Electric Power Engineering of Chalmers University of Technology in Sweden are also gratefully acknowledged. Many thanks to Virginia Mattila, for checking and improving the text of the manuscript.

The research was funded by the Graduate School in Electrical Engineering (Ministry of Education), IVO Transmission Services Ltd, the Tekes Technology Development Centre, Fingrid Plc, Helsinki Energy, Tampere University of Technology and the Academy of Finland. Financial support was also provided by Tekniikan edistämissäätiö, the Ulla Tuominen Foundation and Tampereen kaupungin tiederahasto, which are gratefully acknowledged.

My best love and gratitude are also due to my wife Anna, children Venla and Veikko and to my parents,

Mouhijärvi 3.9.2001

Sami Repo

TABLE OF CONTENTS

LIST OF SYMBOLS AND ABBREVIATIONS

Notations

$\|\| \cdot \|\|$	norm
$\underline{a}^T$, $\mathbf{A}^T$	transpose of vector $\underline{a}$ or matrix **A**
$\mathbf{A}^{-1}$	inverse of matrix **A**
$\mathbf{A}^{\dagger}$	pseudo inverse of matrix **A**
a_i, $\underline{a}_i$	the *i*th element of vector $\underline{a}$ or the *i*th column of matrix **A**
$\mathbf{A}_{ij}$	the element of the *i*th row and the *j*th column of matrix **A**
a^*	voltage collapse point
a_0	nominal value of *a*
$\hat{a}$	estimate of *a*
i, j, k	sub-indices

Symbols

a, b, c	coefficients of polynomial model
A	state matrix
$\underline{b}$	constant vector of linear system
$\cos\phi$	power factor
$\underline{c}$	prototype vector (centre of hidden unit activation function)
C	correlation matrix
E_{max}	maximum of electromagnetic force
$f(\cdot)$	function
I_p	active load current coefficient of polynomial load model
I_q	reactive load current coefficient of polynomial load model
I_{smax}	maximum of stator current
I	identity matrix
j	imaginary operator
J	Jacobian matrix
$\mathbf{J}_x$	Jacobian matrix with respect to $\underline{x}$
K	number of clusters
$\underline{le}$	left eigenvector
L	Lagrangian
n	number of experiments (cases)
N	normal distribution
m	number of original input variables
p	number of input variables

$\underline{p}$	principal component (eigenvector of **R**)
P	active power
P_G	active power of generator
P_p	active load power coefficient of polynomial load model
P	transformation matrix including principal components
q	number of hidden layer units
Q	reactive power
Q_q	reactive load reactive power coefficient of polynomial load model
$Q_{r\,max}$	maximum of generator reactive power limited by excitation current
$Q_{s\,max}$	maximum of generator reactive power limited by stator current
r	residual
$\underline{re}$	right eigenvector
R	= cov(·), covariance matrix
s	error variance
S	set of input variables
t_1	value obtained from the *t*-distribution with a chosen confidence limit
$\tan\phi$	$\frac{Q}{P}$
T	**XP**, transformed data matrix
$\underline{u}$	left singular vector
U	left orthonormal matrix
$\underline{v}$	right singular vector
V	right orthonormal matrix
V	voltage
$\underline{w}$	vector of multipliers
x	model input variable
$\underline{x}$	state vector, input vector
X	reactance
X_d	synchronous reactance
X	data matrix
y	model output variable
$\underline{z}$	cluster centre
Z_p	active load impedance coefficient of polynomial load model
Z_q	reactive load impedance coefficient of polynomial load model
α	exponent of active load
β	exponent of reactive load
δ	voltage angle
$\underline{\varepsilon}$	error vector
$\phi(\cdot)$	activation function (Gaussian function)
λ	eigenvalue
Δ	change, difference

γ	width of activation function
μ	power demand
σ	singular value
$\mathbf{\Sigma}$	diagonal matrix having singular values at diagonal
∂, ∇_x	derivative operator or derivative with respect to $\underline{x}$

Abbreviations

AC	alternating current
BFGS	Broyden, Fletcher, Goldfarb and Shanno quasi-Newton update
DC	direct current
EHV	extra high voltage
GD	gradient descent
HV	high voltage
HVDC	high voltage direct current
IEEE	Institute of Electrical and Electronics Engineers
LM	Levenberg-Marquardt
MSE	mean square error
PC	personal computer
PSS/E	power system simulator for engineering
PV	power-voltage (curve)
RPROP	resilient back-propagation
RTU	remote terminal unit
SCADA	supervisory control and data acquisition
SCG	scaled conjugate gradient
SSE	sum-square error

1 INTRODUCTION

1.1 Background

The following reasons make the management of power systems more difficult than earlier:

- due to increased competition existing power systems are required to provide greater profit or produce the same service at lower costs, thereby increasing the duration of power systems operating close to security and stability limits,
- environmental constraints severely limit the expansion of a transmission network,
- in a deregulated market there is a need for a new kind of voltage and power flow control (for which existing power systems are not designed for),
- the transmission capacity for all transactions in the open access networks needs to be determined,
- fewer operators are engaged in the supervision and operation of power systems.

Although power production, transmission and distribution are unbundled there still exist common interests for these companies: power system adequacy and security. The adequacy of production and transmission capacity is maintained in the long-term and is related to power system planning. The security of a power system is related to power system operation. The security of a power system is a mandatory public good necessary for confidence in the power market. In order to maintain a secure system, the system operator needs to have at his disposal various services called ancillary services from generation and major customers.

The transmission networks need to be utilised ever more efficiently. The transfer capacity of an existing transmission network needs to be increased without major investments but also without compromising the security of the power system. The more efficient use of transmission network has already led to a situation in which many power systems are operated more often and longer close to voltage stability limits. A power system stressed by heavy loading has a substantially different response to disturbances from that of a non-stressed system. The potential size and effect of disturbances has also increased: When a power system is operated closer to a stability limit, a relatively small disturbance may cause a system upset. In addition, larger areas of the interconnected system may be affected by a disturbance.

Voltage stability is concerned with the ability of a power system to maintain acceptable voltages at all buses under normal conditions and after being subjected to a disturbance [Cut98]. The assessment of voltage stability has also become more complicated due to strengthening of power systems. For example, voltages do not indicate the proximity to voltage collapse point in heavily compensated systems even in heavy loading conditions. The transient angle stability is seldom a reason for the restriction of power transfers due to stronger power systems and development of equipment technology compared to past decades, while the power system blackouts occurring all over the world have in the past 20 years mainly been voltage collapses.

Environmental constraints limit the expansion of transmission network and generation near load centres, which has a negative influence on power system voltage stability, because the electrical distance from a generator to a load increases and the voltage support weakens in the load area. The generation today often takes place in fewer and larger units located at considerable distances from major loads. Simultaneous growth in the use of electrical power without a corresponding increase of transmission capacity has brought many power systems closer to their voltage stability limits.

Although restriction of power transfers is seldom needed due to power system security or stability at many power systems, there do exist needs to rebuild parts of the transmission network or the ways in which it is operated. Centralised planning and operation of the power system has enabled its co-ordinated development in past years. The transmission network developed for a vertically integrated power system is not necessarily an optimal nowadays in an unbundled environment; For example, changes in the power production pattern due to market conditions may change the bottlenecks of a transmission network and restrict the power trading in this way. This increases the importance of flexible planning of transmission network.

The transmission network has a key role on the power markets; it makes the whole thing possible. The power trade on the Nordic power market is limited due to lack of transmission capacity. The national capacity bottlenecks are relieved through counter-trading in Finland and Sweden by national grid companies Fingrid and Svenska Kraftnät. The responsibility of the national grid companies is not to resolve the cross-border bottlenecks between Finland and Sweden via counter-trade. The cross-border bottlenecks divide the market into price areas. Network congestion in an otherwise perfect market is not a bad thing, as the cost of market inefficiency can be traded off against the cost of improving the transmission system and thus serves as an economic signal for transmission reinforcement. The cross-border bottleneck between northern Sweden and northern Finland comes from a voltage stability limit. The free power market has increased the number and the amount of short-term electricity trades and willingness for strategic tactics in order to increase the price of electricity. The short-term electricity trade increases the variation in power transfers. The amount of maximum transfers varies a lot, which

makes it difficult to decide the optimum level of transmission network expansions. Open access networks need accurate transmission capacity determination to guarantee secure power system operation for all transactions and information for the players on the market.

These factors have increased the demand for more accurate and up-to-date information in power system operation. Power system planners and operators must define accurately how much power can be safely transferred across the system. The interest in power system available transfer capacity has increased in recent years in order to utilise the transmission network more efficiently, while the determination of available transfer capacity has also become more complicated due to increased uncertainty in the power system planning and operation. The available transfer capacity should be capable of handling all transactions and contingencies. Transmission companies determine the available transfer capacity for the most critical contingencies in certain operational situations. These studies are time-consuming and cannot be done on-line, which is why new methods for voltage stability assessment are needed.

Planning a power system is a technical and an economic optimisation task. Investments made in the production and networks have to be set against the benefits to be derived from improving the reliability of power system. Hence, when planning the power system, we have to compromise between reliability and outage costs. Investment costs can be evaluated easily, but the value of improved reliability cannot be evaluated explicitly. Planning studies examine the adequacy of a power system. The time horizon of planning studies runs from years to decades, but these studies are obviously not accurate enough for power system operation. Security studies on the transmission system are based on existing or near future conditions of the system: The amount of load, network topology, unit commitment, the amount of reserves etc. are known accurately enough to make detailed studies on power system functioning, and the operation limits of transmission system are based on these studies.

The transmission systems are usually reliable due to redundancy in the systems. The reliability of a transmission system is determined according to line overload, protection and power system dynamic behaviour (stability). The transmission system is meshed, why a fault seldom causes an interruption. However, the loss of power system stability may cause a total blackout of the system. It is the interconnection of power systems, for reasons of economy and of improved availability of supplies across broader areas, that makes widespread disruptions possible. Without interconnection, small individual systems would be individually more at risk, but widespread disruptions would not be possible.

Modern society is very vulnerable in the case of power system blackout, the consequences of blackouts being both social and economic. Even short disturbances can be harmful for the process industry, because restarting of the process might take several hours, likewise for air-traffic control and areas that depend on computers. The consequences of

disturbances in office work will be loss of production and information. Many services will be at a standstill, because the production or use of services requires electricity. Long interruptions complicate the use of communication systems, traffic and transportation, water distribution, heating, farming, storage of foodstuffs, etc. In practice, it is not possible to work or to serve without electricity in modern society.

Direct economic consequences of total blackout in Finland are estimated to be a few hundred million Finnish marks[1] [Säh79, Lem94]. In 1994 a study of disturbance cost was made in the Swedish power system [Sve94]. An estimate for the outage cost in Sweden as a whole can be calculated from the following equation, 10 SEK/kW + 24 SEK/kWh. For example, the cost of one hour outage of 10000 MW load is 340 MSEK[1]. Direct costs of outage include loss of production, spoilt raw material, broken equipment, salary costs during the non-productive period and loss of profit, while indirect costs of outage are loss of future orders when an interruption leads to delay in delivering a product, insurance costs and costs of backup power supply.

1.2 Objectives and contributions of the thesis

1.2.1 Topic of the thesis

The research of power system voltage stability during the last 10 years has dealt with modelling of voltage stability, computation of voltage collapse point and enhancement of power system stability. References [Cut98, Kun94, Tay94, and Iee01] provide a good overview of these areas. There has developed a wide variety of modelling principles and of computation and control methods to analyse and control power system voltage stability. The research has mainly been based on analytical methods such as dynamic simulations and load-flow algorithms. The assessment of voltage stability is commonly based on voltage stability margin, but the computation of the margin is time-consuming. The computation methods developed for voltage stability analysis are, in principle, best suited for power system planning. On-line voltage stability assessment has mainly also been based on these computation methods.

The applications of pattern recognition, decision trees, neural networks, fuzzy systems, genetic algorithms and statistical methods (function approximation) are also widely applied to on-line voltage stability assessment. Instead of laws of physics and logic these methods create/use a model, which is based on knowledge or data. Statistical methods and neural networks are black-box models, which are applied when the functioning of a system is unknown or very complex, but there is plenty of data available. The black-boxes are data-driven models, which do not explicitly model the physics of the system, but establish

[1] 1 EUR = 5.94573 FIM ≈ 8.33 SEK (The Swedish krona is independent of the Euro, currency rate as of 8 March 2001)

a mathematical relationship between a large number of input-output pairs measured from the system. The mathematical relationship is a model, which is numerical computed from measurement or statistical data. The term “model-based approach” means in this thesis an approach which is based on data-driven black-box models. Neuro-fuzzy, fuzzy and expert systems, which are grey-box models, may be applied when there is also some knowledge available.

In the thesis the black-box modelling approach was developed for on-line long-term voltage stability assessment. The function to be approximated is the mapping between the pre-disturbance operation point and the voltage stability margin of the most critical contingency. The inputs are active and reactive line flows and bus voltages at a pre-disturbance operation point which are commonly measured in most power systems from almost all lines and buses. Using these inputs guarantees explicit input-output mapping at all operation points. The input variables can take into account changes in the power system load, production, network topology, unit commitment, etc. Good quality data is essential for the approach. The data generation is based on automatic generation of operation and maximum loading points using off-line load-flow computation. The model creation includes following steps: model type selection, data analyses, data pre-processing, estimation of model parameters, and testing of generalisation capability. The on-line procedure of the approach is extremely fast.

The idea of the approach is to enlarge and generalise the existing and widely used security boundary method and to take into account the uncertainty related to power system operation. The approach does not make unnecessary the more traditional computation methods; rather these methods are urgently needed at the off-line computation step of data generation. The use of security boundary method leads to a situation where the power system security limits could be increased in some situations without the fear of insecurity if more accurate and up-to-date security limits were used. Due to the previous reasons the power system cannot be stressed up to maximum limit but a relatively large reliability margin is needed when the security boundary method is applied. This margin is typically a few per cent of total capacity. To allow power transfers increase close to or beyond the security boundary, there should be a possibility to evaluate risks and uncertainties related to security limits.

1.2.2 Objectives of the thesis

The objective of this thesis is to develop a method to be applicable in practice for a model-based voltage stability assessment of long-term large-disturbance voltage stability. The method is suited for transmission system on-line security assessment. The sub-tasks needed to solve the problem, are:

- modelling of voltage stability, i.e. selection of appropriate models of devices for the off-line computation using commercial computation and analysis tools
- contingency ranking for voltage stability studies

- computation of the most critical maximum loading point
- formulation of automatic data generation system
- selection and extraction of model inputs
- black-box modelling (function approximation) of the most critical voltage stability margin.

The main focus of the thesis is on the development of a model-based approach. In order to achieve good and sufficiently general results the accurate approximation of the most critical voltage stability margin requires consideration of the above sub-tasks. The basis of the whole approach is appropriate modelling of power system voltage stability and computation of the most critical voltage stability margins. A large number of power system operation points and voltage stability margins must be computed in order to create an accurate model, which encounters the conflicting requirements of modelling accuracy and computation speed in off-line. However, the on-line computation speed of approach is very fast, less than one second, and the off-line computation speed with existing PCs is fast enough for computation of thousands of data samples in one day. The next step of the model-based approach is the model creation, which also entails the selection and extraction of model inputs, on which the accuracy of the model is mainly based.

This thesis puts forward new ideas for model-based voltage stability assessment. The work accomplished during this project has been published in the following references [Rep97, Rep99, Rep00a, Rep00b, and Rep00c]. The results and contributions of the thesis are:

1. a method to create a model-based approach for on-line voltage stability assessment,
   - The proposed method is a complete approach to on-line voltage stability assessment. The requirements and the proposed solutions are presented to provide a step by step procedure for the use of a model-based approach.
2. a method to approximate the most critical voltage stability margin accurately,
   - The thesis describes first time an application of linear regression models to voltage stability margin approximation.
   - Different solution methods and a comparison of these methods are presented. Feature selection and extraction methods and black-box models are compared in order to find the most suitable combination of methods and models for the power systems studied.
3. an algorithm to compute the most critical voltage stability margin.
   - The thesis also includes improvement of maximum loading point algorithm, development of new voltage stability contingency ranking methods and application of data analysis methods to voltage stability studies.

1.3 Outline of the thesis

Chapter 2 describes the voltage stability phenomena. First the voltage stability, voltage instability and voltage collapse are defined and the aspects of voltage stability are classified, followed by a short description of maximum transfer capacity. Next an introduction for the stability of non-linear system is given. The modelling and the effect of power system components in the long-term voltage stability studies are also described, and scenario of classic voltage collapse concludes the chapter.

Voltage stability assessment in Chapter 3 and black-box modelling in Chapter 4 provide the background information for the voltage stability assessment based on black-box models described in Chapter 5. Chapter 3 is divided into three parts. The first part is a state-of-the-art description of power system security analysis. The second part deals with the computation of voltage stability margin, voltage collapse point and maximum loading point. The computation algorithm of maximum loading point is described in greater detail than others because it is used in the testing of model-based approach. The proposed contingency ranking methods for voltage stability studies are described in the third part.

Chapter 4, principles of black-box modelling, considers linear regression and non-linear neural network modelling, model generalisation, and feature selection and extraction methods. These methods are then applied to the voltage stability assessment in Chapter 6. The parameter estimation of these models is also described here. The generalisation of the model is the most important aspect in modelling. The rest of this chapter considers generalisation improvement; i.e. how model generalisation is managed. The feature selection and extraction methods are used to reduce the input dimension of model-based approach, which is a important and effective tool in the proposed approach.

Chapter 5 is the most important chapter of the thesis, which includes a description of the voltage stability assessment based on black-box model. The information of previous chapters is applied to create the model-based approach. First comes a short introduction to the proposed approach and a comparison to security boundary method and similar approaches proposed earlier, then the requirements of model-based approach are discussed. After that the whole procedure is described step by step in order to provide a comprehensive view of the approach. Finally the implementation possibilities of the approach are discussed. The on-line implementation is proposed to be a part of SCADA and power management system[2].

The proofs of the applicability of the proposed approach are presented in Chapter 6. The proposed approach is tested with IEEE 118-bus test network and a 131-bus equivalent of the Finnish transmission system. The summary is presented in Chapter 7.

---

[2] The power management system is a new type of energy management system intended only for transmission network management, not for whole power system management.

2 VOLTAGE STABILITY

Voltage stability is a problem in power systems which are heavily loaded, faulted or have a shortage of reactive power. The nature of voltage stability can be analysed by examining the production, transmission and consumption of reactive power. The problem of voltage stability concerns the whole power system, although it usually has a large involvement in one critical area of the power system.

This chapter describes the voltage stability phenomena. First voltage stability, voltage instability and voltage collapse are defined and the aspects of voltage stability are classified. Then a short example of maximum transfer capacity is described. After that an introduction to the stability of non-linear system is given. Then the modelling and the effect of power system components in the long-term voltage stability studies are described. The modelling and the effect of following components are considered: synchronous generator, automatic voltage controller, load, on-load tap changer, thermostatic load, and compensation devices. The scenario of classic voltage collapse is also presented to describe the problem.

2.1 Definition and classification of voltage stability

2.1.1 Definition of voltage stability, voltage instability and voltage collapse

Power system stability is defined as a characteristic for a power system to remain in a state of equilibrium at normal operating conditions and to restore an acceptable state of equilibrium after a disturbance [Cut98]. Traditionally, the stability problem has been the rotor angle stability, i.e. maintaining synchronous operation. Instability may also occur without loss of synchronism, in which case the concern is the control and stability of voltage. Reference [Kun94] defines the voltage stability as follows: “The voltage stability is the ability of a power system to maintain steady acceptable voltages at all buses in the system at normal operating conditions and after being subjected to a disturbance.”

Power system is voltage stable if voltages after a disturbance are close to voltages at normal operating condition. A power system becomes unstable when voltages uncontrollably decrease due to outage of equipment (generator, line, transformer, bus bar, etc.), increment of load, decrement of production and/or weakening of voltage control. According to reference [Cut98] the definition of voltage instability is “Voltage instability stems from the attempt of load dynamics to restore power consumption beyond the capability of the combined transmission and generation system.” Voltage control and

instability are local problems. However, the consequences of voltage instability may have a widespread impact. Voltage collapse is the catastrophic result of a sequence of events leading to a low-voltage profile suddenly in a major part of the power system.

Voltage stability can also called “load stability”. A power system lacks the capability to transfer an infinite amount of electrical power to the loads. The main factor causing voltage instability is the inability of the power system to meet the demands for reactive power in the heavily stressed systems to keep desired voltages. Other factors contributing to voltage stability are the generator reactive power limits, the load characteristics, the characteristics of the reactive power compensation devices and the action of the voltage control devices [Cut98]. The reactive characteristics of AC transmission lines, transformers and loads restrict the maximum of power system transfers. The power system lacks the capability to transfer power over long distances or through high reactance due to the requirement of a large amount of reactive power at some critical value of power or distance. Transfer of reactive power is difficult due to extremely high reactive power losses, which is why the reactive power required for voltage control is produced and consumed at the control area.

2.1.2 Classification of power system stability

Power system stability is classified above as rotor angle and voltage stability. A classification of power system stability based on time scale and driving force criteria is presented in Table 2.1. The driving forces for an instability mechanism are named generator-driven and load-driven. It should be noted that these terms do not exclude the affect of other components to the mechanism. The time scale is divided into short and long-term time scales.

Table 2.1. Classification of power system stability [Cut98].

<table>
<tr><td>Time scale</td><td colspan="2">Generator-driven</td><td colspan="2">Load-driven</td></tr>
<tr><td rowspan="2">Short-term</td><td colspan="2">rotor angle stability</td><td colspan="2" rowspan="2">short-term voltage stability</td></tr>
<tr><td>small-signal</td><td>transient</td></tr>
<tr><td rowspan="2">Long-term</td><td colspan="2" rowspan="2">frequency stability</td><td colspan="2">long-term voltage stability</td></tr>
<tr><td>small disturbance</td><td>large disturbance</td></tr>
</table>

The rotor angle stability is divided into small-signal and transient stability. The small-signal stability is present for small disturbances in the form of undumped electromechanical oscillations. The transient stability is due to lack of synchronising torque and is initiated by large disturbances [Kun94]. The time frame of angle stability is that of the electromechanical dynamics of the power system. This time frame is called short-term time scale, because the dynamics typically last for a few seconds.

The voltage problem is load-driven as described above. The voltage stability may be divided into short and long-term voltage stability according to the time scale of load

component dynamics. Short-term voltage stability is characterised by components such as induction motors, excitation of synchronous generators, and electronically controlled devices such as HVDC and static var compensator [Cut98]. The time scale of short-term voltage stability is the same as the time scale of rotor angle stability. The modelling and the analysis of these problems are similar. The distinction between rotor angle and short-term voltage instability is sometimes difficult, because most practical voltage collapses include some element of both voltage and angle instability [Tay94].

When short-term dynamics have died out some time after the disturbance, the system enters a slower time frame. The dynamics of the long-term time scale last for several minutes. Two types of stability problems emerge in the long-term time scale: frequency and voltage problems. Frequency problems may appear after a major disturbance resulting in power system islanding [Kun94]. Frequency instability is related to the active power imbalance between generators and loads. An island may be either under or over-generated when the system frequency either declines or rises.

The analysis of long-term voltage stability requires detailed modelling of long-term dynamics. The long-term voltage stability is characterised by scenarios such as load recovery by the action of on-load tap changer or through load self-restoration, delayed corrective control actions such as shunt compensation switching or load shedding [Cut98]. The long-term dynamics such as response of power plant controls, boiler dynamics and automatic generation control also affect long-term voltage stability [Cut98]. The modelling of long-term voltage stability requires consideration of transformer on-load tap changers, characteristics of static loads, manual control actions of operators, and automatic generation control.

For purposes of analysis, it is sometimes useful to classify voltage stability into small and large disturbances. Small disturbance voltage stability considers the power system’s ability to control voltages after small disturbances, e.g. changes in load [Kun94]. The analysis of small disturbance voltage stability is done in steady state. In that case the power system can be linearised around an operating point and the analysis is typically based on eigenvalue and eigenvector techniques. Large disturbance voltage stability analyses the response of the power system to large disturbances e.g. faults, switching or loss of load, or loss of generation [Kun94]. Large disturbance voltage stability can be studied by using non-linear time domain simulations in the short-term time frame and load-flow analysis in the long-term time frame [Gao96]. The voltage stability is, however, a single problem on which a combination of both linear and non-linear tools can be used.

2.2 Analysis of power system voltage stability

2.2.1 A simple example

The characteristics of voltage stability are illustrated by a simple example. Figure 2.1 shows a simplified two-bus test system. The generator produces active power, which is transferred through a transmission line to the load. The reactive power capability of the generator is infinite; thus the generator terminal voltage V_1 is constant. The transmission line is presented with a reactance (jX). The load is constant power load including active P and reactive Q parts.

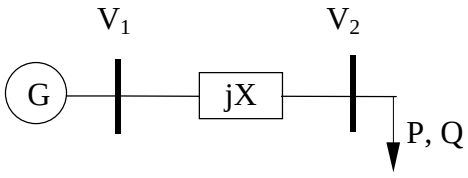

Figure 2.1. Two-bus test system.

The purpose of the study is to calculate the load voltage V_2 with different values of load. The load voltage can be calculated analytically in this simple example. Generally voltages are solved with a load-flow program. The solution of Equation 2.1 is the load voltage for the load-flow equations of the example, when the voltage angle is eliminated.

$$V_2 = \sqrt{\frac{(V_1^2 - 2QX) \pm \sqrt{V_1^4 - 4QXV_1^2 - 4P^2X^2}}{2}} \qquad (2.1)$$

The solutions of load voltages are often presented as a PV-curve (see Figure 2.2). The PV-curve presents load voltage as a function of load or sum of loads. It presents both solutions of power system. The power system has low current—high voltage and high current—low voltage solutions. Power systems are operated in the upper part of the PV-curve. This part of the PV-curve is statically and dynamically stable. The head of the curve is called the maximum loading point. The critical point where the solutions unite is the voltage collapse point [Cut98]. The maximum loading point is more interesting from the practical point of view than the true voltage collapse point, because the maximum of power system loading is achieved at this point. The maximum loading point is the voltage collapse point when constant power loads are considered, but in general they are different. The voltage dependence of loads affects the point of voltage collapse. The power system becomes voltage unstable at the voltage collapse point. Voltages decrease rapidly due to the requirement for an infinite amount of reactive power. The lower part of the PV-curve (to the left of the voltage collapse point) is statically stable, but dynamically unstable [Kun94]. The power system can only operate in stable equilibrium so that the system dynamics act to restore the state to equilibrium when it is perturbed.

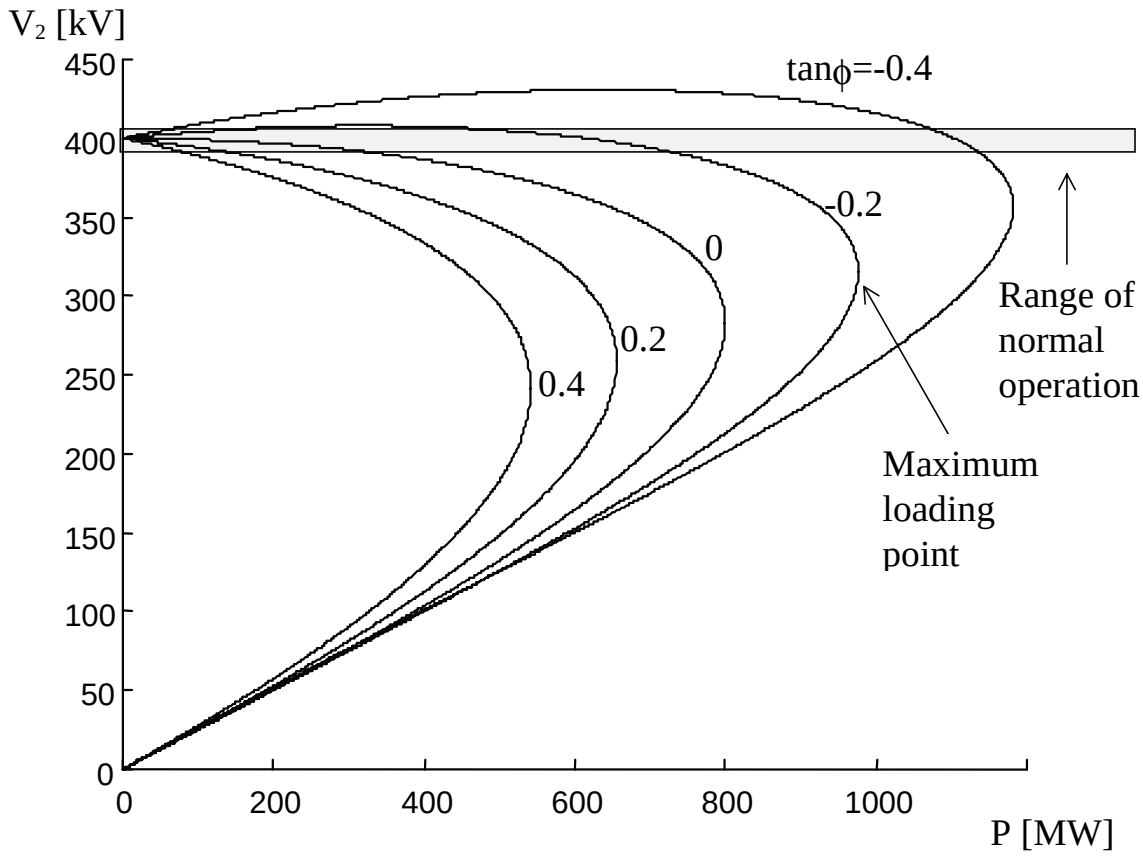

Figure 2.2. PV-curve.

Figure 2.2 presents five PV-curves for the test system (V_1=400 kV and X=100 Ω). These curves represent different load compensation cases (tanϕ=Q/P). Since inductive line losses make it inefficient to supply a large amount of reactive power over long transmission lines, the reactive power loads must be supported locally [Mil82]. According to Figure 2.2 addition of load compensation (decrement of the value of tanϕ) is beneficial for the power system. The load compensation makes it possible to increase the loading of the power system according to voltage stability. Thus, the monitoring of power system security becomes more complicated because the critical voltage might be close to voltages of normal operation range.

The opportunity to increase power system loading by load and line compensation is valuable nowadays. Compensation investments are usually much less expensive and more environment friendly than line investments. Furthermore, construction of new line has become time-consuming if not even impossible in some cases. At the same time new generation plants are being constructed farther away from load centres, fossil-fired power plants are being shut down in the cities and more electricity is being exported and imported. This trend inevitably requires addition of transmission capacity in the long run.

The above description of the voltage stability phenomenon has been limited to a radial system because it presents a simple and a clear picture of the problem. In practical power systems, many factors affect the progress of voltage collapse due to voltage instability. These factors are described in Chapter 2.2.3.

2.2.2 Analysis of voltage stability of non-linear power system

Static and dynamic analysis

Limitations of steady state power system studies (algebraic equations) are associated with stability of non-linear dynamic systems [Iee01]. The dynamics of the power system is modelled as differential equations. If the dynamics act extremely fast to restore algebraic relations between the states, then it can be a good approximation to use the algebraic relations. In dynamic analysis the transition itself is of interest and it checks that the transition will lead to an acceptable operating condition.

The voltage stability is a dynamic phenomenon by nature, but the use of steady state analysis methods is permitted in many cases. Accurate dynamic simulation is needed for post-mortem analysis and the co-ordination of protection and control [Gao96]. The voltage stability assessment of static and dynamic methods should be close to each other when appropriate device models are used and voltage instability does not occur during the transient period of disturbance [Gao96]. In steady state voltage stability studies load-flow equations are used to represent system conditions. In these studies it is assumed that all dynamics are died out and all controllers have done their duty. Steady state voltage stability studies investigate long-term voltage stability. The results of these studies are usually optimistic compared to dynamic studies [Gao96].

The advantage of using algebraic equations compared to dynamic studies is the computation speed. Dynamic simulations are time-consuming and an engineer is needed to analyse the results. However, the stability of the power system cannot be fully guaranteed with steady state studies. The time domain simulations capture the events and chronology leading to voltage instability. This approach provides the most accurate response of the actual dynamics of voltage instability when appropriate modelling is included. However, devices which may have a key role in the voltage instability include those which may operate in a relatively long time frame [Cut98]. These devices include the over-excitation limiter of synchronous generator and the on-load tap changer. It may take minutes before a new steady state is reached or voltage instability occurs following a disturbance. Static analysis is ideal for the bulk of power system studies in which the examination of a wide range of power system conditions and a large number of contingencies is required [Gao96].

Stability of non-linear system

The stability of a linear system can be determined by studying eigenvalues of the state matrix. The system is stable if all real parts of eigenvalues are negative. If any real part is positive the system is unstable. If any real part is zero we cannot say anything. The

stability of a non-linear system can be determined by linearisation of the system at the operating equilibrium. Using the first terms of Taylor series expansion, the function can be linearised. The state matrix is a Jacobian matrix of function determined by the state vector at the operation point. The Jacobian matrix describes the linear system which best approximates the non-linear equations close to the equilibrium. In that case the stability of the non-linear system can be studied like the stability of linear systems in the neighbourhood of operating equilibrium.

Bifurcation analysis

Voltage stability is a non-linear phenomenon and it is natural to use non-linear analysis techniques such as bifurcation theory to study voltage collapse. Bifurcation describes qualitative changes such as loss of stability [Cut98]. Bifurcation theory assumes that power system parameters vary slowly and predicts how a power system becomes unstable. The change of parameter moves the system slowly from one equilibrium to another until it reaches the collapse point. The system dynamics must act more quickly to restore the operating equilibrium than the parameter variations do to change the operating equilibrium. Although voltage collapses are typically associated with discrete events such as large disturbances, device or control limits, some useful concepts of bifurcation theory can be reused with some care. Voltage collapses often have an initial period of slow voltage decline. Later on in the voltage collapse, fast dynamics can lose their stability in a bifurcation and a fast decline of voltage results [Cut98].

Bifurcation occurs at the point where, due to slow changes of parameter, the characteristics of the system change. Bifurcation points where change from stable to unstable occurs, from stationary to oscillatory, or from order to chaos, are the most interesting points in voltage stability studies [Cut98]. These changes may also take place simultaneously. Usually only one parameter, e.g. load demand, is changed at once, in which case there is a possibility to achieve either saddle node or Hopf bifurcation [Dob92].

At the saddle node bifurcation the stable and unstable equilibria coalesce and disappear, then the Jacobian matrix is singular, thus one of the eigenvalues (or singular values) must be zero. The saddle node point is a limiting point between stable and unstable areas. The consequence of the loss of operating equilibrium is that the system state changes dynamically. The dynamics can be such that the system voltages fall dynamically. The complex conjugate eigenvalue pair is located at the imaginary axis at the Hopf bifurcation, in which case oscillation arises or disappears. The Jacobian matrix is non-singular at the Hopf bifurcation. There are also other bifurcations (e.g. pitchfork bifurcation) which are less likely to be found in general equations.

If we consider the example presented in Figures 2.1 and 2.2, the bifurcation parameter is the system loading. The system states are load voltage and angle. As the loading slowly increases, the stable and unstable solutions approach each other and finally coalesce at the

critical loading. The equilibrium solutions disappear at this point, i.e. at a saddle node bifurcation point. Before bifurcation, the system state tracks a stable equilibrium as the loading increases slowly (upper part of the PV-curve). Therefore algebraic equations can be used to follow the operating point. At bifurcation, the equilibrium becomes unstable and the resulting transient voltage collapse requires a dynamic model. However, the detection of the bifurcation point does not require the use of a dynamic model. The detection of saddle node bifurcation points in the case of voltage stability is described in Chapter 3.2.3.

2.2.3 Factors affecting voltage stability

The purpose of the chapter is to describe the modelling of power system and to discuss the effects of power system devices and control to voltage stability. It is well known that slower acting devices such as generator over-excitation limits, the characteristics of the system loads, on-load tap changers and compensation devices will contribute to the evolution of a voltage collapse [Cut98]. The modelling of a power system is similar in long-term voltage stability studies than in traditional load-flow studies. Most components can be modelled with existing models. Fast acting devices such as induction motors, excitation system of synchronous machines, control of HVDC and static var compensators are not described in detail here. These devices have contribution to voltage stability, but the main emphasis is in short-term voltage stability. The analysis and combination of fast and slow acting devices is also difficult with traditional dynamic simulation tools, but may be easily analysed with a fast voltage stability analysis method based on quasi steady state approximation, which consists of replacing the transient differential equations with adequate equilibrium relationships [Cut97].

Reactive power capability of synchronous generator

Synchronous generators are the primary devices for voltage and reactive power control in power systems. According to power system security the most important reactive power reserves are located there. In voltage stability studies active and reactive power capability of generators is needed to consider accurately achieving the best results. The limits of generator active and reactive power are commonly shown with a PQ-diagram (Figure 2.3). The active power limits are due to the design of the turbine and the boiler. Active power limits are constant. Reactive power limits are more complicated, which have a circular shape and are voltage dependent. Normally reactive power limits are described as constant limits in the load-flow programs. The voltage dependence of generator reactive power limits is, however, an important aspect in voltage stability studies and should be taken into account in these studies [Cap78, Löf95b].

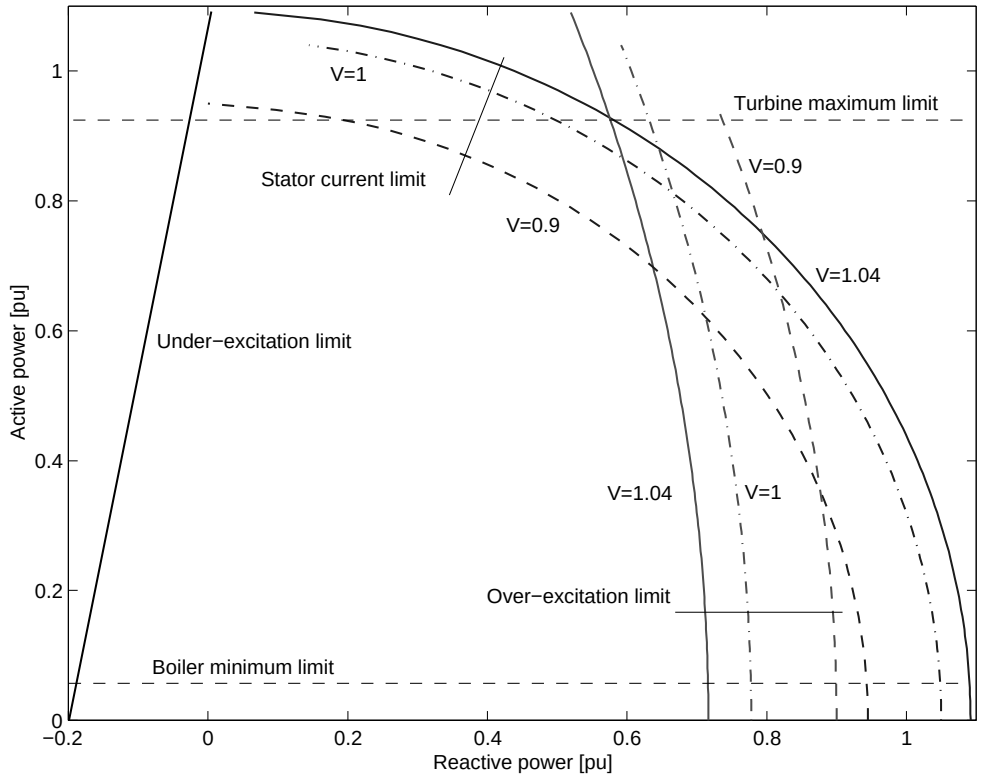

Figure 2.3. PQ-diagram (X_d=0.45 pu, I_{smax}=1.05 pu, E_{max}=1.35 pu).

The limitation of reactive power has three different causes: stator current, over-excitation and under-excitation limits. When excitation current is limited to maximum value, the terminal voltage is the maximum excitation voltage less the voltage drop in the synchronous reactance. The power system has become weaker, because the constant voltage has moved more remote from loads. The voltage dependent limit of excitation current can be calculated from Equation 2.2 [Löf95b], where P_G is active power of generator, E_{max} is the maximum of electromotive force, X_d is synchronous reactance and V is terminal voltage. The reactive power limit corresponding stator current limit can be calculated from Equation 2.3 [Löf95b]. The terminal voltage, the maximum of stator current I_{smax} and the active power of generator P_G determine it.

$$Q_{r\max} = -\frac{V^2}{X_d} + \sqrt{\frac{V^2 E_{\max}^2}{X_d^2} - P_G^2} \tag{2.2}$$

$$Q_{s\max} = \sqrt{V^2 I_{s\max}^2 - P_G^2} \tag{2.3}$$

The shape of both equations is circular. The reactive power limits are presented in Figure 2.3 with three different values of terminal voltage: 1.04, 1.0 and 0.9 pu. The reactive power limit in nominal voltage condition (V=1.04) is defined by the excitation current. The stator current limit should be taken into account because the limit decreases when the voltage decreases. The stator current limit is more restrictive than the excitation current limit with

terminal voltages of 1.0 and 0.9 pu when generator output is higher than 0.8 and 0.35 pu, respectively. Due to voltage dependence the reactive power capability increase when terminal voltage decrease and generator output is less than previous values of output power. The stator current limiter is commonly used in Sweden. It is used to limit reactive power output to avoid stator overloading. The action of the stator current limit is disadvantageous for voltage stability [Joh99]. The stator current limiter decreases the reactive power capability to avoid stator over-heating and causes dramatic decrement in voltage.

Generator reactive power capability from the system point of view is generally much less than indicated by manufactures' reactive capability curves, due to constraints imposed by plant auxiliaries and the power system itself [Adi94]. The steady operation of the power plant may be threatened when the system voltage is low. The necessary auxiliary systems like pumps, fans etc. may stop due to undervoltage, which may cause tripping of the power plant. Choosing optimum positions for the main and auxiliary transformer taps with respect to power system operating conditions may increase the reactive power capability of generator.

Automatic voltage control of synchronous generator

It is important for voltage stability to have enough nodes where voltage may be kept constant. The automatic voltage controllers of synchronous generators are the most important for that. The action of modern voltage controllers is fast enough to keep voltage constant when generators are operated inside PQ-diagrams. The automatic voltage controller includes also the excitation current limiters (over- and under-excitation limiters) and in some cases also the stator current limiter.

In case of a disturbance the excitation voltage is increased to maximum and the excitation current is increased high enough or to its maximum. The short-term maximum of excitation current is commonly twice the long-term maximum. The short-term over-loading capability is important for power system stability. Due to over-heating of excitation circuit the excitation current must be limited after few seconds. The heating coefficients of stator circuit are much larger than those of excitation circuit, why the stator current limiter is not necessary and may be done manually. The over-loading capability of generator may be improved by making the cooling of generator more effective.

Figure 2.4 illustrates the action of automatic voltage controller and current limiters and corresponds to PQ-diagram of Figure 2.3. The terminal voltage is 1.04 pu under voltage control. As the reactive power output increases, hits the generator the excitation current limit, which is dependent on generator output power. The maximum reactive power output under voltage control is 0.67, 0.63 and 0.58 pu when output power is 0.5, 0.75 and 0.9 pu respectively. If the reactive power output further increases, the generator loses controllability of voltage, when the operation point follows the curve of excitation current

limit to the left and the output of reactive power slightly increases but the voltage decreases. The stator current limits are reached at the reactive power outputs of 0.83, 0.70 and 0.60 pu when output power is 0.5, 0.75 and 0.9 pu respectively. The action of stator current limiters is dramatic. The stator current limiter decreases the reactive power capability to avoid stator over-heating, which causes fast decrement in voltage. When the generator output power is increased, the action of stator current limiter becomes more likely because the excitation and the stator current limits move closer to each other.

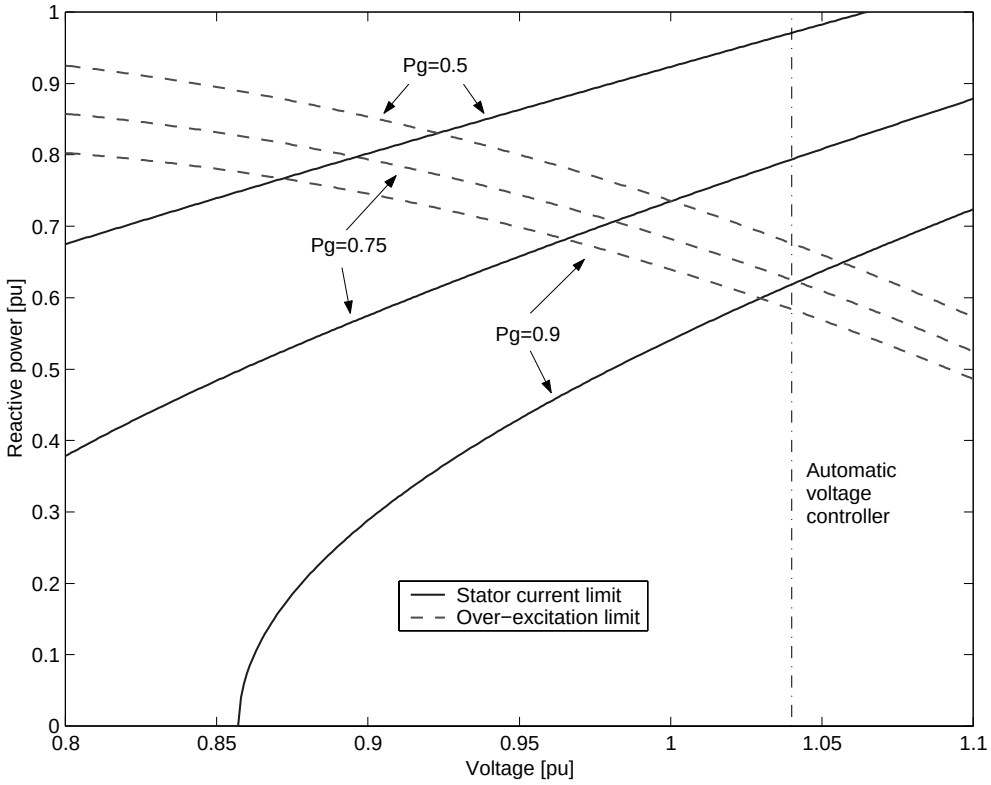

Figure 2.4. QU-diagram (X_d=0.45 pu, I_{smax}=1.05 pu, E_{max}=1.35 pu).

Loads

The modelling of loads is essential in voltage stability analysis. The voltage dependence and dynamics of loads requires consideration in these studies. Power system loads are usually represented as connected to the high voltage bus bars. The modelling of voltage dependence of loads, however, requires proper consideration of voltage control devices. An alternative and more accurate model is the representation of voltage dependent loads at the secondary side of distribution system main transformer including possible tap changer control [Lin96]. The dynamics of loads in long-term voltage stability studies includes the operation of on-load tap changers, operation of compensation, thermostatic loads, protection systems that operate due to low voltage or over-current, and extinction of discharge lamps below a certain voltage and their restart when the voltage recovers [Cut98]. Dynamic models for electrical motors are needed when the power system studied includes a significant amount of motor load.

The voltage dependence of loads is usually modelled with an exponent or a polynomial model. The value of the exponent describes the voltage dependence of the load. Integer values of exponents zero, one and two correspond to constant power, current and impedance loads respectively. The exponent load model is presented in Equation 2.4, where P is active load, Q is reactive load, subscript $_0$ corresponds to nominal values, V is load voltage, α is exponent of active load and β is exponent of reactive load [Cut98]. The typical values for the exponents for different load components are presented in Table 2.2.

$$P = P_0\left(\frac{V}{V_0}\right)^{\alpha},\ Q = Q_0\left(\frac{V}{V_0}\right)^{\beta} \tag{2.4}$$

Table 2.2. Typical values for exponents of load model [Haj98, Tay94].

Load type	α	β
Electrical heating	2.0	- (Q=0)
Television	2.0	5.2
Refrigerator/freezer	0.8-2.11	1.89-2.5
Fluorescent lighting	0.95-2.07	0.31-3.21
Frequency drives	1.47-2.12	1.34-1.98
Small industrial motors	0.1	0.6
Large industrial motors	0.05	0.5

The polynomial load model (also referred to as a ZIP model) is presented in Equation 2.5 [Cut98]. The model sums up the voltage dependent components of integer exponent load models. The parameters of polynomial load models are Z_p, I_p and P_p for active power and Z_q, I_q and Q_q for reactive power, which describe the share of components of the total load. The measured values of parameters Z_p, I_p and P_p, and Z_q, I_q and Q_q for a refrigerator, fluorescent lighting and frequency drives are presented in Table 2.3.

$$P = P_0\left[Z_p\left(\frac{V}{V_0}\right)^2 + I_p\left(\frac{V}{V_0}\right) + P_p\right],\ Q = Q_0\left[Z_q\left(\frac{V}{V_0}\right)^2 + I_q\left(\frac{V}{V_0}\right) + Q_q\right] \tag{2.5}$$

Table 2.3. Measured values of parameters of polynomial load model [Haj98].

Parameter	*Refrigerator/freezer*	*Fluorescent lighting*			*Frequency drives*	
		Device 1	*Device 2*	*Device 3*	*Device 1*	*Device 2*
Z_p	1.19	0.14	0.16	0.34	0.43	3.19
I_p	-0.26	0.77	0.79	1.31	0.61	-3.84
P_p	0.07	0.09	0.05	-0.65	-0.05	1.65
Z_q	0.59	-0.06	0.18	3.03	-1.21	1.09
I_q	0.65	-0.34	-0.83	-2.89	3.47	-0.18
Q_q	-0.24	-0.60	-0.35	0.86	-1.26	0.09

The organisation of comprehensive measurements for the determination of load parameters in the whole power system is a time-consuming task. It requires measuring of load and voltage at each substation separately covering long and various periods. The measurements should include all seasons, weather conditions, days of the week, times of day, special cases like holidays, etc. [Kun94]. This method is used for the verification of load models and determination of load parameters at special substations. In practice the voltage dependence of loads is estimated with a component-based approach [Kun94] which builds up the load model from equipment fed from the substation. The load is first categorised into load classes: industrial, commercial, residential, agricultural, etc. The problem in this approach is the variation of values or properties of load component depending for example on the location of the load. This problem can be avoided if loads are categorised into classes which are typical equipment like large motors, small motors, constant power loads, discharge lamps, thermostatic loads, compensation and distribution system voltage control. The problem in this categorisation is the difficulty to estimate the amount of load in each class. The advantage of the former method is the exact knowledge of equipment voltage dependence.

The properties of the exponent load model are presented in Figure 2.5 for the test system of Figure 2.1 ($\tan\phi$=0). The maximum loading and voltage collapse point of constant power load (α=0) is 800 MW, which corresponds to the PV-curve nose. When α=0.7 (Figure 2.5a), the maximum loading point occurs when the nominal load is about 1000 MW. The voltage collapse point is at 650 MW, when the nominal load is about 1100 MW. The nominal load corresponding the maximum loading point is about 1300 MW, when α=1.3 at Figure 2.5b.

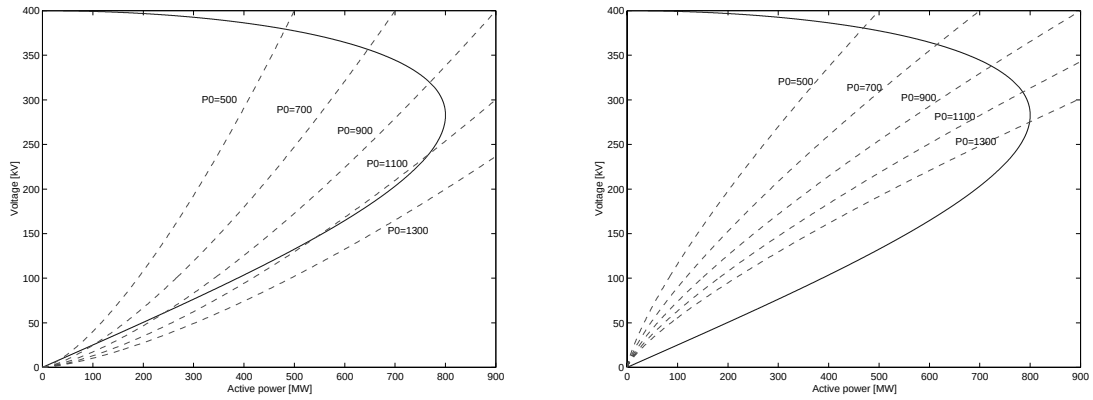

(a) (b)

Figure 2.5. Exponent load model: (a) α=0.7, (b) α=1.3.

Figure 2.6 describes the properties of the polynomial load model for the test system. The voltage dependence of Figure 2.6a load is about the same as the load of Figure 2.5b. The total load consists mainly of constant impedance and current loads. Figure 2.6b shows an extreme case where the total load is unrealistic at the low voltages. The model is not

appropriate for low voltages, because the shape of the second order polynomial is a parabola.

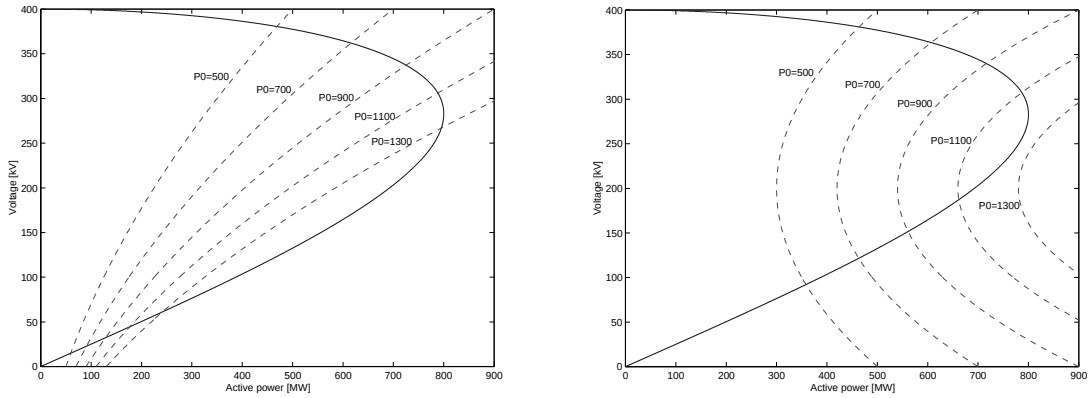

(a) (b)

Figure 2.6. Polynomial load model: (a) Z_p=0.4, I_p=0.5, P_p=0.1, (b) Z_p=1.6, I_p=-1.6, P_p=1.

On-load tap changer

The automatic voltage control of power transformers is arranged with on-load tap changers. The action of tap changer affects the voltage dependence of load seen from the transmission network [Tay94, Cut98]. Typically a transformer equipped with an on-load tap changer feeds the distribution network and maintains constant secondary voltage. When voltage decreases in the distribution system, the load also decreases. The tap changer operates after time delay if voltage error is large enough restoring the load.

The action of an on-load tap changer might be dangerous for a power system under disturbance. The stepping down of the tap changer increases the voltage in a distribution network; thus reactive power transfer increases from the transmission network to the distribution network. Figure 2.7 illustrate the action of tap changer caused by a disturbance seen from the transmission network. The power system operates at point A in the pre-disturbance state. Due to the disturbance the operation point moves to point B, which is caused by decrement of secondary voltage and load dependence of voltage. The load curve represents the state of power system just after the disturbance. After a time delay the tap changer steps down to increase secondary voltage. The operation point seen from the transmission network moves along the post-disturbance PV-curve towards a maximum loading point, which causes decrement of the primary voltage. The tap changer operates until the secondary voltage reaches the nominal voltage at point D. The amount of load at points A and D is equal due to action of tap changer. The operation point D is stable, but quite close the post-disturbance maximum loading point.

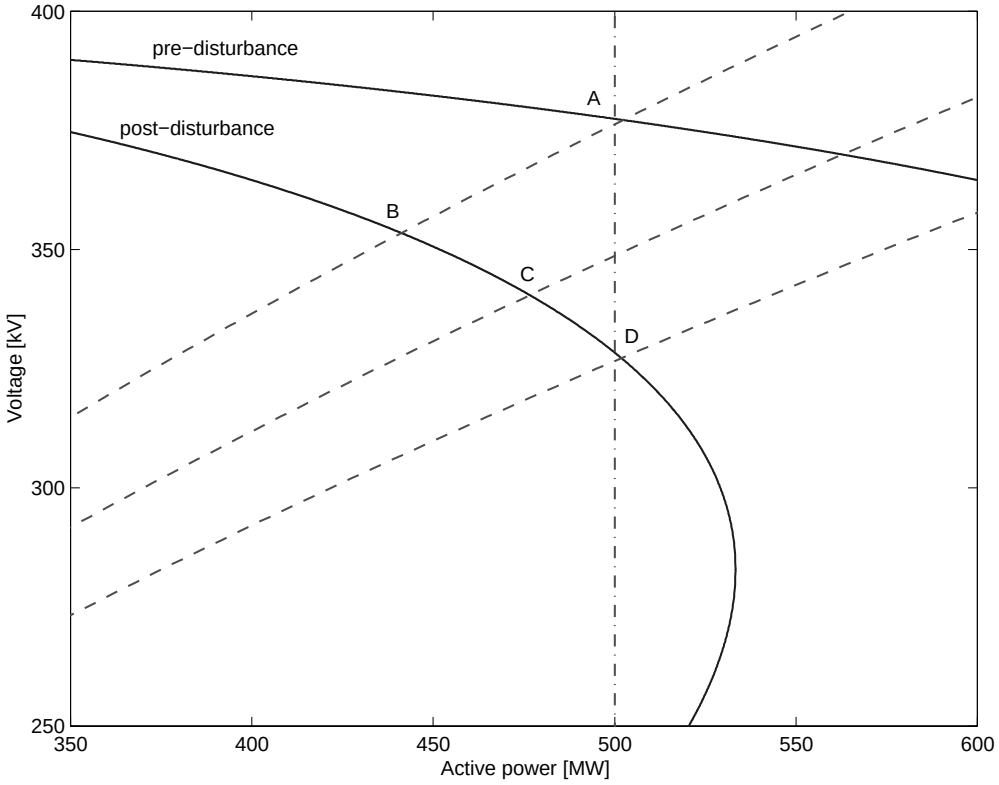

Figure 2.7. The action of on-load tap changer caused by a disturbance.

The voltage dependence of the loads can be seen when the on-load tap changer reaches the tap changer minimum limit, in which case on-load tap changer is not capable of maintaining constant secondary voltage. The step size of the on-load tap changer should also be taken into account in load-flow based long-term voltage stability studies.

The restoration of load may occur although distribution network voltage is not increased to nominal or pre-disturbance value. A thermostat typically controls heating and cooling loads. The energy consumed in the thermostatic loads is constant in the long run. Although heating loads are resistive, the thermostats increase the amount of load if the decrement of load voltage is long enough. The time constants of thermostatic loads are high, which makes this phenomenon slow. The thermostatic load is modelled as constant impedance load with a long time constant [Cut98]. A long interruption or voltage decrement might also cause a phenomenon called cold load pick-up, where the load becomes higher than nominal value due to manual connection of additional load to compensate decreased power supply.

Compensation devices

The aim of reactive power compensation is to improve the performance of power system operation. The compensation is needed to control the reactive power balance of the power system. It is also used for minimising reactive power losses and keeping a flat voltage

profile in the network. The sources of reactive power are located as close to the sinks of reactive power as possible. The transfer of reactive power increases line currents and thus active and reactive power losses. The equipment used for compensation is capacitors, reactors, synchronous generators/compensators and static var compensators.

The reactive power compensation devices should be modelled at the appropriate voltage level including their control logic to ensure the true effect of these devices. Switched shunt compensation is used instead of fixed shunts to take into account the voltage control in the network. The static var compensators can be modelled as a generator when the reactive power demand is within limits, as a capacitor when the reactive power demand is higher than the maximum limit and as a reactor when the reactive power demand is lower than the maximum limit.

2.3 Scenario of classic voltage collapse

Voltage instability may result from at least two scenarios [Cut98]. In the first scenario an increase in demand causes voltage instability. This is seldom the case in the real world. The stability is lost in voltage collapse when the change causes the stable operation point to disappear, due to bifurcation as described above. Initially the fall of voltages is slow, punctuated by fast decline. The dynamic fall of voltages is called voltage collapse, which may include both the transient and the long-term aspects of voltage instability. In practice, the second scenario, which corresponds to a large disturbance, is more important. The large disturbance causes the network characteristics to shrink dramatically. The characteristics of the network and load do not intersect at the instability point. A load increase beyond the voltage collapse point results in loss of equilibrium, and the power system can no longer operate. This will typically lead to cascading outages.

There are different kinds of scenarios of voltage collapse. However, the classic or typical voltage collapse, caused by the long-term voltage instability, is characterised as follows [Kun94, Tay94]:

1. Some EHV transmission lines are heavily loaded, the available generation capacity of the critical area is temporarily reduced e.g. due to maintenance of unit or to market conditions, and reactive power reserves are at the minimum or are located far from the critical area.
2. Due to a fault or any other reason a heavily loaded line is lost. The loading and reactive power losses of remaining lines increase. The total reactive power demand increases due to these reasons.
3. The load voltage decreases, which in turn decreases the load demand and the loading of EHV transmission lines. The voltage control of the system, however, quickly restores generator terminal voltages by increasing excitation. The additional reactive power flow at the transformers and transmission lines causes additional voltage drop at these components.

4. After a few minutes (depending on the time delays of on-load tap changers) the on-load tap changers of distribution substation transformers restore the distribution network voltages. The increased voltage also increases the load demand. The EHV transmission line losses increase, which causes greater voltage drop at these lines.
5. The increased reactive power demand increases the reactive output of the generators. When the generator hits the reactive power limit, its terminal voltage decreases. Its share of reactive power demand is shifted to another generator further away from the critical area. This will lead to cascading overloading of generators. Fewer generators are available for voltage control and they are located far from the critical area. The decreased voltage at the transmission system reduces the effectiveness of shunt capacitors. The system becomes prone to voltage instability, which may lead to voltage collapse.

Voltage instability has become a major concern in many power systems, because systems are operated more often in heavily stressed situations and systems have become more complicated to manage. Historically power system stability has been considered to be based on synchronous operation of the system. However, many power system blackouts all over the world have been reported where the reason for the blackout has been voltage instability. The following list includes some of them:

- France 1978 [Tay94]: The load increment was 1600 MW higher than the one at previous day between 7 am and 8 am. Voltages on the eastern 400 kV transmission network were between 342 and 374 kV at 8.20 am. Low voltage reduced some thermal production and caused an overload relay tripping (an alarm that the line would trip with 20 minutes time delay) on major 400 kV line at 8.26 am. During restoration process another collapse occurred. Load interruption was 29 GW and 100 GWh. The restoration was finished at 12.30 am.
- Belgium 1982 [Tay94]: A total collapse occurred in about four minutes due to the disconnection of a 700 MW unit during commissioning test.
- Southern Sweden 1983 [Löf95a]: The loss of a 400/220 kV substation due to a fault caused cascading line outages and tripping of nuclear power units by over-current protection, which led to the isolation of southern Sweden and total blackout in about one minute.
- Florida USA 1985 [Tay94]: A brush fire caused the tripping of three 500 kV lines and resulted in voltage collapse in a few seconds.
- Western France 1987 [Tay94]: Voltages decayed due to the tripping of four thermal units which resulted in the tripping of nine other thermal units and defect of eight unit over-excitation protection, thus voltages stabilised at a very low level (0.5-0.8 pu). After about six minutes of voltage collapse load shedding recovered the voltage.
- Southern Finland August 1992 [Hir94]: The power system was operated close to security limits. The import from Sweden was large, thus there were only three units directly connected to a 400 kV network in southern Finland. The tripping of a 735 MW generator unit, simultaneous maintenance work on 400 kV line and manual decrease of

reactive power in another remaining generator unit caused a disturbance where the lowest voltage at a 400 kV network was 344 kV. The voltages were restored to normal level about in 30 minutes by starting gas turbines, by some load shedding and by increasing reactive power production.

- WSCC USA July 2 1996 [Tay97]: A short-circuit on a 345 kV line started a chain of events leading to a break-up of the western North American power system. The final reason for the break-up was rapid overload/voltage collapse/angular instability.

3 VOLTAGE STABILITY ASSESSMENT

The power system should be operationally secure, i.e. with minimal probability of blackout or equipment damage. An important part of power system security is the system's ability to withstand the effects of contingencies. A contingency is considered to be an outage of a generator, transformer or line, and their effect is monitored with specified security limits. The objective of power system operation is to keep the power flows and bus voltages within acceptable limits despite changes in load or available resources. From this perspective, security may be defined as the probability of a power system's operating point remaining in a viable state space.

Security assessment is a combination of system monitoring and contingency analysis. It is extremely uneconomical, if not impossible, to build a power system with so much redundancy that failures never cause an interruption of load on a system. Security assessment is analysis performed to determine whether, and to what extent, a power system is reasonably safe from serious interference to its operation. Thus it involves the estimation of the relative robustness of the system in its present state or in near-term future state. Direct security assessment requires calculating the probability that the power system state will move from the normal operation state to the emergency state. Indirect security assessment can be formulated by defining a set of system security variables that should be maintained with predefined limits.

This chapter is divided into three parts. The first part is a state-of-the-art description of power system security analysis, giving a view of a classification of power system states commonly used planning and operating criteria and security assessment tools. The second part deals with the definition of transfer capacity, computation of voltage stability margin, voltage collapse point, and maximum loading point. The proposed contingency ranking methods for voltage stability studies, which are a part of security assessment, are described in the third part.

3.1 Power system security analysis

3.1.1 Analysis and control of operating states

The states of power system are classified into five states: normal, alert, emergency, extreme emergency and restorative [Kun94]. The classification of states is used in the analysis and planning of power system. Figure 3.1 describes these states and the ways in which transition can occur from one state to another.

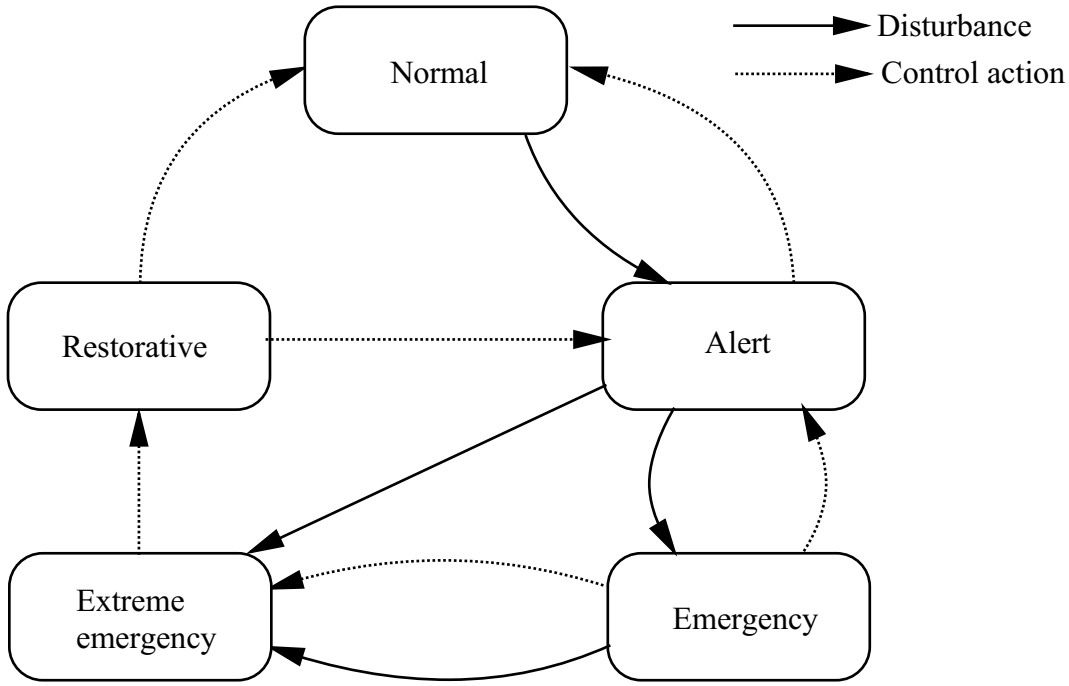

Figure 3.1. Power system operating states.

The operation of a power system is in a normal state most of the time. Voltages and frequency of the system are within the normal range and no equipment is overloaded in this state. The system can also maintain stability during disturbances considered in the power system planning. The security of the power system is described by thermal, voltage and stability limits. The system can also withstand any single contingency without violating any of the limits.

The alert state is similar to the normal state except that the above conditions cannot be met in the case of disturbance. The system transits into the alert state if the security level falls below a certain limit or if the possibility of a disturbance increases e.g. because of weather conditions. All system variables are within the normal range and all constraints are satisfied in the alert operation point. However, the system has been weakened to a level where a contingency may cause a breaking of security limits. This will lead to a transition into an emergency state or in the case of severe disturbance into an extreme emergency state. Control actions, such as generation rescheduling, increased reserve, voltage control, etc., can be used to restore the system back to normal state [Kun94]. If this does not succeed, the system stays in the alert state.

The system transits into the emergency state if a disturbance occurs when the system is in the alert state. Many system variables are out of normal range or equipment loading exceeds short-term ratings in this state. The system is still complete. Emergency control actions more powerful than control actions related to alert state can restore the system to alert state. The emergency control actions include fault clearing, excitation control, fast

valving, generation tripping, generation run-back, HVDC modulation, load curtailment, blocking of on-load tap changer of distribution system transformers and rescheduling of line flows at critical lines [Kun94].

The extreme emergency state is a result of the occurrence of an extreme disturbance or action of incorrect or ineffective emergency control actions. The system is in a state where cascading outages and shutdown of a major part of power system might happen. The system is in an unstable or close to an unstable state. The control actions needed in this state must be really powerful. Usually load shedding of most unimportant loads and separation of system into small independent parts are required in order to transit the system into a restorative state [Kun94]. This is only a possibility, because many production units are shut down due to too high or low frequency or any other reason. The aim of the actions is to save as much of the system as possible from a widespread blackout. If these actions do not succeed, the result is total blackout of the system.

The restorative state is a transition state between the extreme emergency and normal or alert states. It is important to restore the power system as fast and securely as possible in order to limit the social and economic consequences for the population and economy. The restoration time depends on the size of interrupted area, the type of production in the system, the amount of blackstart capability in the system and the possibility to receive assistance from interconnecting systems [Agn96]. The restoration process includes reconnection of all generators, transmission lines, loads, etc. Two major strategies for power system restoration following a blackout are the build-up and the build-down strategy [Agn96]. The build-up strategy is the most commonly used strategy. The system is divided into subsystems where each subsystem should have the capability to blackstart and control voltage and frequency. After the synchronisation of production units loads are gradually connected. The connections to other subsystems are then synchronised.

Power system controls assist the operator in returning the system to a normal state after a disturbance. If the disturbance is small, this may be enough. Operator actions are required for a return to the normal state when the disturbance is large. The control system is highly distributed, which increases the reliability of control. Power system controls are organised as a hierarchical structure, such as

- direct control of individual components (excitation systems, prime movers, boilers, transformer tap changers, HVDC converters, static var compensators, automatically switched shunt compensation)
- an overall power or transmission plant control that co-ordinate the closely linked components
- a system control, which co-ordinates plant controls
- a pool-level master control, which co-ordinates system controls, and imports and exports of power flows.

3.1.2 Planning and operating criteria

Power systems are planned and operated so that the most probable and critical contingencies can be sustained without an interruption or a quality reduction. The power system should be able to continue its operation despite sudden outage of a production unit, transmission line, transformer, compensation device, etc. Outages of power system equipment are typically due to faults (short circuits and earth faults), overloads, malfunctions (false settings or operation actions) or breakdown of equipment. The occurrence of disturbances cannot be predicted, thus the security of the power system needs to be guaranteed beforehand.

The security of the power system is commonly defined based on *(n-1)*-criteria i.e. the system should withstand any single contingency. A system consisting of *n* components should be able to operate with any combination of *n-1* components, thus for any single component outage. This criterion plays an essential role in preventing major disturbances following severe contingencies. The use of criteria ensures that the system will, at worst, transit from the normal state to the alert state. The probability of *(n-2)* contingency increases e.g. when the weather is bad and two transmission circuits are placed on the same towers or when a generator may be relayed out due to a line outage.

The planning of a power system to ensure secure operation at minimum cost is a very complex problem with a potential for enormous financial gains in the solution. The security analysis is required to guarantee the power system's secure operation in all conditions and at all operation points. The purpose of power system planning is to ensure power system adequacy. The analysis is based on forecast cases. The on-line security assessment is needed in the power system operation to guarantee security momentarily, because not all possible future scenarios can be checked beforehand. The purpose of power system operation is to guarantee that a single disturbance cannot cause cascading outages and finally a total blackout.

3.1.3 Security assessment tools

The information to assess power system security is got from the Supervisory Control and Data Acquisition (SCADA) system [Woo96]. It provides the data needed to monitor the system state. Telemetry systems measure and transmit the data. The data consists of voltages, currents, power flows, the status of circuit breakers and switches, generator outputs and transformer tap positions in every substation in a transmission network. The state estimation is used in such a system to combine the raw measurement data with the power system model to produce the best estimate (in a statistical sense) of the power system state [Woo96]. Computers gather the data, process them, and store them in a database where operators can display and analyse them. The computer checks the incoming data against the security limits and notifies the operator in the case of overload or out-of-limit voltage.

The transmission network is controlled and optimised via a power management system. This term is used to refer only to the management of the transmission system as opposed to a energy management system which is applied to composite generation and transmission system. The energy management system also includes the control and optimisation of power production. The power management system gets information from the SCADA system. It includes tools for operation point analysis (load-flow and dynamic simulation programs), contingency analysis (contingency screening and ranking), security assessment and security enhancement (optimal power flow program e.g. to minimise network losses).

Schematic diagram of security assessment

The following description is based on off-line security assessment procedure found through security assessment software (see Figure 3.2). The same procedure can be used in the on-line security assessment, if the execution time is fast enough. The fundamental difference between off-line and on-line security assessment is the difference in input data. On-line security assessment analyses the current operation point given through the SCADA and the power management system, while off-line security assessment ensures the security of a future operation point. It is based on near future planning data, which must be predicted. The future operation points consider network topology, generation dispatch, unit commitment, load level, and power transactions. The uncertainty of these factors causes the need for numerous security assessment studies. As these possible variations increase, the number of operation points which must be studied becomes unmanageable, even in short-term planning cases. In on-line security assessment the variations of network topology, unit commitment and load level need not to be considered. The number of possible variations to be studied becomes manageable and the stability limits obtained on-line are expected to be more accurate. However, the execution time of security assessment is much less in on-line than in off-line mode.

Figure 3.2 is a schematic diagram of security assessment and determination of security limits. The main features of the security assessment are contingency selection, security analysis using either load-flow or time domain simulation, and determination of security limit. Contingency selection helps to identify the critical contingencies for the detailed security analysis. The analysis of all contingencies is too time-consuming and is not necessary in practice. Security analysis uses a short contingency list to check the security of the power system. The short contingency list includes those contingencies which are most probably critical. The traditional approach to planning for voltage security relied on ensuring that pre-contingency and post-contingency voltage levels were acceptable. This criterion is based on equipment tolerances and it ensures safe voltages. However, a system may have healthy pre-contingency and post-contingency voltage levels, but be dangerously close to voltage instability. That is why the security analysis should also provide an index to assure that sufficient voltage stability margin exists.

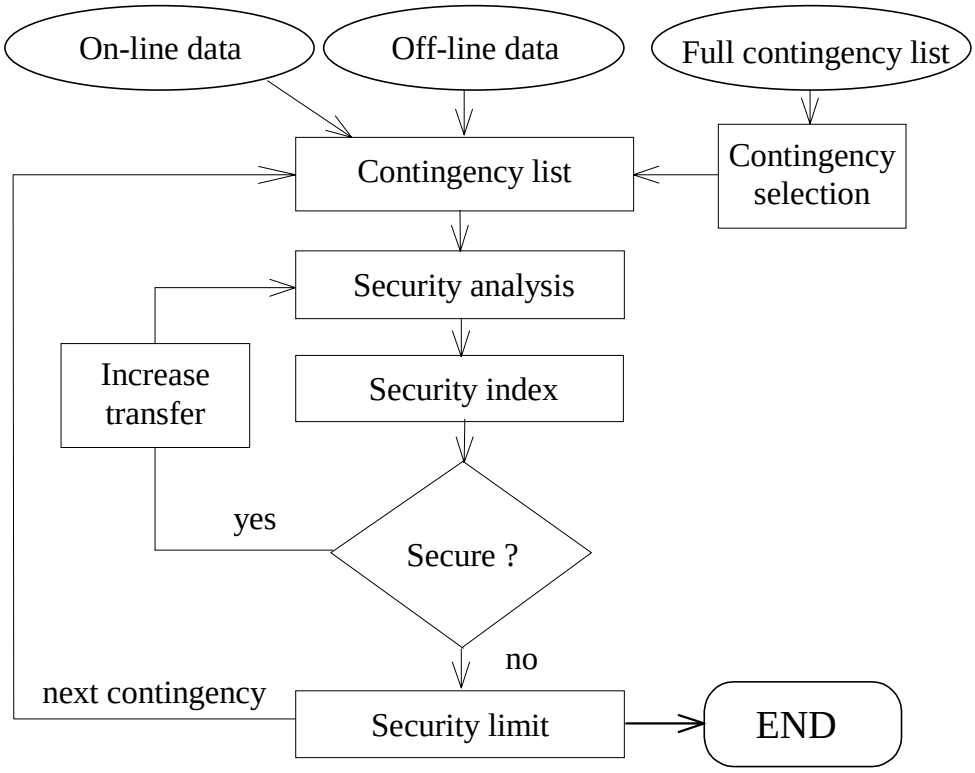

Figure 3.2. Schematic diagram of security assessment and determination of security limits.

The security analysis is done using load-flow in the long-term studies [Vol00b, Aus95] and time-domain or fast time-domain simulation in the dynamic studies [Cut97, Tra00, Eje98a]. The fast time-domain simulation is based on quasi steady-state simulation, which is a compromise between the efficiency of load-flow methods and the accuracy of time-domain simulation. The algorithms must include detailed modelling capabilities and specific requirements, like variable step size integration, early termination, etc., to speed up the security analysis. The security of the system is indicated by a security index, e.g. voltage decline, reactive reserves, thermal overloads or voltage stability margin. The stress on the system can be increased if the system is secure. In this way the security limit, the last point where the system is still secure, is finally found. The procedure described above is not commonly applied for on-line security assessment nowadays, because the computation of security analysis has been too slow.

The security assessment should be done on-line to get a real picture of the power system state. In practice, the security assessment is done every 5-10 minutes, because changes of operation point are normally small and slow, and long-term security analysis of practical size power system takes several minutes, e.g. 12 minutes according to reference [Aus95]. The estimate is based on a computation time (PC 486, 66 MHz) of long-term security limits (about 10 load-flows per PV-curve) for 14 contingencies of a 4000-bus test system. Reference [Hir99] mentions that the dynamic security analysis of 30-40 contingency cases can be done in 20 minutes using parallel processing to determine the transfer limits of a critical interface.

Security boundary method for on-line security assessment

In the absence of on-line analysis capability, the off-line study results must be translated into operating limits and indices that can be monitored by the operators. The on-line security assessment is usually based on off-line computed security limits, e.g. transfer limits at tie-lines. The security limits are stored in a database and monitored on-line by matching the actual power system condition to the nearest matching condition in the database. These security limits are commonly presented to the operator by a security boundary.

The security boundary is a nomogram[3] drawn between off-line computed security limits at the operation space of interesting parameters [Wun95]. The interesting parameters are usually power flows at the critical intersections (e.g. intersections from Sweden to Finland and from northern Finland to southern Finland in the Finnish system, see Chapter 6.2) and bus voltages in weak areas. In this way the security of power system can be monitored in a simple way. Secure operation is very probably guaranteed when the operation point is inside the security boundary. The number of interesting parameters is only two to three due to security boundary presentation problems. Figure 3.3 illustrates a security boundary nomogram for three parameters. The third parameter determines which security boundary should be used in the on-line security assessment.

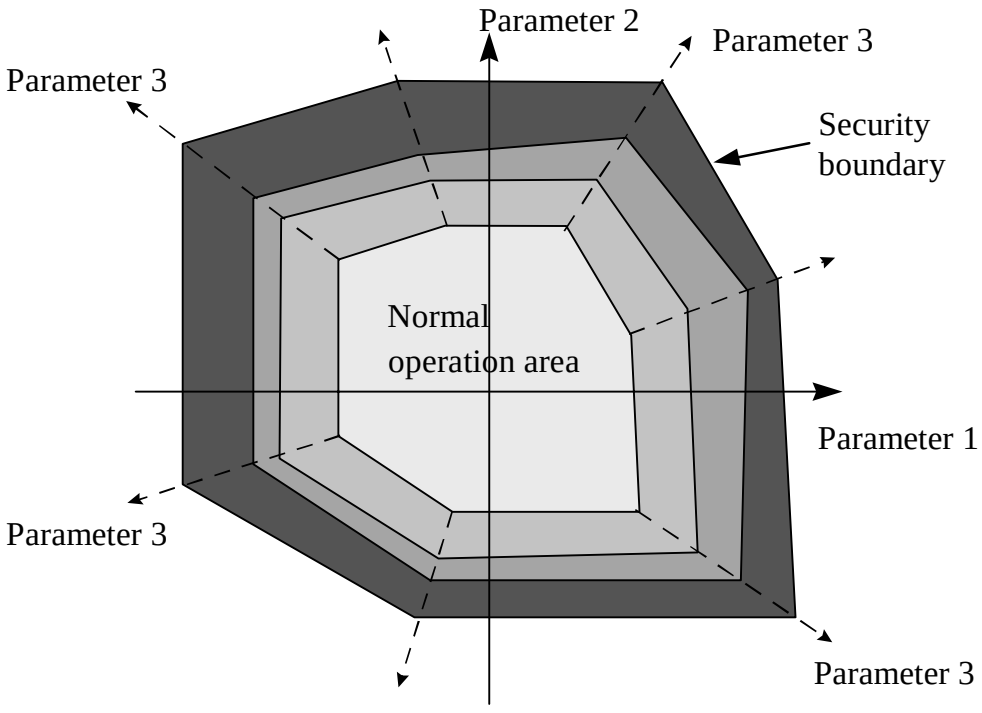

Figure 3.3. Security boundary nomogram.

[3] Nomogram = diagram giving the value of a quantity from those of others when a straight line is drawn between points [Fow86]

Although the use of the security boundary method in the power system security assessment has provided major advantages especially in on-line applications, it has some drawbacks. The accuracy of security assessment in this way is not very good: The security limits tend to be conservative for normal conditions and may be inaccurate for unusual power system conditions. The maximum power flows and the minimum voltages cannot determine power system security explicitly in all possible network topology, loading and production situations, thus the security assessment is usually done for normal conditions and separate security limits are computed for maintenance periods. The accuracy of on-line security assessment is based on

- off-line computed security limits
- coverage of operation points in the operation space
- possibility to approximate power system security with monitored parameters.

3.2 Computation of voltage stability limits

The computation of security limits in the case of voltage stability is described in this chapter, preceded by some definitions of transfer capacity and voltage stability margin. A system with large transfer capacity is generally more robust and flexible than a system with limited ability to accommodate power transfers. The transfer capacity is an indicator of power system security.

3.2.1 Definition of available transfer capacity

The European Transmission System Operators' Association has agreed on a definition of transfer capacity for international electricity exchange [Eur01]. The definition of transfer capacity is important in cases of congestion management and allocation of transfer capacity for market participants. Transmission system operators calculate the transfer capacity, the maximum power that can be transmitted between the systems in both directions. The definition of transfer capacity is distinguished in four terms (see Figure 3.4):

- Total transfer capacity is set by physical limits of transmission systems. The security rules of transmission systems are taken into account in this capacity definition. The capacity limit is set by thermal, voltage and stability limits. The total transfer capacity represents the maximum feasible transfer between the systems, when considering security limits.
- Transmission reliability margin takes into account forecast uncertainties of power exchange. It is necessary to preserve a portion of the transfer capacity in order to ensure that the system remains secure under a wide range of varying conditions. The uncertainty is due to imperfect information from market actors (traders and generation companies) and unexpected events. The further into the future the determination of transfer capacity is made, the greater is the degree of uncertainty in the assumed conditions and, hence, in the transfer capacity. Unexpected events, uncertain

information and uncertainty about power system parameters can be considered as probabilistic events. Transmission system operators according to past experience or statistical methods do the calculation of transmission reliability margin.

- Net transfer capacity is the total transfer capacity minus the transmission reliability margin. It is the maximum transfer capacity that can actually be used and takes into account uncertainties in future power system conditions.
- Available transfer capacity is the net transfer capacity minus notified transmission flow. The notified transmission flow is the transfer capacity already reserved by the contracts already accepted. In principle, a new contract of power exchange requires updating of net transfer capacity and decreases the uncertainty about future conditions. The available transfer capacity is the remaining transfer capacity after the prior allocations of contracted power exchanges. An example of transfer capacities is illustrated in Figure 3.4.

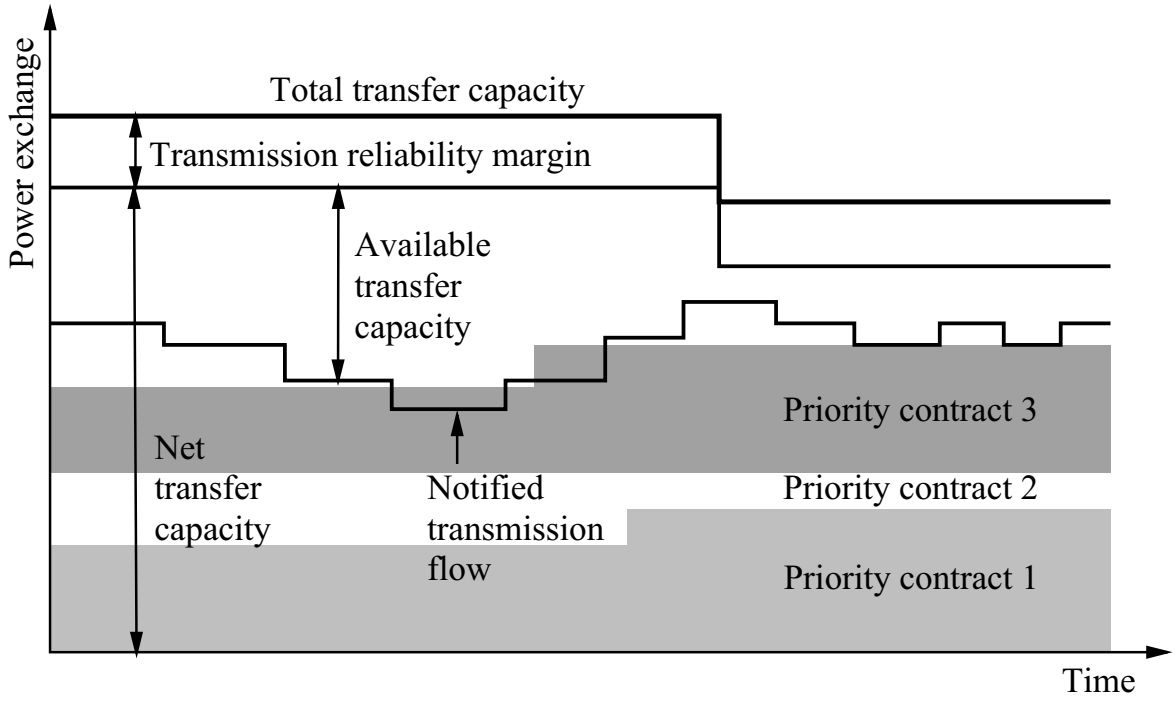

Figure 3.4. Example of transfer capacities.

The definitions of transfer capacities are explained using a simple two-system model which can be used in the “corners or peripheries” of an interconnected system, where the number of interconnections to the adjacent systems is small. The calculation of transfer capacity is much more complex in the case of highly interconnected and meshed systems. The calculation of total transfer capacity is based on modelling and simulation of the effect of power transfer between the systems. The simulation is started from the anticipated power system operation point. The total transfer capacity is calculated by shifting generated power in order to cause additional power exchange between the systems. The power generation is increased at the export area and decreased at the import area. The load of both systems remains unchanged and the shift of generation is stopped when security rules

are not fulfilled in the systems. The total transfer capacity should be calculated in both directions. It is important to note that the calculation of total transfer capacity is based on an assumption of a future generation dispatch scenario, load level and network topology. In order to handle these uncertainties, many total transfer capacities with different scenarios should be calculated.

The available and the net transfer capacity are the values which are usually published for market participants. In the Nordic countries the net transfer capacity values are published to market participants on the Internet for planning purposes on a half-yearly basis or in a week-ahead time frame [Eur01]. In a day-ahead time frame the net or the available transfer capacities are calculated taking outages into account, which is why the total and the net transfer capacities can make discrete steps in the time frame (see Figure 3.4). These values are firm values for the electricity trade. After the electricity trade, the transmission system operators guarantee transactions and manage physical flows by the aid of counter-trading if necessary. The aim of counter-trading is to provide a tool for short-term congestion management [Eur01].

3.2.2 Voltage stability margin

The voltage stability margin is a measure to estimate power system available transfer capacity, net transfer capacity or total transfer capacity. The voltage stability margin is a difference or a ratio between operation and voltage collapse points according to a key parameter (loading, line flow etc.). The voltage collapse point must be assessed in order to guarantee secure operation at the normal operation point and after disturbances. The security of the power system is determined by the most critical post-disturbance margin [Gao96, Cut99]. Figure 3.5 illustrates voltage stability margins in the case of constant power load. The computation of voltage stability margin is time-consuming because many contingencies and post-disturbance margins should be studied. The pre-disturbance margin describes the loadability of a power system and is not interesting from the security point of view.

Basically the computation of the voltage stability margin should be done for all contingencies. This is a time-consuming process and is not necessary in practice. Thereby the most critical voltage stability margin is determined based on a short contingency list as in the general security assessment procedure. If the use of a short contingency list is not fast enough in the on-line voltage stability assessment, the computation of voltage stability margin also needs to be speeded up.

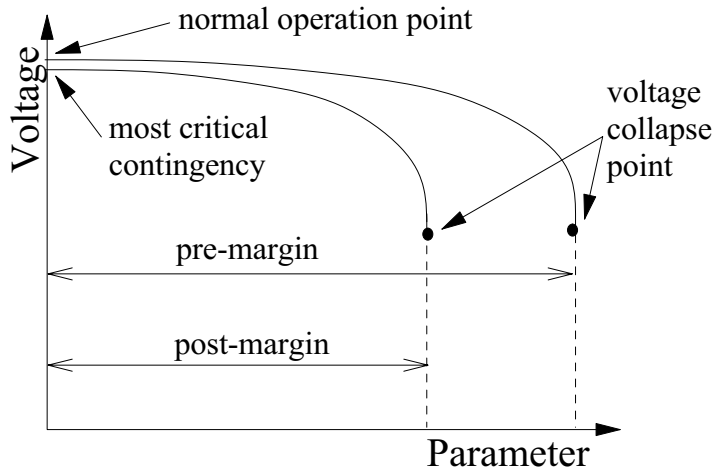

Figure 3.5. Voltage stability margins.

The voltage stability margin is a straightforward, widely accepted and easily understood index of voltage collapse. Other advantages of the voltage stability margin as a voltage collapse index are [Iee01]:

- The margin is not based on a particular power system model and can be used with static or dynamic models independent of the details of the power system dynamics.
- It is an accurate index that takes full account of the power system non-linearity and device limits as the loading is increased.
- Sensitivity analysis may be applied easily and quickly to study the affects of power system parameters and controls [Gre99].
- The margin accounts for the pattern of load increase (computation direction).

3.2.3 Computation of voltage collapse point

Many good voltage stability indices and methods have been created for practical power systems. The most common methods to estimate the proximity of voltage collapse point are minimum singular value [Löf95a], point of collapse method [Cañ92, Cañ93], optimisation method [Oba88, Cut91] and continuation load-flow [Ajj92, Cañ93, Chi95]. These are briefly described and discussed next. Other voltage stability indices are also proposed in the literature like sensitivity analysis [Fla93], second order performance index [Ber98], the energy function method [Ove93], modal analysis [Gao92] and many others which can be found in references [Iee01, Ajj98].

Minimum singular value method

The minimum singular value of load-flow Jacobian matrix has been proposed as an index for quantifying proximity to the voltage collapse point [Löf95a]. It is an indicator available from normal load-flow calculations. The computation of minimum singular value can be done fast with a special algorithm [Löf95a]. The method is based on the analysis of linear system $\mathbf{A}\underline{x}=\underline{b}$. The singular value decomposition of the matrix $\mathbf{A}$ is given in Equation 3.1 [Gol96], where $\mathbf{A}\in \mathrm{R}^{m\times m}$, $\mathbf{U}$ and $\mathbf{V}$ are $m\times m$ orthonormal matrices, the left and right

singular vectors $\underline{u}_i$ and $\underline{v}_i$ are the columns of matrices **U** and **V** respectively, **Σ** is a diagonal matrix (**Σ**=diag{σ_i}), and σ_i is singular value.

$$\mathbf{A} = \mathbf{U}\Sigma\mathbf{V}^T = \sum_{i=1}^{m} \sigma_i \underline{u}_i \underline{v}_i^T \tag{3.1}$$

The singular value decomposition is applied to linearised load-flow equations to analyse power system voltage stability. The analysis studies the influence of a small change in the active and reactive power injections $[\Delta\underline{P}\ \Delta\underline{Q}]^T$ to the change of angle and voltage $[\Delta\underline{\delta}\ \Delta\underline{V}]^T$. The solution of linearised load-flow equations using the singular value decomposition is given in Equation 3.2, where **J** is the load-flow Jacobian matrix.

$$\begin{bmatrix} \Delta\underline{\delta} \\ \Delta\underline{V} \end{bmatrix} = \mathbf{J}^{-1} \begin{bmatrix} \Delta\underline{P} \\ \Delta\underline{Q} \end{bmatrix} = \left(\mathbf{U}\Sigma\mathbf{V}^T\right)^{-1} \begin{bmatrix} \Delta\underline{P} \\ \Delta\underline{Q} \end{bmatrix} = \mathbf{V}\Sigma^{-1}\mathbf{U}^T \begin{bmatrix} \Delta\underline{P} \\ \Delta\underline{Q} \end{bmatrix} \tag{3.2}$$

The inverse of the minimum singular value, $(\min\{\sigma_i\})^{-1}$, will indicate the greatest change in the state variables. Small changes in either matrix **J** or vector $[\Delta\underline{P}\ \Delta\underline{Q}]^T$ may cause major changes in $[\Delta\underline{\delta}\ \Delta\underline{V}]^T$, if $\min\{\sigma_i\}$ is small enough. The minimum singular value is a measure of how close to singularity the load-flow Jacobian matrix is. If the minimum singular value of the load-flow Jacobian matrix is zero, then this matrix is singular i.e. the inverse of the Jacobian matrix does not exist. The operation point does not have a load-flow solution in that case, because the sensitivity of the load-flow solution to small disturbances is infinite. The load-flow Jacobian matrix singularity point is also called the saddle node bifurcation point. Singular vectors can provide information about a power system's critical areas and components. The right singular vector corresponding to the smallest singular value indicates sensitive voltages and angles, i.e. critical areas. The left singular vector corresponding to the smallest singular value indicates sensitive direction for the changes of active and reactive power injections.

It should be remembered that a Jacobian matrix is a linearisation at the operation point and the voltage stability problem is non-linear in nature. If the operation point is far away from the voltage collapse point, then the minimum singular value does not describe the state of the system accurately. The minimum singular value of a load-flow Jacobian matrix is also sensitive to the limitations of generator reactive power, transformer tap changer and compensation device. The minimum singular value method may be applied to a reduced Jacobian matrix in order to improve the profile of the index [Löf95a].

Point of collapse method

The point of collapse method is a direct method. It computes the voltage collapse point, the power demand and corresponding state variables directly without computing intermediate load-flow solutions. The method is based on the bifurcation theory and the singularity of the load-flow Jacobian matrix. In applying bifurcation theory to power systems, the power

demand is often used as the slowly changing parameter. A certain voltage collapse point is found in changes in parameters in a certain direction.

The voltage collapse point corresponds to the loss of equilibrium subject to smooth changes in parameters. The method is used to solve the singularity point of load-flow equations by formulating set of equations which includes load-flow equations and equations describing conditions of singularity [Cañ92]. Many types of bifurcations may occur, but the saddle node bifurcation is the most common in power systems. This occurs at the equilibrium $(\underline{x}^*, \mu^*)$, when the corresponding load-flow Jacobian matrix $\mathbf{J}_x$ is singular. Either Equation 3.3 or 3.4 can be solved to obtain the voltage collapse point, where $\underline{f}$ is the vector function of load-flow equations, $\underline{x}=[\underline{\delta}\ \underline{V}]^T$ is the state vector, μ is the power demand, $\underline{re}$ is the right eigenvector and $\underline{le}$ is the left eigenvector. Equations 3.3a and 3.4a are fulfilled when the load-flow Jacobian matrix is singular and the corresponding eigenvector is not a null vector (this guaranteed according to Equations 3.3c and 3.4c). Equations 3.3b and 3.4b guarantee that load-flow equations are fulfilled at the saddle node bifurcation point.

$$\mathbf{J}_x \underline{re} = \underline{0} \tag{3.3a}$$

$$\underline{f}(\underline{x}, \mu) = \underline{0} \tag{3.3b}$$

$$\|\underline{re}\| \neq 0 \tag{3.3c}$$

$$\underline{le}\mathbf{J}_x = \underline{0} \tag{3.4a}$$

$$\underline{f}(\underline{x}, \mu) = \underline{0} \tag{3.4b}$$

$$\|\underline{le}\| \neq 0 \tag{3.4c}$$

The equations of saddle node bifurcation can be solved by e.g. Newton-Raphson or Broyden (quasi-Newton) iteration techniques [Bas99]. Although the load-flow Jacobian matrix is singular at the bifurcation point, the Jacobian matrix of Equations 3.3 or 3.4 is non-singular at the bifurcation point. The Jacobian matrix of Equations 3.3 or 3.4 is needed to calculate symbolically or numerically [discussion in Par96, Bas99]. The use of the Newton-Raphson method requires good initial values in order to converge to the bifurcation point. The system might have many bifurcation points, but good initial values for the eigenvector guarantees convergence to the nearest voltage collapse point. A good guess for an initial eigenvector is an eigenvector corresponding the smallest eigenvalue at the base case [Cañ92]. Although this is not absolutely guaranteed to be the eigenvalue that eventually goes to zero at saddle node bifurcation point, it is quite likely. The inverse power method or Lanczos method [Gol96] can solve the smallest eigenvalue and corresponding eigenvector. The initial values for the state variables are the state values of load-flow solution at the base case. If the voltage collapse point is far from the base case, convergence problems may emerge. In that case new initial values are computed closer to the collapse point.

When applying the point of collapse method to voltage stability analysis, the information included in the eigenvectors can be used in the analysis of voltage stability [Dob92]. The right eigenvector defines the buses close to voltage collapse. The biggest element of the right eigenvector shows the most critical buses. The left eigenvector defines the bifurcation point normal vector. Selection of the opposite direction of the normal vector is the best way to improve the voltage stability at the collapse point. Thus, the purpose of voltage stability analysis determines which one of Equations 3.3 or 3.4 should be solved. One of the problems of the point of collapse method is convergence to the collapse point from the distant initial point, when reactive power limits of few generators are hit.

Optimisation method

Another direct computation method of voltage collapse point is the optimisation method. In that case the voltage stability margin is maximised according to load-flow equations and power system constraints. When using notation similar to that in the point of collapse method, the optimisation problem is set in Equation 3.5. The optimisation problem is directed by the computation direction. In that sense the optimisation problem is not a global optimisation in the parameter space.

$$\max \mu \tag{3.5a}$$

$$\text{subject to } \underline{f}(\underline{x}, \mu) = \underline{0} \tag{3.5b}$$

The solution of the optimisation problem satisfies the optimality conditions known as Khun-Tucker conditions [Fle90]. The Lagrangian for the equality-constrained problem (Equation 3.5) is defined in Equation 3.6, where $\underline{w}$ is a vector of Lagrangian multipliers. The necessary optimality conditions are defined in Equations 3.7 [Cut98]. Equation 3.7a is similar to Equation 3.3a, thus, the Jacobian $\mathbf{J}_x$ must be singular at the maximum point and the vector $\underline{w}$ is the left eigenvector corresponding the zero eigenvalue.

$$L = \mu + \underline{w}^T \underline{f}(\underline{x}, \mu) \tag{3.6}$$

$$\nabla_x L = \underline{0} \quad \Leftrightarrow \quad \mathbf{J}_x{}^T \underline{w} = \underline{0} \tag{3.7a}$$

$$\nabla_w L = \underline{0} \quad \Leftrightarrow \quad \underline{f}(\underline{x}, \mu) = \underline{0} \tag{3.7b}$$

$$\partial L/\partial \mu = 0 \Leftrightarrow \quad 1 + \underline{w}^T \mathbf{J}_\mu = 0 \tag{3.7c}$$

The solution of non-linear Equations 3.7 can be solved using the Newton method. The load-flow Jacobian matrix is part of the Hessian matrix (Jacobian matrix of Equations 3.7 or Hessian matrix of L) on the linear system. Although the load-flow Jacobian matrix is singular at the solution, the Hessian matrix is not. The vector $\underline{w}$ requires good initial values in order to achieve quick and reliable convergence to the maximum point.

Inequality constraints, like generator reactive power limits, can be included by computing sequence of optimisation problems. First the unconstrained optimisation problem described above is solved. In that case all generators control their voltage as in the base case. The solution of the optimisation problem overestimates the real voltage stability margin. Then

it is estimated, e.g. using linear interpolation technique described in reference [Cut98], which generators are switched to operate at the reactive power limit. A new optimisation problem starting from the previous solution is computed. The procedure is repeated until all constraints are satisfied. The final solution is the voltage stability margin μ^*. An alternative to the above procedure to handle inequality constraints is to use interior point optimisation [Par96, Iri97].

Continuation load-flow method

The purpose of continuation load-flow is to find a continuum of load-flow solutions for a given load/generation change scenario, i.e. computation direction [Ibs96]. It is capable of solving the whole PV-curve. The singularity of continuation load-flow equations is not a problem; therefore the voltage collapse point can be solved. The continuation load-flow finds the solution path of a set of load-flow equations that are reformulated to include a continuation parameter [Ajj92]. This scalar equation represents phase conditions that guarantees the non-singularity of the set of equations. The method is based on prediction-correction technique. The prediction-correction technique applied to the PV-curve solution is illustrated in Figure 3.6. The intermediate results of the continuation process also provide valuable insight into the voltage stability of the system and the areas prone to voltage collapse.

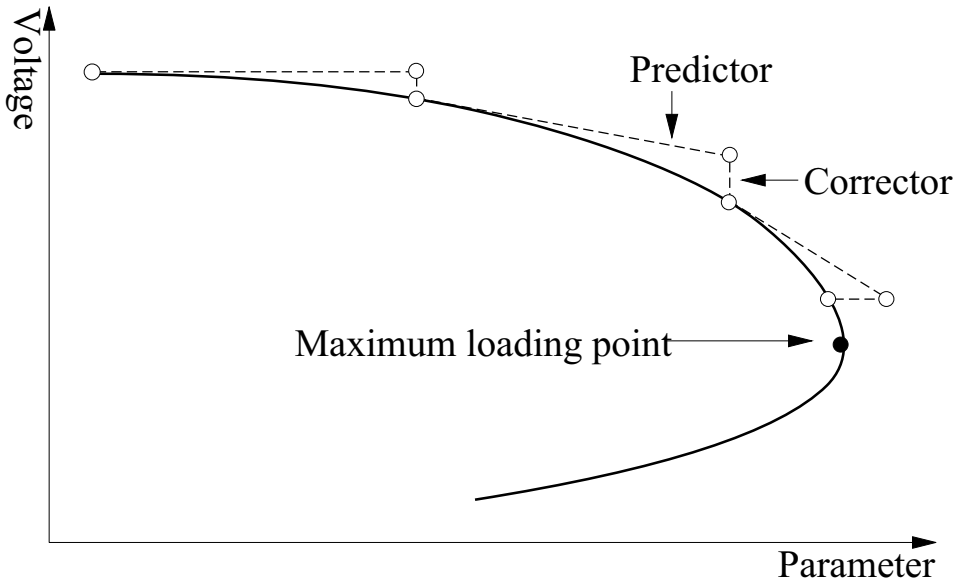

Figure 3.6. PV-curve solution using prediction-correction technique.

The prediction step estimates the next PV-curve solution based on a known solution. Taking an appropriately sized step in a chosen direction to the solution path can make the prediction of the next PV-curve solution. However, the prediction is not necessary, especially at the flat part of the PV-curve [Cut98]. The simplest prediction is the secant of last two PV-curve solutions. The computation of the secant is fast and simple. The tangent of last PV-curve solution is more accurate than the secant, but also requires more computation [Chi95]. The advantage of tangent direction is most valuable around the

PV-curve nose. The step size should be chosen so that the predicted solution is within the radius of convergence of the corrector. The determination of step size can be based on the slope of tangent or the difference between previous predicted and exact solutions [Chi95].

The inexact estimate is corrected using slightly modified load-flow equations at the correction step which is based on e.g. local parameterisation, where one state variable is constant during the computation of correction step [Ajj92]. In Figure 3.6 the constant state variable is the continuation parameter at the first two corrections and the voltage at the last correction. There is no restriction for the continuation parameter, but usually it is the increment of total load.

The maximum loading point can be sensed easily using the tangent vector of PV-curve solution. The tangent component corresponding the continuation parameter is zero at the maximum loading point and becomes negative beyond the maximum point. This method indicates whether or not the maximum loading point has been passed. The exact location of the maximum loading point requires searching with decreasing step size around the maximum point, which is why the point of collapse method and the optimisation method are more effective than the continuation load-flow to find the exact voltage collapse point.

The components of the tangent vector are differential changes in the state variables (voltages or voltage angles) in response to a differential change in system load (continuation parameter). The tangent vector can be used for a sensitivity analysis so that a stability index and identification of weak buses are obtained [Ajj92]. A good method to decide which bus is nearest to its voltage stability limit is to find the bus with the largest ratio of differential change in voltage to differential change in active load for the whole system. This ratio can also be used as a voltage stability index.

3.2.4 Computation of maximum loading point

The maximum loading point can be reached through a load-flow program [Aus95, Gao96, and Rep97]. The maximum loading point can be calculated by starting at the current operating point, making small increments in loading and production and re-computing load-flows at each increment until the maximum point is reached. The load-flow diverges close to maximum loading point because there are numerical problems in the solution of load-flow equations. The load-flow based method is not the most efficient, but has the following characteristics making it appropriate for voltage stability studies:

- good models for the equipment operating limits: generator capability limits, transformer tap ranges, circuit ratings and bus voltage criteria
- good models for the discrete controls: transformer tap steps and switched shunts
- capability to recognise the maximum loading point though the minimum singular value of load-flow Jacobian matrix
- familiar computer modelling, data requirements and solutions algorithms
- option of using the existing computer programs with minor modifications.

Computation algorithm

The computation of the maximum loading point is a parametric analysis of the operating points. The computation algorithm proposed and used in the thesis is presented in Figure 3.7. The algorithm is based on prediction-correction type computation, where loads and production are increased to chosen computation direction. In this way the *n*-dimensional boundary of maximum loading points can be determined in a certain direction. The computation direction is usually used to study how much power can be transferred across a certain intersection (see Chapter 3.2.1). The solution of load-flow corrects the errors due to discrepancy between the prediction and the actual non-linear functioning of the network. The convergence of load-flow is used as a criterion for the acceptance of intermediate results.

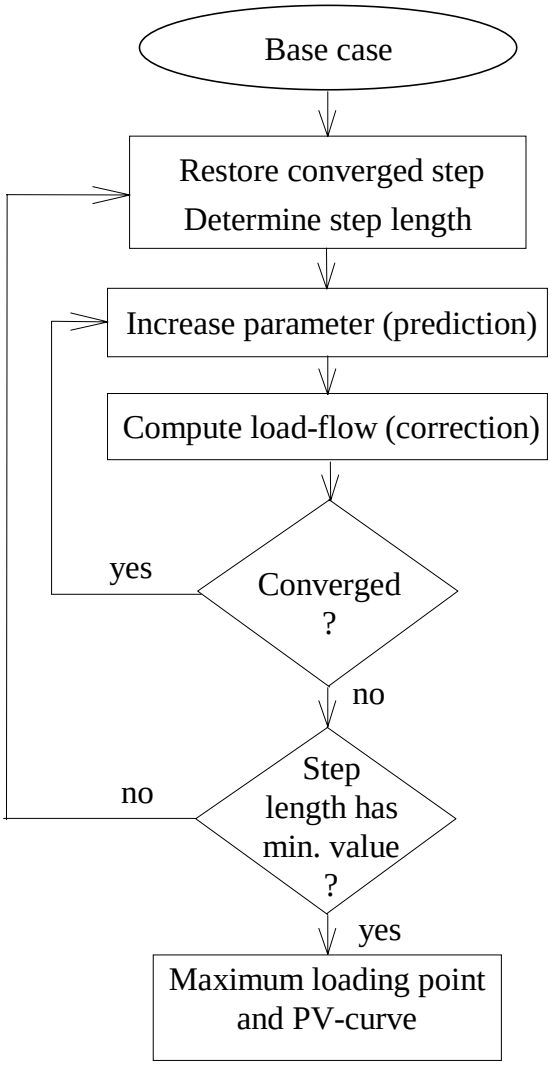

Figure 3.7. Algorithm of maximum loading point computation.

The increment of loads and production is continued until load-flow diverges. The algorithm is then continued with decreased step length. The stopping criterion for the

algorithm is the minimum step length. The accuracy of the proposed method depends on the value of minimum step length. The flat part of the PV-curve can be computed fast. The first few steps may be large, but near the maximum loading point, it must be reduced significantly due to load-flow numerical problems. The computation time is mostly spent at diverged load-flows close to the maximum loading point. The computation time is minimised when the number of diverged load-flows is minimised. The proposed method has proved to reach almost the same solution as the continuation load-flow with constant power loads (see Chapter 6.1.1).

Prediction step

The prediction step of maximum loading point computation can be based on

1. previous load-flow solution (Figure 3.8a)
2. secant of last two load-flow solutions (Figure 3.8b)
3. tangent of previous load-flow solution (Figure 3.8c)
4. fitting of parabolic curve to last three solutions (Figure 3.8d).

The first option uses the previous load-flow solution to predict the next solution. Such prediction is accurate enough on the flat part of the PV-curve. The second and the third option use a straight line to make better predictions than the first one. The secant method is applicable to commercial load-flow programs, because it only requires load-flow solutions. The tangent method requires a Jacobian matrix, which is seldom available. The last option uses curve fitting technique to estimate the maximum loading point. It requires at least three intermediate solutions. The curve fitting technique is described in Chapter 3.3.3.

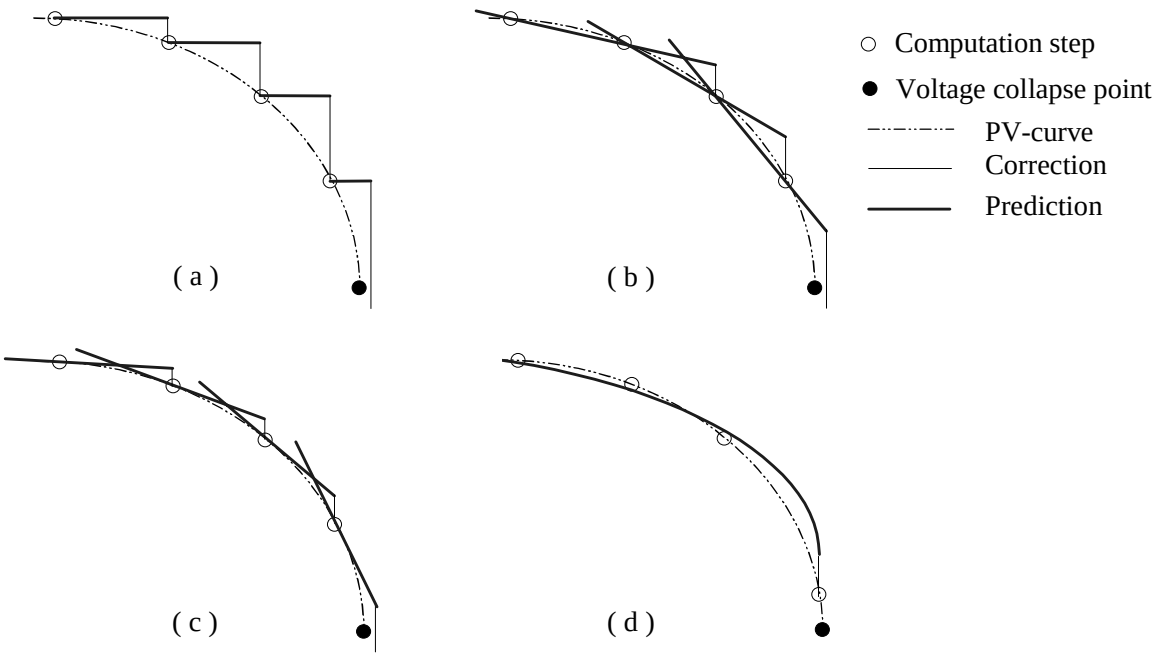

Figure 3.8. The options of prediction steps.

The accuracy of prediction is based on the discrepancy between the prediction and the actual non-linear functioning of the network. The aim of methods two to four is to decrease the prediction error compared to the first option and so to decrease the computation time and improve the convergence near the nose of PV-curve. The convergence of the Newton-Raphson based load-flow algorithm is fast when the algorithm converges. In that case the computation time of the correction step is almost the same regardless of the accuracy of prediction, which is why the first option is efficient especially on the flat part of the PV-curve.

The prediction of the fourth option is the head of the parabolic curve. The curve is fitted by intermediate solutions. The advantage of the option is greatest at the beginning of PV-curve computation when the maximum point is far from the base case. The prediction becomes more accurate when the number of PV-curve solutions increases. Then the step length also becomes short; thus the advantage of curve fitting method is lost.

Step length

The step length of the prediction step is needed to determine in prediction options one to three. The control of step length is automatic in option four. The determination of step length has a strong influence on the computation time of the maximum loading point. A long step can avoid the computation of a few intermediate solutions at the beginning of computation. Similarly, a short step can avoid computation of a few diverged load-flows close to the maximum loading point. The decision of initial step length is therefore based on experience.

The control of step length is crucial for the accuracy of the maximum loading point. When the step length is too long (the prediction error is too large), the load-flow might diverge due to load-flow numerical problems although there exists a load-flow solution. Decreasing the step length of the prediction step when solutions come close to the maximum loading point can ensure better accuracy of maximum loading point. An efficient method for step length control is binary search. The step length is halved based on certain criteria, e.g. voltage or load level, the amount of prediction error, the number of generators at the maximum reactive power limit, the slope of computation direction, the divergence of load-flow or a combination of these. The control of step length is obvious in the case of load-flow divergence. This method is probably the most often used. After a load-flow divergence, the step length is halved and the last converged load-flow solution is restored to a new initial condition. In that case the minimum step length determines the accuracy of the maximum loading point.

3.2.5 Comparison of computation methods

A clear conclusion of the description of the previous computation methods is that all the methods have different functions. They have their own strengths and weaknesses. The combination of all of these methods gives most information in voltage stability analysis.

The choice of the best method for on-line voltage stability assessment is not obvious. The method for on-line voltage stability assessment should be fast enough, robust regarding the algorithm's convergence properties and easy to apply.

The minimum singular value, the continuation load-flow and the maximum loading point methods compute intermediate results of the PV-curve. These methods provide valuable information in the form of voltage stability indices for quantifying proximity to the voltage collapse point and identifying the weakest buses. The algorithms are easy to implement, because they are based on load-flow equations. The intermediate results of these methods can also be used for a quick and approximate analysis of voltage stability in on-line applications. The number of equations is about the same as that in load-flow. The implementation of device limit handling is relatively easy. However, the computation process may be substantially slowed down when the system presents many limits. Nowadays there is also commercial software available for voltage stability analysis, which has applied these methods. These programs, vendors and applied methods are:

- Voltage security assessment tool (VSAT) by Powertech, maximum loading point method and fast time-domain simulation [Vol00b],
- Voltage stability analysis program (VSTAB) by EPRI, continuation load-flow and modal analysis [Gao96], and
- Voltage adequacy and stability tool (VAST) by PowerWorld, maximum loading point method and capability to analyse load-flow Jacobian matrix in Matlab [Vol00a].

The point of collapse method and the optimisation method compute the exact voltage collapse point using a direct method. These methods also provide information related to voltage weak areas and to voltage stability enhancement. Both methods require good initial values in order to converge quickly and correctly. Another drawback is the inclusion of inequality constraints, like generator reactive power limits, in the problems, which requires additional logic to repeat the basic procedure until all constraints are satisfied. Although the basic procedure is fast enough and converges nicely, the inclusion of inequality limits sometimes causes convergence problems. Another obvious disadvantage of these methods is the high computational burden, as the number of equation increases about twofold with respect to the power system load-flow equations. The point of collapse method also has convergence problems when the system is far from the collapse point, especially when device limits are encountered along the solution path.

The maximum loading point method was selected for the model-based approach due to possibility to use commercial software. The implementation of the maximum loading point method and the data generation of the proposed model-based approach could be programmed in PSS/E IPLAN programming language [Pow00a]. In this way a load-flow program could be used which is commonly used in transmission network companies. The accuracy or the computation speed of the method (see Chapter 6.1.1) did not restrict the use of the maximum loading point method in off-line data computation. The execution

time of the maximum loading point method may be further improved by initialising the solution of AC load-flow[4] with the fixed-slope decoupled solution method[5] as proposed in reference [Gra99]. The full Newton solution is then used to refine the AC load-flow solution. In practical applications it is also possible to speed up the execution time by first defining the thermal limits with the DC load-flow solution[6] and then checking the voltage limits and the convergence with the AC load-flow solution. However, the fast DC load-flow solution cannot be used alone, because it cannot identify voltage limits and it is not accurate enough when reactive power flow and voltage deviations are considerable.

The continuous load-flow method is probably the best for on-line application. It is accurate, reliable and moderately fast. The reliability is based on the fact that it has no serious convergence problems due to device limits but the convergence may slow down due to this. The implementation of continuous load-flow is also much easier than that of the point of collapse method or the optimisation method.

3.3 Contingency analysis

The result of the contingency analysis is the classification of the power system into secure and insecure states. This is an essential part of security analysis. The contingency analysis programs are based on a model of the power system and are used to study outages and notify the operators of any potential overloads or out-of-limit voltages. Contingency analysis is a time-consuming process when the number of contingencies is large. The contingency analysis of one thousand outages would take about 16 min, if one outage case were studied in 1 second. This would be useful if the power system conditions did not change over that period of time. Most of the time spent running contingency analysis would go for solutions of the load-flow model that discovers that there are no problems. The on-line contingency analysis is usually performed with a short contingency list using simplified computation methods [Woo96]. The contingency list is selected according to contingency ranking.

3.3.1 Determination of power system post-disturbance state

Contingencies arise due to scheduled outage, component switching in order to optimise power system operation, or unscheduled outage due to a fault. The contingency analysis of scheduled outage is based on a predicted operation point. Component switching in order to optimise power system operation requires contingency analysis of current operation point. The contingency analysis of unscheduled outages is done automatically in the on-line security assessment.

---

[4] Full load-flow solution, where load-flow equations are in complex form [Woo96].

[5] Simplification of full Newton load-flow, where the main idea is to neglect the “weak” interactions between active (reactive) power injections and bus voltages (voltage angles) [Woo96].

[6] Partial load-flow solution, where active power injections and voltage angles are only considered [Woo96].

The contingencies are classified as transmission component (lines, transformers or substation buses) and generator contingencies [Woo96]. The effect of contingency is seen as a change of power flows and voltages in the power system. The outage of a generation unit also increases the production of other generators due to shortage of power production. The modelling of generator contingency requires distribution of generated power to all generators taking part in frequency control. Similarly additional losses caused by contingency should be distributed among generators.

To speed up the execution the contingency analysis procedure uses an approximate model of the power system. The DC load-flow provides accurate results with respect to active power flows. The computation time of DC load-flow is extremely fast, e.g. according to reference [Woo96] the execution time of several thousand outages computed by DC load-flow method was less than 1 min in 1995. The full AC load-flow is required if voltage and reactive power flows are a concern. However, the use of AC load-flow in contingency analysis is impossible if the number of outages is several thousands.

3.3.2 Contingency selection

The selection of contingencies is needed to reduce the computation time of contingency analysis. Operators know from experience which potential outages will cause trouble. The danger is that the past experience may not be sufficient under changing network conditions. There is possibility that one of the cases they have assumed to be safe may in fact present a problem because some of the operators' assumptions used in making the list are no longer correct.

The contingency list is dependent on the power system operation point; thus it must be periodically updated. Another way to reduce the list to be studied is to calculate the list as often as the contingency analysis itself is done. To do this requires a fast approximate evaluation to discover those outage cases which might present a problem and require further detailed evaluation. Many methods have been proposed to solve this problem. The selection of contingencies is based on contingency ranking methods, and contingency ranking is used to estimate the criticality of studied outages. Contingency ranking methods assemble the appropriate severity indices using the individual monitored quantities such as voltages, branch flows and reactive generation.

Evaluation of the contingency list

One way of building the contingency list is based on the fast load-flow solution (usually an approximate one) and ranking the contingencies according to its results. The DC load-flow is commonly used for contingency ranking which is a completely linear, non-iterative, load-flow algorithm. This method is used to eliminate most of the cases and run AC load-flow analysis on the critical cases [Woo96].

The DC load-flow solution may be further speeded up by bounding methods [Bra88]. These methods determine the parts of the network in which active power flow limit violations may occur and a linear incremental solution (by using linear sensitivity factors, i.e. generation shift and line outage distribution factors) is performed only for the selected areas. The solution of AC load-flow may be speeded up by attempts to localise the outage effects and to speed up the load-flow solution. The efficiency of the load-flow solution has been improved by means of approximate/partial solutions (such as following the below described 1P1Q method) or using network equivalents. The bounding method may also be applied to the AC load-flow solution [Bra89]. Another localised method for AC load-flow solution is the zero mismatch method [Bac89].

1P1Q method

A commonly used contingency ranking method is the 1P1Q method [Woo96], where a decoupled load-flow is used to give approximate values for line flows and voltages. The name of the method comes from the solution procedure, where the decoupled load-flow is interrupted after one iteration of active power/voltage angle and reactive power/voltage calculations. A reasonable performance index is given from the solution of the first iteration of decoupled load-flow. The decoupled load-flow has the advantage that a matrix inversion lemma [Deb91] can be incorporated into it to simulate the outage of lines without reinverting the system Jacobian matrix at each iteration. Compared to DC load-flow method, another advantage of decoupled load-flow is the fact that the solution of voltages is given.

The ranking of contingencies is based on the performance index [Woo96]. Estimating the state of the post-disturbance operation point. The performance index is typically a penalty function, which indicates the crossing of limit values of power system parameters, such as voltages and line flows. The index should have a high value for critical contingencies and a low value for non-critical contingencies. The advantage of performance indices is a clear and a simple analysis, the disadvantage being e.g. an unclear setting of limit values for line flows and voltages in the voltage stability analysis. An example of performance index is given in Equation 3.8,

$$PI = \sum_{\substack{all\ lines \\ j}} \left(\frac{P_j}{P_j^{\max}} \right)^{2n} + \sum_{\substack{all\ buses \\ i}} \left(\frac{\Delta|E_i|}{\Delta|E|^{\max}} \right)^{2m} \tag{3.8}$$

where P_j is the line flow at the solution of 1P1Q procedure, $P_j^{\max}$ is the maximum value of line flow, n and m are high numbers, $\Delta|E_i|$ is the difference between the voltage at the solution of the 1P1Q procedure and the base case voltage, and $\Delta|E|^{\max}$ is the value set by operators indicating how much they want to limit voltage changes on the outage.

Consideration of power system non-linearity

The progress of computer and software technology has made it possible to analyse bigger and more demanding studies. A new topic in contingency analysis is the consideration of

non-linear functioning of the power system. Voltage stability analysis requires new kinds of contingency analysis methods due to the non-linearity of the problem. The contingency analysis of voltage stability studies is even more demanding than analysis of single AC load-flow due to the non-linearity of the problem.

Static contingency ranking is traditionally based on the properties of pre and post-disturbance operation points and aims at quickly identifying the contingencies that will lead to some operating limit violation. However, the ranking of contingencies might change due to power system non-linearity when the power system is operated temporarily close to security limits. The objective of voltage stability contingency ranking is ideally to identify the contingency that yields the lowest margin. The ranking should take into account both the disturbance and the direction of system stress. Accurate contingency ranking requires the computation of voltage collapse points for each contingency. The ranking of contingencies is then based on post-disturbance voltage stability margins. The computation of voltage stability margin for each contingency requires a large amount of computation and is not a practical solution to the problem.

Figure 3.9 presents PV-curves for one pre-disturbance case and two post-disturbance cases. Sometimes post-disturbance PV-curves intersect at some parameter value due to power system non-linearity. A typical reason for PV-curve intersection is the action of generator reactive power limit, which causes a strong decrement of load voltages. In practice it is almost impossible to approximate contingency ranking correctly based on pre or post-disturbance operation points, if those are far from the voltage collapse point. The contingency ranking is different seen from the operation point than from the stressed point.

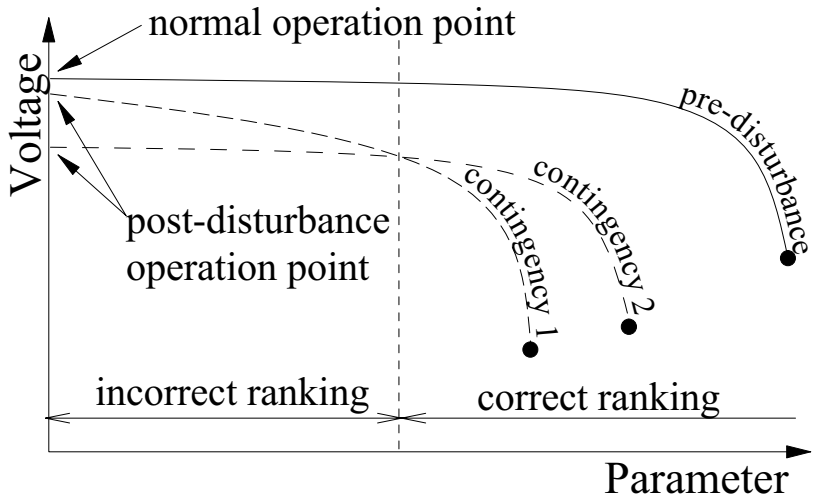

Figure 3.9. Intersection of post-disturbance PV-curves.

3.3.3 Contingency ranking methods for voltage stability studies

The contingency ranking methods for voltage stability analysis approximate the true contingency ranking without the computation of voltage stability margins. If the

contingency ranking is done close to the most critical voltage collapse point (at the stressed operation point), then the ranking can be done more reliably than at the operation point. The methods are based on full load-flow computation for every contingency at a stressed operation point. The methods studied in this thesis are reactive power losses, minimum singular value of load-flow Jacobian matrix, curve fitting technique to approximate voltage stability margin and clustering of contingencies to critical and non-critical contingencies.

Description of previously proposed methods

The contingency ranking methods for voltage stability analysis proposed in the literature are based on sensitivities of voltage stability margin, the curve fitting method, simultaneous computation of multiple contingency cases and parallel/distributed computation algorithms. The sensitivity method [Gre99] computes a PV-curve to obtain a pre-disturbance voltage stability margin. Then linear sensitivities of the margin for each contingency are computed. These sensitivities are then used to estimate the post-disturbance voltage stability margins. The advantage of the method is fast computation compared to other methods. The accuracy of the method is good and can be improved by using quadratic sensitivities. Problems may emerge when contingencies shift the voltage critical area or change the set of generators that are at the reactive power limits at the voltage collapse point.

The curve fitting methods [Eje96, Chi97] compute stable load-flow solutions to approximate the maximum loading point. The PV-curve can be approximated by a second order polynomial. The fitting of a polynomial requires three stable load-flow solutions. The head of the polynomial is an estimate of maximum loading point. In this way the computation of the whole PV-curve is not necessary to approximate the post-disturbance voltage stability margin. However, the method requires solutions of three stable load-flows for each contingency, which is demanding for contingency ranking. Reference [Chi97] proposes a curve fitting method where only two load-flows per contingency are required. However, reference [Zen93] concludes that good results can be obtained with five fitting points which need not be near the maximum loading point to achieve good accuracy.

There are some proposals to calculate multiple contingency cases simultaneously to rank contingencies according to voltage stability [Vaa99, Cut99]. These iterative methods compute load-flows or dynamic simulations to determine the stability of contingency cases in stressed situations. The idea of these methods is to eliminate as many contingency cases as possible at the first iteration. The eliminated contingencies are those which are stable in the stressed situation. Then system stress is decreased to find the most limiting contingencies for the remaining contingencies. The proposed algorithms are efficient regarding computing time, because the number of contingencies can be decreased rapidly.

Contingency ranking is naturally a parallel process. To reduce the execution time, contingency ranking can be employed on a parallel computer [Lem96, Har96, and Eje98b]

or a distributed computer environment [Cha97, San99]. The distributed processing could be based on the client/server model and the parallel virtual machine system [Cha97].

Reactive power losses

The state of power system voltage stability can be described e.g. by reactive power losses. Power system voltage collapse is associated with the reactive power demands not being met because of limitations in the production and transmission of reactive power. When the power system is stressed, reactive power losses increase compared to the operation point. Reference [Rep93] has proposed a performance index that measures reactive power loss in a selected area to rank line outages. The performance index approximates the post-disturbance reactive power losses according to the pre-disturbance load-flow solution. This performance index can be improved by computing the solutions of post-disturbance load-flows. In that case the reactive power losses of outages need not be estimated and the ranking of contingencies can be directly based on them. It is assumed that reactive power losses will be high for critical contingencies and low for non-critical contingencies compared to the pre-disturbance value in the proposed contingency ranking method [Löf95a].

Minimum singular value

The minimum singular value of the load-flow Jacobian matrix is zero at the voltage collapse point. It is used as an indicator to quantify proximity to post-disturbance maximum loading point. The use of the indicator requires the computation of post-disturbance load-flows for each outage. Although singular value decomposition is a linear description of operation point, it is assumed to give a correct enough contingency ranking for voltage stability studies. The intersection of contingency case PV-curves cannot be realised with this method. The value of the minimum singular value of the load-flow Jacobian matrix is also sensitive to limitations and changes of reactive power output. Computing the minimum singular values at the stressed operation point can increase the accuracy of the method.

Curve fitting method

The idea for voltage stability margin approximation with curve fitting technique is taken from references [Eje96, Chi97, and Gre99]. This method needs at least three stable post-disturbance load-flows to approximate the maximum loading point. Computed values are used to fit second order polynomials for chosen power system nodes. The second order polynomial is readily applicable to voltage stability margin approximation because the shape of PV-curve is parabolic. Equation 3.9 represents a second order polynomial.

$$\underline{\mu}_i = a_i \left(\underline{x}_i\right)^2 + b_i \underline{x}_i + c_i, \quad i = 1...n \tag{3.9}$$

The polynomial is defined separately for each power system node i studied. $\underline{\mu}_i=[\mu_i^{(1)}\ \mu_i^{(2)}\ \mu_i^{(3)}]^T$ is the parameter vector, $\underline{x}_i=[x_i^{(1)}\ x_i^{(2)}\ x_i^{(3)}]^T$ is the state variable vector, n is the number of chosen nodes, $\mu_i^{(.)}$ is the chosen parameter (e.g. active or reactive load)

and $x_i^{(.)}$ is a state variable (e.g. voltage or voltage angle). The superscript indicates the post-disturbance load-flow, i.e. the fitting point. The solutions of Equation 3.9 are constants a_i, b_i and c_i when fitting points $(x_i^{(1)},\mu_i^{(1)})$, $(x_i^{(2)},\mu_i^{(2)})$ and $(x_i^{(3)},\mu_i^{(3)})$ are used to fit the set of polynomials.

Constants a_i, b_i and c_i are used to approximate the maximum loading point of the nodes studied. The approximate maximum loading point is the head of the second order polynomial. The head of the maximum loading point is defined for the power system nodes studied by the critical state variable and the critical parameter. The approximate critical state variables and parameters are given in Equations 3.10 and 3.11 respectively. The voltage stability margin is given in Equation 3.12, where is assumed that the first fitting point is computed at the operation point.

$$x_i^* = -\frac{b_i}{2a_i}, \quad i = 1...n \tag{3.10}$$

$$\mu_i^* = a_i\left(x_i^*\right)^2 + b_i\left(x_i^*\right) + c_i, \quad i = 1...n \tag{3.11}$$

$$\mu^* = \frac{\sum_{i=1}^{n}\mu_i^* - \sum_{i=1}^{n}\mu_i^{(1)}}{\sum_{i=1}^{n}\mu_i^*} \tag{3.12}$$

It is necessary to use selected power system nodes to avoid numerical problems in the solution of polynomial coefficients of the curve fitting problem. If any state variables is constant at all fitting points, Equation 3.9 cannot be solved, because it causes singularity problems in the solution of the curve fitting problem. Therefore generator node voltage should not be used.

The accuracy of the voltage stability margin approximated by curve fitting technique is fully dependent on the fitting points. If all the fitting points are located at the flat part of PV-curve, the estimates of critical state variables and critical parameters is sensitive to small changes of fitting points. The voltage stability margin is not sensitive to the estimation errors if the number of power system nodes studied is large enough. It is also possible to remove the critical state variables and parameters which are clearly impossible from the computation of voltage stability margin. When the fitting points are located far from each other, it is possible to get a result where one of the fitting points is at the lower side of the PV-curve. This is a result of incorrect curve fitting, because the fitting points used in the curve fitting should be located at the upper side of the PV-curve. Curve fitting is not explicit, which causes these problems.

The selection of step length in the computation of operation points (using e.g. the maximum loading point method) is critical for the accuracy of voltage stability margin approximation. Computed operation points should not be too far away from each other,

otherwise approximation of maximum loading point may lead to strange results. On the other hand, step length should be large enough to avoid constant voltages in fitting points.

The accuracy of voltage stability margin approximation can also be improved by adding fitting points. The second order polynomial goes through the fitting points exactly if the number of points is three. If the number of fitting points is larger than three, the curve fit is done in the sense of least square error and the polynomial does not necessarily go through the fitting points.

Contingency clustering

Most pattern recognition methods proposed for contingency analysis are based on classification methods [Dac84, Pan73]. The application of classification to contingency ranking requires off-line training of the classifier with a large number of contingency studies. Clustering is distinct from classification methods and tries to find similarities between cases. Reference [Weh95] has proposed an approach to identify the similarities between power system voltages and contingencies by the agglomerative hierarchical clustering method and the Kohonen self-organising feature map.

Because not all groupings can be examined, most clustering algorithms try to find reasonable clusters without having to look at all clusters. Agglomerative hierarchical clustering methods [Joh92] start with individual cases and most similar cases are grouped first. A common measure of similarity is Euclidean distance. Finally all subgroups are fused into a single cluster. Hierarchical clustering methods cannot reallocate cases grouped incorrectly at an earlier level. Also, the size of data may not be large due to amount of computation and the size of the distance matrix. The results of hierarchical clustering are presented as a dendrogram (tree structure). The identification of the group of most critical contingencies is done at selected level of tree structure. The level can be chosen based on statistical analysis or using visualisation of tree structure. Figure 3.10 presents an example of hierarchical clustering which includes three clusters identified at the identification level.

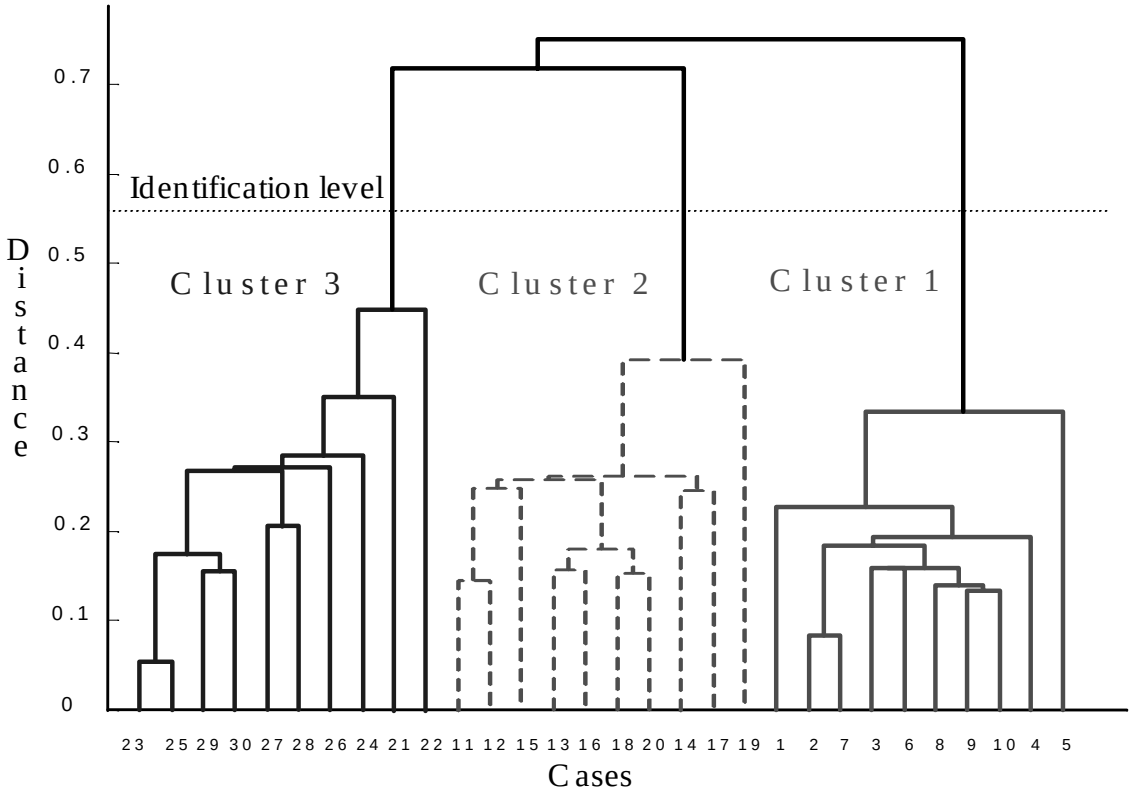

Figure 3.10. Example of hierarchical clustering.

Non-hierarchical clustering methods, which are based on iterative processes, do not restrict clustering in the same way as hierarchical methods. A well known and simple non-hierarchical clustering method is K-means clustering [Tou74]. This is well known, because it is simple and it can manage large data sets [Tou74]. K-means clustering is based on the concept of input vector classification by distance functions and on the minimisation of the sum of squared distances from all points in a cluster domain to the cluster centre. The behaviour of K-means clustering is influenced by the number of cluster centres, the choice of initial centres, the order in which the input vectors are taken and properties of the data [Tou74]. The algorithm will produce acceptable results when the data contain characteristic regions that are relatively far from each other. In practice, the use of K-means clustering will require experimenting with various numbers of clusters as selected by the user. The K-means clustering algorithm is represented in mathematical form in Chapter 4.4.3.

Figure 3.11 presents the clusters found with the K-means clustering method from the same data set as in Figure 3.10, when the number of clusters chosen was three. Small dots are data points and large dots are cluster centres. Both methods found exactly the same clusters in this simple example, but this is not necessarily the case in more complicated studies.

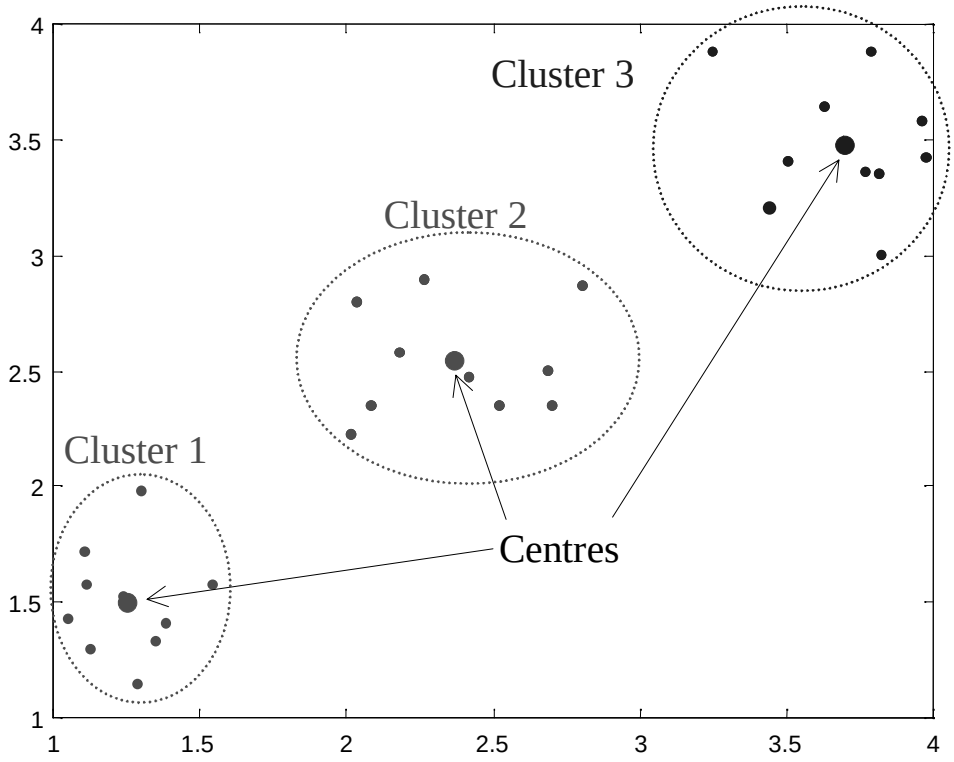

Figure 3.11. Example of K-means clustering.

Contingency clustering is proposed in two steps. First the number of state variables used at contingency clustering is reduced. This reduction is necessary to speed up and to improve the contingency clustering and the step is done using hierarchical clustering methods to analyse interactions of state variables of post-disturbance operation points. For example, voltages can be analysed to find areas where voltages are affected similarly in different operational conditions [Weh95, Son97]. The members of clusters can be replaced by the mean value of state variables at the cluster, for example.

Second, the clustering of contingencies is performed. This is done using K-means clustering. The clustering is done for contingencies (post-disturbance operation points), not for state variables. Clustering is used to find similar contingency cases in order to identify the "critical" groups. Clustering searches for the structure of natural grouping for the post-disturbance operation point data. Clustering methods cannot be used to estimate contingency ranking, but they are used to identify a group of most critical contingencies.

3.3.4 Comparison of contingency ranking methods

The contingency ranking methods described above have different characteristics. The curve fitting technique is the most accurate method, but it also requires a lot of computation compared to other methods. It provides a good approximation for a voltage stability margin in order to rank contingencies. This method can also be used for a first approximation of security analysis in the on-line mode. In the on-line mode the security analysis is usually realised in parallel form, where all contingencies are studied almost

simultaneously. When there are three load-flow solutions available for all contingency cases, the curve fitting technique can be applied to approximate voltage stability margins. The first approximation of voltage stability margins for different contingency cases provides an opportunity to concentrate the computation capacity on the most critical contingencies and eliminate the others. The curve fitting method is the most recommended method of the studied methods due to its accuracy and capability to approximate the voltage stability margin.

Methods based on reactive power losses and minimum singular value are almost equal when considering the accuracy of contingency ranking. The computation of reactive power losses is naturally faster than the computation of the minimum singular value of load-flow Jacobian matrix. Both of these methods are intuitively easy to adapt, because they have clear physical or mathematical explanations considering power system voltage stability. They are easy to implement to existing analysis tools. There are also other similar indices like reactive power reserves which can be combined with the above methods to achieve even better results.

The contingency clustering method is not capable of ranking contingencies. It is a valuable method when a large amount of data of contingency studies is to be analysed. The method provides a way to analyse both the variables and the cases. The purpose of the proposed method is to find similarities in contingency cases in order to find the most critical contingencies. The value of the proposed method is clear when the data includes cases in a wide range of operation points. The data needed in contingency clustering comes from the planning studies and the computation of on-line transfer capacities. When transmission companies start to apply risk management or uncertainty handling in transmission network planning and operation, there are a huge amount of stability studies which must be analysed in a systematic way.

4 PRINCIPLES OF BLACK-BOX MODELLING

This chapter provides the basis of data-driven black-box modelling. Here consideration is given to linear regression and non-linear neural network modelling, model generalisation, and feature selection and extraction methods. The models and methods are described here to provide the basic knowledge about black-box modelling in order to understand their application in Chapters 5 and 6. The models described are regression model, multilayer perceptron and radial base function neural networks. Neural networks may be understood as non-linear and powerful counterpart for traditional statistical methods like regression models from statistics and computer science point of view. The parameter estimation of these models is also described here. The generalisation capability of the model is the most important aspect of modelling. The feature selection and extraction methods are used to compress the information presented for the model. This is important in power system applications, because measurements are redundant.

When we solve real-world problems, we realise that such systems are typically ill-defined, difficult to model, and possess large solution spaces. In these cases, precise models are impractical, too expensive or non-existent. To generate the appropriate solution, we must leverage two kinds of resources: problem domain knowledge of the system and data that characterise the functioning of the system. The data-driven black-box model does not explicitly model the physics of the system, but establish a mathematical relationship between a large number of input-output pairs measured from the system. Black-box models are applied when the functioning of a system is unknown or very complex (there is not enough knowledge to create a physical model, the system is very non-linear and dependent on operation point or the analysis of the system is time-consuming), but there is plenty of data available [Bis95].

For instance, in classical control theory the problem of developing models is decomposed into system identification and parameter estimation. Usually the former is used to determine the order of the differential equations and the latter determines its coefficients. Hence, in this traditional approach we have *model = structure + parameters*. This equation does not change with the application of data-driven black-box model. However, we now have more flexibility to represent the structure, to tune the parameters, and to iterate this process.

The simplest form of black-box models is probably tabulation of measurement data. The data may also be presented with selected prototypes, which are for example the mean

values of certain parts of the data. This form of models may be created by clustering methods. The presentation of the data with tabulation and prototype models is very sparse, because the data is presented only in local points of data set. Local function approximation is a concept where each prototype represent a continuous function in own subset. The radial base function neural network is the most well-known local neural network algorithm, other traditional statistical methods are splines. These models are capable of approximating the functioning of the system at the same level as physical models when sufficiently comprehensive data is available. The multilayer perceptron neural network is capable of global function approximation, i.e. it represents a function in a whole data set. The statistical regression model is also capable of accurate function approximation, but the applicability is usually limited to small scale (the number of parameters is small) and non-complex problems.

4.1 Linear modelling

The linear model is linear regarding its parameters. The applicability of a linear model is much simpler than that of a non-linear model. In most cases it is not necessary to describe all the details of the data. A smooth function which describes the system or the phenomenon reliably is of much more use in the estimation of system state than an exact presentation of the data. Data mapping is modelled in terms of a mathematical function (linear or non-linear model) which contains a number of parameters whose values are determined with the help of the data.

4.1.1 Regression model

Regression analysis [Joh92] is the statistical methodology for predicting values of outputs from a collection of input values. The output of regression model is

$$\underline{y} = \mathbf{X}\underline{w} + \underline{\varepsilon} \tag{4.1}$$

where $\underline{y}$ is the output vector, $\mathbf{X}$ is the data matrix, $\underline{w}$ is the parameter vector and $\underline{\varepsilon}$ is the error vector. The output is a linear function of the parameters. The data matrix describes the function to be modelled. A full quadratic polynomial can be expressed as $\mathbf{X}=[\underline{1}\ \underline{x}_i\ \underline{x}_i\underline{x}_j\ \underline{x}_i^2]$, $i,j=1\ldots p$, where p is the number of input variables. The error distribution is normal distribution $\underline{\varepsilon}\sim N_n(\underline{0},s^2\boldsymbol{I})$, where n is the number of experiments, s is the error variance and $\boldsymbol{I}$ is the identity matrix. The assumptions related to the model are

- the expected value of errors is zero
- the error variance s is constant
- errors do not correlate with each other.

The model parameters are solved by least squares estimation. The estimate minimises the sum-square error (SSE = $\underline{r}^T\underline{r}$) of the residual vector $\underline{r} = \underline{y} - \mathbf{X}\underline{\hat{w}}$, where $\underline{\hat{w}}$ is the estimate of the parameter vector. The minimum of sum-squares error is achieved by solving the normal equations of the least squares estimation problem [Joh92]. The solution of the

problem is a maximum likelihood estimate for the parameter vector. If the columns of the data matrix are independent, there is an explicit solution for the problem. The output and the parameter estimates are given in Equation 4.2, where $\boldsymbol{X}^{\dagger}$ is a pseudo inverse of the data matrix [Net96]. The range of square matrix $\boldsymbol{X}^{\mathrm{T}}\boldsymbol{X}$ is full and thus it has an inverse.

$$\begin{aligned} \underline{\hat{y}} &= \mathbf{X}\underline{\hat{w}} \\ \underline{\hat{w}} &= \mathbf{X}^{\dagger}\,\underline{y} = \left(\mathbf{X}^{T}\mathbf{X}\right)^{-1}\mathbf{X}^{T}\,\underline{y} \end{aligned} \tag{4.2}$$

4.1.2 Confidence limits and model accuracy

A smooth function reliably describing the system studied is of much more use in the estimation of system state than a function that exactly fits the data used in the parameter estimation. The outputs vary slightly due to errors. Because the model outputs are part of equations of parameter estimates, these must also be changed. In order to compute the variance of parameters (confidence limits), an estimate of error variance $\hat{s}$ and a correlation matrix $\boldsymbol{C}$ are needed (Equation 4.3) [Net96]. The value for t_1 is obtained from the t-distribution with a chosen confidence level.

$$\begin{aligned} \text{confidence limits} &= \underline{\hat{w}_i} \pm t_1 \hat{s}\sqrt{\mathbf{C}_{ii}} \\ \hat{s} &= \sqrt{\frac{SSE}{n-p}} \\ C_{ii} &= \left(\mathbf{X}^{T}\mathbf{X}\right)^{-1} \end{aligned} \tag{4.3}$$

Outliers (data points far from the mean of the rest of the data), possibly due to measurement or computation errors, may cause serious errors for parameters. If the error variances of the model are known, then the quality of model can be checked after the parameter estimation. If the error variances are unknown, they can be estimated (Equation 4.3). If the scaled residual $r_i/\hat{s}$ is large, the corresponding data point might be erroneous.

All differentiable functions can be approximated with Taylor series. Therefore it is natural that most data can be represented accurately by polynomial function. We can obtain a better fit by increasing the order of the model, since this increases the number of degrees of freedom in the function, giving it greater flexibility. High order polynomials, however, have problems that appear as high extrapolation errors. Although the polynomial describes the data accurately at the data points, strange curves outside the data points may appear. Therefore polynomial functions are not recommended for extrapolation and high order polynomials should not be used.

Figure 4.1 illustrates an example of bad extrapolation capability of a polynomial model, when there is not enough data. The function to be approximated is a sine function. The data points include small amount of noise. The model is the 10^{th} order polynomial model. The model works nicely at the middle of data following the sine curve. However, there are large errors at the data boundaries due to insufficient amount of data in these areas. The

decrement of model capability area is the only solution to the problem, because the reduction of model order does not remove the extrapolation error.

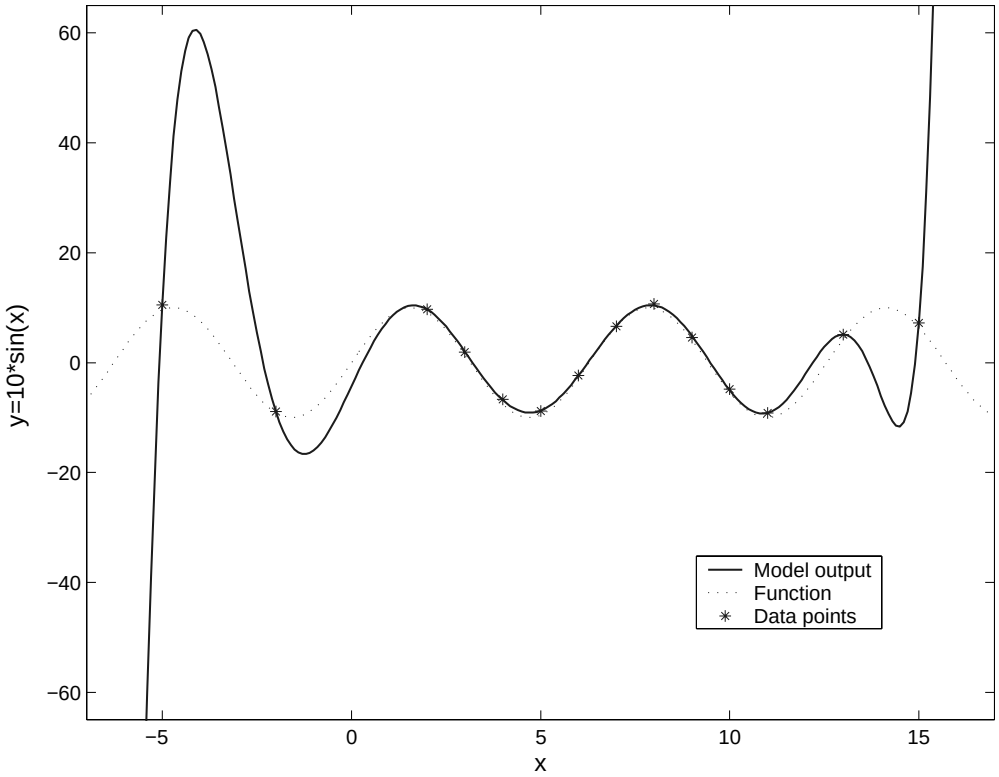

Figure 4.1. Extrapolation error of the 10th order polynomial model.

4.2 Non-linear modelling using neural networks

Neural networks are capable of non-linear function approximation. The importance of neural networks is that they offer a powerful and general framework for representing non-linear mappings. The multilayer perceptron and the radial base function neural networks are probably the best and the most widely used neural networks for function approximation tasks for large problems [Hay94]. A neural network may have any number of hidden layers and arbitrary connections, but only one hidden layer and fully feed-forward connected neural networks are considered in the thesis.

4.2.1 Multilayer perceptron neural network

The information fed into the input layer of a multilayer perceptron neural network is propagated forward through hidden layers to the output layer. The output of the *k*th output unit for one hidden layer network is

$$\hat{y}_k = f^{(2)}{}_k\left(\sum_{j=1}^{q} w_{kj}^{(2)} f^{(1)}{}_j\left(\sum_{i=1}^{p} w_{ji}^{(1)} x_i + w_{j0}^{(1)}\right) + w_{k0}^{(2)}\right) \tag{4.4}$$

where $f^{(2)}_k$ is the *k*th output layer activation function, $w^{(2)}_{kj}$ is the weight by which *k*th output unit multiplies *j*th hidden layer output, $f^{(1)}_j$ is the *j*th hidden layer activation function, $w^{(1)}_{ji}$ is the weight by which *j*th hidden unit multiplies *i*th input, x_i is the *i*th input, $w^{(1)}_{j0}$ is the *j*th hidden layer and $w^{(2)}_{k0}$ is the *k*th output layer bias. Usually the hidden layer activation function is non-linear (e.g. hyperbolic tangent) and the output layer activation function is a pure linear function [Bis95]. Figure 4.2 presents an example of multilayer perceptron neural network. The example presents the network of two inputs, three hidden units and two outputs.

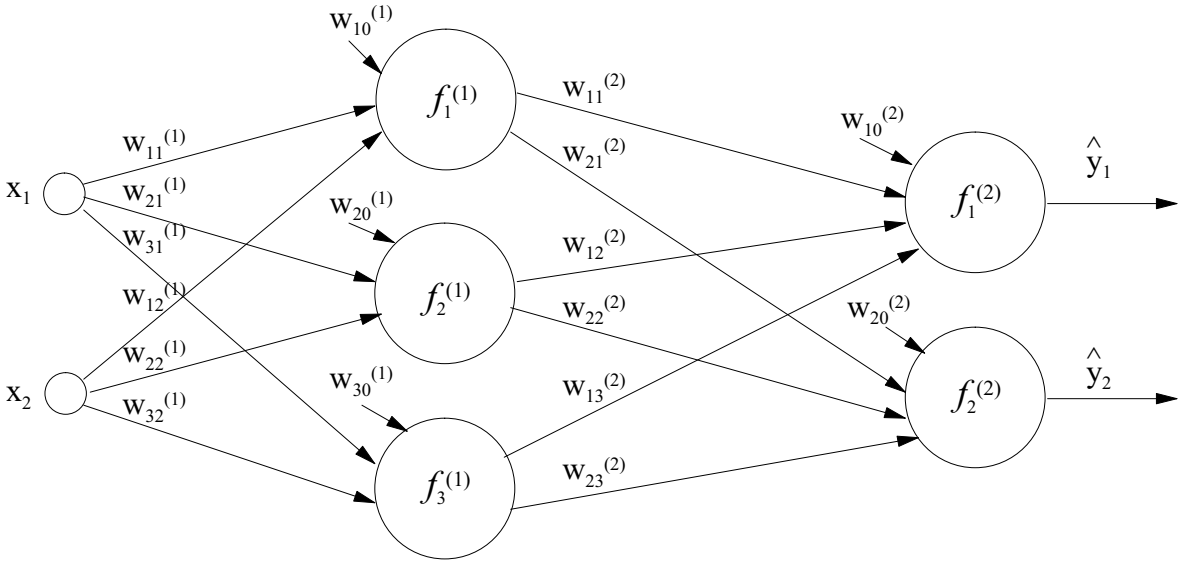

Figure 4.2. Example of a multilayer perceptron neural network.

A multilayer perceptron neural network is a universal approximator [Hay94]. It provides a technique for non-linear function approximation in multidimensional space. A multilayer perceptron neural network can approximate arbitrarily well any continuous function with a finite number of discontinuities when the number of hidden layer units is sufficient and when there is ample training data available. A multilayer perceptron may have one or more hidden layers. A variety of different activation functions may also be used within the same network. It constructs global approximation to non-linear input-output mapping, because many hidden units will contribute to the determination of the output. The number of parameters required presenting a mapping in the desired degree of smoothness is much smaller with a multilayer perceptron neural network than with other neural networks (e.g. radial base network) used for function approximation [Bis95].

The neural network mapping which minimises a sum of square error function is given by the conditional average of the target (true output) data [Bis95]. At any given value of the input variables, the neural network output is given by the average of target with respect to the distribution (conditional density) of the target variables, for that value of input. In other words, the minimum is given by the average of the target data. The value of the residual error is a measure of the average variance of the target data.

4.2.2 Parameter estimation of a multilayer perceptron neural network

The parameter estimation of a multilayer perceptron neural network is an unconstrained non-linear optimisation problem [Bis95]. There is a powerful and computationally efficient method, called error back-propagation, for finding the derivatives of an error function with respect to the parameters of a multilayer perceptron neural network [Bis95]. A commonly used error function is a mean square error. The simplest optimisation algorithm is the gradient descent method [Fle90]. The second order optimisation algorithms (Levenberg-Marquardt, quasi-Newton and conjugate gradient) use the gradient and the Hessian matrix of error function to find the optimum solution [Fle90].

First-order optimisation algorithms

The standard back-propagation training algorithm is based on the gradient descent method. The convergence of gradient descent is slow due to its tendency to zigzag on the flat error surface [Hay94, Mat98b]. A momentum term allows gradient descent to respond not only to the local gradient, but also to recent trends in the error surface [Mat98b]. It allows small features in the error surface to be ignored and prevents getting stuck in the local minimum. The performance of gradient descent is also sensitive to the setting of the learning rate. It may become unstable if the learning rate is too large and might take an enormously long time to converge if the learning rate is set at a small value. The performance of the gradient descent algorithm can be improved with an adaptive learning rate that tries to keep the learning rate at a maximum while holding learning stable [Mat98b].

The slow convergence of gradient descent can be improved with a resilient back-propagation algorithm [Mat98b]. Resilient back-propagation uses only the sign of the derivative to determine the direction of parameter update. If the parameter continues to change in the same direction for several iterations, then the size of parameter change will be increased. Whenever the parameters oscillate, the size of parameter change will be reduced. Resilient back-propagation accelerates training in flat regions of the error function, although it seems a imprecise method [Mat98b].

Second-order optimisation algorithms

Although the error function decreases most rapidly in the direction of a gradient, this does not ensure the fastest convergence. Second order optimisation algorithms use the gradient and the Hessian matrix of error function to find the optimum solution. Second order methods are in principle no more likely to find a global minimum than are first order methods. However, their functioning is better (find better local minimum, more robust convergence and faster) than that of first order methods.

Conjugate gradient algorithms are usually much faster than gradient descent with a momentum term and adaptive learning rate, but are sometimes slower than resilient back-propagation [Mat98b]. In a conjugate gradient a search is made in the conjugate

gradient direction to determine a step size which will minimise the performance function along that line. A scaled conjugate gradient reduces the training time compared to other conjugate gradient methods because it can avoid the time-consuming line search. The conjugate gradient method needs only a little more computer memory than gradient descent or resilient back-propagation. These are used for neural network parameter estimation when there is a large number of parameters. The conjugate gradient methods completely avoid the estimation and storage of the Hessian matrix [Fle90].

Newton's method is an alternative to the conjugate gradient methods for fast optimisation [Fle90]. Its convergence is faster than conjugate gradient methods. Unfortunately it is expensive to compute the Hessian matrix for a multilayer perceptron neural network and there is no guarantee that the Hessian matrix of a multilayer perceptron neural network is always non-singular. Quasi-Newton methods do not require calculation of second derivatives and an approximate Hessian matrix is always non-singular. Quasi-Newton methods are like Newton's method with line search, except that a symmetric positive definite matrix, which is updated at each iteration, approximates that Hessian matrix. The Broyden, Fletcher, Goldfarb and Shanno quasi-Newton update has been the most successful in published studies [Cut87]. The algorithm needs more computation at each iteration and more computer memory than conjugate gradient methods, but it usually converges faster [Mat98b]. Additional computer memory is needed to store an approximate Hessian matrix.

The Newton's method becomes the Gauss-Newton method when the objective function is a sum of squares (non-linear least squares problem) and the approximate Hessian matrix is linear approximation of the residuals [Fle90]. In the Gauss-Newton method, using the information required to determine the first derivative vector, it is possible to approximate the second derivative matrix. The convergence of the Gauss-Newton method may be more rapid than the convergence of quasi-Newton methods. One negative aspect of the Gauss-Newton method is the so-called large residual problem. In this problem the Gauss-Newton method may fail or converge slowly. This problem can be avoided in the Levenberg-Marquardt method, which is a restricted step algorithm [Fle90, Cut87]. The difficulty caused by a non-positive definite Hessian matrix in Newton's method can also be avoided in restricted step algorithms. The Levenberg-Marquardt method is the standard method for non-linear least squares problems due to its fast convergence and robustness [Cut87]. It starts with a gradient descent method with small step size. The Levenberg-Marquardt method becomes more like the Newton method using an approximate Hessian matrix near error minimum due to its faster convergence and better accuracy. The Levenberg-Marquardt algorithm is the fastest method for neural network parameter estimation for moderate size neural networks, especially when accurate results are needed [Mat98b]. The main disadvantage of the Levenberg-Marquardt method is the considerable computer memory requirement.

4.2.3 Radial base function neural network

The radial base function neural network is also widely used for function approximation tasks [Bis95, Hay94]. The radial base function approach introduces a set of q hidden units (radial basis functions), which are radially symmetric non-linear functions ϕ, e.g. Gaussian function. The function depends on the Euclidean distance between input $\underline{x}$ and prototype vector $\underline{c}$, $||\underline{x}-\underline{c}_j||$. The prototype vector is the centre of the hidden unit activation function. The width of the activation function area can be adjusted with the activation function parameter γ. This parameter affects the smoothness of the mapping function. The distance between the input vector and a prototype vector determines the activation of hidden units. In the case of a Gaussian activation function, when the inputs are close to the prototype vector (the distance is small), the unit activates. However, when the inputs are far from the prototype vector, the unit activates only partially or not at all. In this way the hidden units divide the input space into localised areas. The centres of the local areas are given by the prototype vectors of the hidden units. The output of the mapping is then taken to be a linear combination of the basis functions. Equation 4.5 presents the output of kth output unit of a radial base function neural network. The activation function of Equation 4.5 is a Gaussian curve.

$$\hat{y}_k = \sum_{j=1}^{q} w_{kj}\phi_j(\underline{x}) + w_{k0}, \quad \phi_j(\underline{x}) = \exp\left(-\left\|\underline{x}-\underline{c}_j\right\|^2 \Big/ 2\gamma_j^2\right) \tag{4.5}$$

Figure 4.3 presents an example of a radial base function neural network. There are two inputs, three hidden units and two outputs. The purpose of the input layer is to bring inputs to each hidden unit. The number of hidden units is one of the parameters in model creation; i.e. the number of hidden units should be optimised. In practice, the number of hidden units is found by the trial and error method. The parameters of a hidden unit are the centre and the width of activation function. In the case of the Gaussian activation function the output of the hidden unit achieves the maximum, when the distance between the centre of the activation function and the input is zero. The output of the hidden unit becomes zero when the distance is larger than the width of activation function. The output of hidden unit is dependent on distance but not on the direction of distance, which can be taken into account if an unsymmetrical function is used instead of a symmetric function on activation function. The outputs of hidden units are then brought to the output units. When the activation functions of output units are linear, the outputs of radial base function neural network are the linear combination of all inputs weighted by the parameters of output unit (weights between the hidden and the output layer and the bias terms).

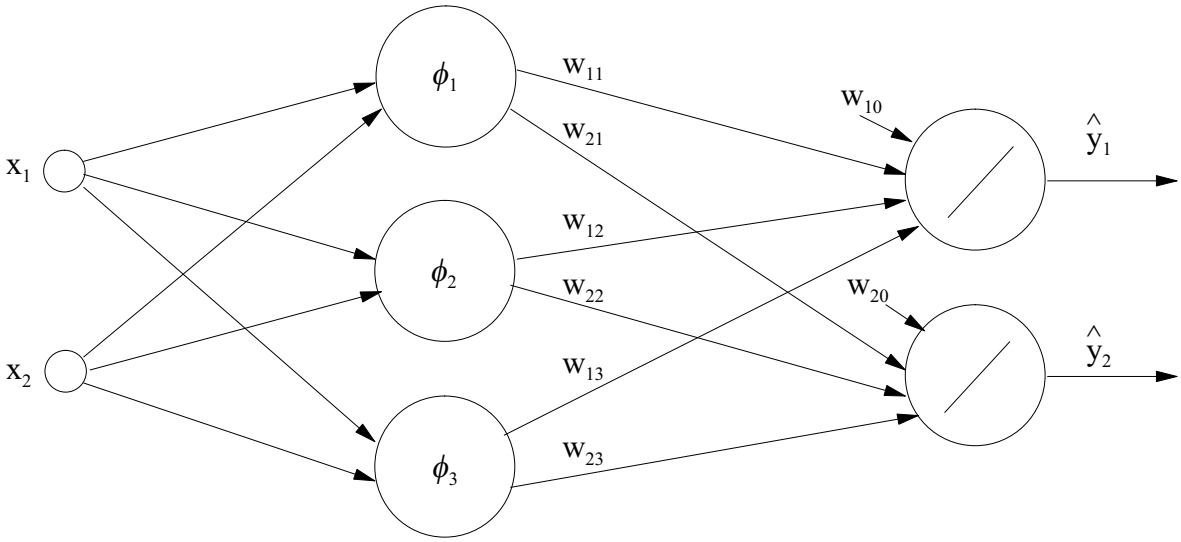

Figure 4.3. Example of a radial base function neural network.

4.2.4 Parameter estimation of a radial base function neural network

The parameter estimation of radial base function neural networks may be substantially faster than that of multilayer perceptron neural networks. The parameter estimation can be done in a fully supervised manner, but the two-stage procedure is less time-consuming and provides adequate learning results [Bis95]. A two-stage parameter estimation procedure includes determination of parameters governing the basis functions ($\underline{c}_j$ and γ_j) by an unsupervised method (e.g. the orthogonal least squares method or K-means clustering) and determination of output layer weights, which requires the solution of the linear problem.

4.2.5 Comparison of multilayer perceptron and radial base function neural networks

The radial base function and multilayer perceptron neural networks are similar. They provide a technique for non-linear function approximation in multidimensional space. Both neural networks are universal approximators. The particular structures of the two neural networks are different. The important differences are as follows [Bis95]:

- The radial base function has a single hidden layer, while the multilayer perceptron may have one or more hidden layers. A variety of different activation functions may also be used within the same multilayer perceptron.
- The radial base function computes the Euclidean distance between the input and the prototype vector for each hidden unit, while the multilayer perceptron computes the inner product of the input and weight vectors of that unit.
- The radial base function constructs local approximations (a few hidden units will have significant activation) to non-linear input-output mapping, while the multilayer perceptron constructs global approximation (many hidden units will contribute to the determination of the output).
- The radial base function is capable of faster parameter estimation than the multilayer perceptron. However, the number of parameters required presenting a mapping in desired degree of smoothness is much larger with the radial base function than with multilayer perceptron.

4.3 Generalisation of model and its improvement

4.3.1 Generalisation

The model has the ability to generalise when the function between inputs and output is computed correctly for a new data set [Bis95]. The best generalisation to the new data is obtained when the mapping represents the underlying systematic aspects of the data, rather capturing the specific details of the data set used for parameter estimation. The output of the mapping typically varies smoothly as a function of the input variables. Thus, it is possible to interpolate i.e. estimate the outputs at intermediate data points, where no data is available. The new data is not used in the parameter estimation or model order selection. The model order selection is the process of selecting the number of parameters. The new data set should, however, belong to the same population as the data used in the parameter estimation and in the model order selection.

The goal of parameter estimation is not to learn an exact representation of the data set, but rather to build a statistical model of the process that generates the data [Bis95]. There will always be some difference between the model output and the true output. A model which is too simple or too inflexible will have a high bias, while a model that has too much flexibility will have a high variance. An excessively simple model will have a low performance due to low accuracy. An excessively complex model may well present the data used in the parameter estimation but may have poor generalisation capability. The bias represents the difference between the average of model output and the true output. The variance represents the average sensitivity of the mapping to a particular data set. The point of best generalisation is determined by the trade-off between these two competing properties, i.e. the model may be neither too simple nor too complex.

Changing the number of parameters in the model can vary the complexity of the model [Bis95]. This is called model order selection and is implemented by comparing a range of models having different numbers of parameters e.g. hidden units. The model order selection is described in Chapter 4.3.2. Other methods to control the complexity of a neural network model are the use of regularisation, early stopping and neural network pruning. These are described in Chapter 4.3.3.

4.3.2 Model order selection

Optimum complexity of the model occurs when the number of degrees of freedom in the model is relatively small compared to the size of the data set. When the number of parameters is too great, the model may over-fit the data set and be therefore less able to generalise [Hay94]. This means that during the parameter estimation period the model no longer improves its ability to approximate the true output, but just starts to learn some random regularities contained in the data set [Sch97]. In that case the mapping is built to fit the data perfectly, thus the bias is zero, but the error variance might be high. The best way

to avoid the over-fitting problem is to use enough data in the parameter estimation and to limit the number of parameters as strictly as possible. This is equivalent to the empirical observation that the error on the new data set has a minimum where the generalisation ability of the model is best before the error again begins to increase [Sch97].

4.3.3 Generalisation improvement of neural network model

There are special methods, like regularisation, early stopping and neural network pruning, to avoid the over-fitting problem [Bis95, Lam97]. The regularisation and the early stopping methods can be used together in the procedure of model order selection. The neural network pruning method is always applied after the procedure of model order selection. The choice of neural network architecture and parameter estimation algorithm also affects the over-fitting problem.

Adding a regularisation term can change the error function of neural network parameter estimation. This is a function with a large value for smooth mapping functions (simple models) and a small value otherwise (complex models). Thus the regularisation encourages less complex models i.e. it is used to improve the generalisation [Hay94, Mat98b]. If a term that consists of the mean square error of neural network parameters (weight decay) is added to the original error function, some of the parameters will have smaller values. In this case the neural network response will be less likely to over-fit.

In the early stopping method the generalisation capability of neural network (validation error) is calculated during the parameter estimation process after each iteration [Lam97, Mat98b]. When the neural network begins to over-fit, the validation error will rise although the parameter estimation error decreases. If the validation error continues rising for a specified number of iterations, the parameter estimation process is stopped and the neural network parameters at the minimum validation error point are returned. In this method the neural network is usually over-parameterised. Despite this the neural network can generalise well enough.

The trial and error method is usually used in the choice of neural network architecture, but more advantageous methods like cascade correlation (growing method) and neural network pruning may also be used [Hay94]. A neural network model having many parameters generally requires a lot of data or else it will memorise well. On the other hand, a neural network model with too few parameters compared with the size and the complexity of the data may not have the capability to generalise at all. The trial and error method usually produces sufficiently good results but does not guarantee the best architecture.

4.4 Feature selection and extraction

The purpose of feature selection and extraction is to reduce the dimensions of the data. The addition of new variables leads to a reduction in the performance of the model beyond a

certain point. The improvement in model accuracy may compensate for the information loss if the right balance is found between the loss of information and the model generalisation capability [Bis95]. Adding more irrelevant variables may increase the noise to a level where it will exceed the useful information.

If each input variable is divided into intervals, then the total number of interval elements in the input space grows exponentially with the dimensionality of input space. Since each interval element in the input space must contain at least one data point, the quantity of data to specify the mapping also needs to grow exponentially. This is called the curse of dimensionality [Bis95]. A function approximation with a limited quantity of data provides a poor representation of mapping when the dimensionality of the input space is increased. This leads to a point where the data is sparse. The accuracy of the mapping can be improved by reducing the dimensionality of the input space. The feature selection and extraction methods are efficient for this task.

The feature selection and extraction methods presented here are the basic statistical methods based on variance and correlation, the principal component analysis and the K-means clustering method. These methods are commonly used and they have been known for a long time. There are numerous other feature extraction methods available like factor analysis [Joh92], partial least squares [Mar89] and independent component analysis [Hyv00]. The principal component analysis is probably the most widely known and applied method of these. That is why it is applied for model-based voltage stability assessment. Other clustering algorithms like ISODATA [Tou74] and the Kohonen self-organising feature map [Koh97] may also be applied to feature selection. Feature selection can also be based on search methods like the branch and bound method [Bis95], but they require a huge amount of computation to estimate parameters for different kind of input variable selections. The advantage of the ISODATA algorithm compared to the K-means algorithm is its ability to find the optimal number of clusters. However, this is not the primary concern of model-based voltage stability assessment. The Kohonen self-organising feature map may be applied to data visualisation.

The purpose of factor analysis is to describe the covariance relationships among variables in terms of a few underlying quantities called factors. Variables within a particular group are highly correlated but have low correlation with variables in a different group. Each group represents a single factor. Factor analysis can be considered an extension of principal component analysis, but the approximation based on it is more complicated [Joh92]. The partial least squares method is also similar to principal component analysis, which is why it is not separately tested. The advantage of partial least squares is its capability to consider the variation of outputs [Mar89]. Independent component analysis is a statistical technique for decomposing a complex data set into independent sub-parts [Hyv00]. It makes a linear transformation, which produces independent components that are maximally independent from each other and simultaneously have interesting

distributions [Hyv00]. All these feature extraction methods make linear transformation for the input data to represent it in a different co-ordinate system.

4.4.1 Statistical methods

In feature selection, the features that best describe the phenomena studied are chosen. Variables that have low variance do not explain changes in the system state [Bis95]. The redundant variables do not yield new information, because the same information is already given by other variables [Bis95]. It is natural to remove them from the data. Redundant variables can be recognised e.g. by correlation analysis.

4.4.2 Principal component analysis

Principal component analysis is based on the transformations that make it possible to reduce the dimensions of the data [Tou74]. It is presumably the most commonly used feature extraction method. The principal components are the linear combinations of the original variables.

The total system variability can be presented by a smaller number of principal components, because there is almost as much information in the first p principal components as there is in the original variables [Tou74, And72]. They represent a new co-ordinate system where the new axes represent the directions with maximum variability. The principal component analysis is based on input data $\mathbf{X}$ covariance matrix $\mathbf{R}$ eigenvalue decomposition. The covariance matrix can be represented by eigenvalues λ_i and eigenvectors $\underline{p}_i$. The number of original variables is m.

$$\mathbf{R} = \mathbf{X}^T\mathbf{X} = \lambda_1 \underline{p}_1 \underline{p}_1^T + \ldots + \lambda_n \underline{p}_m \underline{p}_m^T \tag{4.6}$$

The columns of the transformation matrix of principal component analysis $\mathbf{P}$ are eigenvectors $\underline{p}_i$. The new transformed input matrix $\mathbf{T}$, variances of new variables and covariances of new variables are presented in Equation 4.7. The new transformed input matrix can be calculated by multiplying the original input matrix by the reduced transformation matrix $\mathbf{P}_{\text{red}}$ (p is the number of selected principal components, $p<m$). The variances of new variables are the eigenvalues of the input data covariance matrix. The most important new variables are those whose variances, i.e. covariance matrix eigenvalues, are greatest. The first p principal components explain the variability of original input data almost completely. In addition, the new variables do not correlate with each other, because they are arranged in an orthogonal base.

$$\begin{aligned} &\mathbf{T} = \mathbf{X}\mathbf{P}_{red} = \mathbf{X}\left[\underline{p}_1^T, \underline{p}_2^T, \ldots, \underline{p}_p^T\right] \\ &\text{var}(\underline{t}_i) = \underline{p}_i^T \mathbf{R}\, \underline{p}_i = \lambda_i \\ &\text{cov}(\underline{t}_i) = \underline{p}_i^T \mathbf{R}\, \underline{p}_j = 0, \quad i \neq j \end{aligned} \tag{4.7}$$

Principal component analysis is good at data compression while retaining as much information on the original variables as possible. However, it should be used carefully in real-life approaches, because outliers with high noise level can make it useless. One possible solution for this problem is to feed input data through a filtering function or state estimator before principal component analysis. Sometimes linear transformation should not be used, because essential information about input data may be lost. Then non-linear transformation should be tried [And72].

4.4.3 Clustering

The purpose of clustering methods in feature selection is grouping together sets of similar variables. The advantages with large data sets are the ability to reduce the size of the data set and to find the most meaningful variables for the function approximation task.

K-means clustering is based on the concept of input vector classification by distance functions. K-means clustering is well known, because it is simple and can manage large data sets [Tou74]. It is based on the minimisation of the sum of squared distances from all points in a cluster domain to the cluster centre. It involves the following steps [Tou74]:

1. Choose K initial cluster centres $\underline{z}_1(1)$, $\underline{z}_2(1)$, ..., $\underline{z}_K(1)$. These are usually the first K samples of the data set.
2. At the kth iteration distribute the input vectors $\underline{x}$ among the K cluster domains, using the relation

$$\underline{x} \in S_j(k) \quad if \quad \left\| \underline{x} - \underline{z}_j(k) \right\| < \left\| \underline{x} - \underline{z}_i(k) \right\|, \quad i = 1,2,\ldots K, \quad i \neq j \tag{4.8}$$

   where $S_j(k)$ denotes the set of input variables whose cluster centre is $\underline{z}_j(k)$.
3. Compute the new cluster centres $\underline{z}_j(k+1)$ such that the sum of the squared distances from all points in $S_j(k)$ to the new cluster centre is minimised. This is simply the input variables' mean of $S_j(k)$. Therefore, the new cluster centre is

$$\underline{z}_j(k+1) = \frac{1}{m_j} \sum_{\underline{x} \in S_j(k)} \underline{x}, \quad j = 1,2,\ldots K \tag{4.9}$$

   where m_j is the number of input variables in $S_j(k)$.
4. If $\underline{z}_j(k+1) = \underline{z}_j(k)$ for $j=1,2,...K$, the algorithm has converged and should be ended. All input variables have found their clusters and will not change from one cluster to another. Otherwise go to 2.

The new transformed input matrix is formed from cluster centre mean vectors $\underline{z}_j(k+1)$. In this way the number of new input variables is K. The behaviour of the K-means clustering is influenced by the number of cluster centres, the choice of initial centres, the order in which the input vectors are taken and properties of the data [Tou74]. The algorithm will produce acceptable results when the data contain characteristic regions which are relatively far from each other. In practice, the use of K-means clustering will require experimenting with various numbers of clusters.

5 VOLTAGE STABILITY ASSESSMENT BASED ON BLACK-BOX MODEL

This chapter describes the proposed model-based approach for on-line voltage stability assessment. First the proposed method is introduced and compared to the security boundary method. An overview of the proposed method is given, previously proposed model-based approaches are briefly described, and general requirements of a model-based approach are given. The description of proposed approach is divided into three parts: automatic database generation, model creation and use of model-based approach. Good quality data is essential for the model-based approach. The data generation is based on systematic computation of operation and maximum loading points in off-line. The off-line model creation includes following steps: model type selection, data analyses, data pre-processing, estimation of model parameters, and testing of generalisation capability. The use of model-based approach includes integration and implementation issues of the proposed approach to the SCADA/power management system.

5.1 Introduction to the model-based approach

5.1.1 Overview of the proposed approach

The model-based approach was developed for on-line long-term voltage stability assessment, and the proposed method is based on function approximation. The function to be approximated is the mapping between the pre-disturbance operation point and the voltage stability margin of the most critical contingency. The approach includes both the off-line and the on-line stages. A detailed description of the proposed approach is given in Chapters 5.2-5.4.

The proposed approach is an application in the power management system while the application is a pool or a system-level application in order to assess the security of the whole power system. The model inputs are active and reactive line flows and bus voltages at a pre-disturbance operation point which are commonly measured in most power systems from almost all lines and buses. Using these inputs guarantees explicit input-output mapping at all operation points. The input variables can take into account changes in the power system load, production, network topology, unit commitment, etc.

Off-line stage

The off-line stage of the proposed approach is needed to generate the data and create the models. For a detailed description of the automatic database generation and the model creation procedures see Chapters 5.2 and 5.3 respectively. The data and the models are stored in a database to be used in on-line.

The automatic database generation is based on variation of operation points (see Chapter 5.2.1) and computation of the most critical voltage stability margins (see Chapter 5.2.2). The variation of operation points is based on heuristics and randomness of load, production, voltage control and operation practices. The analysis of operation points is done by load-flow computation. The ranking of contingencies is done for wide variety of operation points before the data generation in order to decrease the computation time of data generation stage, thus the computation of the most critical voltage stability margin includes only few interesting contingencies. The voltage stability margins are determined by the load-flow based on the proposed computation method of maximum loading point (see Chapter 3.2.4). The consideration of pre-disturbance network topologies and unit commitments increases the number of operation points to be studied. The clustering of pre-disturbance operation points based on network topology and unit commitment situations is applied to reduce the number of models.

Three different kind of models, linear regression (see Chapter 4.1.1), multilayer perceptron neural network (see Chapter 4.2.1) and radial base function neural network (see Chapter 4.2.3), are studied in this thesis. The step of model type selection (see Chapter 5.3.1) includes also the selection of model order (see Chapter 4.3.2). The data analysis (see Chapter 5.3.2) is needed to ensure the quality of data and to analyse the functioning and sensitivity of the system for variations in operation conditions. The data pre-processing step (see Chapter 5.3.3) includes consideration of relevance of model inputs, reduction of input vector dimension through feature selection and extraction (see Chapter 4.4) and normalisation of input vector. A candidate model is created by estimating model parameters (see Chapter 5.3.4), which is the numerical part of model creation procedure. The parameter estimation of the models is described in Chapters 4.1.1, 4.2.2 and 4.2.4. The final step of the procedure is the testing of generalisation capability (see Chapter 5.3.5). The black-box model should have capability to generalise (see Chapter 4.3) otherwise the accuracy of the model may be poor. The testing of generalisation should also determine the validity area of the model.

On-line stage

An overview of the proposed method in on-line stage is presented in Figure 5.1. Input variables (line flows and voltages) and information about network topology and unit commitment situation are supplied via SCADA system. The input data may be supplied through a state estimator in order to filter out bad data and to compute estimates for variables which are not measured. The data pre-processing includes normalisation of inputs

and reduction of the number of inputs in order to improve model generalisation capability. This reduction is accomplished by the feature selection and extraction methods (see Chapters 4.4 and 5.3.3). The on-line application of principal component analysis and K-means clustering require multiplication of transformation matrix and input vector and computation of cluster centres (e.g. average values of input variable groups) respectively, which are very fast. Finally a reduced number of inputs is supplied to the model to approximate the voltage stability margin. Several models are required to take into account the most probable combinations of network topology and unit commitment. The current network topology and unit commitment situation is used to choose (classify) the appropriate model (see Chapter 5.2.3). The response of the model-based approach is fast enough to estimate the voltage stability margin at every sequence of SCADA system and much faster if required.

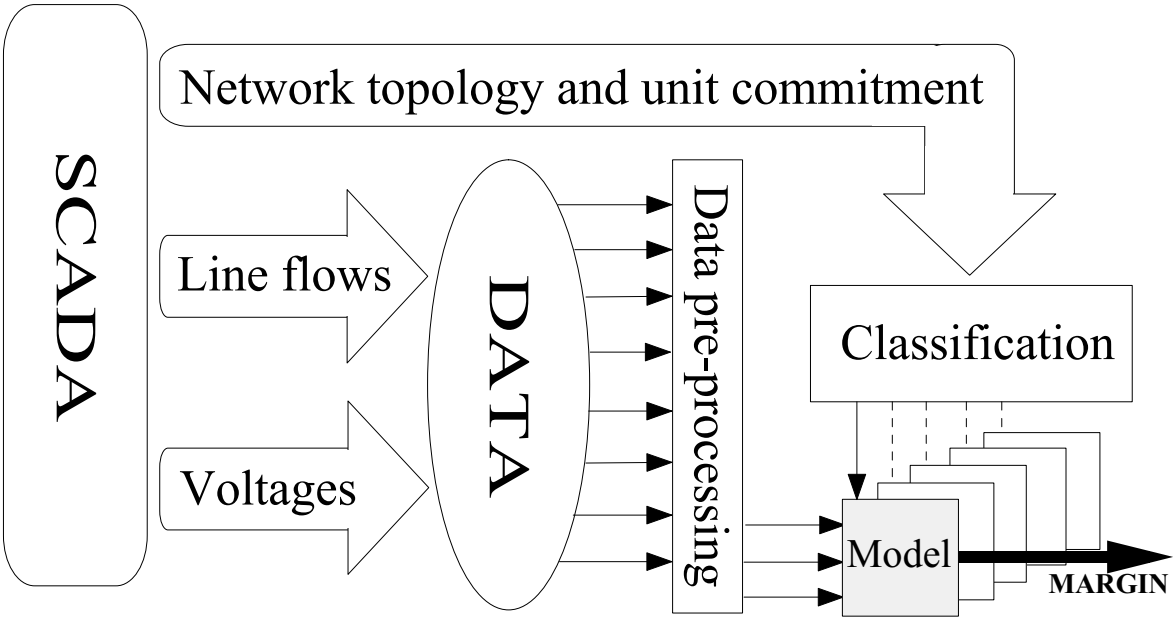

Figure 5.1. Model-based voltage stability assessment.

5.1.2 Comparison to the security boundary method

The security limits of a power system are commonly displayed to the operators by the security boundary nomograms (see Figure 3.3). The nomogram approximates the secure area. It is assumed that the post-disturbance state of a power system can be monitored with selected pre-disturbance parameters. The security limits are based on off-line computed post-disturbance security limits (see Chapter 3.1.3). The number of parameters is usually two or three. The security boundaries are typically computed in off-line using dynamic simulations. To reduce the computation burden, only few contingencies and operation points are studied to determine these limits. In the on-line mode the database is searched to find the most similar off-line computed operation point as the current operation point in the power system, and the corresponding security limit is applied to the current operation point.

The security boundary method does have some disadvantages arising from the limited number of operation points and contingencies used in off-line simulations. The actual operation point is probably different from those cases used in off-line simulations. Likewise there might be operation points where most critical contingencies are different from those used in off-line studies. Therefore two different kinds of approximations have been made in nomograms:

- the linear interpolation between the points of security boundary and
- the insufficient information contained in the selected parameters.

The linear interpolation problem is critical if the security boundary is non-linear, and the number of selected parameters cannot be high due to a representation problem.

The use of the security boundary method leads to a situation in which the power system security limits can be increased in some situations without compromising security if more accurate and up-to-date security limits are used. Due to these previous reasons the power system cannot be stressed up to maximum limit, but a relatively large reliability margin is needed when the security boundary method is applied. This margin is typically a few per cent of total capacity. To allow power transfer increase close to or beyond the security boundary, there should be the possibility to evaluate risks and uncertainties related to security limits. A model-based voltage stability assessment is introduced in this thesis to overcome these problems.

The model-based voltage stability assessment and the security boundary method are essentially similar. The security boundary is understood as a graphical model, but the proposed method is more general and accurate than the security boundary method. Furthermore, the proposed method includes automatic database generation and data pre-processing, which are not included in the security boundary method. The automatic database generation in particular is a major improvement compared to the security boundary method. The data generation part of the model-based approach is commonly omitted in published papers. However, the data generation determines the ability of the whole approach. Data pre-processing is also an essential part of the proposed method. The advantages of the proposed approach compared to the security boundary method are:

- the use of non-linear function approximation between pre-disturbance state variables and post-disturbance security limits
- the use of automatic data generation to overcome the problems caused by limited number of cases and contingencies
- the possibility to use as many variables in the description of pre-disturbance state as required.

5.1.3 Description of previously proposed model-based approaches

Most model-based approaches approximate the long-term voltage stability margin or index with multilayer perceptron neural network. However, there are plenty of other methods like

pattern recognition, expert systems, decision trees and fuzzy systems that are close to function approximation and are applied to on-line voltage stability assessment.

El-Keib and Ma [Elk95] used a multilayer perceptron neural network in voltage stability assessment defining the voltage stability margin by the energy function method. These scholars propose real and reactive power loads and outputs of generators applied as inputs to the neural network. The input vector reduction is accomplished by sensitivity analysis. The neural network was trained with the standard back-propagation method with momentum term and adaptive learning rate.

La Scala et al. [Las96] (and references [Sal95, Cor94]) defined a neural network based approach giving as outputs the voltage stability index for the whole power system and the load bus voltage stability margin for the most critical area. The number of required input variables is large including load powers and voltages, generator powers and voltages and a vector taking into account contingencies that may directly influence the voltage stability margin. This approach requires investigations on input variables to choose those variables that significantly affect the margin. The reduction of inputs is resolved by sharing the assessment of voltage stability among several neural networks. In the neural network parameter estimation a fast learning algorithm based on a least-squares approach was used.

Popovic et al. [Pop98] proposed an approach for voltage stability assessment using neural networks with a reduced set of input data. Hear the reduction of input data is accomplished using self-organised neural network. Neural networks are also used to detect the topology of the power system. The approach consists of a combination of neural networks where the topology of the power system is checked first, then the input data set is reduced and finally the voltage stability margin of considered topology is estimated using a multilayer perceptron neural network. The data for the proposed approach were generated with dynamic simulations. The input variables were voltage phase angles and magnitudes, generator powers and load powers. The standard back-propagation algorithm with momentum term and adaptive learning rate were used in the parameter estimation of multilayer perceptron neural network.

Some papers on dynamic security assessment have also been published, see references [Man97, Edw96]. The extension of the conventional method is a interesting security assessment method based on the security boundary function approximation with neural network [Mcc97, Zho99]. A neuro-fuzzy system has also been introduced for local voltage collapse prediction [Yab96]. Reference [Weh96] proposes a method for contingency severity assessment based on regression trees and a multilayer perceptron neural network. The approach based on the linear regression model proposed by the present author [Rep00b] is the first ever to appear in the literature. The books [Dil96, Weh98] provide an insight into several applications of neural networks and automatic learning techniques in power systems.

The identification of the power system state can also be based on pattern recognition. These methods were already applied in the seventies and eighties [Pan73, Dac84], but they do not provide information about proximity to the maximum loading point. A neural network based classification has been used to classify power system state as secure or insecure [Wee92]. Kohonen self-organising feature map based clustering has been used for the identification and visualisation of voltage weak areas in references [Son97, Weh95] and for voltage stability in reference [Reh99]. The reference [Sin95] has introduced pattern recognition and fuzzy estimation for security assessment.

5.1.4 Requirements of a model-based approach

Automatic data generation is an essential requirement for model-based voltage stability assessment. Monte-Carlo type simulation based on the systematic computation of operation and the voltage collapse points is required to generate the data automatically [Mcc98, Weh96]. The voltage stability margin is sensitive to almost every change in the system conditions that change the flow pattern of the base case. The automatic procedure guarantees good quality data when a wide variety of base cases, computation directions and contingencies are computed. The procedure should also include power system operation practices, a part of the model-based approach commonly omitted from published papers. Another drawback in the proposed methods is the treatment of network topology, unit commitment and contingencies. Some ideas have been put forward concerning this problem in references [Pop98, Wee92], but the number of the models in these methods is high, making them impractical.

Another important stage in the model-based approach is the selection of model inputs and outputs, the former being the statistical feature selection and extraction methods [Pop98, Wee92, Zay96, Muk96, and Rep00c]. The model requires sufficient and suitable inputs for the accurate approximation in the wide range of operation points. The mapping function between inputs and output should be explicit. It is not possible to create explicit mapping based on the bus injections and voltages as in many papers suggest, due to the network topology changes. The model output should be a post-disturbance index, which is the most valuable measure for the power system operator from the power system operation and security perspective.

The model-based approach to voltage stability assessment is most commonly based on neural networks due to their capability to approximate non-linear functions. Many of the previously mentioned papers note that the parameter estimation of neural network is time-consuming. Although the parameter estimation of a neural network is much more time-consuming than, for example, the parameter estimation of a linear regression model, it is not really a limitation for the use of a model-based approach. Computation capacity and power have increased remarkably since most of the previous papers were written. The use of feature selection and extraction methods for the reduction of model inputs decrease

the time required for the neural network parameter estimation significantly. Using second order optimisation algorithms in the parameter estimation of a multilayer perceptron neural network has also improved the situation.

5.2 Automatic database generation

Model creation needs a lot of good quality data to ensure good generalisation capability. The data is computed in this case for two reasons:

- formulation of good quality data from measured values is difficult and time-consuming
- a suitable power system model, however, is needed to compute the voltage stability margins.

Model creation is based on the operation points and the voltage stability margins computed off-line. The data should include all possible network topology, unit commitment, production and loading situations. Power system control and operation practices should also be included in the data generation algorithm to ensure good quality and realistic data. The data should cover operation points both common and rare throughout the operation space. A rare operation point can be e.g. a typical loading situation covered with an untypical generation dispatch. Good quality data is indispensable to an accurate model.

The computation of a data set is done automatically [Rep97], and is essential for large-scale power system studies. It is based on systematic computation of operation and maximum loading points. A load-flow program using a combination of random changes and heuristic rules creates the input data. Computing maximum loading points for chosen contingencies and computation directions creates the output data.

5.2.1 Variation of operation points

The left hand side of Figure 5.2 presents a diagrammatic plan for automatic data generation. To ensure good quality data network topology, unit commitment, loads, production, compensation and transformer tap settings etc. should be varied. For a detailed consideration of network topology and unit commitment in the model-based approach see Chapter 5.2.3.

Variation of load and production

The variation of operation points is based on the random variation of loads and production. The randomness of the variation process should be strong enough to fulfil the operation space of the power system, or then the operation space must be restricted to a small area. The variation procedure should also ensure that operation space does not overlook certain parts of operation space, i.e. the data of operation points should not include gaps. However, purely random variation should not be used, but the experience of power system functioning should be included for the algorithm.

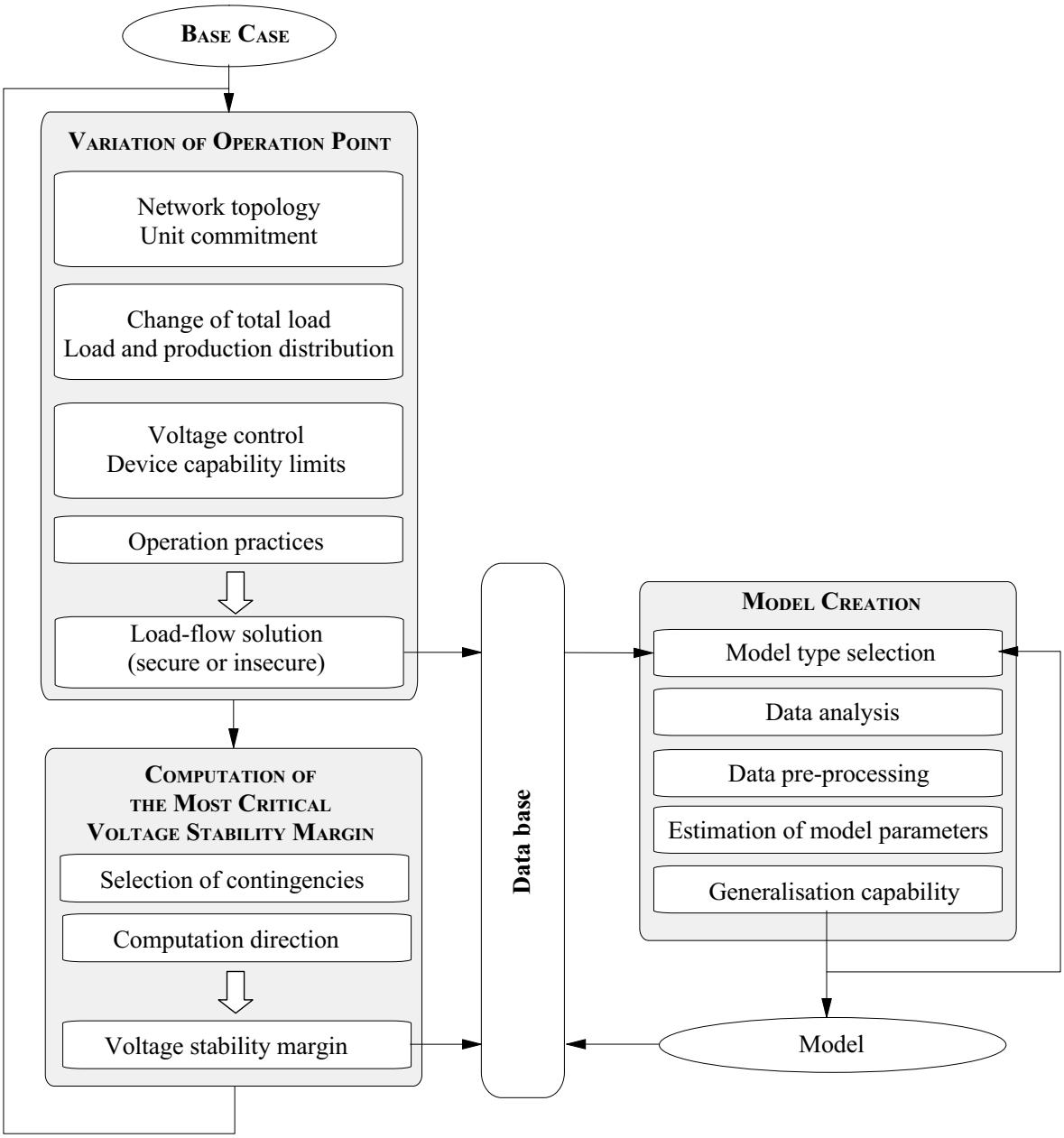

Figure 5.2. Automatic data generation and model creation.

The change of total load is varied with a normal distribution random number generator and added to the base case load. The total load should be varied at least between annual maximum and minimum. Sometimes it might be advisable to generate separate data for each season, thus enables seasonal characteristics of load to be taken into account more precisely. On the other hand unstable cases i.e. cases having zero voltage stability margins should also be included. The change of total load is divided into loads by three different methods: randomly, an equal amount to each load or an amount proportional to the base case load. These methods are used sequentially in automatic data generation. The reactive power load is chosen randomly between certain limits (e.g. $0.06<\tan\phi<0.26$). The modelling of loads should be considered carefully. The use of constant power loads yields pessimistic results compared with voltage dependent loads (see Chapter 2.2.3).

Change in total production is equal to change in total load. The change in production is directed to small units, because it is assumed that large units are base load units, i.e. they produce fairly constant power. The change of total production is divided among generators randomly or proportionally to the maximum active power of the generators. The active power limits of generators, both minimum and maximum, must be taken into account. The procedure of operation point variation should include a logic which also produces cases where the active power output of the generator is zero (operates as a synchronous compensator), instead of limitation of output to the minimum limit in each case.

The modelling of generator reactive power limits and their effect on voltage stability are described in Chapter 2.2.3. Traditionally load-flow programs have presented these limits as constant reactive power limits. The assumption of constant limits is not accurate enough in detailed analysis, therefore voltage dependence of the reactive power limits should also be considered. Some programs use checking activities to be used after the computation of load-flow to check the loading of generators (e.g. activities GCAP and GEOL in PSS/E [Pow00a]).

Control actions (first load-flow)

The new power system situation is calculated by a load-flow. The load-flow model should include generator capability limits, transformer tap ranges, compensation ranges and discrete controls for tap changers and switched shunts. In that case the solution of load-flow provides realistic values for the amount of switched shunts, the position of transformers on-load tap changers and the reactive power production of the generators. The modelling of these devices on the commercial load-flow programs is usually appropriate for long-term voltage stability studies.

Operation practices (second load-flow)

The production of slack bus and the network losses are known after the solution of load-flow. The additional network losses (compared to base case) are distributed to all generators to vary the production of constant power units. If the production of slack bus does not fit within certain limits, the production of constant power units is further changed. The production of constant power units is allowed to change within specified limits (usually a narrow range close to maximum limit).

The consideration of operation practices requires manual control actions. This entails settings of generator transformer tap position, manually switched compensation devices and manually switched transformer taps. Changes in the setting of generator transformer tap positions are exceptional. The probability of that change should be low and related to situations bordering on insecure operation. This is not actually implemented in the data generation system. A minimum singular value of load-flow Jacobian matrix [Löf95a] is a possible means of ascertaining the severity of a new situation.

Manually switched compensation devices and transformer tap settings are frequently changed. The settings of transformer taps are changed randomly between the maximum and the minimum limits with normal distribution random number generator. The manual control of these devices is usually based on voltage level in the transmission network and/or reactive power flow through EHV/HV transformers. The operation of most compensation devices is automatic, but the manual switching of these devices may on occasion be necessary. A common operation practice is to operate generators connected to the EHV network with $\cos\phi=1$ control, i.e. these units do not produce reactive power in normal conditions. Changing the settings of manually switched compensation devices can clear these reactive power reserves.

A new load-flow is needed to verify the results of manual controls and operation practices. The solution of the second load-flow is stored in the database. Such a situation is called normal operation point. These solutions are the model input data. If any contingency load-flow does not converge, the operation point is included in the model input data as a case having a zero voltage stability margin.

5.2.2 Computation of the most critical voltage stability margin

The most critical voltage stability margins are calculated using the maximum loading point method described in Chapter 3.2.4. The maximum loading point can be used to approximate the voltage collapse point quite accurately [Rep97].

Selection of contingencies

The computation of voltage stability margins is performed for chosen contingencies. The selection of contingency is done beforehand to reduce the computation burden during data generation. The selection of the contingencies is based on the contingency ranking methods described in Chapter 3.3.3. Sufficient operation points should be studied in contingency ranking to cover as many kind of operation points as possible. The knowledge of experienced planners and operators may also be exploited. The contingency ranking produces a contingency list for use during data generation. A long contingency list increases the computation time, while a short list might ignore serious contingencies in certain operational conditions.

Computation direction

The most critical voltage stability margin is computed by gradually increasing the load and the production in the specified computation direction. The direction is usually chosen to increase the power transfer through a certain intersection in order to compute the available transfer capacity. Increasing the load in one area and the generation in the adjacent areas yields the load and generation increment. In this way the transmission capacity is determined in one specified direction in a multidimensional operation space. Sometimes the total load is not changed at the computation of available transfer capacity, but the

distribution of production is rearranged in order to determine the maximum power transfer between production areas (see Chapter 3.2.1).

Consideration of the maximum active power limits will cause changes in the computation direction when a maximum limit of a generator is reached during the computation of maximum loading point. In that case the element of computation direction vector corresponding to the generator at the maximum limit must become zero and the share of other elements must increase. This share is found by normalising the new computation direction vector, while the proportions of generators remain unchanged.

The choice of proper computation direction is usually based on experience of power system operation. Restriction of power transfer between different areas of the power system due to a few limiting intersections may occur, but in general there still exist many different possibilities to increase load and production in these areas. One possibility to choose the computation direction is to find the direction corresponding to the minimum voltage stability margin. This can be determined based on eigenvalue analysis of maximum loading point of initial computation direction [Dob93]. An iterative procedure is then used to find a computation direction corresponding to the minimum voltage stability margin. The new computation direction is found in the direction of the normal vector to the tangent vector of the maximum loading point. The normal vector is the left eigenvector of the load-flow Jacobian matrix at the maximum loading point.

The computation direction corresponding to the minimum voltage stability margin represents the worst case, which is dependent on the power system operation point and must be determined separately for each operation point. Another possibility to choose the computation direction is presented in Figure 5.3, showing a system of two generators. If the increased demand is totally taken by generator 1 or 2, the corresponding directions 1 or 2 must be used. Direction 3 represents a case in which both generators respond to equal amounts of the demand. Directions 1, 2 and 3 are parallel at both operation points but the directions of the minimum voltage stability margin are not. The actual operation of the power system is probably close to computation direction 3, where both generators share the increased demand. However, when we study the available transfer capacity of a certain intersection, it is appropriate to consider different computation directions to take into account uncertainties related to the effects of the electricity market. From that point of view it is necessary to compute voltage stability margins in different directions from a common operation point, when the same amount of computation can be used more productively than in the case of minimum voltage stability margin.

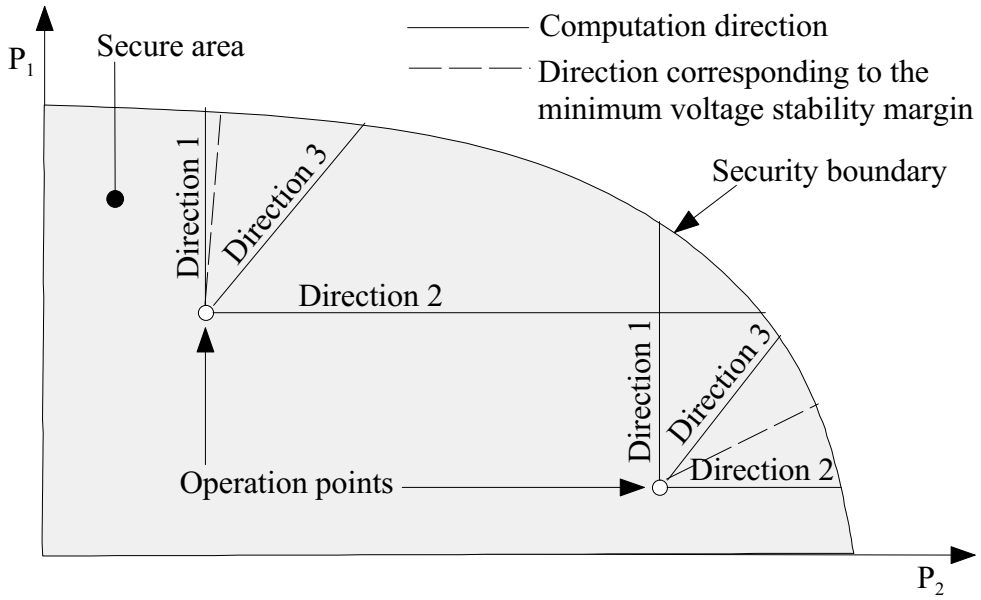

Figure 5.3. Presentation of computation directions in a two-dimensional case.

The most critical voltage stability margin

The most critical voltage stability margin corresponds to a situation where the load-flow of the most critical contingency still converges, but the next step will produce an unstable situation. The procedure of the most critical voltage stability margin is based on simultaneous computation of maximum loading point for chosen contingencies. The computation algorithm and the advantage of simultaneous method are shown by an example in Figure 5.4. The white circle indicates converged load-flow, while the black circle shows the divergence of load-flow. The example has the following steps in increasing demand:

1&2. The solutions of load-flow at the post-disturbance operation point and at the computation steps 1 and 2 are successful in all contingency cases.

3. The load-flow of contingency 3 does not converge at step 3, thus the step length of maximum loading point algorithm is halved to compute more accurate results.
4. The solution of load-flow is successful for both contingencies 3 and 4 at step 4. The load-flow computation for contingencies 1 and 2 is not required, because they converged at step 3, which had higher demand. These contingencies can likewise be omitted at step 5, because the demand is equal to step 3.
5. The load-flow of contingencies 3 and 4 converges at step 5. This is not exceptional, because the convergence of load-flow is dependent on changes in state variables of load-flow algorithm. If the step length of maximum loading point algorithm is too large, the load-flow may diverge although this is not an unstable situation. In that case the divergence of load-flow is caused by numerical problems.
6. All contingencies have a load-flow solution at step 6.
7. The load-flow of contingency 2 diverges at step 7, and the step length of maximum loading point algorithm is again halved.
8. The load-flow of contingency 2 does not converge at step 8.

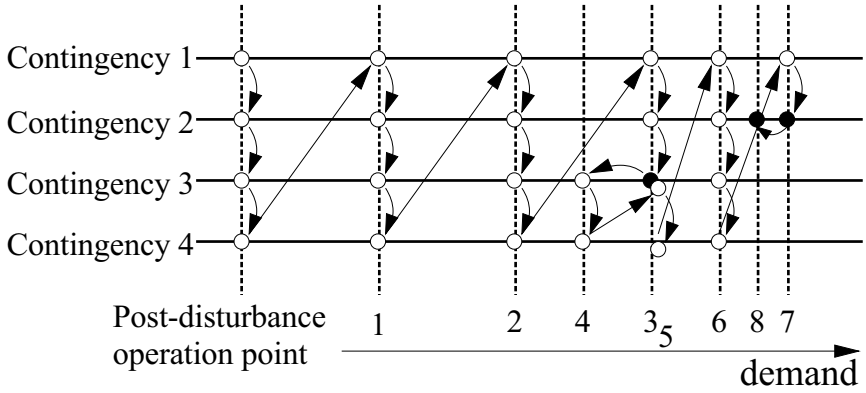

Figure 5.4. Example of the computation of the most critical voltage stability margin.

The maximum loading point corresponding the most critical contingency is step 6, the last step where all contingencies converged. The algorithm could be continued unless contingency 2 converges or the minimum step length of maximum loading point algorithm is reached.

The advantage of the proposed method is the ability to recognise the numerical problems of load-flow. When the load-flow diverges, the halving of step length ensures that this is not due to numerical problems. In the proposed method most of the load-flow cases converge making it fast. In practice, the computation time of one diverged load-flow corresponds roughly to the time of ten converged load-flows.

Modelling of reserves

Here we discuss the active and reactive power reserves of long-term voltage stability studies. These reserves activate due to a disturbance, thus they are applied only in the computation of maximum loading point. It is reasonable to assume that spinning reserves have fully operated in the time frame of long-term voltage stability studies. On the other hand there is a possibility that slower reserves have already released some part of spinning reserves in the study period. In that case these slower reserves should also be considered. The modelling of reserves is straightforward in these studies, the goal being to describe the distribution of power production after the disturbance. Given adequate active power reserves, the production of generators providing the reserve capacity should only be changed due to disturbance. This must be taken into account when considering the share of additional losses and production outage due to a disturbance. In long-term studies it can be assumed that the effect of instantaneous reserves has already disappeared due to generator control actions, thus there is no need to share the additional production caused by a disturbance among all generators.

The instantaneous response of reactive power reserves is determined by automatic voltage control. Such reserves are cleared by switching reactive power compensation. The response time of automatically switched shunt capacitors and reactors in Finland is a few

minutes, which is small enough to be considered in long-term voltage stability studies. Automatically switched compensation devices should therefore be taken into account in the computation of maximum loading point.

5.2.3 Consideration of network topology and unit commitment

The data should include cases from all most probable network topologies and unit commitment situations. However, changes of network topology and unit commitment are not frequent and not all combinations are possible in practice. Changes of network topology can be based on the statistics of line outages and the maintenance scheduling. Total load, electricity market and maintenance scheduling mainly determine the unit commitment changes. The consideration of network topologies and unit commitments increases the number of situations to be studied.

If the data includes only cases from a healthy network (all lines and generators connected), the model cannot be used, for example, during the important transmission line maintenance period. On the other hand it is not practical to create one's own models for each possible network topology and unit commitment combination. The proposed approach is based on a few parallel models: The main attention in the proposed method can be focused without loss of accuracy on the most probable and severe network topology and unit commitment cases instead of all possible cases. This is really important in practical applications, because the number of network topology and unit commitment combinations can thereby be reduced significantly in this way. In practice it is adequate when the outage of the largest production units and most important transmission lines are considered continuously in the on-line voltage stability assessment.

Uncommon cases (e.g. maintenance of certain lines and production units) can be taken into account separately. This means that they are not modelled for all different kinds of operation points, but are modelled individually each time when needed. This procedure significantly reduces the amount of off-line computation. If the generalisation capability of any model is not good enough for a certain maintenance case, it is possible to create a temporary model just for a maintenance period. Predicting the operation situations of the maintenance period can reduce the data generation and model creation time, when the data generation can be focused for a narrow predicted area of operation space.

Clustering can reduce the number of parallel models required. Each cluster includes similar network topologies and unit commitment situations from the voltage stability point of view. The model for the most critical voltage stability margin is then created for each cluster, thus enabling a significant reduction in the number of models. The outage list of transmission lines and generators is used to choose the appropriate model for the current operation point. The rules for the selection of the appropriate model can be simple, such as "choose model x, if one of the generators y_1, y_2 or y_3 is out".

5.3 Model creation

5.3.1 Model type selection

Modelling is started with model type selection (right hand side of Figure 5.2). Although the voltage stability problem is a non-linear phenomenon, it does not mean that linear models (see Chapter 4.1) are not capable of approximating the function between the pre-disturbance operation point and the most critical voltage stability margin. The linear model is linear in respect of its parameters. The function approximated by the linear model can be non-linear. Likewise the non-linear model is non-linear in respect of its parameters.

Neural network models (see Chapter 4.2) are interesting, because they are capable of accurate non-linear function approximation and they tolerate noise in inputs. Most of the model-based approaches are based on neural network models, but the estimation of neural network parameters is time-consuming compared to the parameter estimation of a linear model. The estimation of confidence limits of a neural network requires the use of a Bayesian framework [Bis95]. Linear models are widely used in many other applications. They are also capable of non-linear function approximation and the estimation of confidence limits is straightforward.

Three different kinds of models (linear regression model, multilayer perceptron neural network and radial base function neural network) are applied for on-line voltage stability assessment in the thesis.

1. The linear regression model is selected to
   - determine if the linear model has enough flexibility to approximate the function between the pre-disturbance operation point and the most critical voltage stability margin
   - offer a reference for non-linear models.
2. The multilayer perceptron neural network is selected to
   - apply a flexible and widely used non-linear model for the problem
   - compare the proposed method with methods proposed earlier in the literature.
3. The radial base function neural network is selected to
   - test another widely used non-linear model for the on-line voltage stability assessment.

The choice of model type is based on experiment consisting of the whole model creation procedure, which is repeated until a satisfactory model is found. If the performance of the model is not good enough, the reason may be insufficient amount of data, low quality data, inadequate and/or incorrect inputs or problems in parameter estimation. Usually the linear model is applied first. If the capability of the linear model is good, then the application of more complicated non-linear models is not necessary. The order of polynomial model (linear model) and the number of neural network hidden units are found by trial and error.

5.3.2 Data analysis

The second step is the analysis of data. The analysis of data is used to obtain knowledge that will be used to solve the problem. The data analysis is sometimes called data mining, i.e. the process of extracting valid, unknown and useful information from databases [Ola99]. The input data in this approach cannot on the whole be easily modelled or analysed due to its high dimensionality. Therefore, methods capable of analysing the nature and the structure of the data become a necessity. Data visualisation and the feature selection and extraction methods would be useful for understanding the data.

The data analysis also includes removing of outliers or corrupted data, and data division into training, validation and test data sets (these terms are used in the neural network literature). The training data set is used in the parameter estimation and is the largest data set. The validation data set is used in the selection of model type and order, i.e. when different models are compared to choose the best one. The test data set is used to test the generalisation capability of a chosen model. The division of data sets should be done randomly. The outliers are clearly erroneous data points possibly due to measurement or computation errors. If the data includes wide variations, the generalisation capability of the model can be improved, if distant or “difficult” data points are removed. Unless they are erroneous the removal of these data points is data manipulation, which is an unpleasant and artificial way to create a good model. It is always possible thereby to create a model having the desired characteristics, but the functions presented by the original and manipulated data are not the same.

The generalisation capability of the model is based on the data, which should include all necessary information to create an accurate model. Good quality data have both quantitative and qualitative requirements, and should cover all kinds of operation points, including the necessary variables for appropriate function approximation, the operation points being distributed uniformly into the operation space. If the data does not cover the whole operation space studied, the model tries to extrapolate. The extrapolation capability of the models studied is poor. Although the number of possible operating states is infinite, parameter estimation needs only a reasonable amount of data consisting of typical operating states. The data boundaries must be remembered because the models do not have the ability to extrapolate. There is a risk of a completely incorrect conclusion about the power system voltage stability if the model generalisation capability is not tested carefully. The data boundaries are mainly characterised by network topology and unit commitment.

5.3.3 Data pre-processing

The model input vector consists of active and reactive line flows and voltages. The variables chosen for the inputs describe transmission network and voltage stability phenomena. These inputs also have a direct influence on the output. However, the input space dimension should be kept small to avoid dimensionality problems (see Chapter 4.4). This becomes more important when studying large power systems. The pre-processing of

data becomes much simpler when information about the phenomena studied, is available for the selection of inputs. Considerations in the selection of input variables for on-line voltage stability assessment were that

- the voltage stability margin is sensitive for changes at network topology and unit commitment
- a transmission network cannot be described explicitly with regard only to bus injections
- line flows consist of bus injections and network topology
- voltage stability is related to those cases in which a large amount of power is transferred across the system or the system is operated in stressed condition
- voltage instability is due to difficulty in transferring reactive power over large reactance, which is seen as voltage decline.

Feature selection and extraction

When the dimension of input space is large, the model uses almost all its resources to represent irrelevant portions of the data space. The number of inputs must be reduced to improve the model generalisation capability and to decrease the training time of the neural network model in large-scale applications. The aim of feature selection and extraction is to find features to represent the voltage stability margin by a small number of inputs. The number of variables can be reduced as long as the power system operation states can be reliably separated from each other according to approximated function. The complexity of the model may be significantly reduced when the number of inputs is reduced. This may also improve the performance of the model. The selection of inputs can be made based on empirical knowledge as described above or by using statistical feature selection methods. The number of inputs can also be reduced by feature extraction methods.

The procedure used in the feature selection and extraction in the thesis is as follows:

1. Statistical methods described in Chapter 4.4.1 are first applied to remove variables which do not have enough variance or which correlate with each other.
    - The variance is used to remove variables which are constant. The value of critical variance is dependent on the scale of the variables. If the scale of line flows and voltages is different, different values for critical variances should also be used.
    - The variables with high positive correlation are redundant, thus only one variable should be left in the inputs and the others should be removed. The analysis of the large-scale correlation matrix is difficult, but a first sight into the correlation matrix is obtained via a contour figure of the correlation matrix.
2. Either principal component analysis (Chapter 4.4.2) or K-means clustering (Chapter 4.4.3) is then applied to reduce the number of variables and to extract the information in the data.
    - The application of the principal component analysis is straightforward and structured. First the mean values of input variables must be removed, otherwise the first principal component would explain the mean of the data. Then the

principal components are computed (Equation 4.6). The transformation matrix of Equation 4.7 includes the chosen principal components. The number of chosen principal components is dependent on how much the variability of original data needs to be explained. Usually the few first principal components correspond to over 90 % of the variance cumulation of original variables. The most important principal components are those which correspond to the new variables whose eigenvalues on the covariance matrix are greatest.

- K-means clustering is used to group similar variables. Active and reactive line flows and voltages need to be grouped separately because the grouping of active line flows and voltages, for example, is not meaningful. First the number of clusters for each type of variables is decided. Then the clustering algorithm is tested a couple of times in order to eliminate the influence of the choice of initial centres and the order in which the input vectors are taken. The most difficult part of the procedure is to decide which clustering results will be used in the modelling. The visualisation of clustering results and knowledge of the system and problem studied is required in this step. Finally the cluster centres or the variables representing the clusters are selected as new data.

Normalisation

Usually the raw data is normalised, standardised or re-scaled before modelling [Sar01]. Re-scaling a vector involves adding or subtracting a constant and then multiplying or dividing by a constant. Normalising a vector involes dividing by a norm of the vector, to make the Euclidean length of the vector equal to one. Standardising a vector means subtracting a measure of location and dividing by a measure of scale. Hereafter the term normalisation is used to refer to any of these methods. The usefulness of normalisation of input or output variables is based on its capability to make the parameter estimation process better behaved by improving the numerical condition of the problem [Sar01].

It is possible to normalise the cases or the variables, but here only the normalisation of variables is considered. If the vector contains random values with a Gaussian distribution, one might subtract the mean and divide by the standard deviation, thereby obtaining a random variable with a mean zero and standard deviation of one. Normalisation of cases should be used with caution, because it discards information. If that information is important, then normalisation of cases can be disastrous.

There is a common misconception that the inputs to a multilayer perceptron neural network must be in the interval [0,1]. It is better to have the input values centred on zero than in the interval [0,1]. The normalisation ensures that various default values involved in the initialisation of parameters and termination of algorithm are appropriate. The normalisation of inputs also removes the problem of scale dependence of the initial parameters, i.e. avoids saturation of parameters with bounded intervals. The input variables of multilayer perceptron neural network are combined linearly. It is rarely strictly necessary to normalise

the inputs, because any normalisation of an input vector can be undone by changing the corresponding parameters. In practice, the normalisation can make parameter estimation faster and reduce the risk of getting stuck in local optima [Sar01]. The normalisation of input variables also has different effects on different parameter estimation algorithms for multilayer perceptron neural networks. The first order optimisation methods are generally more scale sensitive than the second order methods.

When the input variables are combined via a distance function in a radial base function neural network, the normalisation of inputs can be crucial. The contribution of input is heavily dependent on its variability compared to other inputs. It is important to normalise the inputs so that their variability reflects their importance [Sar01]. If some input is more important than others, it is normalised to larger variances or ranges than others. In many cases the importance of inputs is unknown, so inputs are normalised to the same range or standard deviation.

If the output activation function has a range of [0,1], then one must ensure that the output estimate values lie within that range. Generally it is better to choose an output activation function suited to the distribution of the outputs. Commonly, if the output variable does not have known upper and lower bounds, the output activation function of multilayer perceptron neural network should be unbounded i.e. a linear function [Bis95]. Normalisation of output variables is used to make sure of good initial parameters. If there are more than one output and the error function is scale sensitive (e.g. means square error function), then it is useful to normalise outputs so that their variability reflects their importance [Sar01]. If the importance of outputs is equal, then it is typical to normalise them to the same range or to the same standard deviation.

5.3.4 Estimation of model parameters

The estimation of model parameters is straightforward when the data analysis and the data pre-processing are done properly. The training data is used in the parameter estimation and the validation data should be used in the model order selection. This step also includes the selection of model type and order. The algorithms of parameter estimation are described briefly in Chapters 4.1.1, 4.2.2 and 4.2.4. The solution of parameter estimation of the linear model is usually explicit. However, the estimation of neural network parameters must be computed a few times in order to eliminate the effect of guesses of initial parameters.

The model order selection is basically an optimisation problem. Usually sufficiently accurate results can be achieved by systematically estimating the parameters of many different kinds of small size models. The model order selection of a neural network model is actually simpler than that of a linear model. In the case of a neural network the model order selection requires only the selection of the number of hidden layer nodes or base functions. The model order selection of the linear model is also substantially related to model type selection. The model order selection becomes much simpler when only one

type of linear model, e.g. a polynomial model, is considered. In that case the model order selection is an optimisation process of selecting the degree of polynomial function.

In the case of a multilayer perceptron neural network the parameter estimation algorithm should also be chosen. According to many test results second order optimisation algorithms are preferable to first order optimisation algorithms although they require more computation power and capacity [Rep00c, Mat98b]. The Levenberg-Marquardt method has been noted the most effective method for many cases. The scaled conjugate gradient method is the best for large-scale applications. Generalisation capability of neural networks can be improved with the special methods described in Chapter 4.3.3. These methods are applied in the parameter estimation step.

5.3.5 Generalisation capability

The final and most important step is the testing of generalisation capability. Computing outputs of the chosen model using inputs of the test data does the testing. Computing the confidence limits may approximate the reliability of the model. The determination of the model validity area is also important, because models are not capable of extrapolating (see Chapter 5.3.2). The over and the under-fitting problems of model generalisation capability are described in Chapter 4.3.2.

The residual of the model output is not actually an error. It should be considered as an uncertainty of the model output, a measure of model accuracy. The values of residuals are combined into a single measure using e.g. a sum square error or a mean square error. The model may be more accurate for some inputs than it is for others. The residual is caused by one of three different reasons:

- the training data may not include the information required to create the model
- the model may be incorrect
- the model should only be used within the operating range determined by the training data.

It should be noted that zero residual will be never achieved. The solutions to increase the accuracy of the model are to collect more data, to create a new model or both of these. Residuals, which appear in some cases but not others, might be caused by insufficient amount of training data at certain areas or by test data which falls outside the training data. Normally the training data is not uniformly distributed to the operating space. If the data is normally distributed, the density of data decreases at the distant areas. If the operating space of the model is kept as wide as the data space, then there might appear large residuals at the distant areas. However, the operating space of the model may be restricted in order to improve the accuracy of the model. This is not a problem in the present application, because there is always the possibility to compute more data points for the areas where the density of points is not high enough.

5.4 Use of the model-based approach

5.4.1 Integration to the SCADA and power management system

The openness of databases, the possibility to export and import information between software programs and the standardisation of application interfaces at the SCADA/power management system improve the possibility to apply a third-party software for power management systems [Vaa01]. The proposed voltage stability assessment approach is an application in SCADA and the power management system (see Figure 5.5).

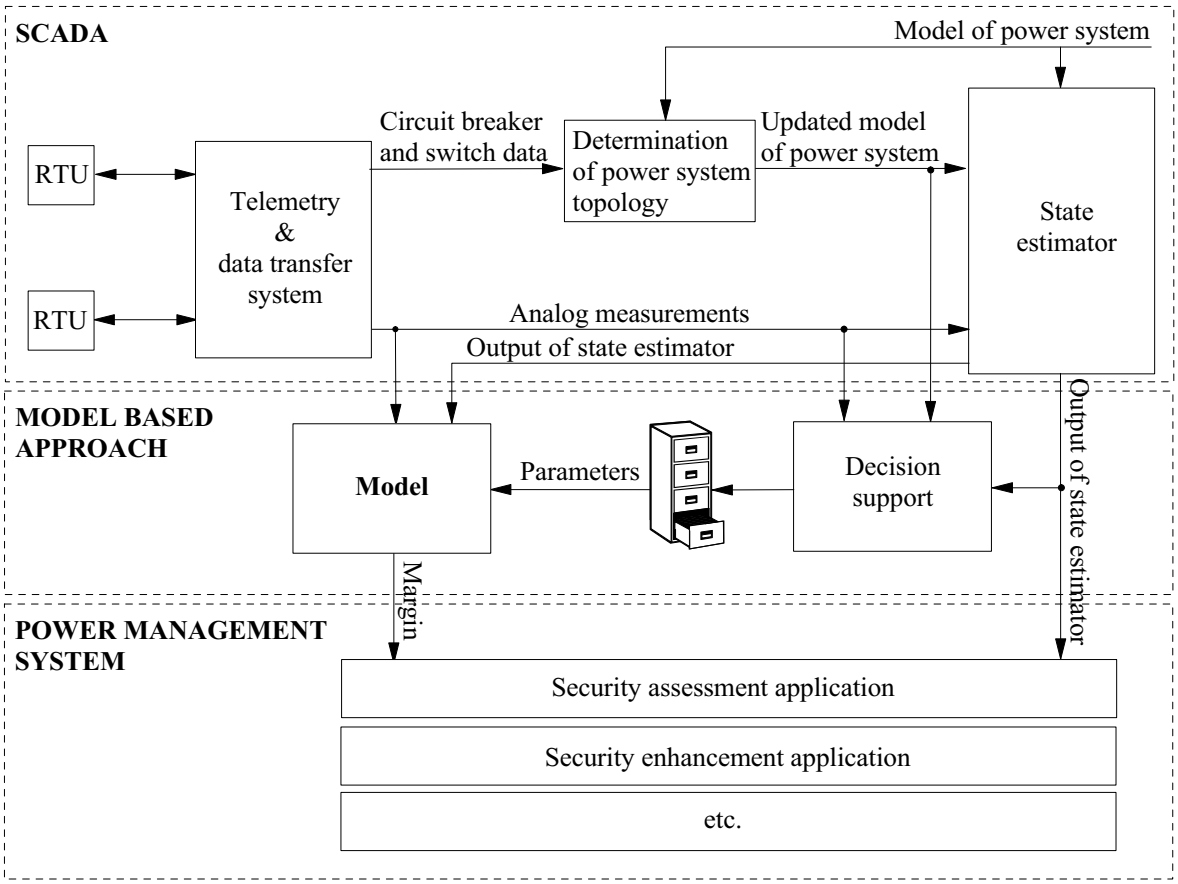

Figure 5.5. On-line implementation of the model-based approach.

The data needed in the on-line application is gathered via the SCADA system. The sequence of measurements is given to the model-based approach to estimate the post-disturbance voltage stability margin of a given situation. The state estimation program can be used to provide better input estimates than raw SCADA measurements for the model. The response of the model-based approach is fast enough to estimate the voltage stability margin of all measurement steps. The application would be implemented to power management system as a third party software.

The transformation matrix of the pre-processing stage, the parameters of the models and the decision rules for choosing an appropriate model for the current operation point are stored in a database. The updating of these does not require special interface, because the interface of the database program may be used. Decision support logic is used to choose

the appropriate model for the current operation point. The logic is based on the updated model of the power system (updated network topology and unit commitment) and the current operation point. The decision support logic, as described in Chapter 5.2.3, checks if the power system condition has changed and which model should be used. Based on this logic the appropriate parameters and the transformation matrix are sent to the modelling function. This function estimates the voltage stability margin, i.e. computes the output of the model. The margin is visualised in the power management system, e.g. at the security assessment application.

The sampling of input variables is 5-10 s, which is fast enough for long-term voltage stability assessment. If the proposed model-based approach for long-term voltage stability assessment is applied to short-term voltage stability assessment, the sampling frequency of the SCADA system may not be high enough. However, the use of phasor measurements via wide area measurement system [Bha99] and synchronisation will increase the accuracy and the sampling frequency of model inputs.

5.4.2 Updating of the models

The reliability of the model-based approach may be improved by taking into account major changes in the power system. Occasionally the accuracy of the model-based approach is checked by computing an exact voltage collapse point of a given situation and comparing the accurate and the estimated results (see Figure 5.6). The advantage of the model-based approach is its fast response compared to the computation time of the exact voltage collapse point. The on-line computation algorithm of the exact voltage collapse point may be used in parallel with the model-based approach. The accuracy of model output may be checked as often as the exact voltage collapse points are computed (on-line updating). Another possibility is to compute the exact voltage collapse point as often as major changes appear in the power system (off-line updating). In that case the algorithm of the exact voltage collapse point must not be an on-line implementation. Many other possibilities also come to mind, which are probably more useful for a specific case.

Figure 5.6 presents the updating procedure of the model-based approach. The on-line updating is part of the third party program of the model-based approach. The exact voltage collapse point is computed as often as possible. The data is supplied through the state estimator because load estimates are needed. The computation direction is obtained from the database. The monitoring of the estimation residual compares the exact voltage collapse point and the corresponding estimate of the voltage stability margin. The estimates of the model and the exact voltage collapse point of same instant are stored in the database in order to monitor the trend of the estimation residual. The updating of parameters is not frequently used, because the estimation residual should take a clear turn for the worse in order to update the parameters. The monitoring of the estimation residual must consider the long-term history of the model, otherwise occasional but large residual might cause unnecessary updating. If the residual increases enough for a long time, then

the parameters of the model are re-estimated. The parameter estimation is done off-line in order to separate these procedures from each other. This makes it possible to use general statistical analysis software or a multipurpose development environment like Matlab. The data for parameter re-estimation is the previously used data plus the results of exact voltage collapse points that are stored in the database.

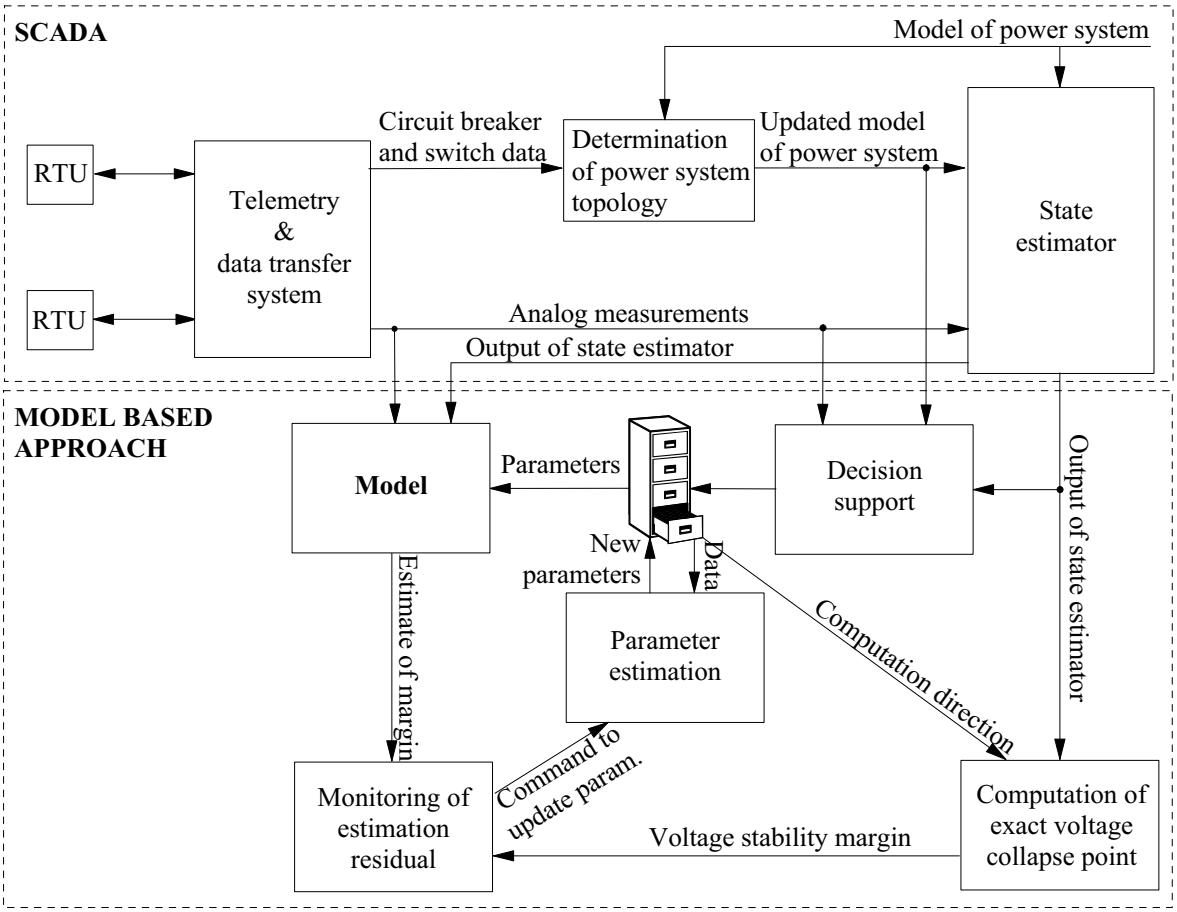

Figure 5.6. Updating of the model-based approach.

The off-line updating of model parameters is simpler than on-line updating. The advantage of on-line updating is its automatic operation, while the disadvantage is the relatively complicated solution. Off-line updating is also based on the computation of the exact voltage collapse point. However, the computation of the exact voltage collapse point and the monitoring of the estimation residual are done off-line. The data for parameter re-estimation should be regenerated in order to take full account of the changes in the power system.

5.4.3 Implementation requirements

The implementation of the approach is simple because the model creation is totally separated from the use of the model. The model creation is done in off-line environment, possibly general statistical analysis software, or a multipurpose development environment like Matlab. These programs usually have the capability to export and import data from

databases. The data generation and the model creation are done entirely in off-line mode. The on-line application is implemented into the SCADA/power management system and the application computes the estimates of voltage stability margin. The on-line updating is also capable of automatically monitoring the estimation residual.

The on-line implementation of the model-based approach does not require major investment in a measurement system, SCADA or a power management system. The approach is based on information available at SCADA or which may be computed with the state estimator. The implementation of the proposed approach is, of course, simpler to realise with open databases and modern SCADA/power management systems. The only major requirement is the ability to implement the third party software to the power management system.

The data generation requires specific software or access to a power system analysis program like PSS/E. The model creation procedure requires a development environment like Matlab, the advantage of PSS/E and Matlab being the option to supplement them by self-made or tailored software. The implementation and the use of the proposed model-based approach also require an expert in black-box modelling and power system analysis. However, it should be noted that a major part of the model-based approach is realised automatically. Special “manual” work is required in the data generation procedure to choose some parameters, in the selection of critical contingencies, in the data analysis, and in the model generalisation testing. The time-consuming procedures like data generation and model parameter estimation are fully automatic.

6 APPLICATION OF THE PROPOSED APPROACH

This chapter includes applications of the proposed approach for IEEE 118-bus test system, which was used for the development of the proposed approach, and 131-bus equivalent of the Finnish transmission system. The equivalent of the Finnish transmission system was used to represent the applicability of the proposed approach to a practical system.

6.1 IEEE 118-bus test system

The details of the proposed approach include the description of test results of computation algorithms for maximum loading point and contingency ranking. The visualisation of post-disturbance operation states describes the characteristics of the system studied, and also shows some possibilities for data analysis. Finally all intermediate steps and results of the model-based approach are presented. Figure 6.1 presents an one-line diagram of the IEEE 118-bus test system. The load-flow data is available at [Pow00b].

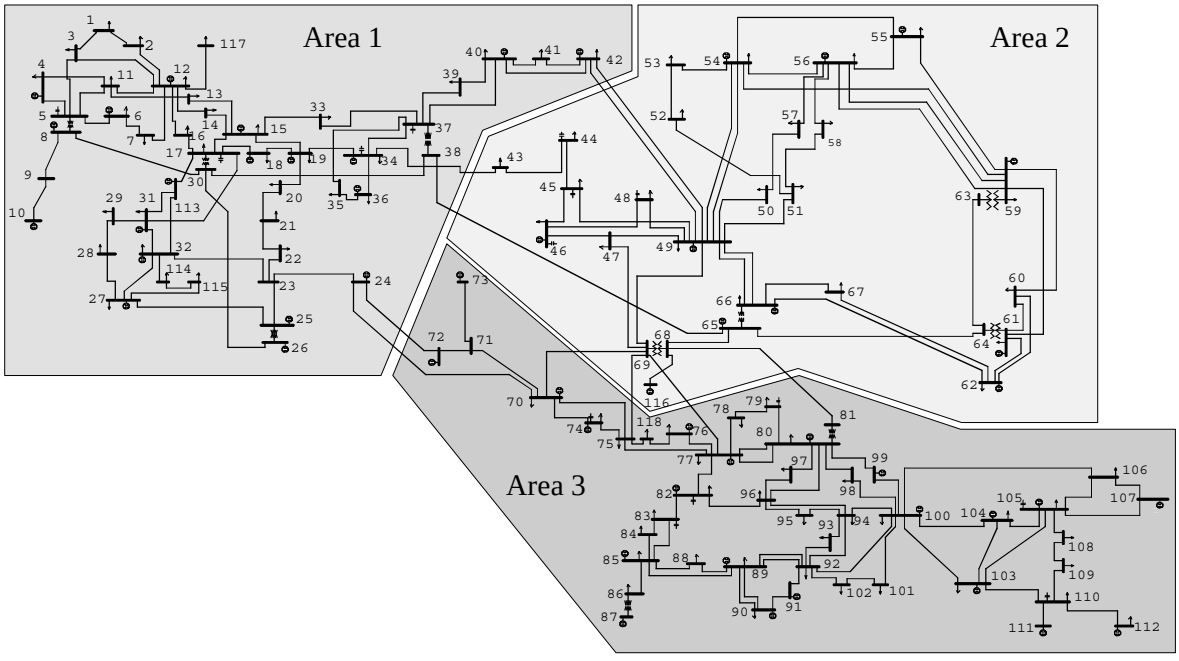

Figure 6.1. IEEE 118-bus test network.

6.1.1 Computation of maximum loading point

Comparison of programs

The computation of maximum loading point can be done simply by using the algorithm described in Chapter 3.2.4. The continuation load-flow method is, however, capable of

solving the whole PV-curve, thus the accuracy of maximum loading point must be better than that of the load-flow method. The programs studied were Pflow (continuation load-flow) [Cañ99], PowerWorld simulator voltage adequacy and stability tool (load-flow) [Vol00a] and the method described in Chapter 3.2.4 which was programmed for PSS/E using IPLAN programming language (load-flow) [Pow00a]. The comparison results are presented in Table 6.1. The comparison was based on the load-flow results of maximum loading points. Loads were modelled as constant power loads. The computation direction for the calculation of voltage stability margin was chosen to increase load at area 1 and production at areas 2 and 3 (Figure 6.1). There are six tie-lines between these areas, which are the bottleneck of the system in the chosen scenario.

Table 6.1. Comparison of maximum loading points.

	Continuation load-flow	*Power World*[7]	*PSS/E Application*[7]
Minimum singular value	$1.4*10^{-4}$	$2.9*10^{-3}$	$2.9*10^{-4}$
Active power losses [MW]	579.06	548.17	551.38
Reactive power losses [MVar]	2270.43	2069.38	2089.61
Slack bus active power [MW]	948.54	929.11	932.4
Slack bus reactive power [Mvar]	50.97	37.19	38.5
Minimum voltage [pu] (bus number)	0.7276 (38)	0.7560 (38)	0.7536 (38)
Generators at the maximum reactive power limit	1, 6, 8, 12, 15, 18, 19, 32, 34, 36, 40, **42**, **46**, 49, 65, **66**, 70, 74, **76**, 113	1,6, 8, 12, 15, 18,19, 32, 34, 36,40, 49, 65, 70, 74, 113	1, 6, 8, 12, 15, 18, 19, 32, 34, 36, 40, **42**, 49, 65, 70, 74, 113
Generators at the minimum reactive power limit	104, 105, 110	**56**, 104, 105, 110	104, 105, 110
Active power transfer 2→1 [MW]	1204.62	1198	1199.8
Reactive power transfer 2→1 [MVar]	549.61	482.18	487.2
Reactive power transfer 1→2 [Mvar]	503.76	492.93	495.7
Active power transfer 3→1 [MW]	334.91	322.16	323.4
Reactive power transfer 3→1 [MVar]	36.51	30.41	31.1
Reactive power transfer 1→3 [MVar]	161.03	148.79	150.0
Voltage stability margin [MW]	1393	1387	1387

The comparison was mainly based on voltage stability margin, whose accuracy was good for both load-flow methods. The difference between the continuation load-flow and the load-flow methods was only 6 MW. The error is not significant. The other results of maximum loading points were used for detailed comparison of methods. The convergence of load-flow algorithm is dependent on the characteristics of the load-flow Jacobian

[7] The initial step length was 300 MW and the minimum step length was 1 MW. The prediction step was based on a previous load-flow solution.

matrix. The Jacobian matrix must be non-singular in order to solve the load-flow equations. However, the Jacobian matrix becomes singular in the voltage collapse point, which is a saddle node bifurcation point. In practice, load-flow programs are not capable of solving cases close to voltage collapse point due to load-flow numerical problems. The value of minimum singular value describes the proximity of the maximum loading point to the voltage collapse point. The continuation load-flow method and the PSS/E application were close to the singularity point. The greatest differences between the continuation load-flow method and load-flow methods can be seen in reactive power. This is due to increased demand for voltage support close to the voltage collapse point. The difference in the minimum voltages is also significant.

The progress of voltage instability in this example was classic with the limitations of generator reactive power outputs and increment of reactive power losses the main reasons for instability. This can be seen from the results of the slack bus reactive power, generators at the maximum reactive power limit and reactive power transfers in Table 6.1. The additional production of reactive power was moved further away from the critical area at the maximum loading point, which further increases reactive power transfers and losses.

The load-flow solutions of PSS/E application beyond the maximum loading point diverged due to oscillations of generator reactive power outputs. The load-flow algorithm could not achieve a solution in which the solutions of load-flow equations were accurate enough and the control logic of generator reactive power limits and terminal voltage fulfilled. The load-flow algorithm could not converge although the number of iterations was increased. Appendix A includes the solution steps of maximum loading point computation for PSS/E application.

The results of PowerWorld were not actually the same as the results of the PSS/E application due to the incorrect control logic of generator reactive power limitation in PowerWorld. The reactive power output of the generator at bus 56 was incorrectly limited to the minimum reactive power limit although the voltage (0.9536 pu) was less than the setting of terminal voltage (0.9540 pu). This also caused differences at adjacent generator reactive power outputs. The active and especially the reactive power losses of PowerWorld maximum loading point were significantly less than in the correct result.

Effect of initial step length and prediction method

The selection of initial step length affects the total computation time and the accuracy of the maximum loading point algorithm. The advantage of binary search is its ability to find almost the same solution regardless of initial step length when the minimum step length is small enough. This is shown in Table 6.2. However, the disadvantage of binary search is its tendency to diverge consecutively at the end of computation. In that case there should be a possibility to further reduce the step length. The number of diverged load-flows

significantly affects the total computation time because the algorithm does not include early termination.

The total computation time of the PSS/E application is largely due to handling of variables and files. This is due to the inefficiency of IPLAN programming language. The time of load-flow computations is only one tenth of the total time. The minimum total computation time was achieved when the number of diverged load-flows was minimised. According to Table 6.2 the minimum computation time was achieved with initial step lengths 300 and 600 MW. In practice, it is advisable to choose the initial step length from the middle. A large initial step might lead to load-flow numerical problems, because the difference between the load-flow initial values and the solution becomes too great. These tests were made with PC (Pentium 350 MHz, 256 Mb RAM).

Table 6.2. Selection of initial step length.

Initial step length [MW]	*Marginal [MW]*	*Total time [s]*	*Time for load-flows [s]*	*# of converged load-flows (# of iterations)*	*# of diverged load-flows (# of iterations)*
100	1387	16.8	1.85	17 (44)	7 (140)
200	1387	13.9	1.71	11 (32)	8 (160)
300	1387	12.0	1.70	7 (22)	9 (138)
400	1387	12.9	1.84	8 (25)	9 (165)
500	1387	13.6	1.94	9 (24)	9 (141)
600	1387	11.8	1.61	5 (18)	10 (147)
700	1387	14.3	1.85	9 (26)	10 (167)

The effect of the prediction step of the maximum loading point algorithm was tested with three methods: no prediction, secant prediction and curve fit prediction. Tests were made with Matlab using the load-flow algorithm of Power System Toolbox [Rog95]. The Matlab application was identical to the PSS/E application, but the results of the Matlab and PSS/E applications are not comparable concerning the computation time. This is mainly due to inefficient control logic of generator reactive power limitation and computation of minimum singular value at each computation step in the Matlab application. The computation of minimum singular values roughly doubles the total computation time.

Figure 6.2 presents the test results of the prediction methods. According to this figure the curve fit prediction is the best one. It increases the step length at the beginning of computation if that is too short. It would be favourable to switch e.g. to secant method, when the maximum loading point is almost reached, due to the approximation inaccuracies of the curve fitting method. In this example the secant prediction is not significantly better than the no prediction method, sometimes even worse. Although the initial load-flow

values in the secant prediction are closer to load-flow solution than that of no prediction method, the number of load-flow iterations is not significantly smaller. This can be seen in Table 6.3.

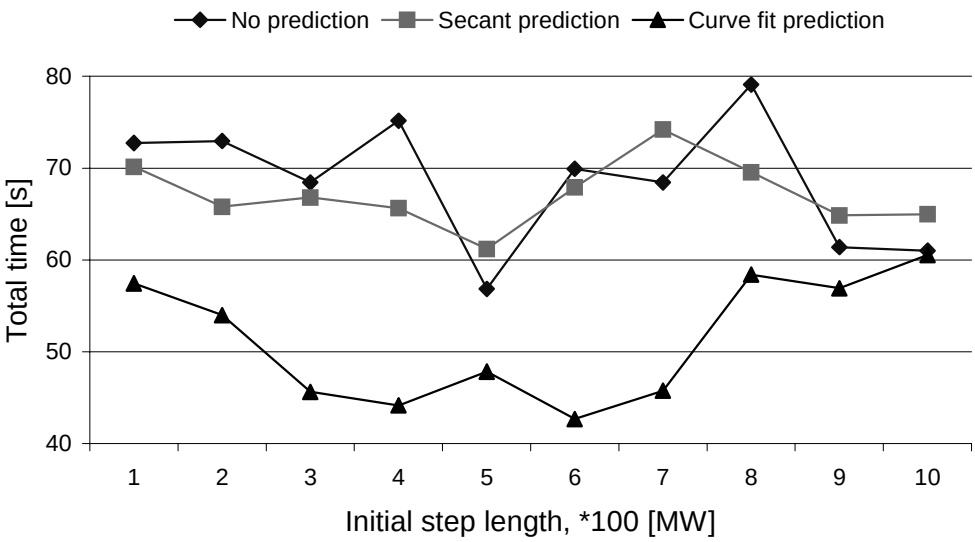

Figure 6.2. Comparison of prediction methods.

Table 6.3. Number of load-flows and iterations of prediction methods.

Initial step length [MW]	*No prediction*		*Secant prediction*		*Curve fit prediction*	
	converged load-flows (iterations)	*diverged load-flows (iterations)*	*converged load-flows (iterations)*	*diverged load-flows (iterations)*	*converged load-flows (iterations)*	*diverged load-flows (iterations)*
100	20 (78)	22 (289)	20 (75)	23 (274)	9 (35)	23 (278)
200	14 (59)	26 (336)	14 (58)	23 (285)	8 (34)	22 (265)
300	11 (45)	24 (329)	11 (46)	23 (316)	8 (32)	20 (212)
400	11 (43)	28 (374)	11 (41)	25 (316)	10 (40)	16 (183)
500	7 (29)	24 (285)	7 (29)	29 (313)	11 (41)	15 (206)
600	9 (37)	25 (352)	9 (38)	24 (339)	10 (42)	16 (171)
700	10 (39)	28 (341)	10 (39)	34 (373)	9 (38)	22 (206)
800	11 (43)	32 (402)	11 (41)	29 (344)	9 (38)	25 (292)
900	7 (28)	26 (309)	7 (27)	26 (329)	8 (32)	23 (281)
1000	7 (29)	28 (312)	7 (29)	33 (340)	11 (43)	27 (283)

6.1.2 Contingency ranking

The ranking of contingencies was done for all *(n-1)*-type contingencies. The number of contingencies was 224 (186 lines and 38 generators). If the line disconnection led to an island, the smaller part of the system was fully disconnected. The power of the disconnected generator was shared over all generators based on their maximum active

power capability. The contingency ranking methods were compared to the true voltage stability margin. The margin was scaled 0…1. The zero margin corresponds to the maximum loading point. The computation direction was chosen to increase load at area 1 and production at areas 2 and 3. The same direction was used for both the computation of pre-disturbance loading situations and the computation of voltage stability margin. The description of the proposed contingency ranking methods is in Chapter 3.3.3.

Reactive power losses

The load-flows were calculated in the base case, base +3 pu, base +6 pu and base +9 pu loading situations in order to rank contingencies based on system reactive power losses. The reactive power losses in pre-disturbance cases were -4.6 pu (base), -3.2 pu (base +3 pu), -0.87 pu (base +6 pu) and 2.8 pu (base +9 pu). In the IEEE 118-bus test system most transmission lines are under their natural loading and the reactive power production of generators is close to zero in the base case.

Table 6.4 presents reactive power losses and contingency ranking (number in parentheses) according to reactive power losses for the 20 most critical contingencies in different loading situations. Numbers referring to the nodes of the test system indicate the contingency. A single number indicates a generator outage and two numbers indicate a branch (line or transformer) outage. The reactive power losses cannot accurately determine the true contingency ranking, but may be used for contingency severity approximation if contingency analysis is done in a stressed situation. The most critical contingencies do not have load-flow solution at base +6 pu and base +9 pu loading situations.

Figure 6.3 presents the contingency analysis based on reactive power losses in the loading situation of base case +9 pu. The solid line represents the post-disturbance voltage stability margin arranged in ascending order (scale on the left hand side of figure). The plus signs indicate reactive power losses for the corresponding contingencies (scale on the right hand side of figure). According to the contingency analysis most contingencies are very stable, because their reactive power losses are not changed compared to the pre-disturbance case. The sensitivity of reactive power losses can be seen in only a few critical contingencies. Not all 20 most critical contingencies can be detected because some of them have low reactive power losses. If a 4 pu reactive power loss severity criterion is used, three critical contingencies cannot be detected (contingencies below the line of severity criterion and left from the line of the 20 most critical contingencies) and 15 non-critical contingencies are incorrectly classified as critical (contingencies above the line of severity criterion and right from the line of the 20 most critical contingencies).

Table 6.4. Reactive power losses.

Rank	*Cont.*	*Base*	*Base + 3 pu*	*Base + 6 pu*	*Base + 9 pu*
1	8-5	-1.47 (1)	1.85 (1)	- (1*)	- (1*)
2	22-23	-3.99 (23)	-2.15 (18)	- (2*)	- (2*)
3	19-20	-4.46 (80)	-2.92 (41)	- (3*)	- (3*)
4	42-49	-2.99 (7)	-0.42 (5)	4.83 (7)	- (4*)
5	42-49	-2.99 (6)	-0.42 (4)	4.83 (6)	- (5*)
6	38-65	-2.88 (5)	0.06 (3)	6.11 (4)	- (6*)
7	9-10	-3.51 (15)	-0.51 (6)	3.98 (8)	11.59 (8)
8	10	-4.88 (217)	-1.88 (12)	2.62 (9)	10.26 (9)
9	8-9	-2.30 (2)	0.70 (2)	5.18 (5)	12.84 (7)
10	38-37	-3.07 (8)	-1.23 (8)	1.93 (11)	6.79 (11)
11	23-24	-4.45 (74)	-3.16 (133)	-0.49 (43)	4.52 (21)
12	12	-3.81 (20)	-1.43 (9)	2.20 (10)	8.07 (10)
13	30-38	-3.80 (19)	-2.74 (28)	-0.34 (37)	4.06 (30)
14	26	-5.14 (223)	-2.98 (49)	0.32 (22)	5.46 (14)
15	11-13	-4.42 (60)	-3.01 (60)	-0.57 (53)	3.35 (48)
16	31	-4.32 (35)	-2.35 (21)	0.78 (15)	5.68 (13)
17	26-30	-2.32 (3)	-0.76 (7)	1.92 (12)	6.21 (12)
18	25	-5.02 (220)	-3.11 (97)	-0.10 (31)	4.53 (19)
19	44-45	-4.44 (68)	-2.93 (43)	-0.32 (35)	3.88 (34)
20	70-71	-4.58 (191)	-3.15 (127)	-0.66 (75)	3.41 (44)

* No load-flow solution.

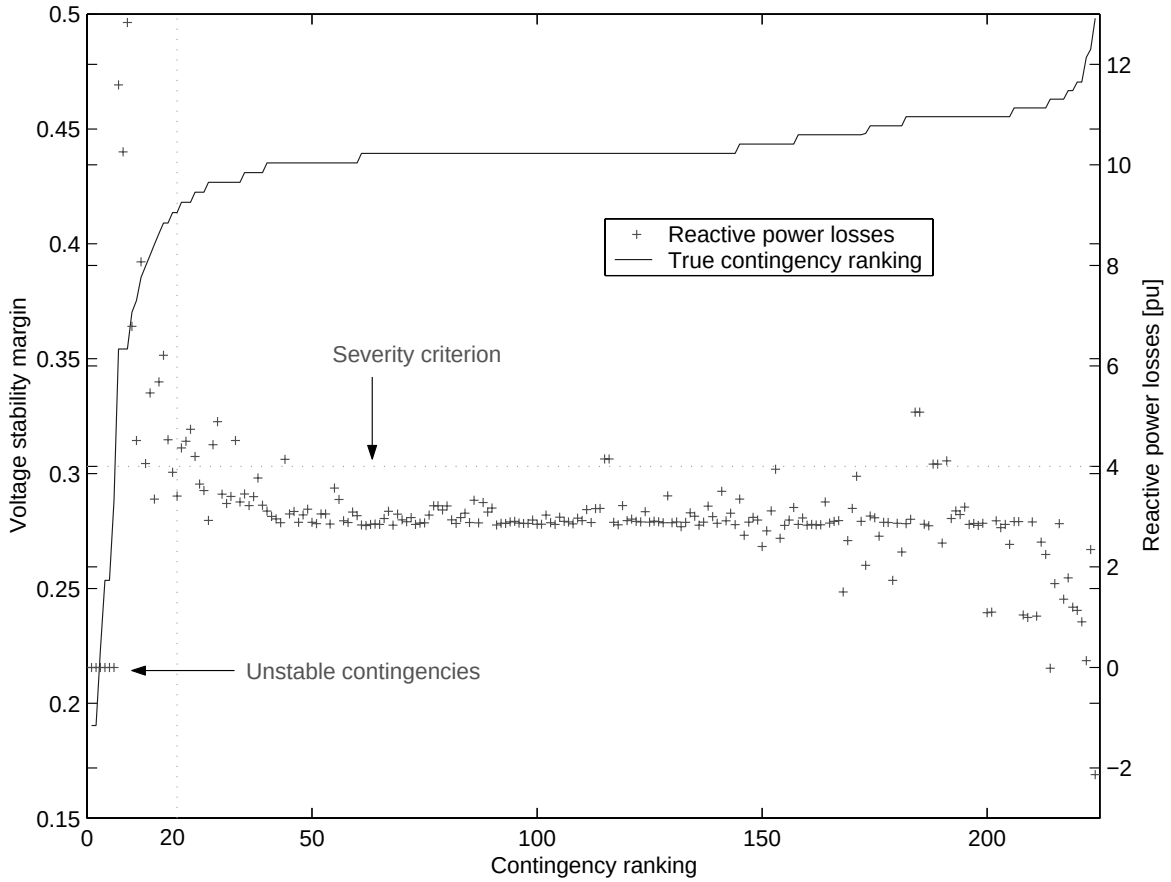

Figure 6.3. Reactive power losses (loading situation of base case +9 pu).

Minimum singular value

The minimum singular values were also calculated for all contingencies in the base case, base +3 pu, base +6 pu and base +9 pu loading situations. The base case minimum singular values were 0.191, 0.183, 0.174 and 0.155 respectively. Table 6.5 presents minimum singular values and ranking (number in parentheses) according to minimum singular values for the 20 most critical contingencies in different loading situations. The contingency ranking is not very accurate. The system stress, however, improves the performance of the index. The minimum singular value indicates the proximity to the maximum loading point, but the comparison of contingency cases is not so straightforward due to power system non-linearities.

Figure 6.4 presents the contingency analysis based on minimum singular values in loading situation of base case +9 pu. The solid line represents the post-disturbance voltage stability margin arranged in ascending order (scale on the left hand side of figure). The plus signs indicate minimum singular values for the corresponding contingency (scale on the right hand side of figure). Most minimum singular values form a curve similar to the true contingency ranking. A severity criterion of 0.14 of minimum singular value was used to detect incorrectly classified contingencies. Three critical contingencies were classified as non-critical (contingencies above the line of severity criterion and left from the line of the 20 most critical contingencies) and seven non-critical contingencies were incorrectly

classified as critical (contingencies below the line of severity criterion and right from the line of the 20 most critical contingencies).

Table 6.5. Minimum singular values.

Rank	*Cont.*	*Base*	*Base + 3 pu*	*Base + 6 pu*	*Base + 9 pu*
1	8-5	0.158 (6)	0.128 (4)	0 (1*)	0 (1*)
2	22-23	0.184 (22)	0.169 (17)	0 (2*)	0 (2*)
3	19-20	0.189 (57)	0.179 (35)	0 (3*)	0 (3*)
4	42-49	0.163 (7)	0.146 (8)	0.100 (6)	0 (4*)
5	42-49	0.163 (8)	0.146 (7)	0.100 (7)	0 (5*)
6	38-65	0.109 (2)	0.094 (1)	0.070 (4)	0 (6*)
7	9-10	0.180 (17)	0.166 (13)	0.143 (12)	0.102 (10)
8	10	0.176 (13)	0.162 (10)	0.140 (11)	0.099 (9)
9	8-9	0.184 (23)	0.170 (18)	0.147 (13)	0.102 (11)
10	38-37	0.186 (29)	0.176 (26)	0.162 (22)	0.140 (24)
11	23-24	0.145 (4)	0.137 (5)	0.125 (9)	0.092 (8)
12	12	0.183 (21)	0.173 (20)	0.156 (18)	0.125 (14)
13	30-38	0.152 (5)	0.143 (6)	0.129 (10)	0.103 (12)
14	26	0.185 (27)	0.176 (25)	0.163 (23)	0.133 (18)
15	11-13	0.190 (84)	0.182 (79)	0.172 (57)	0.151 (54)
16	31	0.186 (31)	0.177 (29)	0.166 (28)	0.138 (23)
17	26-30	0.188 (39)	0.179 (39)	0.165 (26)	0.140 (25)
18	25	0.187 (36)	0.178 (32)	0.167 (34)	0.141 (26)
19	44-45	0.180 (18)	0.172 (19)	0.160 (21)	0.136 (21)
20	70-71	0.167 (9)	0.160 (9)	0.150 (14)	0.127 (15)

* No load flow solution.

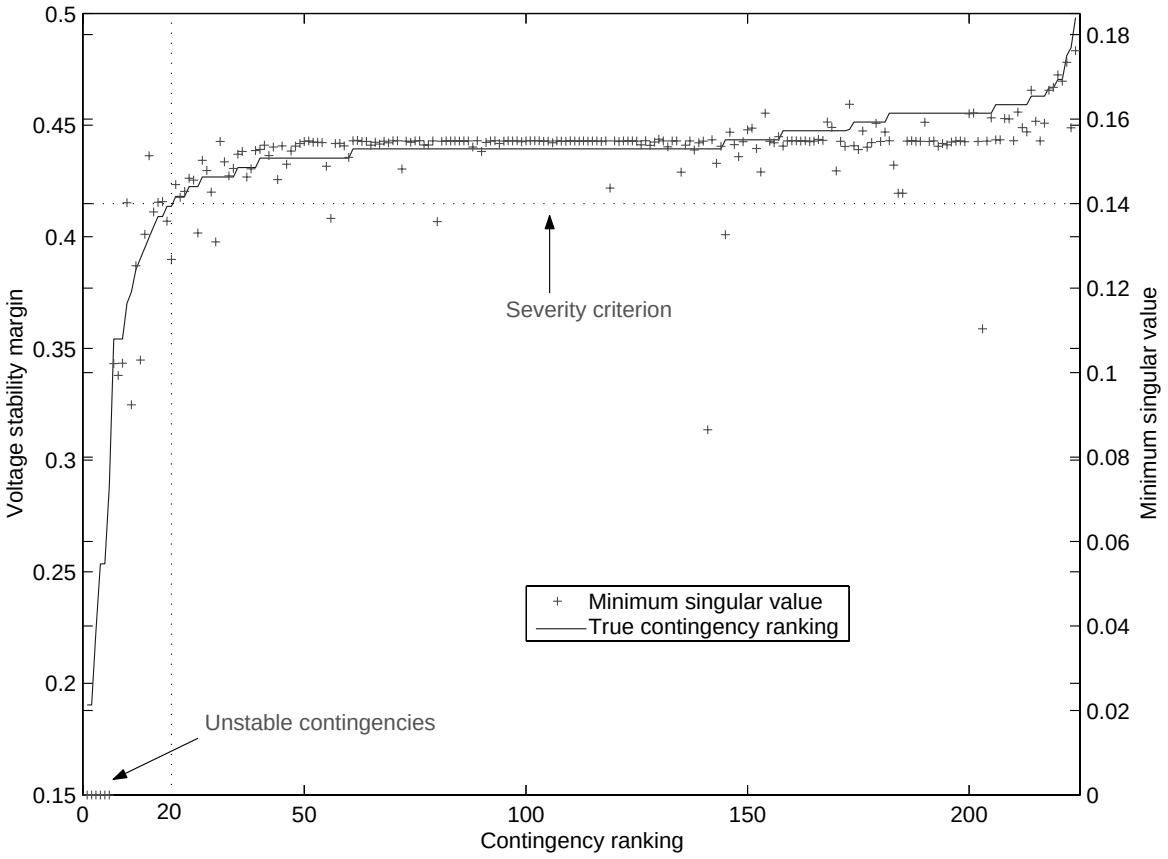

Figure 6.4. Minimum singular values (loading situation of base case +9 pu).

Curve fitting

The curve fitting method was tested with three and four operation point data. The state variables were voltages in loading buses. Angles were used instead of voltages when voltages were constant. The approximated parameters were active power loads. Table 6.6 presents the test results for the 20 most critical contingencies. The columns *Cont.* and *Marg.* represent the contingency and the corresponding voltage stability margins respectively.

The results are fairly good for both voltage stability margin approximation and contingency ranking. The results are the approximate voltage stability margin and contingency ranking (in parentheses). The last row presents the average percentual errors of voltage stability margin approximation for all contingencies in each test. The first three columns present the true contingency ranking based on exact voltage stability margins. The next two columns present curve fitting results of three operation point data. The last two columns presents curve fitting results of four operation point data.

Calculation steps 1, 2 and 3 and 1, 2, 3 and 4 are used in test 1 for three and four point tests respectively. Test 2 uses calculation steps 1, 4 and 5 for three point tests and calculation steps 1, 4, 5 and 6 for four point tests. Test 2 was made to improve the performance of contingency 19-20. The contingency 19-20 is complicated due to fairly constant voltages

in all calculation steps. When the performance of contingency 19-20 was improved by selecting different points for curve fitting, the performance of contingencies 30-38 and 44-45 was decreased in the three point test.

Table 6.6. Curve fitting margins.

	Cont.	*Marg.*	*3 points test 1*	*3 points test 2*	*4 points test 1*	*4 points test 2*
1	8-5	0.190	0.266 (1)	0.253 (1)	0.272 (1)	0.257 (1)
2	22-23	0.190	0.292 (2)	0.287 (4)	0.292 (2)	0.290 (2)
3	19-20	0.223	0.522 (222)	0.369 (6)	0.521 (224)	0.374 (6)
4	42-49	0.254	0.357 (4)	0.274 (2)	0.312 (3)	0.312 (3)
5	42-49	0.254	0.357 (5)	0.274 (3)	0.312 (4)	0.312 (4)
6	38-65	0.288	0.331 (3)	0.321 (5)	0.320 (5)	0.321 (5)
7	9-10	0.354	0.355 (7)	0.389 (9)	0.379 (9)	0.382 (9)
8	10	0.354	0.354 (6)	0.389 (8)	0.379 (8)	0.382 (8)
9	8-9	0.354	0.355 (8)	0.384 (7)	0.377 (6)	0.380 (7)
10	38-37	0.370	0.386 (14)	0.430 (13)	0.419 (19)	0.422 (13)
11	23-24	0.375	0.420 (22)	0.398 (10)	0.411 (14)	0.399 (10)
12	12	0.385	0.380 (11)	0.423 (12)	0.407 (13)	0.409 (12)
13	30-38	0.390	0.385 (13)	0.451 (168)	0.405 (11)	0.430 (15)
14	26	0.395	0.381 (12)	0.432 (14)	0.404 (10)	0.428 (14)
15	11-13	0.400	0.421 (25)	0.442 (20)	0.425 (24)	0.441 (29)
16	31	0.405	0.380 (10)	0.418 (11)	0.378 (7)	0.403 (11)
17	26-30	0.409	0.434 (47)	0.437 (17)	0.413 (16)	0.431 (16)
18	25	0.409	0.393 (15)	0.444 (25)	0.412 (15)	0.435 (18)
19	44-45	0.414	0.428 (34)	0.459 (199)	0.423 (21)	0.437 (20)
20	70-71	0.414	0.445 (72)	0.445 (31)	0.438 (52)	0.446 (46)
Average error [%]			2.2	2.9	2.2	3.1

Figure 6.5 presents four operation point (test 2) test results for all contingencies. Most voltage stability margin approximations are higher than the true margins. However, the ranking of contingencies is correct enough for all contingencies. A severity criterion (voltage stability margin 0.43) is used to distinguish between critical non-critical contingencies. According to this criterion three critical contingencies are classified as non-critical (contingencies above the line of severity criterion and left from the line of the 20 most critical contingencies) and no non-critical contingencies are classified as critical. Peaks in the approximate voltage stability margins can be dangerous if they are large enough and in a suitable place (e.g. contingency 19-20). They are due to numerical problems in the curve fitting, which in turn are mainly due to fairly constant state variable values at different operation points.

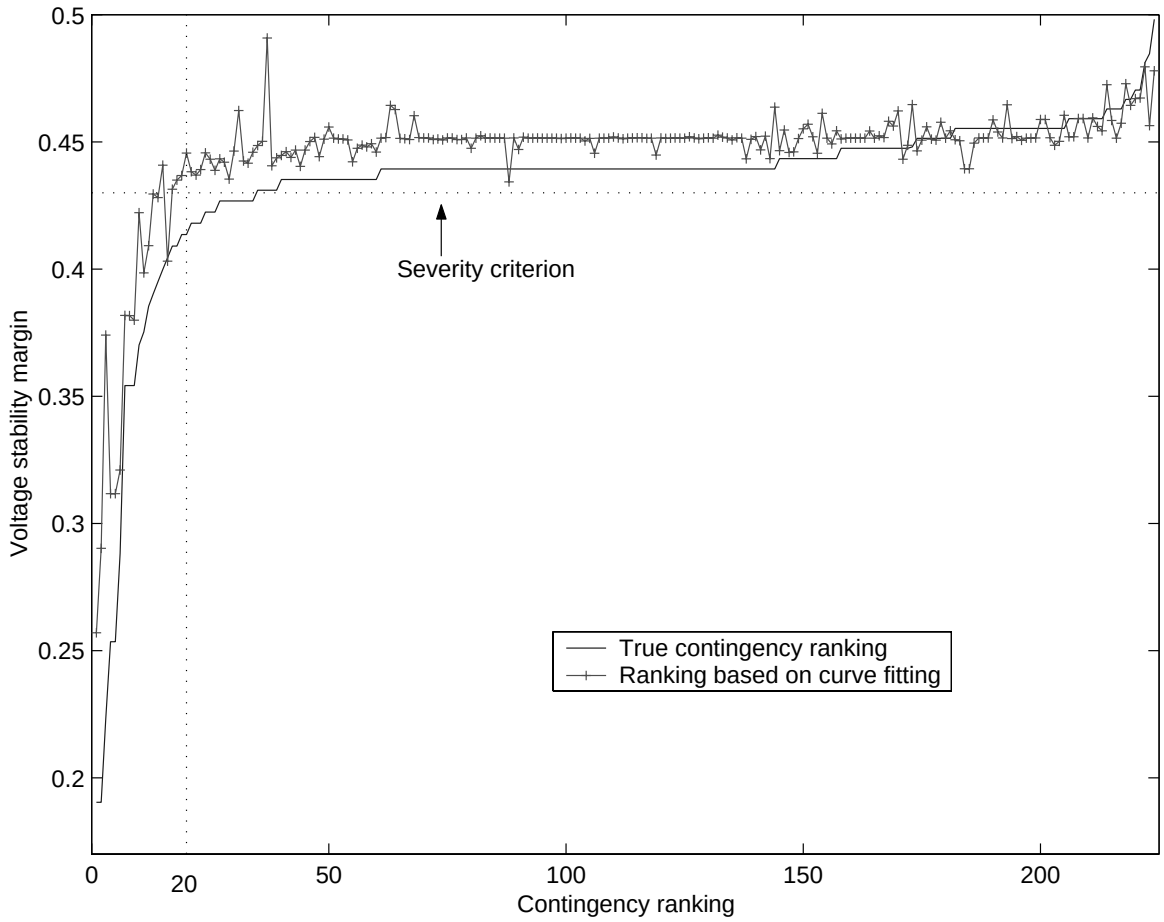

Figure 6.5. Contingency ranking of four operation point (test 2) curve fitting method.

Contingency clustering

The use of K-means clustering in the contingency ranking is studied in different loading situations (base, base +3 pu, base +6 pu, base +9 pu). The effect of initial cluster centre guesses was eliminated by repeating the procedure 100 times.

The data pre-processing is important for the performance of clustering. The features studied were active and reactive line flows, voltages and active power transfers between areas. The chosen features were 15 voltages of load buses and active power transfers between areas. The feature selection was based on agglomerative hierarchical clustering. Furthermore, the data was standardised to improve its capability. The number of clusters (20 in these studies) also affects the performance of clustering. The number of contingency clusters should be large enough to offer one cluster for each natural grouping in the data. When the number of clusters was increased, more non-critical contingencies were included in the critical clusters. The largest cluster was found to be the non-critical cluster. The grouping of critical clusters could not be used for contingency ranking. This method is only capable of indicating which contingencies are the critical ones.

The test results are presented in Table 6.7. The results are percentages and characterise how many times the corresponding contingency is assigned to the critical cluster. The

K-means clustering can group critical contingencies fairly reliably into critical clusters. The grouping of contingencies 11-13 and 70-71 seems to be more difficult than that of others. The performance of K-means clustering improves only slightly when the system stress increases.

Table 6.7. K-means contingency clustering.

Rank	*Cont.*	*Base*	*Base +3 pu*	*Base +6 pu*	*Base +9 pu*
1	8-5	97	100	100	97
2	22-23	94	95	100	97
3	19-20	94	96	100	97
4	42-49	98	100	100	97
5	42-49	98	100	100	97
6	38-65	97	99	100	97
7	9-10	100	99	98	99
8	10	100	99	98	99
9	8-9	100	99	98	99
10	38-37	98	100	96	98
11	23-24	97	91	100	100
12	12	100	99	98	99
13	30-38	100	91	97	99
14	26	100	99	98	99
15	11-13	79	85	82	73
16	31	99	97	94	97
17	26-30	100	99	100	98
18	25	99	97	94	99
19	44-45	94	95	97	99
20	70-71	77	91	91	98

The critical clusters also include non-critical contingencies. The numbers of critical and all contingencies in the critical clusters are presented in Table 6.8. In 100 %, contingencies grouped every time into a critical cluster, are only counted. In 95 %, contingencies grouped more often than 95 times into a critical cluster, are counted, and so on. At the level of 90 % the clustering of critical contingencies is fairly good and the total number of contingencies in critical clusters is small. The correct clustering of all critical contingencies is not possible unless almost all contingencies are grouped into critical clusters.

Table 6.8. Content of critical clusters.

[%]	*Base*		*Base +3 pu*		*Base +6 pu*		*Base +9 pu*	
	A	*B*	*A*	*B*	*A*	*B*	*A*	*B*
100	7	15	4	8	8	20	1	14
95	15	31	14	46	16	43	19	64
90	18	70	19	67	19	73	19	65
85	18	100	19	105	19	114	19	91
80	18	126	20	152	20	141	19	119
75	20	221	20	224	20	161	19	218
70	20	224	20	224	20	224	20	224

A= the number of critical contingencies in "critical" clusters
B= the total number of contingencies in "critical" clusters

6.1.3 Visualisation of results of contingency analysis

The visualisation of operation points is needed to analyse the results of contingency analysis and database generation. This visualisation gives an overview of the data, and thus is part of data analysis step of model creation procedure. The visualisation of the results of database generation is presented in Chapter 6.1.4. Here the visualisation is presented for the results of the contingency analysis. This analysis was done to find out the effect of power system uncertainty on contingency ranking and severity of cases. In order to select the most critical contingencies for database generation, it is necessary to analyse a large number of cases at different operation points. Therefore the data is not the same as in the previous study on contingency ranking. The most critical contingencies are the same as in Chapter 6.1.2 but in a different order. The number of operation points is increased to 100 and the operation points are generated using the database generation procedure. The data included post-disturbance voltage stability margins with respect to all *(n-1)*-type contingencies.

Visualisation of voltage stability margins

Figure 6.6 presents the contour figure of post-disturbance voltage stability margins, which clearly indicates the most critical contingencies and cases (small voltage stability margin corresponds to dark colour in the figure). The zero value of the voltage stability margin corresponds to the voltage collapse point. The margin is determined according to the total load. The most critical contingencies according to the post-disturbance margins calculated are contingencies 46 (outage of line 8-5), 67 (outage of line 22-23), 134 (outage of line 38-65) and 63 (outage of line 19-20). The next critical contingencies are 105 (outage of line 42-49), 104 (outage of line 42-49), 45 (outage of line 8-9), 3 (outage of generator 10), 89 (outage of line 38-37), 47 (outage of line 9-10) and 68 (outage of line 23-24). The information included in the figure includes the post-disturbance margins calculated for 22400 different situations. Without the use of visualisation methods the analysis of so many post-disturbance margins is almost impossible.

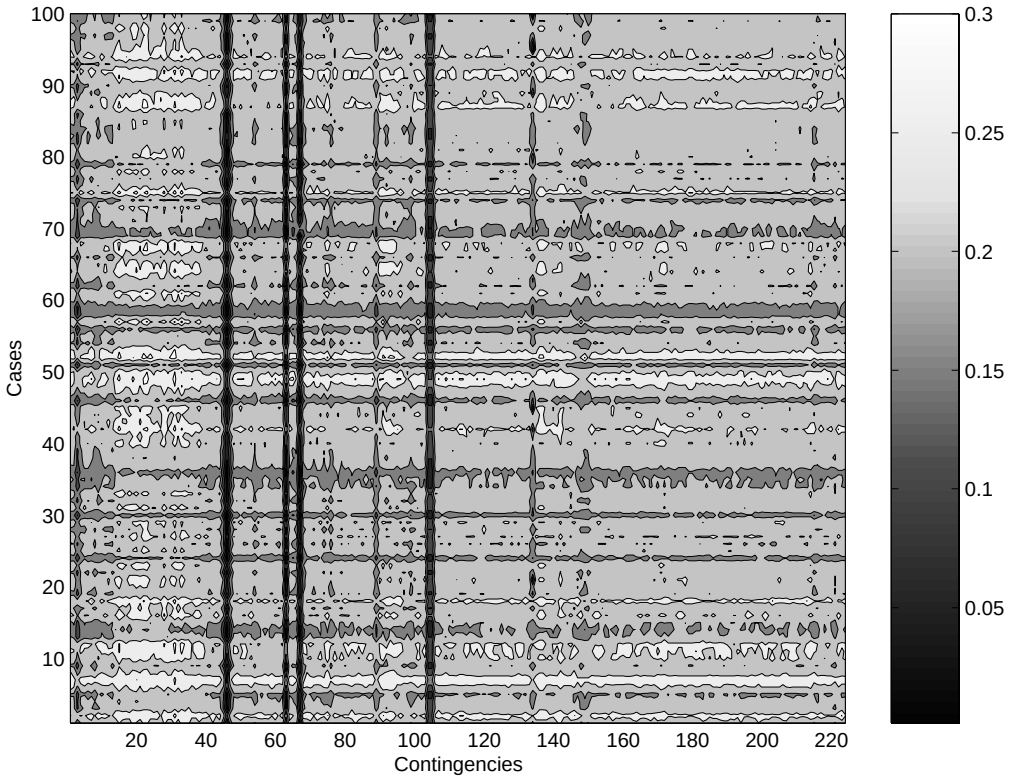

Figure 6.6. Post-disturbance margins.

The post-disturbance voltage stability margins are studied further in Figure 6.7. According to the histogram of all margins most cases and contingencies are very stable. The average margin is 0.22 and the standard deviation is 0.035. In the next subfigure (top right-hand corner) each contingency is sorted in ascending order. The subfigure shows the variation in the voltage stability margin for each contingency. In addition, the four most critical contingencies can be clearly separated (four lowest curves). The bottom subfigure represents the most critical margins in different cases and the corresponding contingency.

Figure 6.8 presents the deviation of post-disturbance margins (presented by box and whisker) for a few contingencies. The box has lines at the lower quartile, median and upper quartile values. The whiskers are lines extending from each end of the box to show the extent of the rest of the data. If any margin value is identified as an outlier, it is marked with a plus sign. The figure shows clearly that contingencies 46, 63 and 67 are much more severe compared to the rest of the contingencies. Contingencies 45 and 47 are next in severity. Most contingencies are close to the post-disturbance margin mean value.

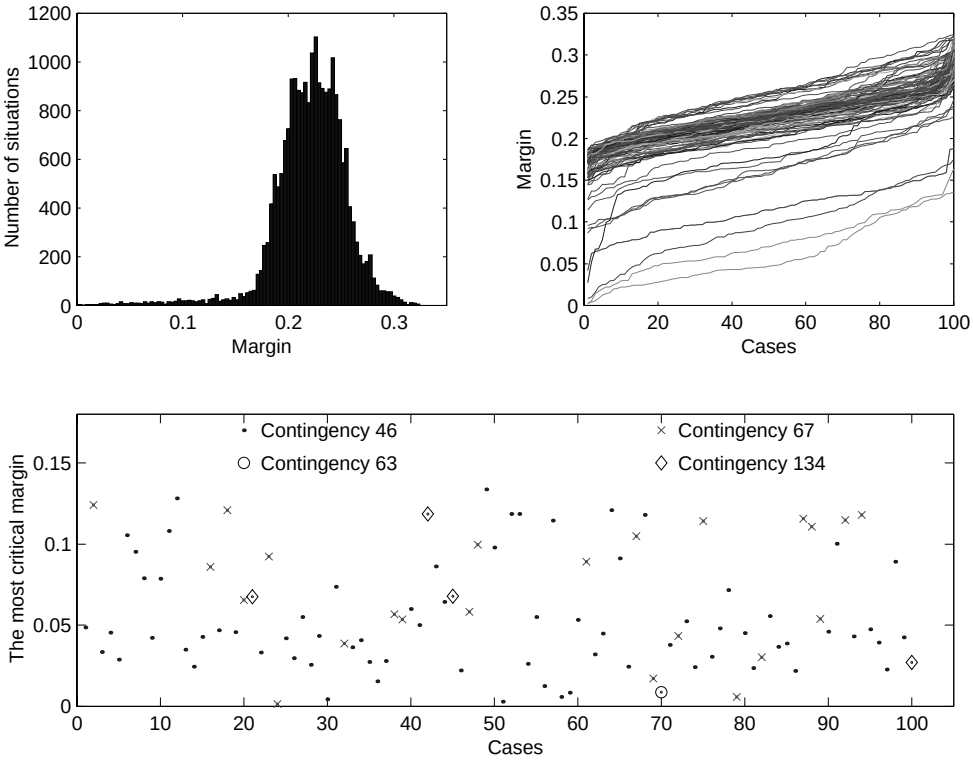

Figure 6.7. More detail analysis of margins.

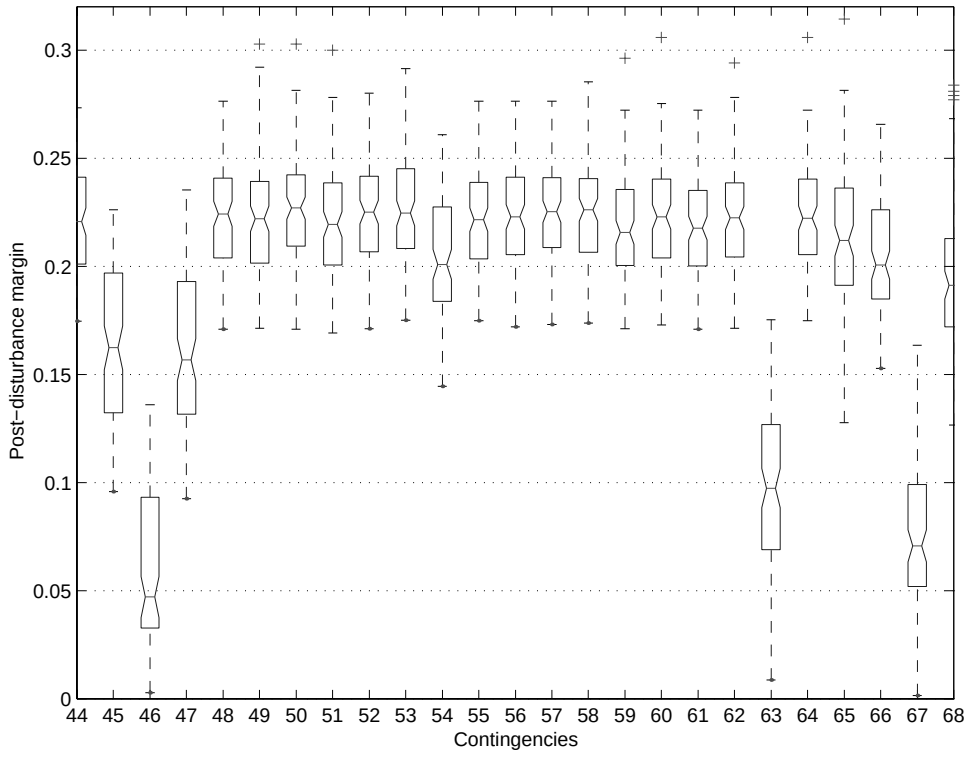

Figure 6.8. Post-disturbance margin variation.

Classification of severe and non-severe operation points

The visualisation of power system state is straightforward and the analysis of figures is clear when the post-disturbance margins are calculated. The state of power system voltage stability can also be analysed by many other indices, which are typically calculated at the post-disturbance operation point to avoid the computation of the whole PV-curve. The accuracy of such indices cannot be 100 % in all situations, because the voltage stability problem is non-linear in nature. Next the post-disturbance operation points of the previous study are analysed to identify severe cases and contingencies. All operation points were classified into two groups, severe and non-severe, in order to visualise the power system state with its variables. The situation is called severe when the voltage stability margin is less than 0.2. The number of severe and non-severe situations is 4665 and 17735 respectively.

Figure 6.9 presents the histograms of active power line flows of lines 38-65 and 8-9 and voltages of bus 21 at the post-disturbance operation point. Severe situations are presented in dark grey and non-severe situations in light grey. According to the line flows presented it is hard to say where the border between severe and non-severe situations is. It is clear that the line flow of line 38-65 should not exceed -4 pu to maintain the non-severe state. This is important because the line is the main tie-line between areas 1 and 2. However, some situations can be severe even at a very low value of line flow. This indicates the impossibility of explaining all changes in the system state by this variable. When the line flow (absolute value) increases, the share of severe situations also increases indicating that uncertainty of system state and risk of voltage instability is increasing.

Another interesting variable is line flow 8-9. It seems to behave similarly to line flow 38-65. However, a small number of severe situations is located near zero flow. The line 8-9 is the only route for bus 10. Bus 10 includes a generator, which is important for voltage stability. In situations when the generator is disconnected (flow at line 8-9 is almost zero) a large amount of power is needed to transfer from areas 2 and 3 to area 1 and that is why these situations are likely to be severe. The voltage at bus 21 is one of the weakest in the system. Most of the situations have normal operation voltage (>0.9 pu). All voltages below 0.9 pu are severe situations, but not all those above 0.9 pu are non-severe. The voltage at bus 21 indicates clearly the severity of the system although some uncertainty still persists.

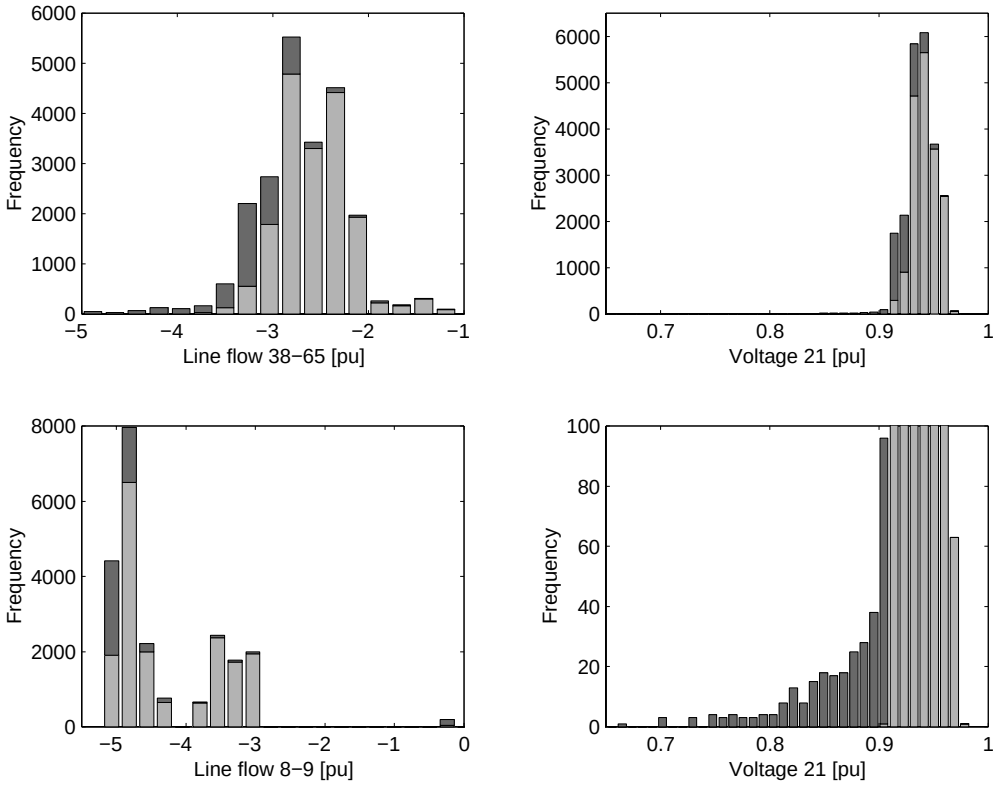

Figure 6.9. Classification of line flows and voltages.

The combination of line flow at line 38-65 and voltage at bus 21 is used for more detailed analysis. These variables cannot classify severe and non-severe situations into totally separate groups. Despite that, the use of two variables gives more information than the use of separate variables. Figure 6.10 indicates clearly that situations where the voltage is below 0.9 pu or the line flow is less than -4 pu are severe. There is an overlapping area when the voltage is between 0.9-0.95 pu and the line flow is between -1.5 - -4 pu. Inside this area there exist severe and non-severe situations, thus the classification of system severity is uncertain in this area. These situations should be studied more carefully to identify the variables which can separate severe and non-severe situations. The addition of a new variable makes the analysis of the figure, however, difficult.

Use of principal component analysis to simplify the data visualisation

The principal component analysis is used to transform active power flows and voltages into a new co-ordinate system. Principal components do not have physical meaning, but can be used to analyse the data and the analysis can be simplified significantly. The data studied is presented with first and second principal components (90 % of the variability of data studied can be explained with these). The first two principal components are studied to find out the severity of contingencies and cases. The colour of dots is used to separate situations: dark grey indicates a severe and light grey indicates a non-severe situation according to the voltage stability margin.

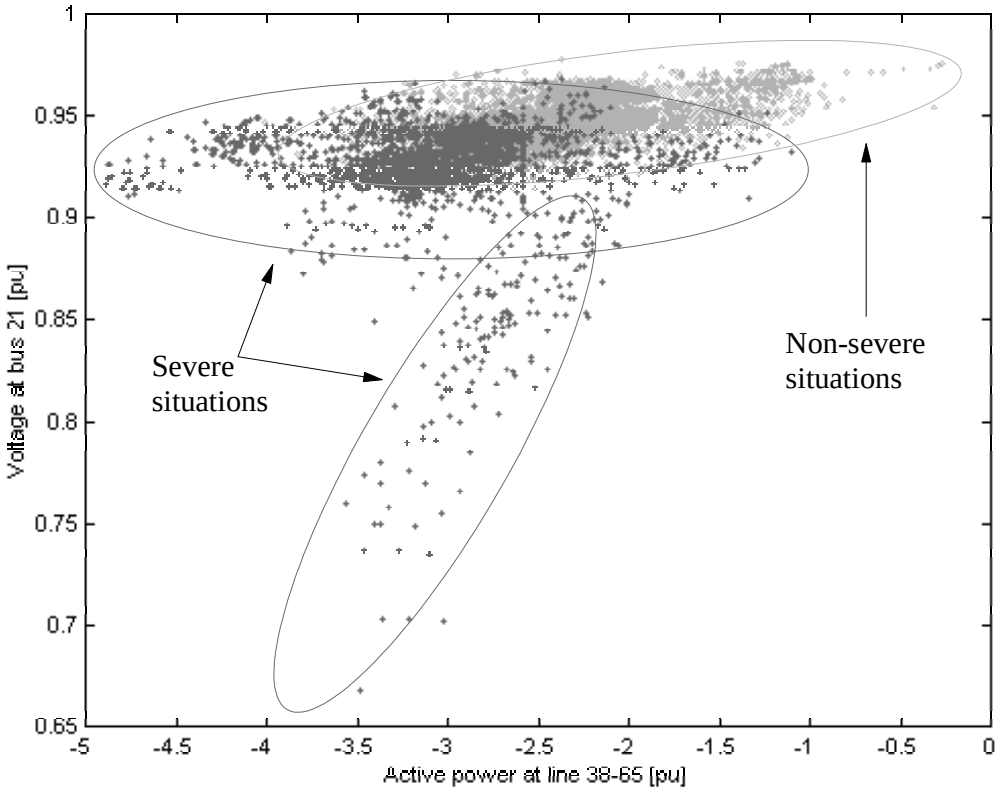

Figure 6.10. Two-dimensional analysis of system severity.

Figure 6.11 presents the groups of distinct contingencies. Contingencies 3 (bus 10 generator outage), 45 (outage of line 8-9) and 47 (outage of line 9-10) are severe and are all related to generator bus 10. These contingencies have a different effect on the system than other contingencies have. Contingencies 28, 31 and 33 are outages of generators at buses 100, 110 and 113 respectively. They are non-severe contingencies and that is why they are located in a different part of the figure than contingencies 3, 45 and 47. The analysis of other contingencies is not as clear as the analysis of the contingencies presented. They are located in the middle overlapping each other.

The analysis of cases shows the possibility to separate them (Figure 6.12). It was decided to classify cases into four groups: most severe, severe, non-severe and least severe. The analysis of cases also shows that the severity of a case can be explained well with the first principal component. The second principal component is needed, otherwise the distinct contingencies (see Figure 6.11) are misclassified. Further analysis showed that a case is all the more severe the farther left it is located. The least severe case seems to differ from this because it is located next to the severe group.

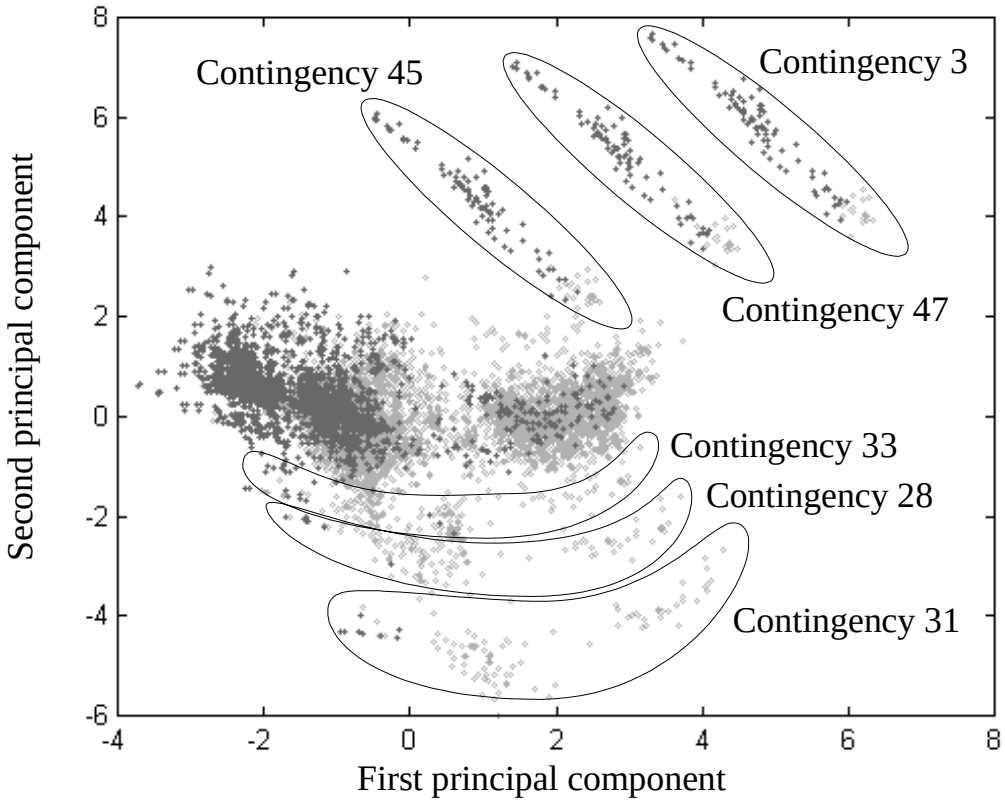

Figure 6.11. Analysis of contingencies with principal components.

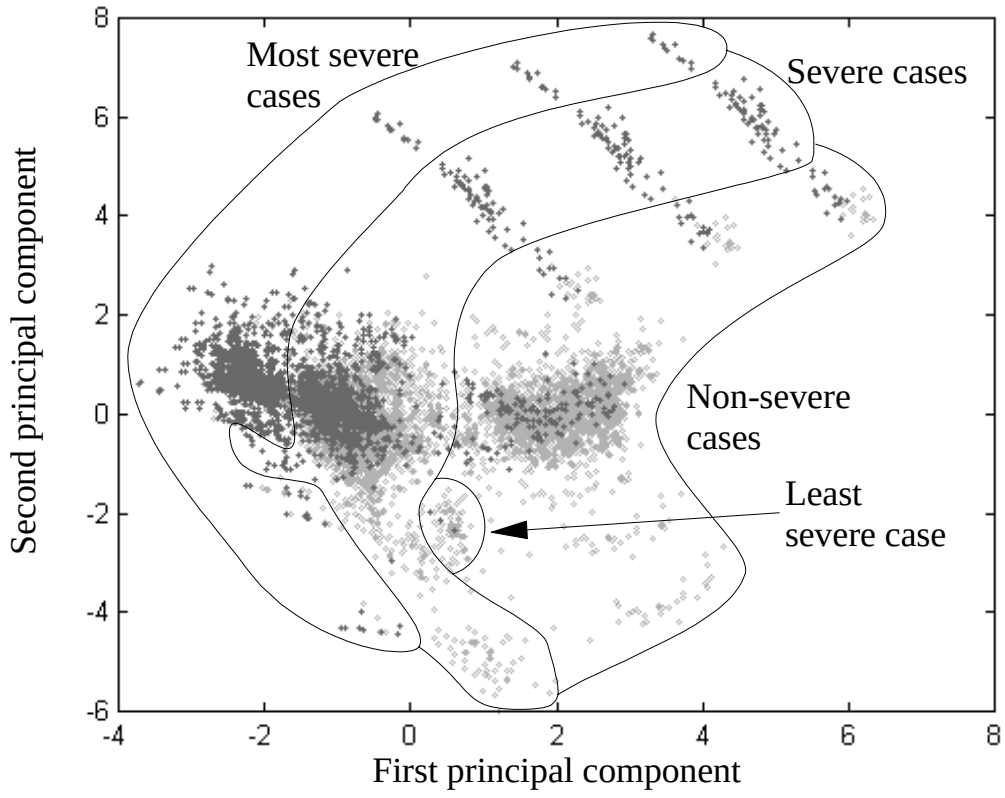

Figure 6.12. Analysis of cases with principal components.

6.1.4 Model creation for approximation of voltage stability margin

Chapters 6.1.1 to 6.1.3 describe the characteristics of the maximum loading point algorithm, contingency ranking methods and visualisation of results of contingency analysis. These are done before the data generation and model creation procedures. Finally the most important results of the thesis, the model-based approximation of post-disturbance voltage stability margin, are presented. First the analysis of data is presented to describe the operation space of the system. The feature selection and extraction methods are then applied to reduce the dimension of inputs and a comparison results of parameter estimation algorithms and feature selection and extraction methods are also presented. The comparison of models is presented to find out the best and structure. Finally the results of generalisation capability and generalisation improvement testing are analysed.

Data analysis

The number of training, validation and test cases was 4370, 772 and 100 respectively. The computation direction was chosen to increase the load at area 1 and the production at areas 2 and 3. The total active power load was varied ±10 pu around the base case. The training data included cases from a healthy network, i.e. all lines and generators were connected at the normal operation points. Active and reactive power line flows from one end of a line and bus voltages in pre-disturbance state were selected for model inputs. The total number of inputs was 490 (186 lines and 118 buses), which is too much for modelling purposes. The output was the most critical post-disturbance voltage stability margin. The contingency list included four contingencies, tripping off two generators from the production areas (66 and 89), line inside the load area (8-30) and the main tie-line between areas 1 and 2 (38-65). The chosen contingencies are different from the most critical contingencies identified in Chapters 6.1.2 and 6.1.3.

Here we present some electrical variables of training, validation and test data to visualise and to analyse the data used in the model-based approach (see Figure 6.13). The training data is presented with dots (·) and the test data with circles (o). The top subfigure represents the distribution of the post-disturbance margin with respect to the total active power load. The voltage stability margin is the ratio of the total load of post-disturbance maximum loading point and the total load of pre-disturbance normal operation point. The value of voltage stability margin one corresponds to the voltage collapse point. The top subfigure clearly indicates the effect of the total load on the voltage stability margin. On the other hand it shows the uncertainty related to them. The bottom left subfigure represents the data operation space according to the first two principal components. It is not possible to show the overview of the whole data space, but the principal component analysis makes it possible to reduce the dimensions of the data. The first two principal components are used to show the data instead of the original 490 dimensional data. The bottom right subfigure is the distribution of the minimum voltage in the post-disturbance maximum loading point (PoC, point of collapse). The whole distribution is within the

normal voltage range, which makes it impossible to detect the maximum loading point with the minimum voltage.

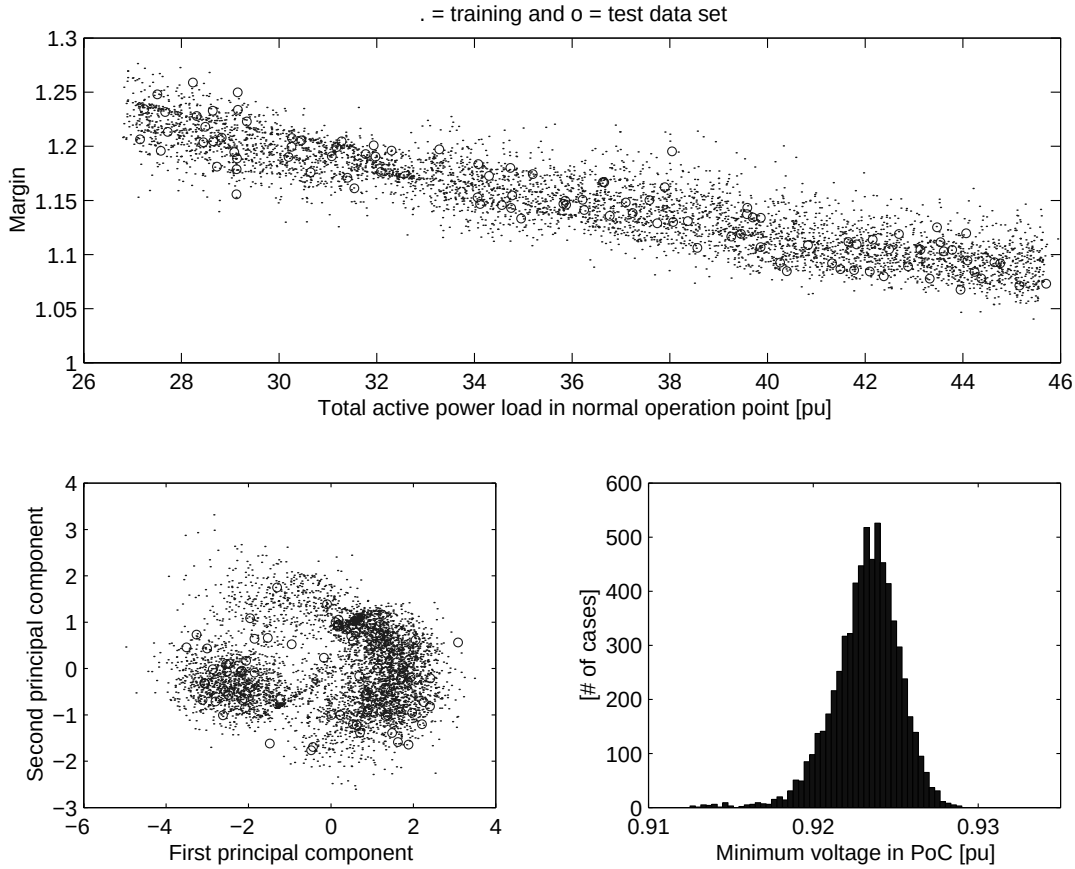

Figure 6.13. Data distribution in the operation space.

Figure 6.14 presents the distribution of the tie-line flows at normal operation point and at maximum loading point. The top subfigures present transfer from area 2 to area 1. The average transfer has increased approximately 1.7 pu from the normal operation point to the post-disturbance maximum loading point. Only a few cases cross 4 pu transfer in the post-disturbance maximum loading point. On the other hand the maximum transfer limit can in some cases be as low as 3.2 pu. The fixed transfer limit will lead to inefficient use of the transmission network. The middle subfigures represent transfer from area 3 to area 1. The uncertainty at the maximum transfer limit is larger in these tie-lines than between areas 1 and 2, although the maximum power is smaller. The bottom subfigures represent the transfer between areas 2 and 3. The wide distribution of the power transfers is due to the changes in the unit commitment and the generation dispatch at areas 2 and 3.

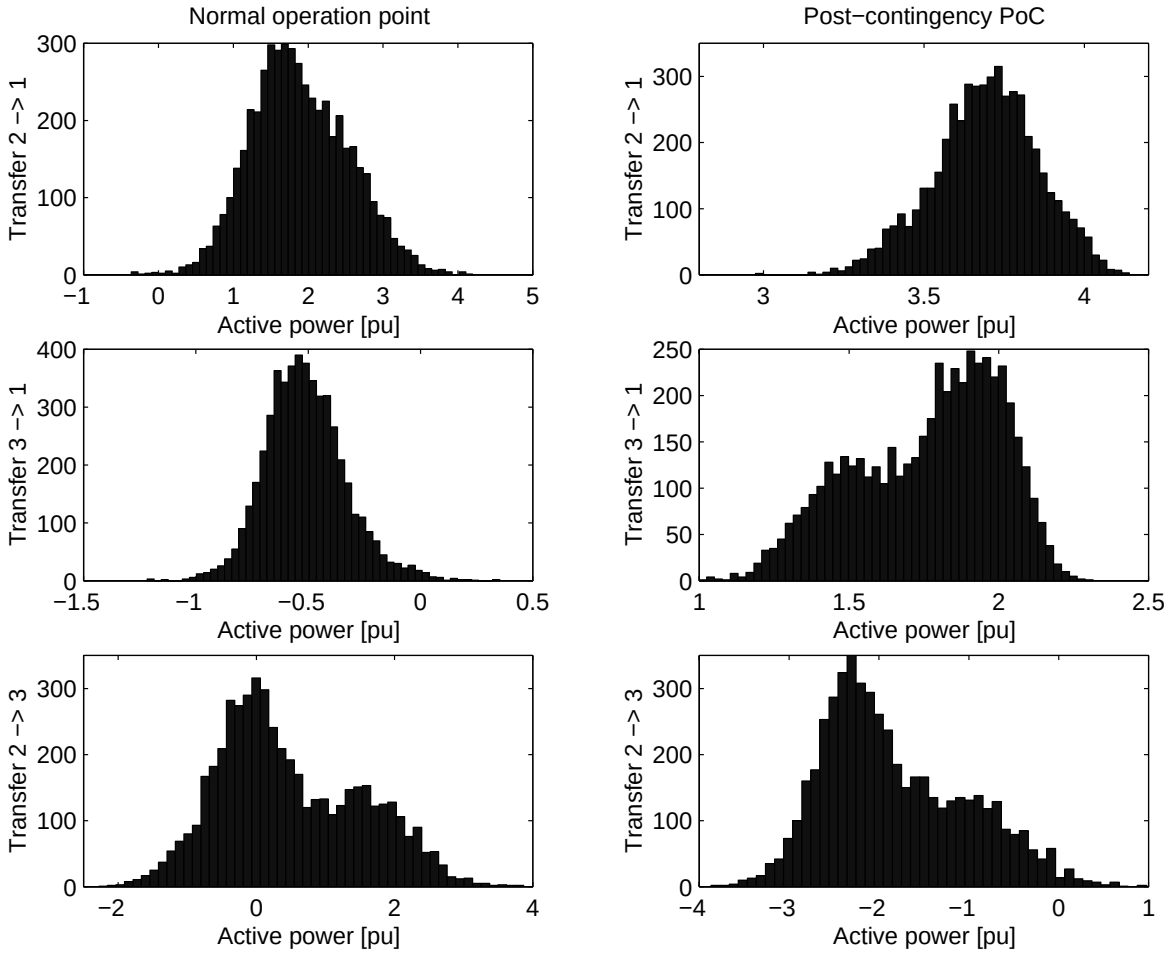

Figure 6.14. Active power transfers.

Feature selection and extraction

The redundant variables of the data have to be removed in order to improve the generalisation ability of the model and the performance of the parameter estimation algorithm. The low variance variables do not explain the changes in the system state, and it is natural to remove them from the data. In this way, we were able to reduce the number of variables to 434 (8 active line flows, 15 reactive line flows and 33 voltages were removed).

The number of model inputs was reduced from 434 to 10 with the principal component analysis. The first principal component explains 50 % of the variability of all variables (see Figure 6.15). Ten first principal components correspond to 91 % of the variance cumulation (the straight line, scale on the right hand side of figure). The reduction of inputs is highly significant and easy to do. The main disadvantage is the large computer memory requirement. Heavy computation of principal component analysis is required once. The transformation matrix of principal components is used in the on-line procedure. The on-line procedure (input vector reduction and model output computation) takes less than 1 second with a PC (Pentium 350 MHz with 256 Mb RAM).

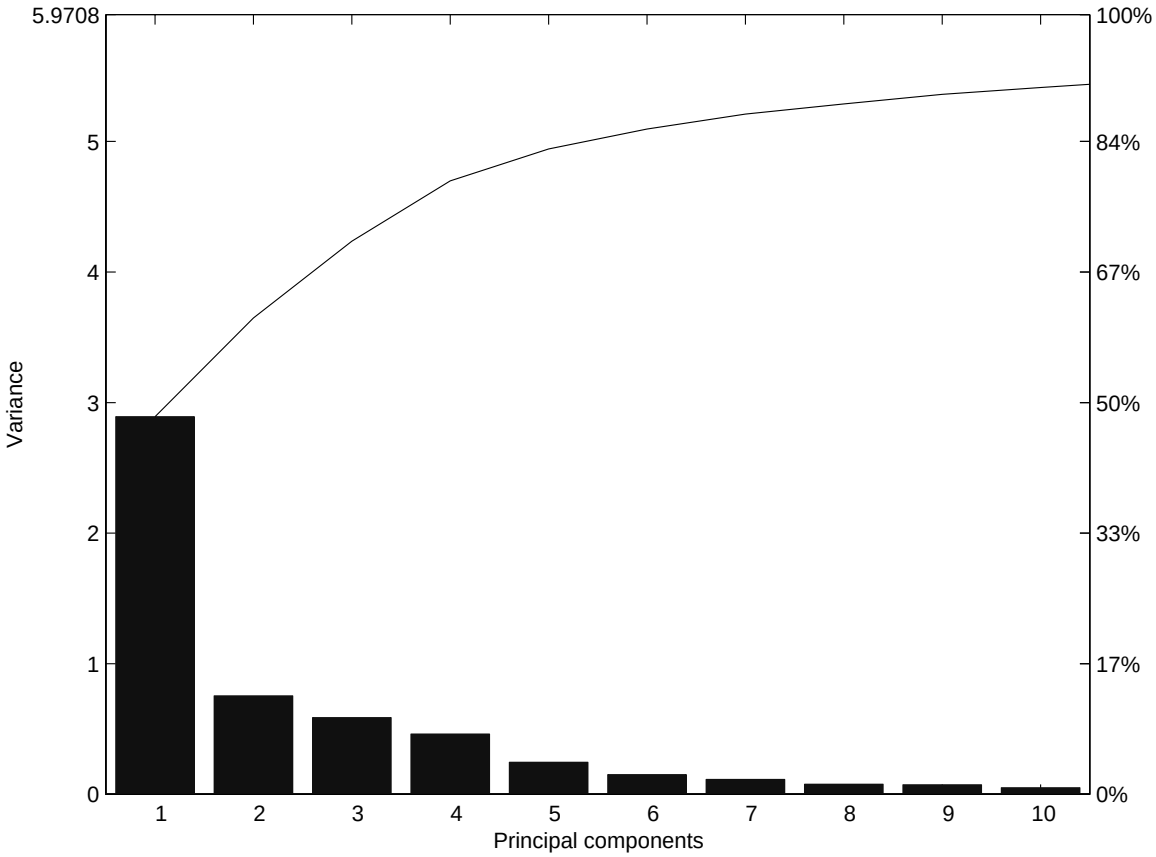

Figure 6.15. First ten principal components and variance cumulation.

The selection of model inputs is not as easy with the K-means clustering as with the principal component analysis. The number of cluster centres for active line flow, reactive line flow and voltage were 10, 15 and 15 respectively. Although the K-means algorithm is fast and can manage a large amount of data, the total computation time is longer than that of the principal component analysis. K-means clustering cannot recognise the physical relationship but searches for a statistical one. Due to this problem, the clustering is done separately for each variable group (active line flows, reactive line flows and voltages), while the reduction of variables is done by representing each cluster by its centre. The number of variables in the clusters varies between 1 and 33.

Figure 6.16 shows the histograms of the cluster centres. The clusters of active power flow are mainly based on the statistical properties of the data. The mean value and the standard deviation of cluster centres are presented in Table 6.10 in ascending order. Some of the clusters of reactive power flow have a physical meaning. For example cluster number 1 includes lines which are below surge impedance load, cluster number 11 includes lines from generator buses 24, 40 and 107 which are always under-excited and cluster number 15 includes only transformers. The voltage clusters are also mainly characterised by the statistical properties of the data. Due to the local property of the power system voltage buses close to each other are grouped more likely into the same clusters than distant buses. Certain clusters may include distant buses which have similar voltage distribution.

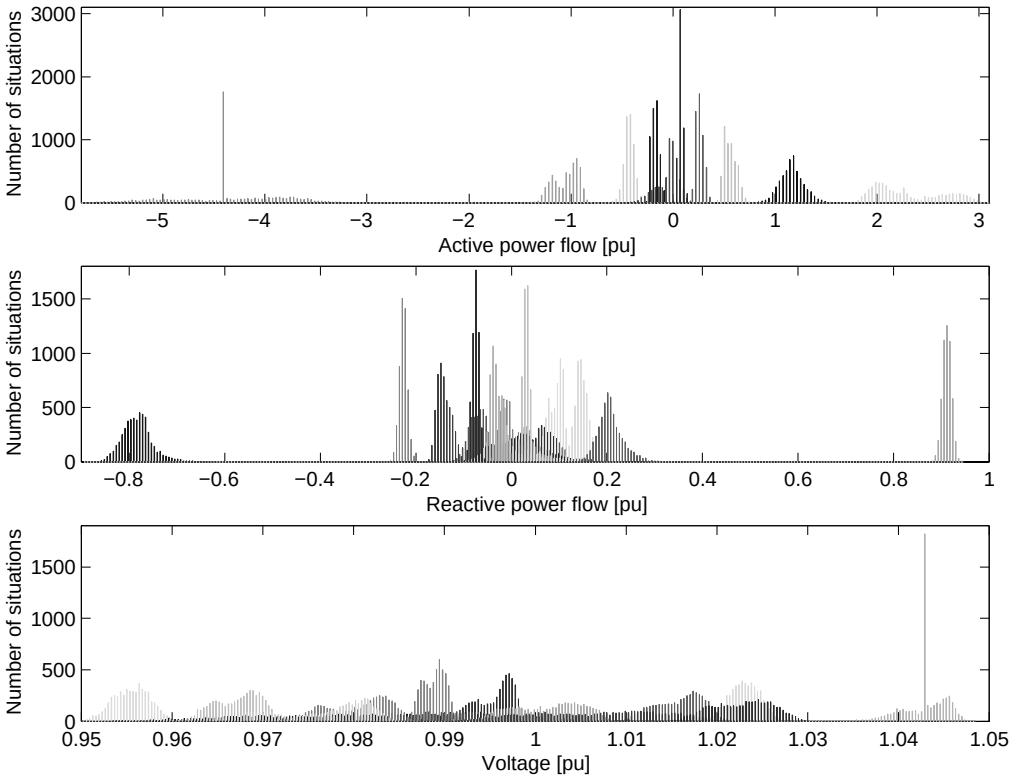

Figure 6.16. Histograms of cluster centres.

Table 6.10. The mean value and the standard deviation of cluster centres.

Cluster	*Active line flow*		*Reactive line flow*		*Voltage*	
	Mean	*Std*	*Mean*	*Std*	*Mean*	*Std*
1	-4.4	0.54	-0.78	0.073	0.9555	0.0023
2	-1.04	0.18	-0.23	0.030	0.9672	0.0029
3	-0.43	0.16	-0.14	0.037	0.9764	0.0062
4	-0.16	0.088	-0.077	0.025	0.9787	0.0107
5	-0.057	0.16	-0.041	0.061	0.9805	0.0041
6	0.064	0.092	-0.032	0.024	0.9881	0.0089
7	0.27	0.092	-0.008	0.045	0.9888	0.0085
8	0.56	0.13	0.0064	0.033	0.9888	0.0016
9	1.2	0.24	0.015	0.052	0.9957	0.0024
10	2.3	0.41	0.031	0.022	1.0013	0.0042
11	-	-	0.045	0.049	1.0067	0.0076
12	-	-	0.092	0.034	1.0158	0.0028
13	-	-	0.15	0.031	1.0226	0.0035
14	-	-	0.21	0.049	1.0230	0.0020
15	-	-	0.91	0.027	1.0429	0.0023

Comparison of parameter estimation algorithms and feature selection and extraction methods

Two feature selection methods (principal component analysis and K-means clustering) and five parameter estimation algorithms of a multilayer perceptron neural network were studied to find the best combination. The parameter estimation algorithms studied were Levenberg-Marquardt (LM), Broyden, Fletcher, Goldfarb and Shanno (BFGS) update for the quasi-Newton optimisation algorithm, scaled conjugate gradient (SCG), resilient back-propagation (RPROP) and gradient descent (GD) with adaptive learning rate and momentum term. Each algorithm was studied with a different number of hidden layer nodes with the trial and error method. Furthermore, parameters were initialised five times to attain as good a local minimum as possible. Studies were made with PC (Pentium 90 MHz and 64 Mb RAM) and Matlab [Mat98b, Nør97].

The results of the parameter estimation algorithms and principal component analysis are presented in Figure 6.17. The error in Figure 6.17a is the mean square error (MSE). The LM optimisation algorithm is best according to validation error. The BFGS is almost as good as the LM. Other optimisation algorithms are in the following order: SCG, RPROP and GD. The minimum validation error was achieved with the LM algorithm and with nine hidden layer nodes. Figure 6.17b presents training times for all algorithms with respect to number of hidden layer nodes. The number of iterations used for different algorithms was LM 100, BFGS, SCG and RPROP 1000 and GD 10000 iterations. The LM algorithm is again the best one. The LM algorithm is obviously the best choice when the number of parameters is not great.

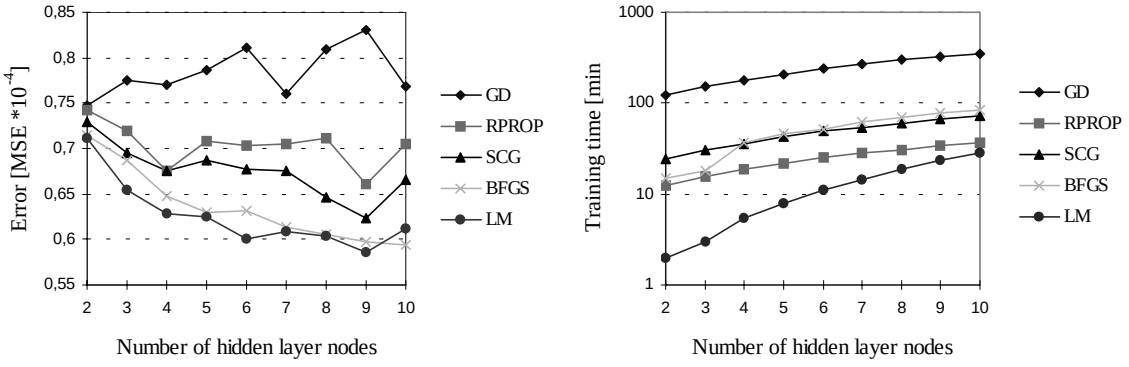

(a) (b)

Figure 6.17. Principal component analysis: (a) Validation errors and (b) training times with different parameter estimation algorithms.

The results of K-means and parameter estimation algorithms study are presented in Figure 6.18a. Again the LM optimisation algorithm is the best one, and the BFGS is almost as good as the LM. The performance of SCG, RPROP and GD is reduced significantly compared with the study of principal component analysis. The minimum validation error (LM with eight hidden layer nodes) is less than with principal component analysis. However, the total number of parameters is much greater with K-means than with principal

component analysis, because the number of inputs is greater. Figure 6.18b presents neural network training times for all algorithms with respect to the number of hidden layer nodes. The training time of all algorithms is longer than that with principal component analysis. This is due to the greater number of parameters. When the number of parameters is increased, the time needed for parameter estimation increases rapidly with the LM. According to the training time requirement, the BFGS algorithm is much better than the LM. Unfortunately, fast parameter estimation algorithms like RPROP and SCG do not work well enough.

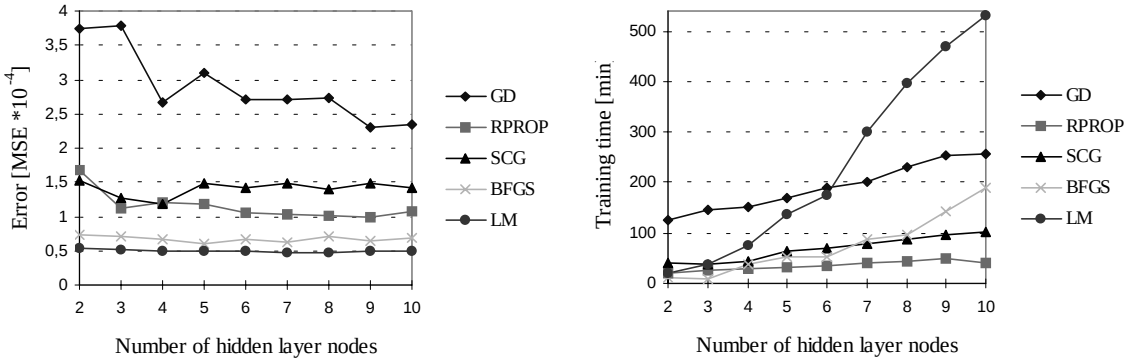

Figure 6.18. K-means: (a) Validation errors and (b) training times with different parameter estimation algorithms.

When principal component analysis is used in feature selection and extraction, fewer input variables can be used to guarantee good generalisation than when using the K-means method. The use of principal component analysis is also more straightforward and easier than using the K-means method. The neural network validation errors were found to be at the same level with both methods. When the size of data is huge, the computation of principal component analysis needs special algorithms for singular value decomposition.

The LM optimisation algorithm was found to be the best. When the number of neural network parameters increases, the LM algorithm needs a lot of computer memory and the training time becomes long. In that case the BFGS or the SCG optimisation algorithms should be used. Given the findings of the present study, the use of GD is not recommended.

Comparison of models

This chapter presents the comparison of linear and non-linear models for the approximation of post-disturbance voltage stability margin. The models studied were linear regression, multilayer perceptron neural network and radial base function neural network. The number of inputs was 10. The inputs were the ten first principal components.

The linear model was tested with polynomial models, and the selection of model order was tested with a few simple models. The results of the most successful models are presented in

Table 6.11, and the models are compared according to MSE, residual maximum (max(r)), residual mean value (mean(r)), residual standard deviation (std(r)) and number of parameters. The accuracy of models was good, the best result being achieved with the full quadratic model and a surprisingly good result being achieved with the pure linear model. This indicates the strong linear dependency between the input and the output. If the number of parameters is highlighted instead of the accuracy, then a model including a cubic term should be used. Parameter estimation (solution of the least square estimation problem) took a few seconds depending on the number of parameters. These studies were made with PC (Pentium 350 MHz and 256 Mb RAM) and Matlab [Mat98a].

Table 6.11. Comparison of linear models.

Model	*MSE* $[10^{-5}]$	*Max(r)* $[10^{-2}]$	*Mean(r)* $[10^{-4}]$	*Std(r)* $[10^{-3}]$	*# of param.*
$y=[1\ \underline{x}]\underline{\beta}$	10.2	4.79	-10.0	10.1	11
$y=[1\ \underline{x}\ \underline{x}^2]\underline{\beta}$	10.1	4.85	-11.0	10.0	21
$y=[1\ \underline{x}\ \underline{x}^3]\underline{\beta}$	9.62	4.66	-9.36	9.8	21
$y=[1\ \underline{x}\ \underline{x}^4]\underline{\beta}$	10.2	4.79	-11.0	10.0	21
Full quadratic	7.01	4.04	-9.15	8.3	66

The number of hidden layer units for a multilayer perceptron neural network was optimised by estimating parameters for different numbers of hidden layer units. Table 6.12 presents the results computed by the Levenberg-Marquardt optimisation algorithm [Nør97]. The parameter estimation procedure for all numbers of hidden layer units with single initial values took approximately 26 minutes. The performance of all multilayer perceptron neural networks was very good. Both the MSE and the residual maximum have a minimum point. The optimum number of hidden layer units was 7. The mean and the standard deviation of the residuals were close to zero in all cases.

Table 6.12. Comparison of multilayer perceptron neural networks.

Hidden units	*MSE* $[10^{-5}]$	*Max(r)* $[10^{-2}]$	*Mean(r)* $[10^{-4}]$	*Std(r)* $[10^{-3}]$	*# of param.*
1	7.64	3.96	-12.0	8.7	13
2	7.12	3.87	-8.83	8.4	25
3	6.54	3.84	-6.61	8.1	37
4	6.27	3.85	-7.40	7.9	49
5	6.14	3.81	-7.24	7.8	61
6	6.06	3.80	-6.51	7.8	73
7	5.97	3.68	-7.01	7.7	85
8	6.15	3.75	-6.35	7.8	97
9	6.12	3.73	-7.37	7.8	109
10	6.17	3.81	-5.07	7.8	121

The basis functions of radial base function neural network were estimated using the K-means clustering and the solution of the linear problem [Bis00]. The results, presented in Table 6.13, were almost as good as the results of the multilayer perceptron neural network. However, it should be noted that the number of parameters is much greater. According to the test results the best radial base function neural network has 40 base functions. The whole parameter estimation procedure for all numbers of hidden units with single initial values took about 45 minutes.

Table 6.13. Comparison of radial base function neural networks.

Hidden Units	*MSE* $[10^{-5}]$	*Max(r)* $[10^{-2}]$	*Mean(r)* $[10^{-4}]$	*Std(r)* $[10^{-3}]$	*# of param.*
10	9.09	4.12	11.0	9.5	121
20	7.72	4.22	9.51	8.7	241
30	7.06	4.02	8.86	8.4	361
40	6.84	4.0	8.50	8.2	481
50	6.88	4.02	8.60	8.3	601
60	6.93	4.04	8.70	8.3	721
70	6.89	4.06	8.21	8.3	841
80	6.89	4.04	8.79	8.3	961
90	6.91	4.09	7.91	8.3	1081
100	6.87	4.06	7.80	8.3	1201

The comparison results of the model type selection is presented in Table 6.14. The comparison of models was mainly based on the accuracy of the models. The number of parameters required and the model creation time were used as subsidiary criteria. The weights of the criteria are presented in percentages. The best model type got three points, the next two points and the last got one point for each criterion. The comparison of model types is based on the weighted sum of points. According to these criteria the models studied were in the following order: multilayer perceptron neural network, full quadratic polynomial and radial base function neural network.

Table 6.14. Comparison of models.

	Multilayer perceptron	*Quadratic Polynomial*	*Radial base Function*
Accuracy (50 %)	3	1	2
Parameters (25 %)	2	3	1
Creation time (25 %)	2	3	1
Weighted sum	2.5	2	1.5

Generalisation capability

The generalisation capability of models was studied with the test data set. Figures 6.19 and 6.20 show two examples of these tests. The output estimates of the multilayer perceptron

neural network were very accurate with seven hidden unit networks (Figure 6.19). The maximum residual was 2.1 %. The top subfigure presents the true and the estimated outputs in ascending order for the test data set. The order of outputs does not have meaning in practice. The residuals between the true and the estimated outputs are shown in the middle subfigure. The bottom subfigure presents the histogram of output residuals. The mean value of output residuals is about zero and the distribution of residuals is similar to normal distribution.

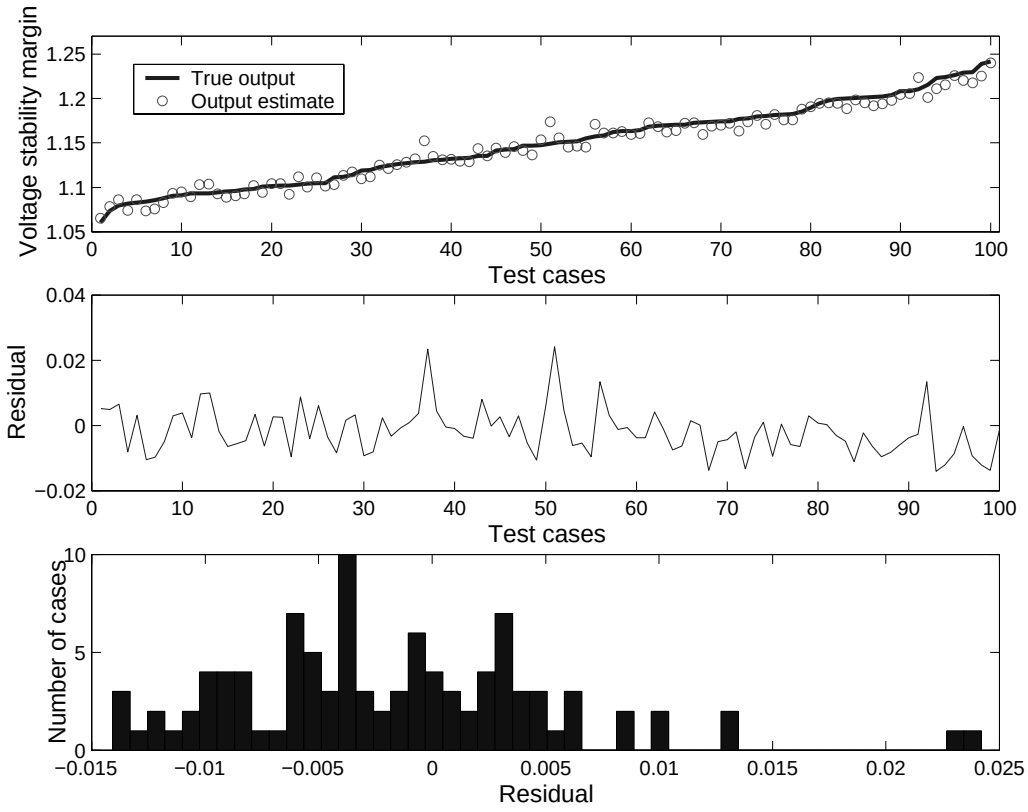

Figure 6.19. Multilayer perceptron neural network output estimates and errors.

The confidence limits of parameter estimates are used to describe the distribution of model outputs. This property is demonstrated with the full quadratic polynomial model. Figure 6.20 presents 95 % confidence limits, the estimates of model output and the true outputs. This figure provides valuable information about the performance of the model throughout the output range, showing the model's ability to approximate the voltage stability margin more accurately in the middle of the range than at the extremities. This is essential information, because the reliability of the model is a important factor in the decision-making on operation control.

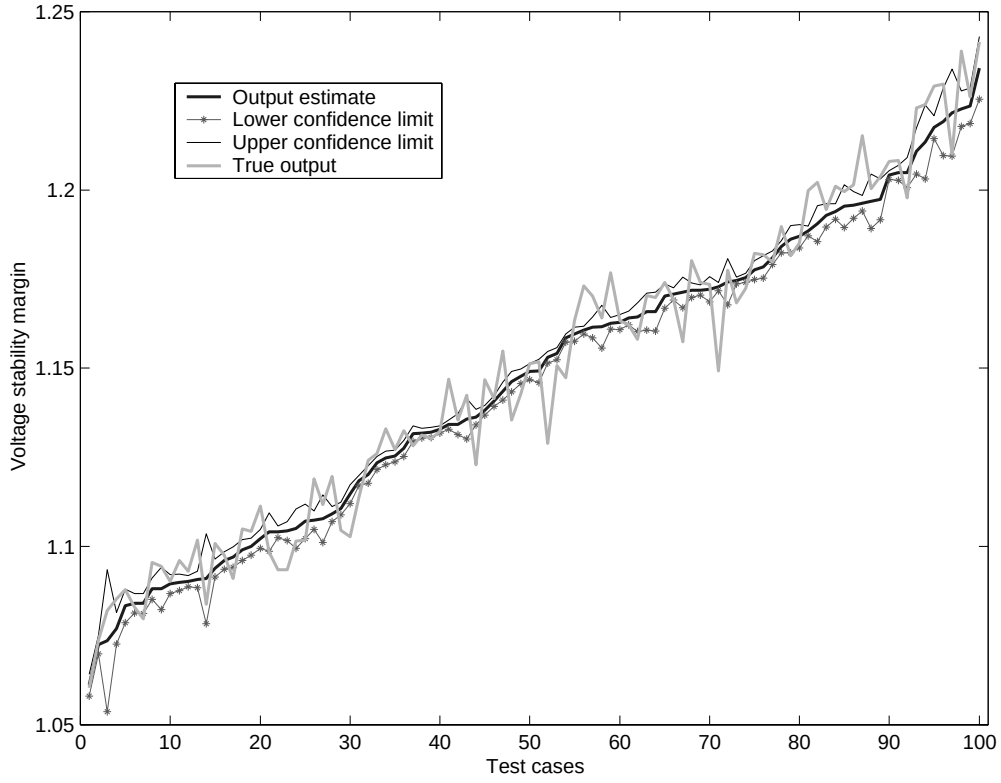

Figure 6.20. Confidence limits and output estimates of the full quadratic polynomial model.

Generalisation improvement

The generalisation of the multilayer perceptron neural network can be improved with the special methods described in Chapter 4.3.3. When the early stopping method was tested with different parameter estimation algorithms it was found that generalisation did not improve, but the number of iterations was reduced in all cases. The generalisation capability of the GD algorithm was reduced, because parameter estimation was stopped too soon. The generalisation capability of other algorithms was about the same as without early stopping. The average number of iterations was 65 (LM), 150 (BFGS), 145 (SCG), 425 (RPROP) and 340 (GD). According to this study early stopping can be used to reduce the parameter estimation time of the multilayer perceptron neural network.

Regularisation was tested with the LM optimisation algorithm. The generalisation capability was only slightly better than that of the best neural network model given by the trial and error method. The use of regularisation allows larger neural networks to be used without loss of generalisation capability. In this way the neural network design time can be reduced, because it is not necessary to study many different kinds of neural network structures.

Pruning was tested with the best multilayer perceptron neural network structure and the used technique was optimal brain surgeon [Nør97]. The starting point of pruning requires a well generalised neural network. This means that neural network pruning is suitable only for the fine tuning of a model, not for neural network design. It is effective in the reduction of neural network parameters. Without a significant decrement in the generalisation capability, about half of the neural network parameters could be removed. This may indicate that there are still too many input variables.

6.1.5 Summary of the IEEE 118-bus test system

Chapter 6.1 has shown the test results of the maximum loading point algorithm, the contingency ranking methods, the data visualisation methods, and the model-based voltage stability assessment. The accuracy of the maximum loading point algorithm is good enough when compared to other similar methods. The disadvantage of the algorithm is the relatively long computation time. This could be improved with the proposed step length control and prediction step methods. Four different contingency ranking methods were tested, of which the curve fitting method was found to be the most accurate. The reactive power loss and the minimum singular value methods could be used to indicate the proximity to the maximum loading point. The contingency clustering method could be used for the analysis of large a amount of data of the contingency analysis. The data visualisation methods are valuable in the data analysis of the model creation procedure. Here the visualisation was also made for the results of contingency analysis.

The model-based voltage stability assessment is capable of approximating the most critical voltage stability margin very accurately and the model creation could be done in reasonable time. This is the main result of this chapter. The use of feature selection and extraction methods is an essential requirement for the accurate model and the fast response of the parameter estimation algorithm. Principal component analysis was found to be attractive for this purpose. The parameter estimation of the multilayer perceptron neural network was also tested. According to the test results the second order optimisation algorithms should always be used in the parameter estimation. The Levenberg-Marquardt algorithm especially was found to be robust and moderately fast when the number of parameters was not large. Different model types (linear regression, multilayer perceptron neural network and radial base function neural network models) were also compared, the best results resulting from the multilayer perceptron neural network, although almost equally good results were achieved with all model types.

6.2 Equivalent of the Finnish transmission network

Figure 6.20 presents the Finnish 400 kV and 220 kV transmission network in 1999. The Finnish network has interconnections to Sweden, Norway, and Russia. The AC interconnections to Sweden are located in northern Finland and the DC interconnection, Fenno-Skan HVDC link, is located in south-western Finland. The connection to Russia is a

back-to-back HVDC connection (the Vyborg link). The annual energy consumption in Finland was 78 TWh in 1999 [Nor99], and the installed production capacity was about 16.5 GW [Nor99]. Energy consumption occurs mainly in the southern part of the country, the main part of the energy being generated by hydro and thermal (nuclear, coal, and gas) power plants. Hydro power plants are situated mainly in northern Finland and thermal power plants in the coastal area of southern Finland. In 1999, 14 % of electrical energy was imported [Nor99]. The operational conditions of the Finnish transmission network are typical for a system with a long distance power transmission, where stability problems, especially voltage stability, are to be considered when the power transmission increases from Sweden to northern Finland and from northern to southern Finland.

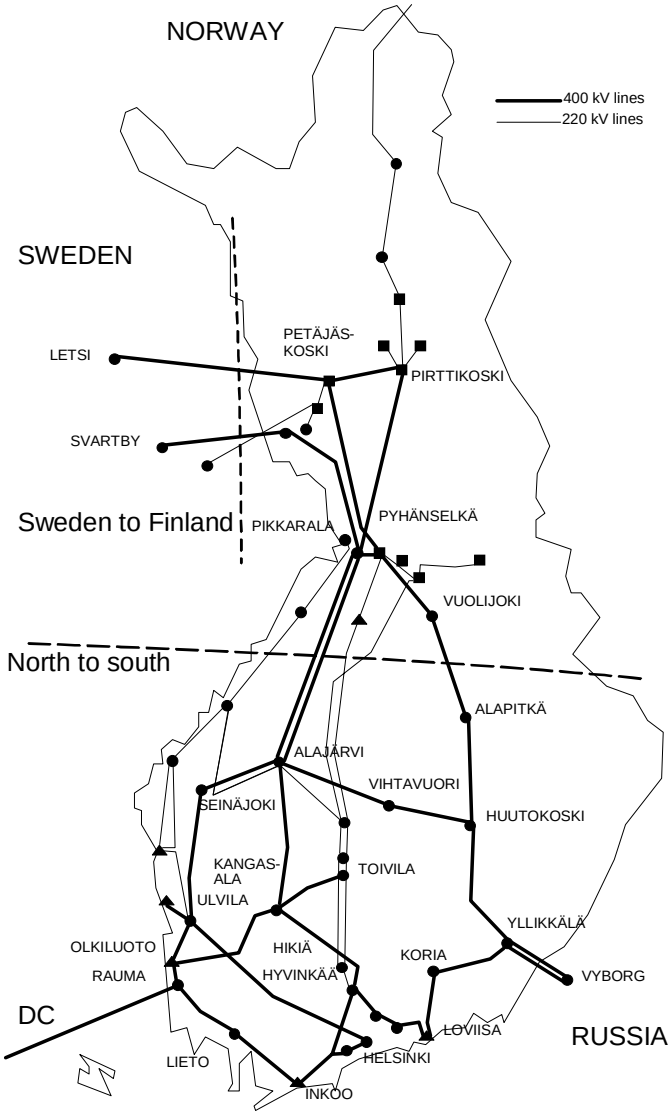

Figure 6.20. The Finnish 400 kV and 220 kV transmission network in 1999.

The analysis of the proposed method was not as complete as for the IEEE 118-bus test system. For example, the analysis of contingencies was totally omitted. The test results were computed for a single contingency situation, the outage of the largest power plant. The analysis of line outages was too complicated due to the reaction of the equivalent

system. The total load and production in the base case were 10932 MW and 9627 MW, respectively. The import from Sweden was 829 MW and the transfer to southern Finland was 790 MW. It is typical for winter cases that AC import from Sweden to northern Finland is not close to the maximum limit due to the high production in southern Finland.

The proposed model-based voltage stability assessment was tested on the equivalent of the Finnish transmission network to ascertain the applicability and the problems on the real system. The equivalent system (131 buses and 236 branches) included the entire 400 kV transmission network. The 220 kV network was partly made equivalent and the 110 kV network were completely made equivalent. The description of the Swedish power system was rough: it had six buses that included a slack bus, one generator and two loads. The connection to northern Norway was disconnected. The Fenno-Skan HVDC link and the Vyborg link to Russia were described as loads, because the characteristics of these correspond to constant power load. The Fenno-Skan HVDC link exported power to Sweden (27…82 MW in the generated data). The Vyborg link imported about 750 MW to Finland.

6.2.1 Computation and analysis of the data

The computation direction of maximum loading point was chosen to increase the AC import from Sweden to Finland and the transfer from northern to southern Finland. The locations of intersections are marked on Figure 6.20. These intersections are the main bottlenecks of the Finnish transmission network. The pre-disturbance data for the model-based approach included cases between the base case and 10 pu above the base case. The pre-disturbance cases were all healthy cases. The number of cases was 10767. Of these 10 % did not fulfil the (*n-1*)-criterion, i.e. the load-flow did not converge at the post-disturbance situation. These cases are called unstable. Next the computed data was analysed by intersection transfers, bus voltages and system loading.

The transfers of intersections Sweden to Finland and north to south are presented in Figure 6.21. The figure includes histograms of the pre-disturbance operation points and the maximum transfers according to the (*n-1*)-criterion. The maximum transfers are determined by computing the post-disturbance maximum loading points and subtracting the effect of generator outage from the intersection transfers. The light and dark grey histograms include stable and unstable operation points respectively. The base value of active power flow corresponds to the maximum transfer limit of AC interconnection between Sweden and Finland determined by the deterministic (*n-1*)-criterion and detailed dynamic simulations.

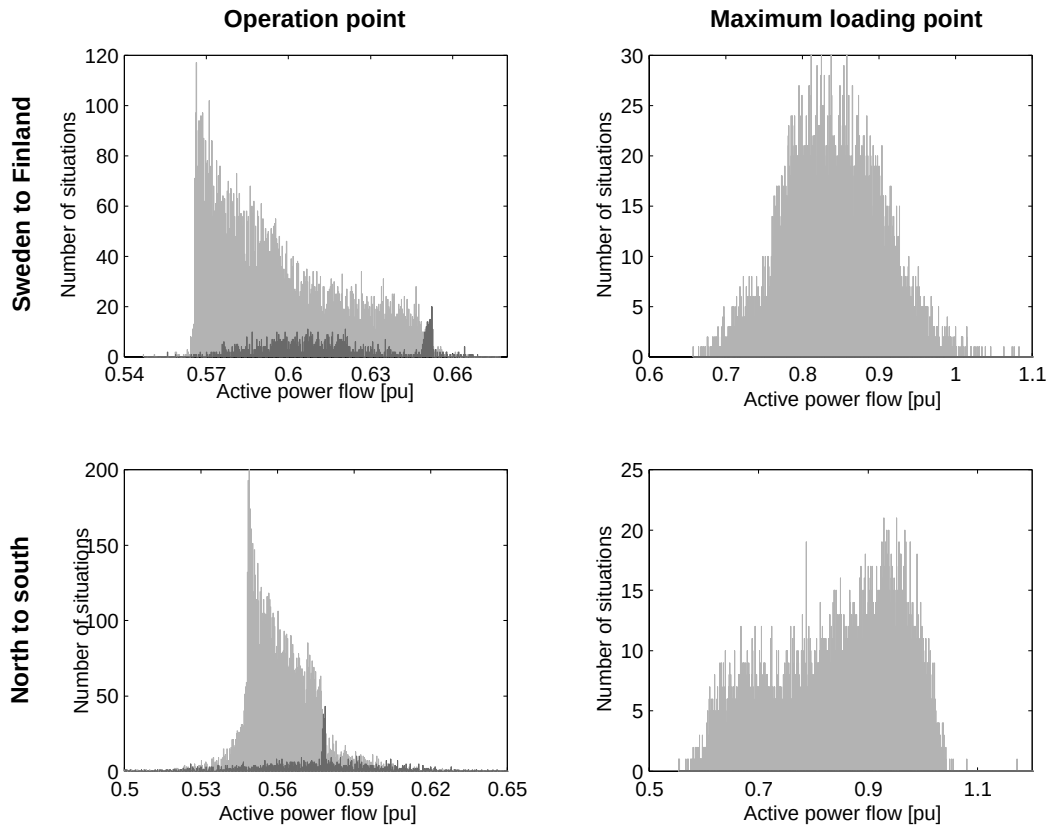

Figure 6.21. Active power flows of intersection transfers.

The operation points of the intersection between Sweden and Finland are well below the real maximum transfer limit. The distribution of transfers of operation points is concentrated for low values. A major part of imported power is further transferred to southern Finland. It is noteworthy that unstable operation points have a wide distribution. The reasons for the unstable cases could be inconvenient loading/production situation (real unstable case) or load-flow numerical problems (unreal unstable case). It is assumed that unstable cases are real unstable cases. This assumption is made due to difficulty in separating real and unreal unstable cases. Some of the unstable cases have low intersection transfers at the operation point due to high production in southern Finland. This clearly indicates the effect of production variation at the data generation stage. Because the system represents a winter case, the probability of power production increment was increased in southern Finland in the variation of operation points. The security assessment becomes difficult when the intersection transfers are the parameters monitored in the on-line security assessment as the possibility of the occurrence of stable and unstable cases at similar transfer situations makes the security assessment uncertain.

The system was unable to achieve the real maximum transfer limit in all cases, which is due to the use of equivalent transmission network model and the exceptional load/production situations in the computed data. An accurate model of the Swedish power system would improve the situation considerably. In that case the maximum transfer limit

would be higher. The base case of the equivalent system represents a lightly loaded transfer situation. Slightly better results would be achieved if the power transfers were higher in the base case. The reactive power balance of the equivalent system is based on the light transfer situation, when the line compensation is not always appropriate and the voltage level is unacceptably low in high transfer situations. The maximum transfers of the intersections also have wide distributions, the lowest computed transfer limit being about 0.65 pu and the highest limit above 1 pu for the intersection of Sweden and Finland. This makes the security assessment with intersection transfers even more complicated.

Figure 6.22 presents the pre-disturbance voltages. The voltages of buses 108 and 131 are the lowest of the pre-disturbance cases. However, these buses are equivalent nodes, thus the physical meaning of these buses is not clear. The lowest voltages of the 400 kV network were found in buses 17 and 33. The light and the dark grey indicate stable and unstable cases respectively. The voltages of buses 17, 33 and 108 seem to be good indicators of the system state. Although there is overlapping of stable and unstable cases, the distributions of unstable cases are much narrower than the distributions of stable cases and the unstable cases have the lowest voltages. The voltage of bus 131, however, makes the analysis of voltage quite complicated. However, all voltages are within the ±10 % voltage variation limits, which makes the decision on secure level of voltage difficult.

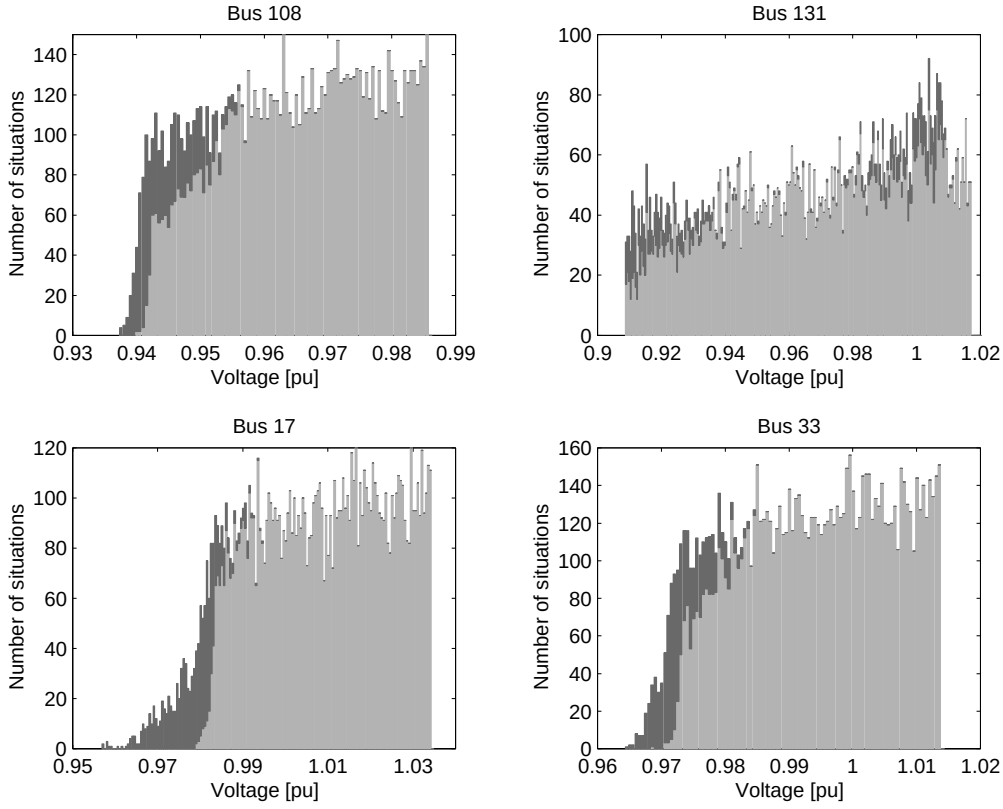

Figure 6.22. Lowest pre-disturbance voltages.

The third figure of computed data (Figure 6.23) presents the function between the total active power load and the post-disturbance voltage stability margin. The voltage stability margin is calculated as a difference of the total load between the post-disturbance maximum loading point and the pre-disturbance operation point. The dots (·) indicate the training data and the circles (o) indicate the test data. It clearly shows the effect of total load on the voltage stability margin, but also the uncertainty of this. The unstable cases (zero margins) are all heavily loaded. The bottom subfigure presents the minimum voltages at the pre-disturbance normal operation point (light grey) and at the post-disturbance maximum loading point (dark grey). If the minimum voltage of the whole system is used as an indicator for security assessment, it is clear that the minimum of system voltages should not be lower than 0.9 pu in any case. However, the minimum voltage is mainly from the equivalent nodes, which do not actually exist.

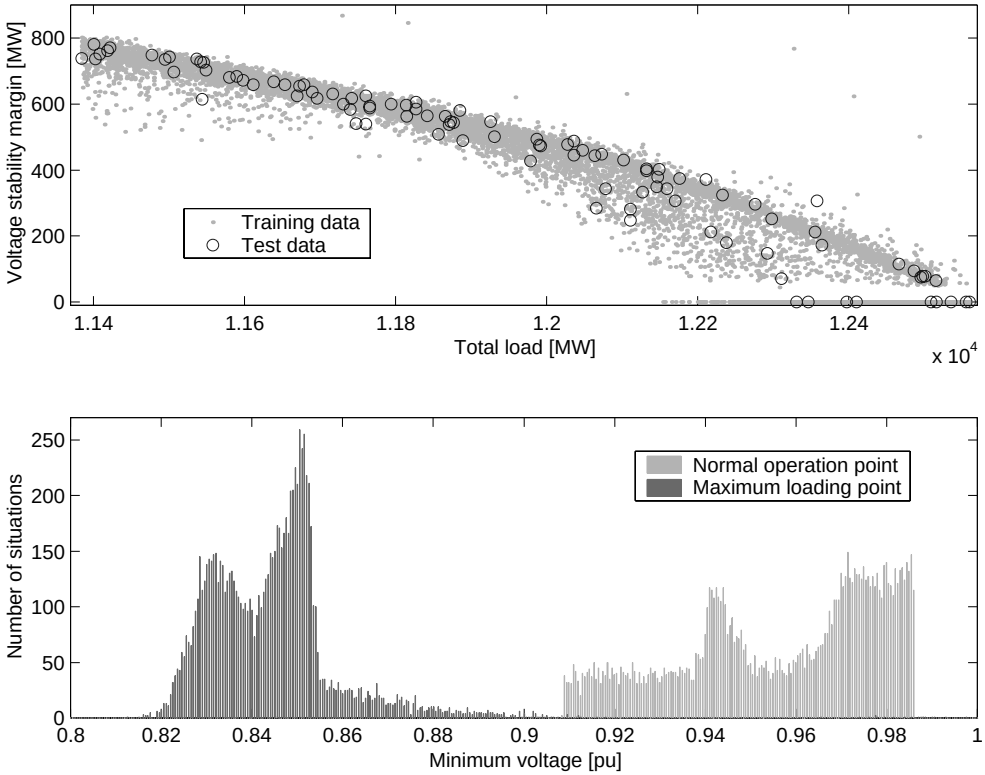

Figure 6.23. Voltage stability margin vs. total load and histograms of minimum voltages.

6.2.2 Modelling of post-disturbance voltage stability margin

The data was divided into training, validation and test data sets. The number of training, validation and test cases was 9151, 1516 and 100 respectively. The data included the pre-disturbance operation points and the post-disturbance voltage stability margins. The voltage stability margin is the ratio of the total load of post-disturbance maximum loading point and the total load of pre-disturbance operation point. Thus, the value of voltage stability margin one corresponds to the voltage collapse point. The inputs of the model

were chosen from the non-equivalent variables. The input variables were active and reactive line flows from one end of the line and bus voltages. The number of variables was 239 (98 lines and 43 buses). The reduction of input variables was based on the computation of variances (11 variables were removed) and the principal component analysis. The ten first principal components chosen for model inputs, could explain 96 % of the variability of all variables.

Table 6.15 presents the comparison results of linear models using a polynomial model. The comparison is based on MSE, maximum, mean value and standard deviation of residual, and number of parameters. The accuracy of all models is good. The pure linear model ($\underline{y}=[1\ \underline{x}]\underline{\beta}$) also has relatively good results when the number of parameters is considered. The difference of accuracy of the models is insignificant. The different measures of model accuracy (MSE and maximum residual) moreover give contradictory results. The best model was chosen mainly based on MSE, because it measures "global" properties instead of maximum residual, which measures more or less "local" properties of the model. Based on these arguments, the best model is the full quadratic model. The mean value and the standard deviation of residuals of all models are close to zero, thus there is no significant bias or variation. The parameter estimation time was a few seconds with PC (Pentium 350 MHz and 256 Mb RAM) and Matlab [Mat98a].

Table 6.15. Comparison of linear models.

Model	*MSE* $[10^{-5}]$	*Max(r)* $[10^{-2}]$	*Mean(r)* $[10^{-4}]$	*Std(r)* $[10^{-3}]$	*# of param.*
$\underline{y}=[1\ \underline{x}]\underline{\beta}$	1.39	1.95	0.246	3.7	11
$\underline{y}=[1\ \underline{x}\ \underline{x}^2]\underline{\beta}$	1.05	1.99	-0.227	3.2	21
$\underline{y}=[1\ \underline{x}\ \underline{x}^3]\underline{\beta}$	1.39	1.92	0.254	3.7	21
$\underline{y}=[1\ \underline{x}\ \underline{x}^4]\underline{\beta}$	1.12	1.86	-0.021	3.4	21
Full quadratic	1.01	2.22	-0.218	3.2	66

The parameters of the multilayer perceptron neural network were estimated with the Levenberg-Marquardt optimisation algorithm [Nør97]. The number of hidden units, i.e. the number of parameters, was chosen using the trial and error method. The trials included five different initial values for each parameter case. Table 6.16 presents the validation results. The results of all multilayer perceptron neural networks are very good. According to MSE and maximum residual the multilayer perceptron neural network is more accurate than the polynomial model. However, the time needed for the parameter estimation is much longer for multilayer perceptron neural network than for linear models. The column *Time* in Table 6.16 indicates the time needed for the parameter estimation of a single trial. The best neural network structure includes eight hidden units. The selection of the best structure was mainly based on the MSE, because the maximum residual does not have a clear minimum point. The mean value and the standard deviation of residual are close to zero.

Table 6.16. Comparison of multilayer perceptron neural networks.

Hidden Units	*MSE [10^{-5}]*	*Max(r) [10^{-2}]*	*Mean(r) [10^{-4}]*	*Std(r) [10^{-3}]*	*Time [s]*	*# of param.*
1	0.864	1.56	0.110	2.9	11	13
2	0.686	1.48	0.606	2.6	56	25
3	0.680	1.47	0.580	2.6	97	37
4	0.681	1.48	0.628	2.6	144	49
5	0.674	1.61	0.847	2.6	208	61
6	0.631	1.58	0.409	2.5	285	73
7	0.669	1.48	0.754	2.6	376	85
8	0.628	1.55	0.455	2.5	475	97
9	0.670	1.49	0.594	2.6	585	109
10	0.73	1.58	0.725	2.7	774	121

Table 6.17 shows the validation results of the radial base function neural network. The accuracy of radial base function neural networks is almost as good as the accuracy of multilayer perceptron neural networks. However, the number of parameters in radial base function neural networks is much greater than that in multilayer perceptron neural networks. The best results were achieved with radial base function neural network having 40 basis functions. Although the number of parameters is much greater with the radial base function neural network than with the multilayer perceptron neural network, the parameter estimation time is shorter when the optimum neural network structures are compared. The test was made with Netlab toolbox [Bis00].

Table 6.17. Comparison of radial base function neural networks.

Hidden Units	*MSE [10^{-5}]*	*Max(r) [10^{-2}]*	*Mean(r) [10^{-4}]*	*Std(r) [10^{-3}]*	*Time [s]*	*# of param.*
10	0.892	1.66	0.664	3.0	112	121
20	0.784	1.66	0.283	2.8	212	241
30	0.724	1.65	0.071	2.7	312	361
40	0.671	1.59	0.539	2.6	413	481
50	0.655	1.69	0.373	2.6	514	601
60	0.651	1.65	0.560	2.6	615	721
70	0.647	1.62	0.571	2.5	718	841
80	0.633	1.61	0.455	2.5	828	961
90	0.636	1.61	0.605	2.5	930	1081
100	0.628	1.61	0.484	2.5	1039	1201

Figure 6.24 presents the results of the generalisation test of the multilayer perceptron neural network with eight hidden units. The test cases cover the whole data space, which can be seen from the Figure 6.23. The output estimates are very accurate. The maximum residuals are 1.5 % and 0.73 % for validation and test data respectively. The top subfigure

presents the output estimates and the true voltage stability margins. The model outputs are marked with a circle (o) and the true output is the light grey line. The output residuals are presented in the middle subfigure. There is no trend in the residual, which means that the model is equally good throughout the data space. The bottom subfigure is the histogram of output residuals in MWs. The maximum residual is less than 90 MW. Most of the residuals are ±40 MW.

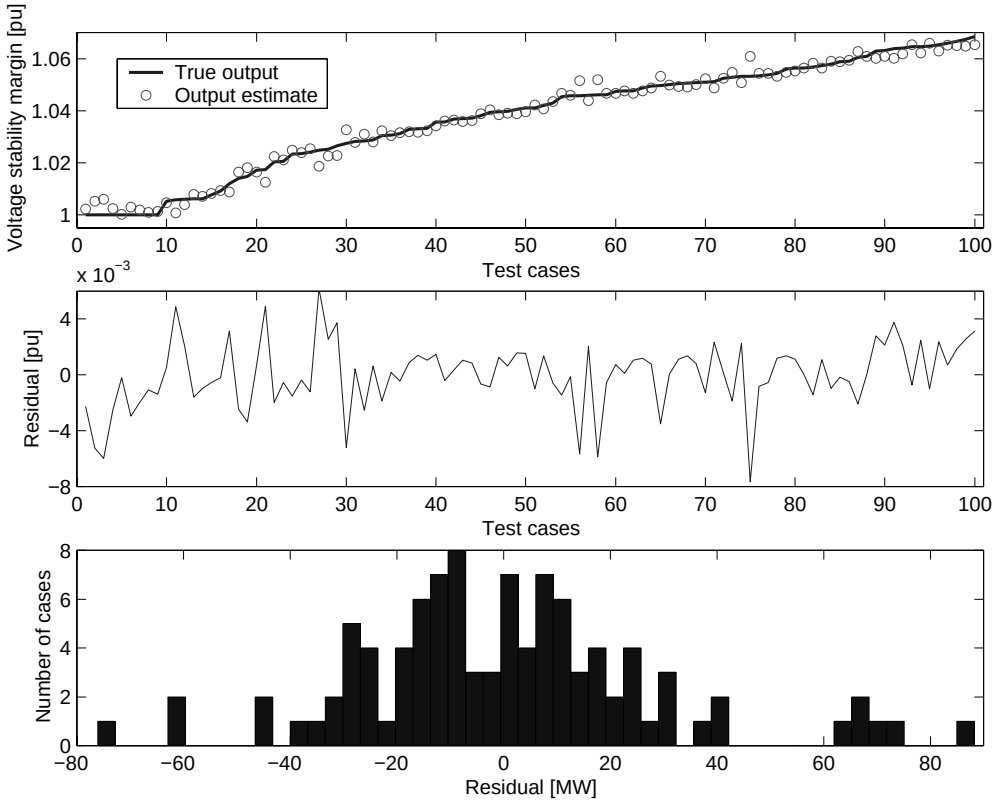

Figure 6.24. Generalisation test of multilayer perceptron neural network, eight hidden units.

The uncertainty of model parameters can be estimated with confidence limits. The output estimates of the model usually have narrow distributions. Figure 6.25 shows 95 % confidence limits for the full quadratic polynomial model. The figure also shows the true outputs and the output estimates of the model. The model has the ability to approximate the voltage stability margin more accurately in the middle than at the extremities of the data range. The model has some difficulties in approximating the unstable cases (margin=1), which is indicated by peaks in the lines of the confidence limits.

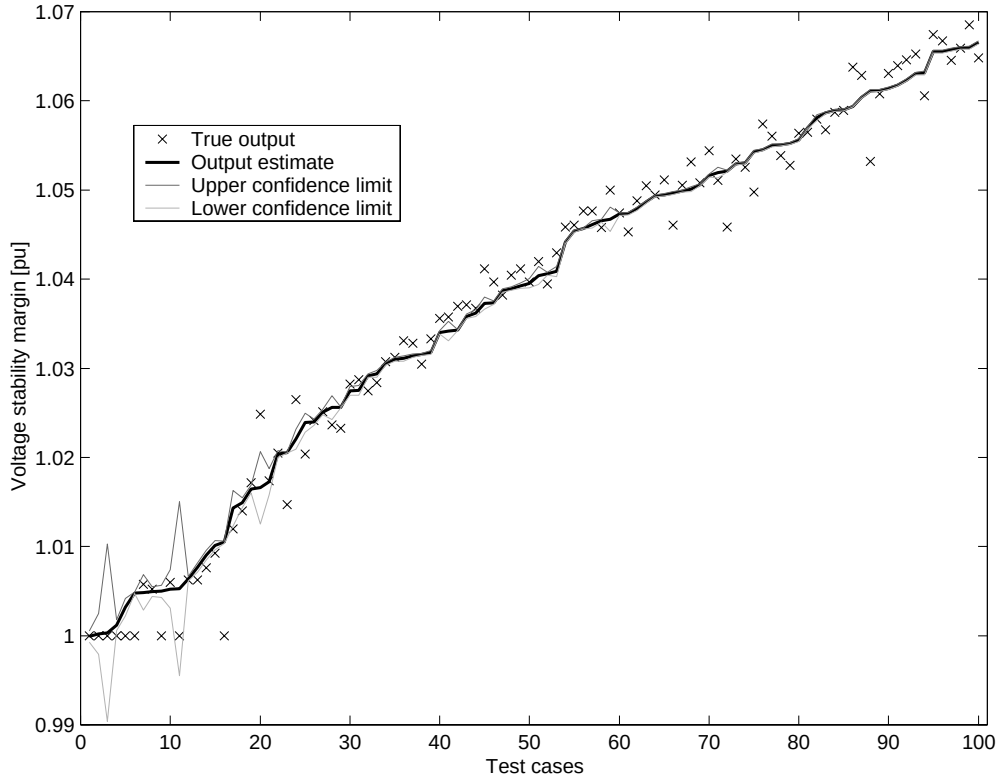

Figure 6.25. Generalisation test and confidence limits of full quadratic model.

6.2.3 Summary of the Finnish transmission network

The model-based approach was applied to the equivalent of the Finnish transmission network. The equivalent system presented a winter case. The system was studied to find the maximum transfer capacity from Sweden to Finland. The use of the equivalent system caused some troubles in the computation of maximum transfers. The representation of Swedish power system especially was inadequate. The equivalent system was also created in a light transfer situation, when the line compensation was not always appropriate and the voltage level was unacceptably low in high transfer situations. The maximum transfer capacity of the cases generated varied between 0.65…1.1 pu compared to the actual maximum value, which was determined by dynamic simulations. It was also found that the maximum transfer capacity has a wide distribution and the security assessment based on the intersection transfers studied includes some uncertainty. The voltage level was found to indicate the state of the power system more clearly than the intersection transfers do. However, the pre-disturbance voltages are always within the normal operation range.

The test results of the equivalent system are similar to results of the IEEE 118-bus test system. The accuracy of the model is even slightly better in the equivalent system than in the test system. The multilayer perceptron neural network was again found to be the best one. The feature extraction and the parameter estimation were based on the principal component analysis and the Levenberg-Marquard algorithm respectively. The maximum

residual of model output estimate was 90 MW and most residuals were ±40 MW. According to the test results the model-based approach is applicable to a real system, however practical implementation would require a more detailed power system model that could represent the performance of the real system.

6.3 Applicability to practical power systems

Practical power systems consist of thousands of nodes and branches, and hundreds of generators, loads and other devices. The number of possible operating points is infinite. This fact complicates the applicability of the model-based approach to practical systems, but does not make it impossible. The computation power and capacity of computers and capability of numerical methods are enough today for the power system analysis of any size system. Of course there are limits to computer memory and so on, but detailed analysis of the whole European transmission system is seldom needed. A typical study model represents a part of a practical system that may be a detailed description of some local part of the system or an equivalent system where a major part of practical system is described with equivalents. The reduction of the power system model is dependent on the problem studied. The number of possible operating points may also be reduced when the knowledge and the experience of the functioning and operating practices of the system are considered. The consideration of the probability of operating points considerably reduces the number of unusual combinations of network topologies and unit commitments which require consideration.

A detailed voltage stability study of the Finnish power system, for example, requires a description of the transmission network at least in Finland and in northern Sweden, a description of the major generators and loads in both countries, and a detailed description of loads and load parameters in the critical area. If the studies are made with a power system model including all Nordic countries, the number of uncertain parameters increases to great number. The uncertainty is related to the parameters of power system components, operation practices and knowledge of the functioning of the system. Therefore some compromises between the size of the system model and the accuracy of system modelling must be made.

The proposed model-based approach has some interesting characteristics, which may be put to use in practical power systems. The on-line security assessment of power systems has traditionally been based on the monitoring of intersection transfers, bus voltages etc. in order to maintain the security of the power system. This approach is a deterministic one, hence it is not easy to take the uncertainty of the power system into account. The model-based approach is a step towards a stochastic security assessment where the uncertainty of the power system is fully modelled.

6.3.1 Computation of data

The computation of data is the most essential part of the model-based approach. The data consists of possible pre-disturbance operation points and corresponding post-disturbance voltage stability margins. The computation of data may be put in parallel form to compute an enormous amount of data in a fraction of the time compared to the serial form of computation. The progress of computer and software technology should also be taken into account in the development of computation methods. The computation capacity of computers has increased following Moore's law for the last 20 years. The parallel computation can nowadays be realised on a local area network with PCs using client/server model or NT/Linux clusters [Cen00]. The computation time of available transfer capacity can be reduced by distributed or parallel computation methods, e.g. distributed contingency analysis [San99] and available transfer capability [Eje98b], which are already available. These also make possible the updating of the data in reasonable time. One of the advantages of the proposed approach is the ability to add more data later on if necessary. The storage of the data is not a problem, because the capacity of data storage devices is already sufficient.

The consideration of power system functioning and operation practices requires the help of power system planners and operators. The experience and the knowledge of these people is valuable, but that information cannot be the only source of information on the variation of pre-disturbance operation points, for the selection of critical contingencies, and for the computation of voltage stability margins. The stochastic nature of the system must somehow be taken into account. One possibility to accommodate the uncertainty is to analyse the historical data of operating points. Another possibility is to create scenarios of possible operation points. The scenarios are especially needed to create unstable and close to unstable operation points, because the amount of historical data from these points is usually small. The scenarios of possible but unusual operation points and the information of functioning and operation practices of the power system are included in the automatic data generation procedure. The procedure adds some randomness to the data in order to create different kinds of operation points. The historical data can provide answers to questions like:

- what kind of network topologies are most probable and what kind of topologies have never been experienced
- what kind of unit commitments are possible and what kind are not
- how much can the power production of generators vary, i.e. how are they actually operated
- how much do loads vary and what is the annual maximum and minimum of the total load
- what is the probability of contingencies.

The most critical post-disturbance voltage stability margins are then computed. The computation burden of the security analysis must be reduced by contingency selection and

ranking methods. This is important in practical systems where the number of possible contingencies is thousands. However, it might be dangerous to rely only on usual critical contingencies. The contingency ranking at unexceptional operation points may be different than at usual operation points. That is why the contingency list used in the computation of maximum loading point must include critical contingencies for a wide variety of operation points. The determination of computation direction may be based on the analysis of historical data or the power system planner or operator may predetermine it. Special attention must also be paid to the reactive power limits of generators, load parameters and operation practices of reserves and voltage control devices. The computation of the maximum loading point may be done using load flow or dynamic simulation.

6.3.2 Model creation

The aspects of feature selection and extraction and of the generalisation capability of the proposed approach are critical in large-scale applications at the model creation stage. Feature selection and extraction is an essential action to overcome the computation burden at the parameter estimation step and to improve model generalisation ability. The proposed feature selection and extraction methods are also capable for large-scale applications. The use of principal component analysis may require a special algorithm designed for large data sets. However, the number of inputs may be reduced to few with principal component analysis dependent on the size of data set. The generalisation ability of the model is improved by the use of feature selection and extraction methods. This is due to the ability to avoid the curse of dimensionality problem when the dimension of the data set is decreased.

The generalisation capability of the model is also dependent on the procedures of parameter estimation, especially with neural networks, and on the selection of model type. The accuracy of the model is better with multilayer perceptron neural networks than with polynomial models. The accuracy of the polynomial model is good enough, especially when the time needed for the parameter estimation procedure is also considered. However, the parameter estimation of a neural network with a large-scale data set is possible today as in reference [Koh00] with a massive self-organising map. The computation capacity and power is steadily increasing, which further solves the problem of computation time. The parameter estimation of the multilayer perceptron neural network should be done with second order optimisation algorithms, which are more robust than first order algorithms.

7 SUMMARY

The thesis proposed a model-based approach for the on-line assessment of long-term voltage stability. It also includes descriptions of the voltage stability problem, on-line voltage stability assessment, computation methods of voltage collapse point, contingency ranking methods for non-linear problems and black-box modelling. The proposed approach is intended for the determination of the power system state and the estimation of the available transfer capacity, and may be implemented as a decision support tool for the power management system.

The proposed model-based approach approximates the most critical post-disturbance voltage stability margin, and the thesis includes a step by step procedure for its application. The approach requires the computation of a large amount of training data, the condensing of all voltage stability assessment sub-problems into a few sub-problems, and the creation of models. Efficient methods for voltage stability margin computation, contingency ranking and automatic data generation were also proposed. Principal component analysis and K-means clustering were used to reduce the number of inputs and to improve model generalisation capability. Advanced optimisation methods (second order optimisation algorithms) were presented for the parameter estimation of multilayer perceptron neural network. These are faster and more robust than the standard back-propagation. Three different models a linear regression model (polynomial model), a multilayer perceptron neural network and a radial base function neural network were tested.

The approach was successfully applied to the approximation of the most critical post-disturbance voltage stability margin of the IEEE 118-bus test system and a 131-bus equivalent system of the Finnish power system. The results prove the ability of the proposed approach to approximate the voltage stability margin. The test results also show the comparison of different feature selection and extraction methods, parameter estimation algorithms and model types. The best results were achieved with the multilayer perceptron neural network and principal component analysis. The advantage of linear polynomial models compared to neural networks is the fast parameter estimation and capability to easily estimate the uncertainty of model parameters with confidence limits.

7.1 Advantages of the proposed method

Basically the model-based approach and the security boundary method are similar. The security boundary is understood as a graphical model, but the proposed method is more

general and accurate. Furthermore, the proposed method includes automatic database generation and data pre-processing, which are not included in the security boundary method. The automatic database generation in particular is a major improvement compared to the security boundary method. The proposed method is one step to fully automatic security analysis, which also considers the uncertainties related to on-line stability studies. Nowadays, the computation and analysis of uncertainties related to transmission network operation requires a lot of manual work to set up operational scenarios and to analyse stability studies. The proposed method applies the computation power and capacity available today to utilise existing transmission equipment more efficiently. The advantages of the proposed approach are:

- The on-line procedure of the model-based approach is extremely fast
- It has the ability to interpolate between the operation points used in the training
- The clustering of pre-disturbance operation points based on network topology and unit commitment situations is applied to reduce the number of models and to take into account different network topology, unit commitment, production, loading situations etc.
- The approach is not restricted to neural networks. The application of a linear regression model to on-line voltage stability assessment is proposed first time in the thesis.

The advantage of the model-based approach compared to conventional security boundary nomograms is the extension of two-dimensional analysis to the multidimensional space. The function approximation of the voltage stability margin could also be non-linear. The non-linear approximation makes it possible to estimate the margin more accurately and thus gives a better estimate of system security. This may allow the transfer capacity to be increased in some cases if the reliability margin of available transfer capacity can be decreased. The accuracy and applicability of the proposed approach is based on the automatic generation of good quality data and the use of feature selection and extraction methods in data pre-processing. The modelling and computation of the power system are based on existing methods and tools.

The security boundary nomograms are usually based on a few manually computed and analysed operation points, when there is a danger that the model may extrapolate. The accurate modelling requires the use of many different kinds of operation points in order to ensure enough data for good interpolation. The automatic procedure also ensures that the analysis of computed cases does not limit the data generation. The data generation part of the model-based approach is commonly omitted in published papers. However, the data generation determines the ability of the whole approach. This part of the approach was described in detail in this thesis.

The high dimensionality of power system operation space may be taken into account in the proposed approach. The number of model inputs does not have a maximum limit rather the number of inputs is selected by the model generalisation capability. The accuracy of the

model can be improved in this way. The information loss in the feature selection and extraction of the model-based approach is fairly small compared to that of the security boundary method. The feature selection and extraction methods studied are useful and important for the generalisation capability of the models. The proposed method also applies different input variables than reported in previously published papers. The line flows are applied to represent changes in the network topology and unit commitment.

7.2 Disadvantages of the proposed method

The disadvantage of the model-based approach is the requirement of time-consuming computation during data generation, model creation and model updating. Models should be updated when the power system or its operation practices have changed considerably. However, this is a disadvantage of all model-based on-line security assessment methods, including the conventional security boundary method. The updating of models requires re-computation of the data and the models. The data generation and pre-processing of the large-scale power systems (ten thousands of variables) require a lot of computation power and capacity. Moreover, the potentiality of transfer capacity increment based on the proposed approach is not yet clear or commonly accepted.

It is possible in the future that on-line voltage stability assessment will be based on similar tools than off-line assessment today, i.e. exact computation of the most critical voltage stability margin. In that case the approximation of voltage stability margins or security boundary will no longer be necessary. The computation power and capacity versus the cost is continuously increasing, which supports the above forecast. The computation time can be reduced by distributed or parallel computation methods, e.g. distributed contingency analysis and available transfer capability, which are already available.

The risk management and the uncertainty handling of the transmission network are becoming more important due to changes in the power system planning and operation environment. The proposed approach is a non-deterministic security assessment method, which is capable of modelling and evaluating the uncertainties of pre-disturbance operation points. Another important aspect, the uncertainty of contingencies, is not considered at all, because the (*n-1*)-criterion is applied. The uncertainty of contingencies is considered in probabilistic security assessment, where the probability of contingencies and the consequences of contingencies are considered concurrently.

REFERENCES

[Adi94] Adibi M.M. and Milanicz D.P., Reactive capability limitation of synchronous machines, *IEEE Transactions on Power Systems*, Vol. 9, No. 1, February 1994, pp. 29-35.

[Agn96] Agneholm E., *The restoration process following a major breakdown in a power system*, Licentiate thesis, Technical report No. 230L, Chalmers University of Technology, Gothenburg, Sweden, 1996, 123 p.

[Ajj92] Ajjarapu V. and Christ C., The continuation power flow: a tool for steady state voltage stability analysis, *IEEE Transactions on Power Systems*, Vol. 7, No. 1, February 1992, pp. 416-423.

[Ajj98] Ajjarapu V. and Lee B., Bibliography on voltage stability, *IEEE Transactions on Power Systems*, Vol. 13, No. 1, February 1998, pp.115-125.

[And72] Andrews H.C., *Introduction to mathematical techniques in pattern recognition*, John Wiley & Sons, New York, USA, 1972, 242 p.

[Aus95] Austria R.R. et al., Integrated approach to transfer limit calculations, *IEEE Computer Applications in Power*, January 1995, pp. 48-52.

[Bac89] Bacher R. and Tinney W.F., Faster local power flow solutions: The zero mismatch approach, *IEEE Transactions on Power Systems*, Vol. 4, No. 4, November 1989, pp. 1345-1351.

[Bas99] Bastman J. et al., Comparison of solution algorithms in point of collapse method, *Proceedings of 13th Power system computation conference*, Trondheim, Norway, June 1999, pp. 451-455.

[Ber98] Berizzi A. et al., First and second order methods for voltage collapse assessment and security enhancement, *IEEE Transactions on Power Systems*, Vol. 13, No. 2, May 1998, pp. 543-549.

[Bha99] Bhargava B., Synchronized phasor measurement system project at Southern California Edison Co., *Proceedings of IEEE PES Summer Meeting*, 1999, pp. 16-22.

[Bis95] Bishop C.M., *Neural networks for pattern recognition*, Clarendon Press, Oxford, UK, 1995, 482 p.

[Bis00] Bishop C.M. and Nabney I., *Netlab toolbox*, the toolbox for Matlab is available at http://www.ncrg.aston.ac.uk/netlab/, 2000.

[Bra88] Brandwajn V., Efficient bounding method for linear contingency analysis, *IEEE Transactions on Power Systems*, Vol. 3, No. 1, February 1988, pp. 38-42.

[Bra89] Brandwajn V. and Lauby M.G., Complete bounding method for AC contingency screening, *IEEE Transactions on Power Systems*, Vol. 4, No. 2, May 1989, pp. 724-728.

[Cañ92] Cañizares C.A. et al., Point of collapse method applied to AC/DC power systems, *IEEE Transactions on Power Systems*, Vol. 7, No. 2, May 1992, pp. 673-680.

[Cañ93] Cañizares C.A. and Alvarado F.L., Point of collapse and continuation methods for large AC/DC systems, *IEEE Transactions on Power Systems*, Vol. 8, No. 1, February 1993, pp. 1-8.

[Cañ99] Cañizares C.A. and Alvarado F.L., *UWPFLOW Continuation and direct methods to locate fold bifurcation in AC/HVDC/FACTS power systems*, the software is available at http://iliniza.uwaterloo.ca/~claudio/software/pflow.html, 1999.

[Cap78] Capasso A. and Mariani E., Influence of generator capability curves representation on system voltage and reactive power control studies, *IEEE Transactions on Power Apparatus and Systems*, Vol. 97, No. 4, July/August 1978, pp. 1036-1040.

[Cen00] Center for Scientific Computing, *Pilot project for PC clusters*, the information is available at http://www.csc.fi/metacomputer/pckluster/, 2000.

[Cha97] Chan K.W. et al., On-line dynamic-security contingency screening and ranking, *IEE Proceeding on Generation, Transmission and Distribution*, Vol. 144, No. 2, March 1997, pp. 132-138.

[Chi95] Chiang H.-D. et al., CPFLOW: a practical tool for tracing power system steady-state stationary behavior due to load and generation variations, *IEEE Transactions on Power Systems*, Vol. 10, No. 2, May 1995, pp. 623-630.

[Chi97] Chiang H.-D. et al., Look-ahead voltage and load margin contingency selection functions for large-scale power systems, *IEEE Transactions on Power Systems*, Vol. 12, No. 1, February 1997, pp. 173-179.

[Cor94] Cory B.J. et al., Towards a neural network based voltage stability assessment, *Proceedings of International Conference on Intelligent Systems Application on Power Systems*, Montpellier, France, 1994, pp. 529-534.

[Cut87] Cuthbert T.R., *Optimization using personal computers with applications to electrical networks*, John Wiley & Sons, New York, USA, 1987, 474 p.

[Cut91] Van Cutsem T., A method to compute reactive power margins with respect to voltage collapse, *IEEE Transactions on Power Systems*, Vol. 6, No. 1, February 1991, pp. 145-153.

[Cut97] Van Cutsem T. and Mailhot R., Validation of a fast voltage stability analysis method on the Hydro-Quebec system, *IEEE Transactions on Power Systems*, Vol. 12, No. 1, February 1997, pp. 282-288.

[Cut98] Van Cutsem T. and Vournas C., *Voltage stability of electric power systems*, Kluwer academic publishers, Boston, USA, 1998, 378 p.

[Cut99] Van Cutsem T. et al., Determination of secure operating limits with respect to voltage collapse, *IEEE Transactions on Power Systems*, Vol. 14, No. 1, February 1999, pp. 327-333.

[Dac84] Sa Da Costa J. and Munro N., Pattern recognition in power system security, *Electrical Power & Energy Systems*, vol. 6, no. 1, January 1984, pp. 31-36.

[Deb91] Debs A.S., *Modern power systems control and operation: A study of real-time operation of power utility control centres*, Kluwer academic publishers, Boston, USA, 1991, 361 p.

[Dil96] Dillon T.S. and Niebur D., *Neural networks applications in power systems*, CRL Publishing, London, UK, 1996, 404 p.

[Dob92] Dobson I., Observations on the geometry of saddle node bifurcation and voltage collapse in electrical power systems, *IEEE Transactions on Circuits and systems—I: Fundamental theory and applications*, Vol. 39, No. 3, March 1992, pp. 240-243.

[Dob93] Dobson I. and Lu L., New methods for computing a closest saddle node bifurcation and worst case load power margin for voltage collapse, *IEEE Transactions on Power Systems*, Vol. 8 No. 3, August 1993, pp. 905-911.

[Edw96] Edwards A.R. et al., Transient stability screening using artificial neural networks within a dynamic security assessment system, *IEE Proceeding on Generation, Transmission and Distribution*, Vol. 143, No. 2, March 1996, pp. 129-134.

[Eje96] Ejebe G.C. et al., Methods for contingency screening and ranking for voltage stability analysis of power systems, *IEEE Transactions on Power Systems*, Vol. 11, No. 1, February 1996, pp. 350-356.

[Eje98a] Ejebe G.C. et al., Online dynamic security assessment in an EMS, *IEEE Computer Applications in Power*, January 1998, pp. 43-47.

[Eje98b] Ejebe G.C. et al, Available transfer capacity calculations, *IEEE Transactions on Power Systems*, Vol. 13, No. 4, November 1998, pp. 1521-1527.

[Elk95] El-Keib A.A. and Ma X., Application of artificial neural networks in voltage stability assessment, *IEEE Transactions on Power Systems*, Vol. 10, No. 4, November 1995, pp. 1890-1896.

[Eur01] European Transmission System Operators, *Net transfer capacities and available transfer capacities in the internal market of electricity in Europe, Information for user*, the information is available at http://www.etso-net.org/, 2001.

[Fla93] Flatabø N. et al., A method for calculation of margins to voltage instability applied on the Norwegian system for maintaining required security level, *IEEE Transactions on Power Systems*, Vol. 8, No. 3, August 1993, pp. 920-928.

[Fle90] Fletcher R., *Practical methods of optimization*, John Wiley & Sons, Chichester, UK, 1990, 436 p.

[Fow86] Fowler F.G. and Fowler H.W., *The pocket Oxford dictionary of current English*, Oxford University Press, Oxford, UK, 1986, 1057 p.

[Gao92] Gao B. et al., Voltage stability evaluation using modal analysis, *IEEE Transactions on Power Systems*, Vol. 7, No. 4, November 1992, pp. 1529-1536.

[Gao96] Gao B. et al., Towards the development of a systematic approach for voltage stability assessment of large-scale power systems, *IEEE Transactions on Power Systems*, Vol. 11, No. 3, August 1996, pp. 1314-1324.

[Gol96] Golub G.H. and van Load C.F., *Matrix computations*, The Johns Hopkins University Press, Baltimore, USA, 1996, 694 p.

[Gra99] Gravener M.H. and Nwankpa C., Available transfer capability and first order sensitivity, *IEEE Transactions on Power Systems*, Vol. 14, No. 2, May 1999, pp. 512-518.

[Gre99] Greene S. et al., Contingency ranking for voltage collapse via sensitivities from a single nose curve, *IEEE Transactions on Power Systems*, Vol. 14, No. 1, February 1999, pp. 232-238.

[Haj98] Hajagos L.M. and Danai B., Laboratory measurements and models of modern loads and their effect on voltage stability studies, *IEEE Transactions on Power Systems*, Vol. 13, No. 2, May 1998, pp. 584-591.

[Har96] Harsan H. et al., Combining parallel processing and cyclic approach to speed-up the static security analysis, *Proceedings of the 12th Power Systems Computation Conference*, Dresden, Germany, August 1996, pp. 932-938.

[Hay94] Haykin S., *Neural networks, a comprehensive foundation*, Prentice Hall, New Jersey, USA, 1994, 696 p.

[Hir99] Hirsch P. and Lee S., Security applications and architecture for an open market, *IEEE Computer Applications in Power*, July 1999, pp. 26-31.

[Hir94] Hirvonen R. and Pottonen L., Low voltages after a disturbance in the Finnish 400 kV network, *Proceedings of the International symposium on Bulk Power System Voltage Phenomena III*, Davos, Switzerland, August 1994.

[Hyv00] Hyvärinen A. and Oja E., Independent component analysis: algorithms and applications, *Neural networks*, Vol. 13, No. 4-5, 2000, pp. 411-430.

[Ibs96] Ibsais A. and Ajjarapu V., Voltage stability-limited interchange flow, *Electric power systems research*, Vol. 38, 1996, pp. 91-95.

[Iee01] IEEE/PES Power System Stability Subcommittee Special Publications, *Voltage stability assessment, procedures and guides*, Final draft, available at http://www.power.uwaterloo.ca, January 2001.

[Iri97] Irisarri G.D. et al., Maximum loadability of power systems using interior point non-linear optimization method, *IEEE Transactions on Power Systems*, Vol. 12, No. 1, February 1997, pp. 162-169.

[Joh92] Johnson R.A. and Wichern D.W., *Applied multivariate statistical analysis*, Prentice Hall, London, UK, 1992, 642 p.

[Joh99] Johansson S.G., Mitigation of voltage collapse caused by armature current protection, *IEEE Transactions on Power Systems*, Vol. 14, No. 2, May 1999, pp. 591-599.

[Koh97] Kohonen T., *Self-organizing maps*, Springer-Verlag, Berlin, Germany, 1997, 426 p.

[Koh00] Kohonen T. et al., Self organization of a massive document collection, *IEEE Transactions on Neural Networks*, Vol. 11, No. 3, May 2000, pp. 574-585.

[Kun94] Kundur P., *Power system stability and control*, McGraw-Hill, New York, USA, 1994, 1176 p.

[Lam97] Lampinen J., Advances in neural network modeling, *Proceedings of the Tool environments and development methods for intelligent systems*, Oulu, Finland, April 1997, pp. 28-36.

[Las96] La Scala M. et al., A neural network-based method for voltage security monitoring, *IEEE Transactions on Power Systems*, Vol. 11, No. 3, August 1996, pp. 1332-1341.

[Lem96] Lemaitre C. And Thomas B., Two applications of parallel processing in power system computation, *IEEE Transactions on Power Systems*, Vol. 11, No. 1, February 1996, pp. 246-253.

[Lem94] Lemström B. And Lehtonen M., *Kostnader för elavbrott*, Nordisk Ministerråd, TemaNord report 1994:627, Copenhagen, Denmark, 1994, 125 p, (in Swedish, includes English summary).

[Lin96] Lind R. and Karlsson D., Distribution system modelling for voltage stability studies, *IEEE Transactions on Power Systems*, Vol. 11, No. 4, November 1996, pp. 1677-1682.

[Löf95a] Löf P-A., *On static analysis of long-term voltage stability*, PhD thesis, Royal Institute of Technology, Stockholm, Sweden, 1995, 197 p.

[Löf95b] Löf P.-A. et al., Voltage dependent reactive power limits for voltage stability studies, *IEEE Transactions on Power Systems*, Vol. 10, No. 1, February 1995, pp. 220-226.

[Man97] Mansour Y. et al., Large scale dynamic security screening and ranking using neural network, *IEEE Transactions on Power Systems*, Vol. 12, No. 2, May 1997, pp. 954-960.

[Mar89] Martens H. And Næs T., *Multivariate calibration*, John Wiley & Sons, Guildford, UK, 1989, 419 p.

[Mat98a] The Math Works Inc., *Usering MATLAB*, Natick, Massachusetts, USA, 1998.

[Mat98b] The Math Works Inc., *Neural network toolbox user's guide*, Natick, Massachusetts, USA, 1998.

[Mcc97] McCalley J.D. et al., Security boundary visualization for systems operation, *IEEE Transactions on Power Systems*, Vol. 12, No. 2, May 1997, pp. 940-947.

[Mcc98] McCalley J.D. et al., Power system security boundary visualization using neural networks, *Proceedings of the Bulk Power Systems Dynamics and Control IV – restructuring*, Santorini, Greece, August 1998, pp. 139-156.

[Mil82] Miller T.J.E., *Reactive power control in electric systems*, John Wiley & Sons, New York, USA, 1982, 381 p.

[Muk96] Muknahallipatna S. and Chowdhury B.H., Input dimension reduction in neural network training – case study in transient stability assessment of large systems,

Proceedings of International Conference on Intelligent System Applications to Power Systems, Atlanta, Florida, USA, 1996, pp. 50-54.

[Net96] Neter J. et al., *Applied linear regression models*, Irwin, Chicago, USA, 1996, 720 p.

[Nor99] *Nordel annual report 1999*, the report is available at http://www.nordel.org/, 1999.

[Nør97] Nørgaard M., *Neural network based system identification toolbox*, Technical University of Denmark, the toolbox for Matlab is available at http://www.iau.dtu.dk/research/control/nnsysid.html, 1997.

[Oba88] Obadina O.O. and Berg G.J., Determination of voltage stability limit in multimachine power systems, *IEEE Transactions on Power Systems*, Vol. 3, No. 4, November 1988, pp. 1545-1552.

[Ola99] Olaru C. and Wehenkel L., Data mining, *IEEE Computer Applications in Power*, Vol. 12, Issue 3, July 1999, pp. 19-25.

[Ove93] Overbye T.J., Use of energy methods for online assessment of power system voltage security, *IEEE Transactions on Power Systems*, Vol. 8, No. 2, May 1993, pp. 452-458.

[Pan73] Pang C.K. et al., Application of pattern recognition to steady state security evaluation in a power system, *IEEE Transactions on Systems, Man and Cybernetics*, Vol. smc-3, No. 6, November 1973, pp. 622-631.

[Par96] Parker C.J. et al., Application of an optimisation method for determining the reactive margin from voltage collapse in reactive power planning, *IEEE Transactions on Power Systems*, Vol. 11, No. 3, august 1996, pp. 1473-1478.

[Pop98] Popovic D. et al., Monitoring and assessment of voltage stability margins using artificial neural networks with a reduced input set, *IEE Proceeding on Generation, Transmission and Distribution*, Vol. 145, No. 4, July 1998, pp. 355-362.

[Pow00a] *Power system simulator for engineering (PSS/E-26.1), Program manual*, Power Technologies Inc., Schenectady, New York, USA, 2000.

[Pow00b] *Power systems test case archive*, the archive is available at http://www.ee.washington.edu/research/pstca/, 2000.

[Reh99] Rehtanz C., Visualisation of voltage stability in large electric power systems, *IEE Proceeding on Generation, Transmission and Distribution*, Vol. 146, No. 6, November 1999, pp. 573-576.

[Rep97] Repo S. and Bastman J., Neural network based static voltage security and stability assessment, *Proceedings of the IASTED international conference High technology in the power industry*, Orlando, Florida, USA, October 1997, pp. 45-51.

[Rep99] Repo S. and Järventausta P., Contingency analysis for a large number of voltage stability studies. *Proceedings of the IEEE Power Tech '99 Conference*, Budapest, Hungary, August 1999.

[Rep00a] Repo S. et al., Data analysis in static voltage stability analysis, *Proceedings of the 6th International Conference on Probabilistic Methods Applied to Power Systems* (PMAPS), Madeira, Portugal, September 2000.

[Rep00b] Repo S. et al., Development of model based voltage stability margin approximation, *Proceedings of the 5th International Conference on Advantages in Power System Control, Operation and Management*, Hong Kong, October 2000, pp.201-205.

[Rep00c] Repo S., Neural network parameter estimation and dimensionality reduction in power system voltage stability assessment, *Soft computing in industrial applications*, Editors: Suzuki Y. et al., Springer-Verlag, London, 2000, pp. 191-202.

[Rep93] Reppen N.D. et al., Performance of methods for ranking and evaluation of voltage collapse contingencies applied to a large-scale network, *Proceedings of the Athens Power Tech conference*, Athens, Greece, September 1993, pp. 337-343.

[Rog95] Rogers G. and Chow J., Hands-on teaching of power system dynamics, *IEEE Computer Application in Power*, January 1995, pp. 12-16.

[Sal95] Salatino D. et al., Online voltage stability assessment of load centers by using neural networks, *Electric Power Systems Research*, 32, 1995, pp. 165-173.

[San99] Riquelme Santos J. et al., Distributed contingency analysis: practical issues, *IEEE Transactions on Power Systems*, Vol. 14, No. 4, November 1999, pp. 1349-1354.

[Sar01] Sarle W.S. (editor), *Neural network FAQ*, the FAQ locates at ftp://ftp.sas.com/pub/neural/FAQ.html, 2001.

[Sch97] Schittenkopf C. et al., Two strategies to avoid overfitting in feedforward networks, *Neural networks*, Vol. 10, No. 3, 1997, pp.505-516.

[Sin95] Sinha A.K., Power system security assessment using pattern recognition and fuzzy estimation, *Electrical Power & Energy Systems*, Vol. 17, No. 1, 1995, pp. 11-19.

[Son97] Song Y.H. et al., Kohonen neural network based approach to voltage weak buses/areas identification, *IEE Proceeding on Generation, Transmission and Distribution*, Vol. 144, No. 3, May 1997, pp. 340-344.

[Sve94] Svensk Energi, *Avbrottskostnader för elkunder*, Report, Sweden, 1994, 80 p.

[Säh79] Sähköntuottajien yhteistyövaltuuskunta, *Report on the value of non-distributed energy*, English summary of report 1/79, Helsinki, Finland, 1979, 37 p.

[Tay94] Taylor C.W., *Power system voltage stability*, McGraw-Hill, New York, USA, 1994, 273 p.

[Tay97] Taylor C.W. and Erickson D.C., Recording and analyzing the July 2 cascading outage, *IEEE Computer Applications in Power*, January 1997, pp. 26-30.

[Tou74] Tou J.T. and Gonzalez R.C., *Pattern recognition principles*, Addison-Wesley, Massachusetts, USA, 1974, 377 p.

[Tra00] *Transient security assessment tool (TSAT)*, Product brochure, Powertech Labs Inc, the information is available at http://www.powertech.bc.ca/, 2000.

[Vaa99] Vaahedi E. et al., Voltage stability contingency screening and ranking, *IEEE Transactions on Power Systems*, Vol. 14, No. 1, February 1999, pp. 256-261.

[Vaa01] Vaahedi E. et al., A future application environment for B.C. Hydro's EMS, *IEEE Transactions on Power Systems*, Vol. 16, No. 1, February 2001, pp. 9-14.

[Vol00a] *Voltage adequacy and stability tool (VAST)*, Product brochure, PowerWorld Corporation, the information is available at http://www.powerworld.com/, 2000.

[Vol00b] *Voltage security assessment tool (VSAT)*, Product brochure, Powertech Labs Inc, the information is available at http://www.powertech.bc.ca/, 2000.

[Wee92] Weerasooriya S. et al., Towards static-security assessment of a large-scale power system using neural networks, *IEE Proceeding on Generation, Transmission and Distribution*, Vol. 139, No. 1, January 1992, pp. 64-70.

[Weh95] Wehenkel L., A statistical approach to the identification of electrical regions in power systems, *Proceedings of the Stockholm Power Tech conference*, Stockholm, Sweden, June 1995, pp. 530-535.

[Weh96] Wehenkel L., Contingency severity assessment for voltage security using non-parametric regression techniques, *IEEE Transactions on Power Systems*, Vol. 11, No. 1, February 1996, pp. 101-111.

[Weh98] Wehenkel L., *Automatic learning techniques in power systems*, Kluwer Academic Publishers, Boston, USA, 1998, 280 p.

[Woo96] Wood A.J. and Wollenberg B.F., *Power generation, operation and control*, John Wiley & Sons, New York, USA, 1996, 569 p.

[Wun95] Wunderlich S. et al., An inter-area transmission and voltage limitation (TVLIM) program, *IEEE Transactions on Power Systems*, Vol. 10, No. 3, August 1995, pp. 1257-1263.

[Yab96] Yabe K. et al., Conceptual designs of AI-based systems for local prediction of voltage collapse, *IEEE Transactions on Power Systems*, Vol. 11, No. 1, February 1996, pp. 137-145.

[Zay96] Zayan M.B. et al., Comparative study of feature extraction techniques for neural network classifier, *Proceedings of International Conference on Intelligent System Applications to Power Systems*, Atlanta, Florida, USA, 1996, pp. 400-404.

[Zen93] Zeng Z.C. et al., A simplified approach to estimate maximum loading conditions in the load flow problem, *IEEE Transactions on Power Systems*, Vol. 8, No. 2, May 1993, pp. 646-652.

[Zho99] Zhou G and McCalley J.D., Composite security boundary visualisation, *IEEE Transactions on Power Systems*, Vol. 14, No. 2, May 1999, pp. 725-731.

APPENDICES

Appendix A

The computation of maximum loading point is presented here step by step. The title in bold face indicates the progress of computation (converged/diverged load-flow) and the value of voltage stability margin. The computation algorithm is based on binary search, the initial step length is 300 MW, the minimum step length is 1 MW. No prediction method was used at the prediction step.

Base case:

```
ITER   DELTAP   BUS     DELTAQ   BUS     DELTA/V/   BUS   DELTAANG   BUS
  0    0.0720(   30)    1.2968(   30)     0.01852(   30)   0.00566(    1)
  1    0.0014(   30)    0.0245(   30)     0.00040(   30)   0.00019(  113)
  2    0.0000(   56)    0.0000(    5)
REACHED TOLERANCE IN   2 ITERATIONS
LARGEST MISMATCH:    0.00 MW    0.00 MVAR     0.00 MVA-BUS     5 [OLIVE       ]
SYSTEM TOTAL ABSOLUTE MISMATCH:              0.03 MVA
```

First step, +300 MW

```
ITER   DELTAP   BUS     DELTAQ   BUS     DELTA/V/   BUS   DELTAANG   BUS
  0    0.0857(  115)    0.0490(   21)     0.01967(   21)   0.21508(  117)
  1    0.0159(   38)    0.0661(   38)     0.00194(   38)   0.00643(   21)
  2    0.0001(   65)    0.0038(   12)     0.00152(  103)   0.00044(  103)
  3    0.0000(  100)    0.0000(   68)
REACHED TOLERANCE IN   3 ITERATIONS
LARGEST MISMATCH:    0.00 MW    0.00 MVAR     0.00 MVA-BUS    68 [SPORN       ]
SYSTEM TOTAL ABSOLUTE MISMATCH:              0.03 MVA
```

Second step, +600 MW

```
 ITER   DELTAP   BUS     DELTAQ   BUS     DELTA/V/   BUS   DELTAANG   BUS
  0    0.0857(   40)    0.0490(   21)     0.02149(   21)   0.22731(  117)
  1    0.0232(   65)    0.1460(   34)     0.00679(    1)   0.00989(  117)
  2    0.0002(   65)    0.1230(   36)     0.00701(   36)   0.00174(   40)
  3    0.0001(   36)    0.0009(   36)     0.00005(   36)   0.00004(   40)
  4    0.0000(  116)    0.0000(   68)
 REACHED TOLERANCE IN   4 ITERATIONS
 LARGEST MISMATCH:    0.00 MW    0.00 MVAR     0.00 MVA-BUS    68 [SPORN       ]
 SYSTEM TOTAL ABSOLUTE MISMATCH:              0.03 MVA
```

Third step, +900 MW

```
 ITER   DELTAP   BUS     DELTAQ   BUS     DELTA/V/   BUS   DELTAANG   BUS
  0    0.0857(   11)    0.0490(   21)     0.03911(   21)   0.25598(  117)
  1    0.0568(   65)    0.3843(   65)     0.00874(   38)   0.02382(  117)
  2    0.0018(   65)    0.0021(   65)     0.00015(   43)   0.00049(  117)
  3    0.0000(   34)    0.0000(   68)
REACHED TOLERANCE IN   3 ITERATIONS
LARGEST MISMATCH:    0.00 MW    0.00 MVAR     0.00 MVA-BUS    68 [SPORN       ]
 SYSTEM TOTAL ABSOLUTE MISMATCH:              0.03 MVA
```

Fourth step, +1200 MW

```
ITER   DELTAP   BUS     DELTAQ   BUS     DELTA/V/   BUS   DELTAANG   BUS
  0    0.0857(   35)    0.0490(   21)     0.05311(   21)   0.31232(  117)
  1    0.1156(   65)    0.4014(   49)     0.01907(   43)   0.05523(  117)
  2    0.0078(   65)    0.0061(   49)     0.00101(   43)   0.00286(  117)
  3    0.0000(   65)    0.0000(   38)
REACHED TOLERANCE IN   3 ITERATIONS
LARGEST MISMATCH:    0.00 MW    0.00 MVAR     0.00 MVA-BUS    65 [MUSKNGUM      ]
 SYSTEM TOTAL ABSOLUTE MISMATCH:              0.03 MVA
```

First diverged load-flow, +1500 MW

```
 ITER   DELTAP   BUS     DELTAQ   BUS     DELTA/V/   BUS   DELTAANG   BUS
  0    0.0857(   42)    0.0490(   21)     0.10322(   43)   0.45727(  117)
  1    0.3231(   65)    0.4483(   40)     0.24799(   43)   0.57111(  117)
  2    0.7121(   65)    2.5431(   42)     0.26036(   43)   0.50949(  117)
  3    0.4661(   65)    0.2662(   65)     0.45783(   43)   0.83538(  117)
  4    2.1675(   65)    0.8141(   38)     0.21128(   40)   0.38463(   19)
  5    0.4976(   65)    1.3663(   34)     0.15415(   43)   0.31640(  117)
  6    0.3264(   65)    0.2129(    8)     0.13315(   43)   0.35518(  117)
  7    0.3115(   65)    1.5812(   40)     0.18069(   43)   0.40309(  117)
  8    0.4276(   65)    0.1025(   56)     0.12815(   43)   0.32750(  117)
  9    0.3014(   65)    1.2356(   40)     0.20516(   43)   0.42576(  117)
 10    0.4800(   65)    0.1832(   56)     0.13312(   43)   0.31364(  117)
 11    0.2924(   65)    0.7003(   40)     0.41652(   43)   0.85581(  117)
 12    2.2174(   65)    0.7907(   38)     0.20100(   40)   0.38370(  117)
 13    0.4985(   65)    1.4540(   34)     0.15220(   43)   0.30480(  117)
 14    0.3045(   65)    0.2140(    8)     0.14164(   43)   0.37571(  117)
 15    0.3687(   65)    1.7006(   40)     0.17829(   43)   0.40295(  117)
 16    0.4308(   65)    0.0928(   65)     0.14519(   43)   0.37651(  117)
 17    0.3852(   65)    1.6094(   40)     0.19306(   43)   0.41679(  117)
 18    0.4303(   65)    0.1141(   56)     0.13156(   43)   0.33519(  117)
 19    0.3149(   65)    1.1888(   40)     0.20990(   43)   0.43128(  117)
 20    0.5027(   65)    0.1994(   56)
TERMINATED AFTER 20 ITERATIONS
BUS X--- NAME ---X    QGEN    QMAX    QMIN VOLTAGE V-SCHED
   42 HOWARD          300.0   300.0  -300.0 1.08180 0.98500
   49 PHILO           210.0   210.0   -85.0 1.04215 1.02500
   66 MUSKNGUM        200.0   200.0   -67.0 1.08025 1.05000
   72 HILLSBRO        100.0   100.0  -100.0 1.05165 0.98000
   74 BELLEFNT          9.0     9.0    -6.0 0.96549 0.95800
WARNING:   5 PLANTS INCORRECTLY AT VAR LIMIT
LARGEST MISMATCH:  -50.27 MW   -9.64 MVAR    51.19 MVA-BUS    65 [MUSKNGUM      ]
 SYSTEM TOTAL ABSOLUTE MISMATCH:            271.00 MVA
```

Fifth step, +1350 MW

```
 ITER   DELTAP   BUS     DELTAQ   BUS     DELTA/V/   BUS   DELTAANG   BUS
  0    0.0429(   42)    0.0245(   21)     0.05161(   43)   0.22864(  117)
  1    0.0819(   65)    0.0446(   38)     0.01699(   43)   0.04888(  117)
  2    0.0064(   65)    0.0041(   40)     0.00168(   43)   0.00388(  117)
  3    0.0000(   65)    0.0000(   38)
REACHED TOLERANCE IN   3 ITERATIONS
LARGEST MISMATCH:    0.00 MW    0.00 MVAR     0.00 MVA-BUS    65 [MUSKNGUM      ]
 SYSTEM TOTAL ABSOLUTE MISMATCH:              0.04 MVA
```

Second diverged load-flow, +1500 MW

```
 ITER   DELTAP   BUS     DELTAQ   BUS     DELTA/V/   BUS   DELTAANG   BUS
  0    0.0429(   42)    0.0493(   40)     0.13611(   43)   0.40593(  117)
  1    0.3163(   65)    1.0612(   42)     0.22390(   43)   0.41753(  117)
  2    0.4797(   65)    0.1518(   56)     0.12803(   43)   0.30978(  117)
  3    0.2818(   65)    0.7786(   40)     0.25202(   43)   0.48995(  117)
  4    0.6814(   65)    0.3160(   56)     0.15399(   43)   0.33720(  117)
```

```
   5    0.3613(   65)    0.3736(    8)     0.95528(   43)   1.95678(  117)
   6    5.4664(   65)    6.2958(   66)     3.71444(   38)   2.84355(   42)
   7   12.0643(   24)    9.4970(   37)    57.26264(   21)  49.19350(  117)
 BLOWN UP AFTER   8 ITERATIONS
BUS X--- NAME ---X    QGEN    QMAX    QMIN VOLTAGE V-SCHED
    1 RIVERSDE         15.0    15.0    -5.028.38663 0.95500
    4 NWCARLSL         300.0   300.0  -300.021.63682 0.99800
    6 KANKAKEE         50.0    50.0   -13.023.63087 0.99000
    8 OLIVE           300.0   300.0  -300.019.77946 1.01500
   10 BREED           200.0   200.0  -147.020.48315 1.05000
   12 TWINBRCH        120.0   120.0   -35.023.89572 0.99000
   15 FTWAYNE          30.0    30.0   -10.0 8.25223 0.97000
   18 MCKINLEY         50.0    50.0   -16.0 6.75746 0.97300
   19 LINCOLN          24.0    24.0    -8.0 3.83903 0.96300
   24 TRENTON         300.0   300.0  -300.0 3.94257 0.99200
   25 TANNRSCK        140.0   140.0   -47.0 1.41584 1.05000
   27 MADISON         300.0   300.0  -300.0 1.97455 0.96800
   31 DEERCRK         300.0   300.0  -300.0 3.92066 0.96700
   32 DELAWARE         42.0    42.0   -14.0 2.35443 0.96400
   34 ROCKHILL         24.0    24.0    -8.0 1.36867 0.98600
   40 WEST END        300.0   300.0  -300.0 1.88734 0.97000
   55 WAGENHLS         -8.0    23.0    -8.0 0.94771 0.95200
   70 PORTSMTH         32.0    32.0   -10.0 1.79668 0.98400
   72 HILLSBRO        100.0   100.0  -100.0 3.77177 0.98000
   74 BELLEFNT         9.0     9.0    -6.0 1.32597 0.95800
   77 TURNER          70.0    70.0   -20.0 1.01028 1.00600
  113 DEER CRK        200.0   200.0  -100.0 7.60513 0.99300
WARNING:  22 PLANTS INCORRECTLY AT VAR LIMIT
LARGEST MISMATCH:******** MW******** MVAR********* MVA-BUS     5 [OLIVE        ]
 SYSTEM TOTAL ABSOLUTE MISMATCH:        71776872.00 MVA
```

Third diverged load-flow, +1425 MW

```
 ITER   DELTAP   BUS     DELTAQ   BUS     DELTA/V/   BUS   DELTAANG   BUS
   0    0.0214(   42)    0.0246(   40)     0.06806(   43)   0.20298(  117)
   1    0.0814(   65)    0.4830(    8)     0.40103(   43)   0.77397(  117)
   2    1.7871(   65)    0.7211(   38)     0.19741(   40)   0.32924(  117)
   3    0.3409(   65)    2.1128(   65)     0.13526(   36)   0.24122(  117)
   4    0.1874(   65)    0.1672(   34)     0.06454(   43)   0.16367(  117)
   5    0.0701(   65)    0.3549(    8)     2.88514(   43)   5.64493(  117)
BLOWN UP AFTER   6 ITERATIONS
BUS X--- NAME ---X    QGEN    QMAX    QMIN VOLTAGE V-SCHED
   34 ROCKHILL         24.0    24.0    -8.0 1.28403 0.98600
   36 STERLING         24.0    24.0    -8.0 1.33082 0.98000
   40 WEST END        300.0   300.0  -300.0 1.07342 0.97000
   42 HOWARD          300.0   300.0  -300.0 1.08028 0.98500
WARNING:   4 PLANTS INCORRECTLY AT VAR LIMIT
LARGEST MISMATCH: 2654.15 MW 5554.57 MVAR  6156.12 MVA-BUS    38 [EASTLIMA     ]
 SYSTEM TOTAL ABSOLUTE MISMATCH:          39094.76 MVA
```

Sixth step, +1387 MW

```
 ITER   DELTAP   BUS     DELTAQ   BUS     DELTA/V/   BUS   DELTAANG   BUS
   0    0.0106(   42)    0.0122(   40)     0.03358(   43)   0.10015(  117)
   1    0.0201(   65)    0.2318(    8)     0.01279(   43)   0.02966(  117)
   2    0.0021(   65)    0.0012(    8)     0.00111(   43)   0.00261(  117)
   3    0.0000(   65)    0.0006(   42)     0.00072(   43)   0.00138(  117)
   4    0.0000(   65)    0.0000(   68)

 REACHED TOLERANCE IN   4 ITERATIONS
LARGEST MISMATCH:    0.00 MW    0.00 MVAR     0.00 MVA-BUS    68 [SPORN        ]
 SYSTEM TOTAL ABSOLUTE MISMATCH:              0.03 MVA
```

Fourth diverged load-flow, +1424 MW

```
 ITER   DELTAP   BUS     DELTAQ   BUS     DELTA/V/   BUS   DELTAANG   BUS
   0    0.0106(   39)    0.0122(   40)     0.96992(   43)   1.89413(  117)
   1    5.1248(   65)    6.3190(   66)     3.75410(   38)   2.80770(   42)
   2   10.2414(   70)    8.1925(   37)     3.21182(   21)   2.62705(   39)
   3   23.6262(   21)   16.9396(   22)    10.39036(   35)  12.93018(   35)
BLOWN UP AFTER   4 ITERATIONS
BUS X--- NAME ---X    QGEN    QMAX    QMIN VOLTAGE V-SCHED
    6 KANKAKEE          50.0    50.0   -13.0 1.00682 0.99000
    8 OLIVE            300.0   300.0  -300.0 1.05162 1.01500
   12 TWINBRCH         120.0   120.0   -35.0 0.99260 0.99000
   31 DEERCRK          300.0   300.0  -300.0 1.03991 0.96700
   36 STERLING          24.0    24.0    -8.0 1.18175 0.98000
   42 HOWARD           300.0   300.0  -300.0 1.20393 0.98500
   49 PHILO            210.0   210.0   -85.0 1.26493 1.02500
   56 SUNNYSDE          15.0    15.0    -8.0 0.96738 0.95400
   66 MUSKNGUM         200.0   200.0   -67.0 1.12875 1.05000
   73 SARGENTS        -100.0   100.0  -100.0 0.52005 0.99100
   76 DARRAH            -8.0    23.0    -8.0 0.81417 0.94300
WARNING:  11 PLANTS INCORRECTLY AT VAR LIMIT
LARGEST MISMATCH:  589.47 MW 8533.22 MVAR  8553.56 MVA-BUS    34 [ROCKHILL      ]
 SYSTEM TOTAL ABSOLUTE MISMATCH:           45587.14 MVA
```

Fifth diverged load-flow, +1405 MW

```
 ITER   DELTAP   BUS     DELTAQ   BUS     DELTA/V/   BUS   DELTAANG   BUS
   0    0.0051(   39)    0.0059(   40)     0.47188(   43)   0.92153(  117)
   1    1.7896(   65)    2.9324(   66)     0.51000(   43)   0.64495(  117)
   2    0.4676(   65)    0.6244(   65)     0.13557(   43)   0.20207(   41)
   3    0.1105(   49)    0.0609(   24)     0.09168(   43)   0.13934(  117)
   4    0.0595(   65)    0.0238(   70)     0.55026(   43)   1.05855(  117)
   5    3.3906(   65)    1.7422(   38)     0.26819(   40)   0.47662(  117)
   6    0.8215(   65)    0.7306(   38)     0.13497(   43)   0.32835(  117)
   7    0.3278(   65)    0.2018(   38)     0.06492(   43)   0.16731(  117)
   8    0.0591(   65)    0.1756(    8)     0.02782(   43)   0.07008(  117)
   9    0.0133(   65)    0.3156(   40)     0.72429(   43)   1.39809(  117)
  10    3.4955(   65)    4.6899(   66)     1.94387(   43)   1.42228(   42)
  11    5.1826(   42)    1.5472(   65)     0.14143(   40)   0.80054(   42)
  12    0.4507(   42)    1.6827(   49)     0.17806(   21)   0.44865(   21)
  13    0.2431(   37)    0.1296(   42)     0.14200(   43)   0.24491(   40)
  14    0.1375(   49)    0.0396(   65)     0.07735(   43)   0.13456(  117)
  15    0.0430(   65)    0.0162(   65)     0.04142(   43)   0.08760(  117)
  16    0.0204(   65)    0.3746(   42)     0.11129(   43)   0.22447(  117)
  17    0.1315(   65)    0.0475(   42)     0.05353(   43)   0.12463(  117)
  18    0.0441(   65)    0.3325(   40)     0.04530(   43)   0.09110(  117)
  19    0.0209(   65)    0.3345(   42)     0.12447(   43)   0.24911(  117)
  20    0.1650(   65)    0.0587(   42)
TERMINATED AFTER 20 ITERATIONS
LARGEST MISMATCH:  -16.50 MW   -3.95 MVAR    16.96 MVA-BUS    65 [MUSKNGUM      ]
 SYSTEM TOTAL ABSOLUTE MISMATCH:           76.88 MVA
```

Sixth diverged load-flow, +1396 MW

```
 ITER   DELTAP   BUS     DELTAQ   BUS     DELTA/V/   BUS   DELTAANG   BUS
   0    0.0026(   39)    0.0030(   40)     0.23597(   43)   0.46082(  117)
   1    0.5105(   65)    1.3351(   66)     0.17336(   43)   0.28456(  117)
   2    0.1388(   65)    0.1041(   65)     0.07295(   43)   0.11551(   10)
   3    0.0374(   65)    0.0184(   72)     0.05794(   43)   0.09501(  117)
   4    0.0243(   65)    0.0143(   46)     0.03168(   43)   0.05887(  117)
   5    0.0093(   65)    0.1580(   42)     0.21052(   43)   0.40850(  117)
   6    0.4729(   65)    0.1502(   38)     0.10901(   39)   0.22602(  117)
   7    0.1596(   65)    0.0661(   38)     0.03814(   43)   0.10306(  117)
   8    0.0295(   65)    0.1991(    8)     0.04718(   43)   0.09243(  117)
   9    0.0241(   65)    0.2411(  113)     0.10990(   43)   0.21018(  117)
  10    0.1234(   65)    0.0386(   40)     0.05247(   43)   0.11183(  117)
```

```
 11   0.0366(   65)   0.1867(    8)    0.04617(   43)   0.09235(  117)
 12   0.0239(   65)   0.2256(  113)    0.13018(   43)   0.24922(  117)
 13   0.1746(   65)   0.0540(   40)    0.06601(   43)   0.13900(  117)
 14   0.0574(   65)   0.1498(    8)    0.01895(   43)   0.05018(  117)
 15   0.0069(   65)   0.1770(   40)    0.02935(   43)   0.05399(  117)
 16   0.0077(   65)   0.1617(   42)    0.20012(   43)   0.38876(  117)
 17   0.4272(   65)   0.1334(   38)    0.10306(   39)   0.21606(  117)
 18   0.1449(   65)   0.0586(   38)    0.03674(   43)   0.09917(  117)
 19   0.0270(   65)   0.0778(   40)    0.07390(   43)   0.14155(  117)
 20   0.0543(   65)   0.1052(   66)
TERMINATED AFTER 20 ITERATIONS
LARGEST MISMATCH:   -0.02 MW   10.52 MVAR    10.52 MVA-BUS    66 [MUSKNGUM     ]
 SYSTEM TOTAL ABSOLUTE MISMATCH:             46.63 MVA
```

Seventh diverged load-flow, +1391 MW

```
 ITER   DELTAP   BUS     DELTAQ   BUS     DELTA/V/   BUS   DELTAANG   BUS
  0   0.0011(   39)   0.0013(   40)    0.10490(   43)   0.20486(  117)
  1   0.1071(   65)   0.4499(   66)    0.06811(   43)   0.12042(  117)
  2   0.0351(   65)   0.0154(   65)    0.02526(   43)   0.04102(  117)
  3   0.0046(   65)   0.0053(   46)    0.06015(   43)   0.11727(  117)
  4   0.0366(   65)   0.0103(   65)    0.01800(   43)   0.04150(  117)
  5   0.0048(   65)   0.1015(   40)    0.02448(   43)   0.04500(  117)
  6   0.0055(   65)   0.0545(   42)    0.31664(   43)   0.60887(  117)
  7   0.8643(   65)   1.8983(   66)    0.26459(   43)   0.39243(  117)
  8   0.2434(   65)   0.2222(   65)    0.09572(   43)   0.13092(   40)
  9   0.0480(   65)   0.0202(   65)    0.03711(   43)   0.05808(  117)
 10   0.0091(   65)   0.0044(   46)    0.05408(   43)   0.10512(  117)
 11   0.0292(   65)   0.0084(   65)    0.01065(   43)   0.02720(  117)
 12   0.0020(   65)   0.1140(   40)    0.02379(   43)   0.04306(  117)
 13   0.0050(   65)   0.0569(   42)    0.35496(   43)   0.68256(  117)
 14   1.0631(   65)   2.1570(   66)    0.28975(   43)   0.43434(  117)
 15   0.2545(   65)   0.2639(   65)    0.08757(   43)   0.12662(   40)
 16   0.0400(   49)   0.0579(   24)    0.06582(   43)   0.09168(   33)
 17   0.0262(   65)   0.0125(   70)    0.02393(   43)   0.03850(  117)
 18   0.0041(   65)   0.0062(   46)    0.06756(   43)   0.13261(  117)
 19   0.0468(   65)   0.0146(   40)    0.02586(   43)   0.05687(  117)
 20   0.0090(   65)   0.0819(   40)
TERMINATED AFTER 20 ITERATIONS
BUS X--- NAME ---X    QGEN    QMAX    QMIN VOLTAGE V-SCHED
   42 HOWARD          300.1   300.0  -300.0 1.00188 0.98500
WARNING:   1 PLANTS INCORRECTLY AT VAR LIMIT
LARGEST MISMATCH:    0.20 MW    8.19 MVAR     8.20 MVA-BUS    40 [WEST END     ]
 SYSTEM TOTAL ABSOLUTE MISMATCH:             12.38 MVA
```

Eighth diverged load-flow, +1389 MW

```
 ITER   DELTAP   BUS     DELTAQ   BUS     DELTA/V/   BUS   DELTAANG   BUS
  0   0.0006(   39)   0.0007(   40)    0.05247(   43)   0.10246(  117)
  1   0.0274(   65)   0.0963(   66)    0.02573(   43)   0.04570(  117)
  2   0.0055(   65)   0.0027(   73)    0.02805(   43)   0.05420(  117)
  3   0.0076(   65)   0.0024(   65)    0.05877(   43)   0.11368(  117)
  4   0.0342(   65)   0.1439(   66)    0.03118(   43)   0.05584(  117)
  5   0.0080(   65)   0.0030(   65)    0.02798(   43)   0.05346(  117)
  6   0.0074(   65)   0.0024(   65)    0.08777(   43)   0.16941(  117)
  7   0.0748(   65)   0.3525(   66)    0.05394(   43)   0.09672(  117)
  8   0.0230(   65)   0.0096(   65)    0.01808(   43)   0.02923(  117)
  9   0.0024(   65)   0.0038(   46)    0.02875(   43)   0.05686(  117)
 10   0.0083(   65)   0.0026(   65)    0.00699(   43)   0.01500(  117)
 11   0.0006(   65)   0.0406(   42)    0.09491(   43)   0.18176(  117)
 12   0.0860(   65)   0.4011(   66)    0.05914(   43)   0.10581(  117)
 13   0.0272(   65)   0.0117(   65)    0.01954(   43)   0.03173(  117)
 14   0.0027(   65)   0.0033(   46)    0.02843(   43)   0.05557(  117)
 15   0.0080(   65)   0.0025(   65)    0.00525(   43)   0.01164(  117)
```

```
 16    0.0004(   65)    0.0419(   42)     0.09816(   43)   0.18797(  117)
 17    0.0919(   65)    0.4237(   66)     0.06157(   43)   0.10999(  117)
 18    0.0293(   65)    0.0128(   65)     0.02072(   43)   0.03358(  117)
 19    0.0031(   65)    0.0033(   46)     0.02837(   43)   0.05536(  117)
 20    0.0080(   65)    0.0025(   65)
TERMINATED AFTER 20 ITERATIONS
BUS X--- NAME ---X    QGEN    QMAX    QMIN VOLTAGE V-SCHED
   42 HOWARD          300.1   300.0  -300.0 0.98556 0.98500
WARNING:   1 PLANTS INCORRECTLY AT VAR LIMIT
LARGEST MISMATCH:   -0.80 MW   -0.25 MVAR     0.83 MVA-BUS    65 [MUSKNGUM      ]
 SYSTEM TOTAL ABSOLUTE MISMATCH:              3.82 MVA
```

Ninth diverged load-flow, +1388 MW

```
 ITER   DELTAP   BUS     DELTAQ   BUS     DELTA/V/   BUS   DELTAANG   BUS
  0    0.0003(   39)    0.0003(   40)     0.02625(   43)   0.05127(  117)
  1    0.0069(   65)    0.0020(   65)     0.01905(   43)   0.03590(  117)
  2    0.0034(   65)    0.0011(   65)     0.46641(   43)   0.89574(  117)
  3    2.4381(   65)    1.1360(   38)     0.23702(   40)   0.39590(  117)
  4    0.5312(   65)    1.4847(   65)     0.12930(   43)   0.27519(  117)
  5    0.2563(   65)    0.1136(   38)     0.05003(   43)   0.12877(  117)
  6    0.0295(   65)    0.1125(    8)     0.01499(   43)   0.03773(  117)
  7    0.0038(   65)    0.0565(   40)     0.01958(   43)   0.03577(  117)
  8    0.0037(   65)    0.0912(  113)     0.00531(  113)   0.01044(  117)
  9    0.0003(   65)    0.0201(   42)     0.03071(   43)   0.05868(  117)
 10    0.0092(   65)    0.0028(   65)     0.02002(   43)   0.03754(  117)
 11    0.0037(   65)    0.0012(   65)     0.03590(   43)   0.06859(  117)
 12    0.0127(   65)    0.0158(   42)     0.01874(   43)   0.03698(  117)
 13    0.0039(   65)    0.0913(  113)     0.00531(  113)   0.01047(  117)
 14    0.0003(   65)    0.0201(   42)     0.03069(   43)   0.05863(  117)
 15    0.0092(   65)    0.0028(   65)     0.02002(   43)   0.03754(  117)
 16    0.0037(   65)    0.0012(   65)     0.03604(   43)   0.06886(  117)
 17    0.0128(   65)    0.0159(   42)     0.01888(   43)   0.03725(  117)
 18    0.0040(   65)    0.0912(  113)     0.00531(  113)   0.01053(  117)
 19    0.0003(   65)    0.0201(   42)     0.03064(   43)   0.05855(  117)
 20    0.0092(   65)    0.0028(   65)
TERMINATED AFTER 20 ITERATIONS
LARGEST MISMATCH:   -0.92 MW   -0.28 MVAR     0.96 MVA-BUS    65 [MUSKNGUM      ]
 SYSTEM TOTAL ABSOLUTE MISMATCH:              4.47 MVA
```

Tampereen teknillinen korkeakoulu
PL 527
33101 Tampere

Tampere University of Technology
P. O. B. 527
FIN-33101 Tampere Finland